UNIVERSITY OF THE
WITWATERSRAND,
JOHANNESBURG

Extending McCabe-Thiele Diagrams to Multicomponent Distillation Systems

Naadhira Seedat (300319)

Doctor of Philosophy in Engineering by Research only:

School of Chemical and Metallurgical Engineering

Faculty of Engineering and the Built Environment

University of the Witwatersrand

Johannesburg, South Africa

2022

Supervisors:

Dr Shehzaad Kauchali

Prof Bilal Patel

University of the Witwatersrand, Johannesburg, South Africa

Faculty of Engineering and the Built Environment

School of Chemical and Metallurgical Engineering

Plagiarism Declaration for Postgraduate Research

I Naadhira Seedat (Student number: 300319) am a student registered for PhD in Chemical Engineering in the year 2022. I hereby declare the following:

I am aware that plagiarism (the use of someone else's work without their permission and/or without acknowledging the original source) is wrong.

I confirm that the work submitted for assessment for the above course is my own unaided work except where I have explicitly indicated otherwise.

I have followed the required conventions in referencing the thoughts and ideas of others.

I understand that the University of the Witwatersrand may take disciplinary action against me if there is a belief that this is not my own unaided work or that I have failed to acknowledge the source of the ideas or words in my writing.

Student Signature: 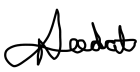

Date: 13/07/2022

DECLARATION

I hereby declare this thesis as my own unaided work. It is being submitted for the Degree of Doctor of Philosophy in Engineering to the University of the Witwatersrand, Johannesburg. It has not been submitted for any degree or examination in any other University

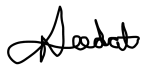

……

Naadhira Seedat

……13…… day of ……July…… year ….....2022.....

ABSTRACT

A novel graphical technique for the preliminary design of multicomponent distillation systems has been developed in this work. The graphical technique is akin to McCabe-Thiele diagrams for binary distillation systems. The method is presented in a two-dimensional (2D) scheme and is simple, intuitive and non-iterative in nature, hence retaining all the inherent characteristics of the McCabe-Thiele method.

Several graphical techniques have been developed for the preliminary design of multicomponent distillation systems in 2D. The methods have started with the fundamentals of the binary McCabe-Thiele method but have lost vital information inherent in their simplifying assumptions. The novel graphical technique presented in this work is not limited by simplifying assumptions, and retains the simplicity and inherent elements of the binary McCabe-Thiele method as well as visually depicting the behaviour of all the components in the system.

This work postulates a novel approach to calculating and depicting the equilibrium relationship between vapour and liquid compositions as a series of contours of vapour-liquid equilibrium (VLE) allowing designers and students alike to analyse systems behaviour as well as determine preliminary design variables in order to initialize rigorous process simulations.

The method of plotting the contours of VLE is presented such that the behaviour of each component in a system can be analysed in order to identify if a separation would be simple or difficult, and contain azeotropes and tangent pinches. The graphical technique is applied to ternary systems to develop a method of calculating the minimum number of stages at total reflux for both ideal and non-ideal systems.

A simple graphical method is proposed to allocate the minimum reflux for ternary ideal and non-ideal systems for transition, sharp direct and indirect splits using the transition point theory presented by Stichlmair (2005). Once the minimum reflux is calculated, the method of determining the number of theoretical stages and feed stage location is unpacked. The method is simple and can be applied to both ideal and non-ideal systems. The preliminary design parameters obtained from the graphical technique were initialised and converged as a feasible column design using Aspen Plus^{TM}. The graphical method has also been extended to the design of quaternary systems. A general method has been presented for the design of higher order systems for feed stage location although this work depicts applications to systems with less than five components.

Finally, the finite reflux graphical method was applied to determine design parameters for ternary reactive-hybrid distillation processes. The notion of reactive difference point cascades presented by Lee et al., (2000) was extended to ternary reactive-hybrid columns for ideal and non-ideal systems such that the powerful visual insights of non-reactive distillation processes are retained. Using the reactive difference point cascades, a simple graphical technique is derived to determine design parameters for different reactive-hybrid distillation column configurations. Particular attention to columns with reaction on the feed stage and in the rectifying section only is analysed. In addition, the method of determining design parameters for reaction in the rectifying section and feed stage as well as stripping section only is presented. Besides reaction on the feed stage, the other column configurations have been applied only to ideal systems with no net change in the number of moles. The design parameters obtained from the graphical technique for reaction on the feed stage were initialised and produced a feasible design that correlated with simulations on Aspen Plus^{TM} for a non-ideal system with a net change in the number of moles.

The novel graphical method in this thesis are practical for early stage design such that rigorous simulators can be initialised with the design parameters obtained. The graphical method is applicable to reactive and non-reactive systems.

DEDICATION

I dedicate this work to my dear parents, Dr AK Seedat and Anisha Seedat, my children, Eesa and Esra, and my beloved husband, Mohamed Riyaadh Ismail. The creator has blessed me by granting me the love and support from you all. I love you all dearly

ACKNOWLEDGMENT

In the name of Allah, the most gracious and ever merciful.

First and above all, I praise and I am immensely grateful to ALLAH, the Almighty for showering his mercy and blessings on me and giving me the strength and capabilities to complete my thesis.

There are many people to whom I am truly grateful for their help and without whom it would not have been possible for me to complete this thesis. Dr Shehzaad Kauchali and Prof Bilal Patel, my supervisor and co-supervisor respectively, who have guided me in completing this thesis and the related publications. Thank you so much for the encouragement, advice and support.

The Department of Higher Education, Science and Technology and the National Research Fund (NRF) of South Africa for financial support to extend my knowledge and complete the required research for this thesis.

My loving family, Husband, Children, Mum, Dad, Sisters, Father-in-law and Mother-in-law. Thank you for the love, support and patience during the completion of this PhD. God has blessed me by having you all in my life.

Contents

List of Figures

List of Tables

Nomenclature

Symbols

x	liquid mole fraction
y	vapour mole fraction
K	equilibrium constant
i	component *i*
j	component *j*
k	component *k*
l	component *l*
x_i	liquid mole fraction of component *i*
y_i	vapour composition of component *i*
x_j	liquid mole fraction of component *j*
y_j	vapour composition of component *j*
x_k	liquid mole fraction of component *k*
y_k	vapour composition of component *k*
CR_{jk}	ratio of component *j* and component *k*
CR_{ik}	ratio of component *i* and component *k*
CR_{ij}	ratio of component *i* and component *j*
CR	component ratio
α_{ik}	relative volatility of component *i* and k
α_{jk}	relative volatility of component *j* and *k*
α_{kj}	relative volatility of component *k* and *j*
x_{C7}	liquid mole fraction of n-heptane
x_{C9}	liquid mole fraction of n-nonane
x_{C6}	liquid mole fraction of n-hexane
y_{C6}	vapour mole fraction of n-hexane
K_{C7}	equilibrium constant of n-heptane
K_{C9}	equilibrium constant of n-nonane
K_{C6}	equilibrium constant of n-hexane
$CR_{C7/C9}$	component ratio of n-heptane and n-nonane

x_A	liquid mole fraction of component A
x_B	liquid mole fraction of component B
x_C	liquid mole fraction of component C
y_A	vapour mole fraction of component A
y_B	vapour mole fraction of component B
y_C	vapour mole fraction of component C
$x_{Acetone}$	liquid mole fraction of component acetone
$x_{Benzene}$	liquid mole fraction of component benzene
$x_{Chloroform}$	liquid mole fraction of component chloroform
$y_{Acetone}$	vapour mole fraction of component acetone
$y_{Benzene}$	vapour mole fraction of component benzene
$y_{Chloroform}$	vapour mole fraction of component chloroform
$CR_{\frac{Benzene}{Chloroform}}$	component ratio of benzene and chloroform
Ki	equilibrium constant for component *i*
$K_{acetone}$	equilibrium constant for acetone
$K_{chloroform}$	equilibrium constant for chloroform
x_D	liquid distillate mole fraction
x_B	liquid bottoms mole fraction
y_{eqm}	vapour equilibrium composition
x_{eqm}	liquid equilibrium composition
$CR_{C6/C9}$	component ratio of n-hexane and n-nonane
$CR_{\frac{Acetone}{Chloroform}}$	component ratio of acetone and chloroform
$CR_{F,jk}$	feed component ratio of component *j* and component *k*
$CR_{F,ik}$	feed component ratio of component *i* and component *k*
$CR_{F,ij}$	feed component ratio of component *i* and component *j*
$x_{F,j}$	liquid feed composition for component *j*
$x_{F,k}$	liquid feed composition for component *k*
$x_{F,i}$	liquid feed composition for component *i*
R_{min}	minimum reflux ratio
S_{min}	minimum reboil ratio
$R_{gradient}$	gradient of rectifying operating line
$S_{gradient}$	gradient of bottoms operating line
$y_{D,i}$	vapour distillate composition for component *i*

$y_{F,i}^{*}$	liquid equilibrium composition corresponding to the liquid feed composition, $x_{F,i}$, for component *i.*
$x_{F,i}$	liquid feed composition for component i
$x_{D,i}$	liquid distillate composition of component *i*
$x_{B,i}$	liquid bottoms composition of component *i*
$y_{B,i}$	vapour bottoms composition of component *i*
$x_{TR,i}^{*}$	liquid composition of the transition point for component *i* in rectifying section
$y_{TR,i}^{*}$	vapour composition of the transition point for component *i* in rectifying section
$x_{TB,i}^{*}$	liquid composition of the transition point for component *i* in bottoms section
$y_{TB,i}^{*}$	vapour composition of the transition point for component *i* in bottoms section
$CR_{F,E/P}$	ratio of feed composition of ethanol and propanol
$CR_{F,M/P}$	ratio of feed composition of methanol and propanol
$CR_{F,M/E}$	ratio of feed composition of methanol and ethanol
$\alpha_{(\frac{M}{P})}$	relative volatility of methanol/n-propanol
$\alpha_{(\frac{M}{E})}$	relative volatility of methanol/ethanol
x_M	liquid composition of methanol
y_M	vapour composition of methanol
q	thermal state of feed
α_{ME}	relative volatility of methanol/ethanol
α_{BC}	relative volatility of benzene/chloroform
$x_{TB,B}^{*}$	liquid composition of the transition point for component B in bottoms section
$y_{TB,B}^{*}$	vapour composition of the transition point for component B in bottoms section
x_F	liquid feed mole fraction
x_D	liquid distillate mole fraction
$x_{B,}$	liquid bottoms mole fraction
R	reflux
D	distillate
V_n	total vapour flowrate on stage *n* in rectifying section
L_{n+1}	total liquid flowrate on stage *n+1* in rectifying section
$V_{n,i}$	vapour flowrate on stage *n* in rectifying section for component *i*
$L_{n+1,i}$	liquid flowrate on stage *n+1* in rectifying section for component *i*
$y_{n,i}$	vapour composition on stage *n* in rectifying section for component *i*
$x_{n+1,i}$	liquid composition on stage *n+1* in rectifying section for component

L_n	reflux is the amount of liquid returned back to the column
S	reboil ratio
L_{m+1}	total liquid flowrate on stage *m+1* in bottoms section
$y_{m,i}$	vapour composition on stage *m* in bottoms section for component *i*
L_m	Reboil is the amount of vapour returned back to the column
$x_{m+1,i}$	liquid composition on stage *m+1* in bottoms section for component *i*
D	Bottoms
$y_{q,i}$	vapour composition of component *i* in the feed
$x_{q,i}$	liquid composition of component *i* in the feed
$x_{methanol}$	liquid mole fraction of component Acetone
$x_{ethanol}$	liquid mole fraction of component Benzene
$x_{n\text{-}propanol}$	liquid mole fraction of component Chloroform
$CR_{E/P}$	ratio of composition of ethanol and propanol
$CR_{M/P}$	ratio of composition of methanol and propanol
$\hat{x}^{1,s}$	node pinch in the stripping section
x^0	first point for feasible design
y_R	vapour composition in on feed stage in rectifying section
y_S	vapour composition in on feed stage in stripping section
x_R	liquid composition in on feed stage in rectifying section
x_S	liquid composition in on feed stage in stripping section
x_l	liquid mole fraction of component *l*
y_l	vapour composition of component *l*
α_{lk}	relative volatility of component *l* and *k*
α_{ji}	relative volatility of component *j* and *i*
α_{ki}	relative volatility of component *k* and *i*
α_{li}	relative volatility of component *l* and *i*
CR_{lk}	ratio of component *l* and component *k*
CR_{ki}	ratio of component *k* and component *i*
CR_{li}	ratio of component *l* and component *i*
CR_{ji}	ratio of component *j* and component *i*
n	total number of components in mixture
x_{C10}	liquid mole fraction of n-decane

g	ratio of the molar latent heat of vaporization of component *i* and molar latent heat of vaporization of the component with the lowest molar latent heat of vaporization in the mixture
λ_{HK}	molar latent heat of vaporization of the component with the lowest molar latent heat of vaporization in the mixture
λ_i	molar latent heat of vaporization of component *i*
ξ_n	reaction extent on stage n
v_T	sum of the stoichiometric coefficients
ξ	total of the reaction molar turnover flowrate on the feed stage
v_i	stoichiometric coefficient of component i
$x_{\bar{F},i}$	molar composition of component i in the pseudo-feed.
$\delta_{R,i}$	reaction difference point of component i
V_i	vapour flowrates leaving the feed stage
$\bar{L}_i$	liquid flowrates leaving the feed stage
$\bar{V}_i$	vapour flowrates entering the feed stage
L_i	liquid flowrates entering the feed stage
Δh_R	heat of reaction
H_V	enthalpy of the feed at the dew point
h_F	enthalpy of the feed
h_L	enthalpy of the feed at the bubble point
CR1,(isobut/meth)	ratio of isobutene and methanol
CR1,(isobut/MTBE)	ratio of isobutene and MTBE
$y_{methanol}$	vapour mole fraction of methanol
$y_{isobutene}$	vapour mole fraction of isobutene
y_{MTBE}	vapour mole fraction of MTBE
$\sum_{n=1}^{n} \xi_n$	sum of the reaction molar turnover flowrate occurring on all stages from the top stage to stage n
v	stoichiometric coefficient vector
c_P	product coefficient vector
c_R	reactant coefficient vector
$\delta^r{}_{R,i,n}$	reactive difference point for reaction in the rectifying section
$\sum_{m=1}^{m+1} \xi_{m+1}$	sum of the reaction molar turnover flowrate occurring on all stages from the top stage in the bottoms section to stage m+1
$\delta^s{}_{R,i,n}$	reactive difference point for reaction in the stripping section
x_{D1}	adjusted distillate composition for reactive stage 1 in rectifying section

x_{D2}	adjusted distillate composition for reactive stage 2 in rectifying section
x_{B1}	adjusted bottoms composition for reactive stage 1 in stripping section

Greek letters

α	relative volatility
λ	latent heat of vaporization
ξ	reaction extent
δ	reactive difference point

Subscripts

i	component *i*
j	component *j*
k	component *k*
l	component *l*
C6	component n-hexane
C7	component n-heptane
C9	component n-nonane
C10	component n-decane
A	component A
B	component B
C	component C
eqm	equilibrium
D	distillate
B	bottoms
F	feed
min	minimum
M	methanol
E	ethanol
P	n-propanol
l	component *l*
MTBE	Methyl tert-butyl ether
R	reaction
n	stage *n*
m	stage *m*
P	product
R	reactant

LK	light key
IK	intermediate key
HK	heavy key
$\hat{F}$	pseudo-feed
V	vapour
L	liquid
T	total

Superscripts

TM	trade mark

Abbreviations

2D	two dimension
BOL	bottoms operating line
B	bottoms
bpt	boiling point
BVM	boundary value method
CMO	constant molar overflow
CRV	constant relative volatility
CTEMO	elemental mass overflow
D	distillate
DCM	distillation curve map
DWC	divided-wall column
E	ethanol
eqm	equilibrium
F	feed
FUG	Fenske-Underwood-Gilliland
HK	heavy key
IK	intermediate key
LK	light key
MBT	mass balance triangle
M	methanol
min	minimum

MTBE	Methyl tert-butyl ether
NRTL	non-random two-liquid
nbpt	normal boiling point
OL	operating line
P	n-propanol
q-line	feed line
R	reflux
RCM	residue curve map
ROL	rectifying operating line
S	reboil
SSLM	shortest stripping line method
$x_{B,\ pinch}$	pinch bottoms product
$x_{D,\ pinch}$	pinch distillate product
VLE	vapour-liquid equilibrium

Chapter 1

Introduction

In this introduction, a brief overview and importance of the topic is stated, and the aim and contribution to the field of separation engineering is presented.

1.1 Overview

Separation processes are an essential and integral part of all chemical processes. Chemical processes require efficient separation of products from reactants, by-products and impurities, amongst other applications. Distillation is widely used in the petroleum, chemical, pharmaceutical and food industries. According to Stichlmair et al., (2021) distillation will continue to be the dominant process for separation in these industries. Distillation processes constitute approximately 90-95% of all separations in industry (Humphrey, 1995). In 2012, there were in excess of 40 000 distillation columns in use in the USA alone (White, 2012). Hence distillation processes are generally the most widely used separation processes in industry. Distillation accounts for up to 40% of energy consumption in chemical plants in the USA (White, 2012). In addition, Górak & Sorensen, (2014) state that distillation accounts for up to 50% of the capital and operation costs in industrial plants. Extensive research has been conducted on energy saving intensified distillation technologies such as reactive distillation, divided wall columns, internally heat integrated columns and thermally coupled columns (Kiss et al., 2019). This clearly demonstrates the need for efficient methods of distillation design to lower both capital and operational costs.

Current practice for distillation design is for designers to synthesise process flowsheets, set the operating parameters and input the information into a rigorous equilibrium tray simulation (Partin, 1993). Rigorous simulators such as the RadFrac model using Aspen Plus™ software are generally used for distillation design (Skiborowski et al., 2018). The simulator then performs a rating calculation at the operating parameters for the process (Partin, 1993). It can be challenging to determine the required operating parameters to initialize the process specifications in a simulator and the designer is not guaranteed that the design is feasible (Partin. 1993). Preliminary design tools, such as empirical short-cut and graphical methods, are used to determine design variables such as minimum reflux, minimum number of stages at total reflux and feed stage location (Gani & Bek-Pedersen, 2000). Once determined using a preliminary design tool, the above listed operating parameters are used to initialize a rigorous simulator to perform detailed design and optimization simulations (Fidkowski et al., 1991). Essentially, the preliminary design procedure should serve as a precursor to the rigorous simulation process. This ensures the competent use of the simulation tools. Hence both procedures play an important role in the overall distillation design procedure (Mathias, 2009).

Graphical methods are an attractive preliminary design tool that can not only be utilised for determining design parameters but also aid in the visual analysis and understanding of the behaviour of the components required to be separated. Graphical methods depict mass and energy balances as well as vapour-liquid equilibrium (VLE) in a 'picture'. The depiction of VLE provides the designer with powerful visual insights into identifying feasible designs, azeotropes, pinch points (minimum energy requirements) and possible operational issues (Mathias, 2009). Short-cut and rigorous simulators do not provide the visual insights that graphical methods offer.

McCabe and Thiele developed the McCabe-Thiele diagram, a graphical preliminary design tool, to gain behavioural insights and calculate design parameters for binary distillation systems (McCabe & Thiele, 1925; Lee et al., 2000). For decades, the McCabe-Thiele diagram has provided engineers with a quick tool which enabled effective design and operational analysis of binary distillation processes (Lee et al.,

2000). The design parameters obtained from the McCabe-Thiele method are used to initialise rigorous simulators such that converged solutions are achieved, hence enhancing the competent use of rigorous simulators.

Several graphical techniques have been developed for the preliminary design of reactive and non-reactive multicomponent distillation systems in two dimensions (2D). The methods have started with the fundamentals of the binary McCabe-Thiele method but have lost vital information inherent in their simplifying assumptions. A simple and comprehensive graphical method for multicomponent systems similar to the McCabe-Thiele method for binary systems is lacking. Most methods use approximations of reducing a ternary system to a binary-pseudo system (Hengstebeck, 1946). The work in this thesis addresses the need for a comprehensive, simple and effective preliminary design tool for multicomponent reactive and non-reactive systems in the form of a graphical method such that both visual insights and design parameters can be determined fairly quickly to aid rigorous and detailed design calculations.

1.2 Aim of the Thesis

The aim of the work in this thesis is to provide a simple and effective alternative graphical design technique for the analysis and preliminary design of reactive and non-reactive multicomponent systems. The novelty of the work is the representation of the equilibrium relationship between vapour (x) and liquid (y) compositions as a series of contours of vapour-liquid equilibrium (VLE). From the foundation of the VLE representation the following outcomes are possible:

(1) the behaviour of the components in the system such as identifying the type of separation (easy or difficult), azeotropes and tangent pinch points can be identified;
(2) the minimum number of stages at total reflux can be calculated graphically for ternary ideal and non-ideal systems;

(3) the minimum reflux for transition, sharp direct and indirect splits can be calculated for both ternary ideal and non-ideal systems from a simple graphical method;
(4) the number of theoretical stages and feed stage location is determined for ternary ideal and non-ideal systems at finite operating reflux;
(5) the combined graphical method for designing distillation columns is adapted to provide a general outline method for higher order systems and hence applied to quaternary systems;
(6) the graphical technique is extended to reactive-hybrid distillation systems for reaction on the feed stage for ternary ideal and non-ideal systems, rectifying section only, stripping section only and a combination of feed stage and rectifying section reaction for ternary ideal systems.

Each contribution presented above is elaborated on in a chapter in the thesis overview outline below.

1.3 Thesis Outline

The majority of the work presented in this thesis has been published in two journal articles whilst the third is to be submitted for review. Each chapter is presented in the form of a journal article with an introduction and conclusion such that it can be read independently. Since each chapter is in a journal format, a certain overlap in ideas will be noticed from one chapter to the next. Details of the publication relating to the specific chapter will be stated under each chapter outline.

CHAPTER 2 provides a brief literature review that covers the most applicable conceptual and preliminary design tools under the categories of empirical short-cut, traditional graphical and residue curve map (RCM) based graphical methods.

CHAPTER 3 forms the foundation of the graphical technique providing the derivations and methods of plotting the contours of VLE. Once the VLE is plotted the visual insights of the behaviour of the system can be analysed. It is shown how

to identify the type of separation (easy or difficult), azeotropes, as well as tangent and pinch points

The work in this chapter has been published as: Seedat, N., Kauchali, S., Patel, B., **2020**. Novel representation of vapour-liquid equilibrium curves for multicomponent systems: design of total reflux distillation columns. *Chem. Eng. Res. Des*. 155, pp. 22-39.

CHAPTER 4 uses the novel method of plotting VLE presented in Chapter 3 to determine the minimum number of stages at total reflux. The method is akin to the binary McCabe-Thiele method, but has been extended to ternary ideal and non-ideal systems. Depending on the nature of the split, either sharp direct or indirect, the direction of stepping off stages begins at the bottoms and distillate product respectively. The method for stepping off stages in either direction is explained and depicted in the form of examples.

The work in this chapter has been published as: Seedat, N., Kauchali, S., Patel, B., **2020**. Novel representation of vapour-liquid equilibrium curves for multicomponent systems: design of total reflux distillation columns. *Chem. Eng. Res. Des*. 155, p. 22-39.

CHAPTER 5 presents a simple graphical tool for the calculation of minimum reflux for ideal and non-ideal ternary systems. The method can be applied to transition, sharp direct and indirect splits. The method is based on the occurrence of transition points when a sharp direct and indirect split goes through a saddle point. The method for all three types of splits is demonstrated using examples of ideal and non-ideal ternary systems.

The work in this chapter has been published as: Seedat, N., Kauchali, S., Patel, B., **2021**. A graphical method for the preliminary design of ternary simple distillation columns at finite reflux. *SAJCE*. 37, pp. 99-109.

CHAPTER 6 demonstrates the graphical method of calculating the number of theoretical stages required in a sharp direct and indirect separation. Due to the

nature of the separations being an inverse of each other, the methods and rules of each split are discussed and the methods presented in examples for both ideal and non-ideal distillation systems. In addition, the analysis of feed stage location and how to determine a feasible range of feed stages can be visually located without any further calculation, whilst stepping off stages to find the theoretical number of stages. An initialisation of a rigorous simulation with the design parameters obtained from the graphical techniques showed a feasible converged distillation column design. A consolidated general procedure for all the steps required in the preliminary design stage is presented and applied to an ideal quaternary system An extension of plotting contours of VLE for ternary systems to higher order systems is presented. In addition, the method for total reflux (Chapter 4) and finite reflux (Chapter 6) for ternary systems has also been extended to higher order systems. The method is demonstrated for a sharp direct split for a quaternary ideal system in a sharp split. Nonetheless, the method can be applied to higher order systems, non-ideal mixtures and sharp indirect splits. Finally, an algebraic extension of the method to cases in which constant molar overflow (CMO) does not hold is presented.

The work in this chapter has been published as: Seedat, N., Kauchali, S., Patel, B., **2021**. A graphical method for the preliminary design of ternary simple distillation columns at finite reflux. *SAJCE*. 37, p. 99-109.

CHAPTER 7 applies the methods from Chapters 3 and 6 to a more complex problem of designing reactive-hybrid distillation columns for a single reaction. The graphical technique combines the novel representation of the contours of VLE (Chapter 3), the graphical method of determining design parameters at finite reflux (Chapter 6), and the theory of reactive difference point cascades (Lee et al., 2000). A combination of these notions results in a simple graphical technique to determine design parameters for reaction on the feed stage for ideal and non-ideal systems. The production of methyl tert-butyl ether (MTBE) from the reaction of isobutene and methanol results in a highly non-ideal system with a net change in the number of moles. An initialisation of a rigorous simulation with the design parameters for the production and recovery of MTBE obtained from the graphical technique

showed a feasible converged distillation column design for the non-ideal system for the feed stage reaction. The graphical method is also extended for column configurations for reactions in the rectifying section only, feed and rectifying section, and stripping section only, for ideal systems with no net change in the number of moles.

The work in this chapter will be submitted for publication as: Seedat, N., Kauchali, S., Patel, B., A graphical method for the preliminary design of ternary reactive-hybrid distillation columns at finite reflux.

CHAPTER 8 concludes and summarises the important aspects of the thesis.

REFERENCES

Fidkowski, Z.T., Malone, M.F., Doherty, M.F., **1991**. Nonideal Multicomponent Distillation: Use of Bifurcation Theory for Design. *AIChE J*. 37(12), pp. 1761-1779.

Gani, R. & Bek-Pedersen, E., **2000**. Simple New Algorithm for Distillation Column Design. *AIChE J*. 46(6), pp. 1271-1274.

Górak, A. & Sorensen, E., **2014**. Distillation: Fundamentals and Principles. *Elsevier: Academic Press*: London

Hengstebeck, R.J., **1946**. A Simplified Method for Solving Multicomponent Distillation Problems. *Trans. AIChE*. 42, pp. 309-329.

Humphrey, J.L., **1995**. Separation processes: Playing a critical role. *Chem. Eng. Prog*. 91(10), pp. 31-45.

Kiss, A.A., Jobson, M., Goa, X., **2019**. Reactive Distillation: Stepping Up to the Next Level of Process Intensification. *Ind. Eng. Chem. Res.* 58(15), pp. 5909−5918.

Lee, J.W., Hauan, S., Lien, K.M., Westerberg, A.W., **2000**. A graphical method for designing reactive distillation columns. II. The McCabe-Thiele method. *Proc. R. Soc. Lond. A*. 456(2000), pp. 1965-1978.

Mathias, P.M., **2009**. Visualizing the McCabe-Thiele Diagram. *Chem. Eng. Prog*. 105(12), pp. 36-44.

McCabe, W.L. & Thiele, E.W., **1925**. Graphical Design of Fractionating Columns. *Ind. Eng. Chem.* 17(6), pp. 605-611.

Partin, L.R., **1993**. Use Graphical Techniques to Improve Process Analysis. *Chem. Eng. Prog*. 89(1), pp. 43-48.

Skiborowski, M., Recker, S., Marquardt, W., **2018**. Shortcut-based optimization of distillation-based processes by a novel reformulation of the feed angle method. *Chem. Eng. Res. Des*. 132, pp. 135-148.

Stichlmair, J.G., Klein, H., Rehfeldt, S., **2021**. Distillation: Principles and Practice. *John Wiley & Sons*: New Jersey.

White, D.C., **2012**. Optimize energy use in distillation. *Chem. Eng. Prog.* 108(3), pp. 35-41.

Chapter 2

Literature Review

2.1 Introduction

The aim of this chapter is to establish context and relevance of the work developed in this thesis. Each subsequent chapter contains a detailed introduction into the specific topic investigated in the chapter. The detailed introduction has been published in journal articles and hence is sufficient to understand the content of each chapter. In this chapter, a brief outline and review summary of the overall distillation design process as well as the well-established preliminary design methods in the categories of empirical short-cut method, traditional graphical methods and RCM based graphical method will be provided.

2.2 Importance of Distillation as a Separation Process

Separation processes are an essential and integral part of all chemical processes. Chemical processes require efficient separation of products from reactants, by-products and impurities, amongst other applications. There are different methods of separation used in industry, namely membrane separation, crystallization, liquid-liquid extraction, absorption and distillation amongst others. Distillation has been the primary method of separation to separate binary as well as multicomponent systems into purer products for over 5000 years (Górak & Sorensen, 2014). To this day, distillation is the most important and effective method of separating multicomponent mixtures (Stichlmair et al., 2021). Distillation is widely used in the petroleum, chemical, pharmaceutical and food industries. According to Stichlmair

et al., (2021) distillation will continue to be the dominant process for separation in these industries.

Distillation accounts for up to 50% of operational and capital costs in the chemical and petrochemical industries (Górak & Sorensen, 2014). In recent years, cost effective distillation systems in terms of energy and capital costs have gained a lot of prominence. (Bahadori & Vuthaluru, 2010). Examples of energy-saving intensified distillation technologies are reactive distillation, divided wall columns, internally heat integrated columns and thermally coupled columns as well as combinations of the different technologies (Kiss et al., 2019). The ongoing research into energy efficient distillation processes clearly demonstrates the need for efficient methods of distillation design to lower both capital and operational costs (Górak & Sorensen, 2014).

Chapter 8 focuses on the development of graphical methods for determining preliminary design variables for reactive distillation in a ternary system. Reactive distillation is one of the most successful applications of process intensification technologies of the past century (Kiss et al., 2019). Reactive distillation combines reaction and separation in a single intensified unit such that both capital and operating costs are reduced (Orjuela et al., 2016). Reactive distillation in general has shown capital and energy savings of between 15% and 80% over conventional set-ups (Harmsen, 2007). The design of reactive distillation systems is more complex than simple distillation columns. Combined separation and reaction feasibility factors need to be considered, unlike conventional distillation and reactor design which accounts individually for the respective design and feasibility factors. Hence a simple graphical technique is imperative to efficiently design reactive-hybrid distillation processes without adopting the traditional method of transformation of composition coordinates.

2.3 Overall Distillation Design Process

Traditionally, distillation design involved synthesizing process flowsheets, setting the operating parameters and inputting the information into a rigorous equilibrium tray simulation (Partin, 1993). It can be challenging to determine the required operating parameters to initialize the process specifications in a simulator. This methodology did not guarantee a feasible design or a converged solution as rigorous simulators provide no visual insights or understanding of the process. Hence, the incorporation of techniques such as graphical tools is required to complement and enhance the effective use of rigorous simulators.

The distillation design procedure consists of three crucial stages, namely the conceptual, preliminary and detailed/optimization design phases. The conceptual design phase is the first screening process to determine the feasibility of a desired separation by analysing the behaviour of the system. In the conceptual design stage, graphical methods are invaluable tools as they provide crucial visual insights into the behaviour of systems. Residue curve maps (RCMs), distillation curve maps (DCMs) and McCabe-Thiele diagrams have been used frequently in the conceptual design of multicomponent zeotropic, azeotropic and reactive distillation systems (Widago & Seider, 1996). By identifying if a desired separation is infeasible, prior to preliminary and detailed design calculations convergence issues are prevented.

Key design parameters such as minimum reflux, theoretical number of stages at finite reflux, feed stage location and reactive stage location (reactive distillation only) are determined using preliminary design tools (Gani & Bek-Pedersen, 2000; Almeida-Rivera et al., 2004). These design parameters serve as a starting point for the initialisation of rigorous simulations using simulation packages such as Aspen Plus™ such that a converged solution is obtained with the first simulation. Obtaining a starting point for detailed design is of utmost importance as it eliminates tedious trial-and-error calculations. Essentially, the conceptual and preliminary design procedures serve as a precursor to the rigorous simulation process and ensure the effective and competent use of rigorous simulators.

Preliminary design tools can be categorised into two main methods: short-cut/empirical methods and graphical methods (Kister, 1992).

Many short-cut empirical, traditional graphical and computational-graphical methods have been developed in order to design binary as well as multicomponent distillation systems. This review will summarize the different preliminary design tools under the categories of short-cut empirical, graphical and residue curve map (RCM) based graphical methods.

2.4 Empirical Short-Cut Methods

Empirical short-cut methods are commonly used to determine preliminary design variables with fairly simple and quick calculations. Empirical short-cut methods assume constant molar overflow (CMO) and constant relative volatility (CRV) and do produce inaccuracies in the estimated variables (Reyes et al., 2000 ; Van Winkle, 1967; Kister, 1992). Nevertheless, the methods are often used by students and designers in the preliminary design phase as the estimated values provide a suitable starting point for rigorous simulations. The main advantage of graphical methods over empirical short-cut methods is the visual insights gained whilst determining design parameters. Short-cut methods are numerical in nature therefore provide no visual depiction for gaining insight into the behaviour of systems.

In this section, a summary of the short-cut methods for preliminary design variables such as minimum number of stages at total reflux, minimum reflux, theoretical number of stages and feed point location at finite reflux will be presented. Additionally, the empirical short-cut empirical method for determining design parameters for reactive distillation will be discussed.

Operation at total reflux results in no distillate and bottoms products being withdrawn such that the minimum number of stages to obtain the required product specification is determined (Bahadori & Vuthaluru, 2010). Total reflux columns are defined to have a single continuous section unlike finite reflux columns which have

a rectifying and stripping section (Castillo et al., 1998). Minimum reflux and reboil are defined as the lowest amount of liquid and vapour returned to a column from the distillate and bottoms product respectively, to achieve the desired separation. The minimum reflux and reboil ratio primarily determines the minimum energy requirements of a distillation process, but the investment cost would also reach infinity (Stichlmair et al., 1993). Minimum reflux and reboil represent a lower, thermodynamically defined operating limit which corresponds to an infinite number of stages and also to an infeasible operating point (Koehler et al, 1995; Górak & Sorensen, 2014). Hence, if a column is designed with a lower number of stages, the product specification will not be achieved. Thus minimum reflux and total reflux operation are extreme operational bounds in distillation columns. A desired separation can only be achieved if operation is between these bounds, hence highlighting the importance of determining operating variables at these limits (Bahadori & Vuthaluru, 2010).

2.4.1 Total Reflux

The Fenske (1932), Underwood (1948) and Winn (1958) equations calculate the minimum number of stages in simple columns (one feed, with two products) for ideal binary and multicomponent systems. The Fenske (1932) and Underwood (1948) equations assume constant relative volatilities (α), whereas the Winn (1958) equation uses the vapour−liquid equilibrium constant, (K). The Winn equation is deemed more robust than the Fenske and Underwood equations for systems which the relative volatility is strongly dependent on temperature (Cao et al., 2014). Nevertheless, all these equations are limited to ideal systems. The model of plotting the contours of VLE in the proposed graphical method, presented in this thesis, is not restricted to CRV: any appropriate thermodynamic model can be used to model ideal and non-deal systems. Additionally since the method is graphical in nature it can be adapted to non-CMO operation, simply illustrated by non-linear operating lines on the McCabe-Thiele diagrams.

2.4.2 Minimum Reflux

The Underwood (1948) method is the most frequently used short-cut method to determine minimum reflux (Górak & Sorensen, 2014). Underwood (1948) used the notion of 'pinches' proposed by McCabe & Thiele (1925) to develop an empirical equation to calculate minimum reflux for multicomponent mixtures, but which are limited to CMO and CRV. The Underwood (1948) equation simply relates the feed compositions and relative volatilities with the state of the feed and hence finds a factor that calculates the minimum reflux using the distillate composition. The Underwood (1948) method yields fairly accurate values for minimum reflux, if the assumptions of CMO and no intermediate distribution of keys in the distillate and bottoms hold for the process to be designed (Perry & Green, 1999). If the assumptions of CMO and constant relative volatility do not hold between the two pinch point regions, considerably inaccurate values for the minimum reflux are obtained, yielding incorrect design specifications (Perry & Green, 1999). Numerous publications have modified the Underwood (1948) equation for non-ideal multicomponent systems (Bausa et al., 1998), multicomponent complex columns (Barnes et al., 1972; von Watzdorf et al., 1999; Yaws et al., 1981) and extractive distillation (Brüggemann & Marquardt, 2004).

Additional short-cut correlations for determining minimum reflux are also presented by Colburn (1941), Gilliland (1940) and Brown & Martin (1939). The Colburn method (1941) is a modification of the Underwood (1948) equation by accounting for the distribution of intermediate components. Colburn (1941) used two equations to determine the key composition in the rectifying pinch and hence the minimum reflux of the key components (Van Winkle, 1967; Reyes et al., 2000). The value obtained is corrected to account for the non-heavy key component in the upper zone and the non-light key in the lower zone (Van Winkle, 1967). According to Reyes et al., (2000), the Colburn (1941) method can yield fairly accurate estimates of minimum reflux in certain applications. The Gilliland (1940) correlation produces the same results as the Underwood (1948) method but does not require iterative calculations as it is a single equation (Reyes et al., 2000). Van

Winkle, (1967), recommends the Brown-Martin method for systems that do not require great accuracy, such as multicomponent hydrocarbon distillation systems. This method is the simplest and requires fewer calculations, but minimum reflux values obtained from the method are conservative such that the actual minimum reflux is less than that calculated (Van Winkle, 1967; Kister, 1992). The proposed method, presented in this thesis, of determining the minimum reflux using McCabe-Thiele diagrams is applicable to ideal and non-ideal systems and accommodates distributed keys by the novel representation of the contours of VLE (Chapter 3) for all components in the system.

2.4.3 Finite Reflux

Smoker (1938), Gilliland (1940) and Erbar & Maddox (1961) provide empirical correlations to determine the number of theoretical separation units at finite reflux for multicomponent systems. The Smoker (1938) equation requires the calculation of the number of stages in the rectifying and stripping section separately in order to calculate the total number of stages (Soliman, 2009). Erbar & Maddox (1961) and Gilliland (1940) provide a correlation between the number of stages and reflux by calculating the minimum reflux and stages using Underwood and Winn/Fenske respectively (Kister, 1992). The Gilliland (1940) correlation in general uses the Fenske equation whilst either Winn or Fenske is used for Erbar and Maddox (1961). According to Kister (1992), the Erbar and Maddox (1961) correlation is more accurate at lower refluxes than the Gilliland (1940) correlation.

The most well-known and applied short-cut method to determine the number of theoretical stages is known as the Fenske-Underwood-Gilliland (FUG) method. Gilliland (1940) provided the correlation between minimum reflux and stages in graphical form which was later adapted into an empirical equation (Soliman, 2009). Although the variables determined from the FUG method produce inaccuracies and uncertainties, it provides quick initial estimates sufficient for a good starting point. The proposed graphical method, in this thesis, does not require additional calculation such as estimating the number of minimum stages to calculate the

number of stages required. Once the contours of VLE are plotted and the operating reflux is known, the number of stages is determined graphically in one calculation.

2.4.4 Feed Stage Location

The Fenske (1932) (part of the FUG method) and Kirkbride (1944) equations are empirical correlations that determine the feed stage location for multicomponent systems. Both these equations require additional calculations in order to locate the feed stage. The FUG method requires the minimum reflux and number of stages to be calculated a priori in order to determine the theoretical number of stages and feed stage location. The Kirkbride (1944) equation requires numerous additional calculations to determine the number of stages in the rectifying and bottoms section, as well as product flowrates and product specifications, in order to calculate the feed stage location. The proposed graphical method, presented in this thesis, does not require any additional calculations (there is no need to calculate the minimum number of stages or product flowrates). Once the contours of VLE are plotted, a priori, the number of stages and the feed stage are determined simultaneously.

2.4.5 Reactive Distillation

The above stated short-cut methods have not been adapted to reactive distillation processes and hence applicability is limited to non-reactive columns. Short-cut methods are based on using approximate equations derived from making simplifying assumptions such as CRV and CMO (Taylor & Krishna, 2000). Chemical reactions influence the process in reactive distillation and hence these simplifying assumptions do not hold for reactive distillation processes. Short-cut methods are therefore not appropriate for reactive distillation design (Taylor & Krishna, 2000).

2.4.6 Closing Remarks

In conclusion, empirical short-cut methods are often used in preliminary design calculations as they are quick to apply and provide sufficient starting points (not without inaccuracies) for initialisation of rigorous simulator designs. Empirical short-cut methods rely on making several assumptions, such as CRV and CMO, and hence are not applicable to non-ideal and azeotropic systems (Reyes et al., 2000; Wasylkiewicz et al., 2000). The proposed graphical method, presented in this thesis, will be applicable to ideal and non-ideal systems. Short-cut methods require many additional calculations to determine design variables, unlike the proposed graphical method. Nevertheless the design variables obtained from the proposed graphical method will be compared with the design variables obtained from short-cut methods for ideal systems, in the design problems studied in this thesis.

2.5 Traditional Graphical Methods

According to Ryan (2001): 'If a picture is worth 1,000 words, then a good graph is worth 5,000 lines of computer code'. Graphical tool are powerful visual tools that not only provide insight into the behaviour of systems for conceptual design, but also serve as preliminary design tool to determine design parameters (Partin, 1993; Ho et al., 2010). Hence, graphical tools are effective in the conceptual and preliminary design stages and serve as the best assistant to rigorous simulations. The McCabe-Thiele (1925) and Ponchon-Savarit methods are classified as traditional or conventional graphical methods (Ho et al., 2010).

2.5.1 Ponchon-Savarit Method

The Ponchon-Savarit method for binary distillation accounts for enthalpy effects in stepping off stages due to varying molar overflow rates (Lee et al., 2000b). The VLE is depicted as tie lines on a two-dimension (2D) diagram that plots vapour and liquid enthalpy as a function of composition (Lee et al., 2000b). The number of

stages is determined by stepping off stages using the VLE tie lines as a function of the product compositions, state of the feed and condenser duty (Lee et al., 2000b). The Ponchon-Savarit method has been extended to binary reactive columns by Lee et al., (2000b).

Espinosa et al., (1993) and Sánchez-Daza et al., (2003) have extended the Ponchon-Savarit method to multicomponent reactive distillation. Espinosa et al., (1993) used the transformed composition variables of Barbosa & Doherty (1987) to reduce ternary systems to binary systems. The model incorporates the energy and mass balances under reaction equilibrium, hence the Ponchon-Savarit method is used to determine key design variables (Espinosa et al., 1993). The composition space is reduced due to the transformed variables resulting in some visual insights being lost. Sánchez-Daza et al., (2003) used the elements mass balance concept, first presented by Pérez-Cisneros et al., (1997), to depict a ternary system graphically. The mixture could contain three components, but must contain binary elements. In order that the equilibrium curve can be represented as an 'element' VLE curve, and not a component VLE curve, assuming constant total elemental mass overflow (CTEMO) the equilibrium curves can be plotted on an x-y diagram. Factoring in heat effects allows the plot of an equivalent diagram to perform the Ponchon-Savarit method to determine key design parameters (Sánchez-Daza et al., 2003). The methods by Sánchez-Daza et al., (2003) are limited if the system contains more than two elements and non-key components cannot be neglected. Lee et al., (2000b; 2000c) extended the original Ponchon-Savarit method to binary reactive distillation systems without transforming the composition variables. The Ponchon-Savarit method is based on the lever arm rule developed extensively by Hauan et al., (2000) and reactive difference points (Hauan et al., (1999, 2000); Lee et al., 2000a). From these two concepts, a set of new operating lines is derived from the energy and mass balances. The number of stages can be determined by stepping off stages on the Ponchon-Savarit diagram, using the difference points for a reactive cascade (Lee et al., 2000b).

The Ponchon-Savarit method for non-reactive and reactive processes are limited to binary distillation systems. The graphical methods based on the Ponchon-Savarit method for reactive distillation also require the conversion to transformed composition variables.

2.5.2 Binary McCabe-Thiele Method

The McCabe-Thiele method is arguably the most well-known, simple and effective graphical design method used to date for the design of binary distillation processes (Kong & Maravelias, 2019). The popularity and effectiveness of using McCabe-Thiele diagrams as a binary distillation design tool is the powerful pictorial understanding of the behaviour of a system, in addition to quantitatively determining design parameters (Neri et al., 1998). Every chemical engineer has been taught and has drawn a McCabe-Thiele diagram to design binary distillation processes (Mathias, 2009). McCabe & Thiele diagrams plot the VLE, and mass balance in the form of rectifying, bottoms and feed operating lines on a 2D x-y plot. The minimum number of stages is determined by stepping off stages between the VLE curve and the 45 degree line. At total reflux, the operating lines approach unity and coincide with the 45 degree line (McCabe & Thiele, 1925). At minimum reflux/reboil, a distillation column exhibits a pinch point (unless tangent pinch controls minimum reflux/reboil). On a McCabe-Thiele diagram for binary distillation, pinch points can be visually identified on a 2D plane. At a pinch point, the compositions of the vapour and liquid remain constant. Hence, approaching a pinch point requires an infinite number of stages (Stichlmair et al., 1993). In binary distillation, a double pinch occurs above and below the feed stage (only if no tangent pinch exists) (Stichlmair et al., 1993). This can be seen visually as the rectifying and bottoms operating lines intersect each other and the equilibrium curve on the feed line of the light key (LK) component for binary systems. The number of stages required at finite reflux is determined by stepping off stages between the VLE and the applicable operating line. The feed location is at the feed operating line of the light key component. The original McCabe-Thiele method is limited to binary systems.

2.5.3 Extension of Binary McCabe-Thiele Method for Reactive Distillation

Reactive-hybrid distillation columns incorporate both reactive and non-reactive stages in a column in order to obtain the desired product which otherwise cannot be obtained from a fully reactive column (Dragomir & Jobson 2005). Lee et al., (2000c) and Sundmacher & Qi (2003) presented the McCabe-Thiele method for ideal reactive binary systems. The Sundmacher & Qi (2003) method incorporates the Damköhler number to analyse the conceptual design of different configurations namely: fully reactive columns, hybrid columns and a non-reactive column on top of a reactive reboiler. The method is confined to isomerization reaction in which there is no net change in the number of moles as well as not being extended to non-ideal and multicomponent mixtures. Lee et al., (2000c) developed methods of using the McCabe-Thiele diagram to design binary reactive-hybrid distillation processes with particular interest in reaction on the feed stage. Lee et al., (2000c; 2000d) derived a modified q-line (feed line) for a decomposition reaction on the feed stage which requires accounting for the thermal conditions of the feed, if the heat of reactions and heat of vaporization are not comparable. For feed stage reactions, the concept of a pseudo-feed is introduced (Lee et al., 2000c). For reaction in the stripping or rectifying section only, a set of new reactive operating lines is derived by adding the normalized reactant/product coefficient to the non-reactive McCabe-Thiele operating lines (Lee et al., 2000c). This allows the diagram to be constructed in a finite composition space (Lee et al., 2000d). The method of determining the number of stages remains the same for binary non-reactive processes with stepping off stages between the VLE and new reactive operating lines. The Lee et al., (2000c) and Scundmacher & Qi (2003) methods are limited to binary systems and isomerization/decomposition reactions.

2.5.4 Traditional Graphical Methods for Non-Reactive Multicomponent Systems

Several adaptations of the McCabe-Thiele method for both reactive and non-reactive distillation processes have been made to multicomponent systems. Cope & Lewis (1932), Brown et al., (1932), Jenny (1939), Hengstebeck (1946) and Marek (1954) presented graphical methods for multicomponent mixtures. The first and integral step of a graphical method is the accurate depiction of the VLE from which the behaviour of the system can be analysed. The VLE of a component in a multicomponent mixture is also influenced by the other components present in the mixture and cannot be approximated by a single VLE curve (Cope & Lewis, 1932; Marek, 1954). Hence, an appropriate method of plotting VLE needs to account for the influence of the other components in the system. The VLE is required to be plotted once a priori, after which various design simulations can be investigated and optimized. A comparison of the methods presented by the above-listed authors to represent the VLE needs to be established. The most well-known adaptation of the McCabe-Thiele diagram to multicomponent distillation is the Hengstebeck (1946) method. The Hengstebeck method assumes no intermediate components between the key components, hence treating the systems as pseudo-binary mixture of the key components (or 'effective' key components) (Hengstebeck, 1946). The result is the graphical plot of the light key component on an x-y axis with a single VLE curve that represents the pseudo-binary system. Hence, the transformed pseudo-binary plot resembles that of binary processes. If intermediate components between the key components cannot be neglected, the equivalent pseudo-binary VLE curve will be inadequate.

The Cope & Lewis (1932) method plots the equilibrium curves as a straight line at different temperatures using Raoult's law for all components. The representation of the VLE is limited to systems that obey Raoult's law and cannot be applied to non-ideal systems. Marek (1954) plots the VLE for the light key, at constant liquid compositions of the heavy key whilst the heavy key is plotted at constant liquid composition of the light key. The interaction of the intermediate key with the heavy

and light key is neglected. The Brown et al., (1932) method requires the calculation of limiting values at minimum and total reflux in order to determine the VLE compositions of the three components. The method proposed by Jenny (1939) plots the equilibrium curves for one component in the rectifying section (heavy key) and one component in the stripping section (light key) hence prior knowledge of the key components is essential. The methods of representing VLE presented by Jenny (1939), Cope & Lewis (1932), and Brown et al., (1932) do not account for the influence of the other components in the system on each other. The methods proposed by Jenny (1939), Cope & Lewis (1932), Marek (1954) and Brown et al., (1932) have also not been applied to other equilibrium relationships other than the ideal equilibrium model presented in their respective work. The proposed graphical method solves the above-mentioned issues by the novel representation of the equilibrium relationship between x and y, as a series of contours of VLE for each component over the composition space on individual x-y 2D plots. Additionally, the method is applicable to any thermodynamic model and hence applicable to non-ideal systems.

The Hengstebeck (1961) method to calculate minimum reflux and stages, feed stage location and theoretical number of stages, follows the same method for the binary McCabe-Thiele method since the system is reduced to a single plot. Marek (1954) does not present a method to determine minimum reflux and stages. The number of stages is determined by stepping off stages between the operating lines and the appropriate VLE curve represented by the composition of heavy key for the light key on an x-y diagram. According to Marek (1954), the feed stage is located such that the fewest number of stages is required. Cope & Lewis (1932) did not demonstrate a method to determine minimum reflux and stages. The Cope & Lewis (1932) method requires the determination of the temperature profile in the column in order to determine the distribution of components in the product streams. The temperature on each stage is determined by graphical trial-and-error from the equilibrium curves (Cope & Lewis 1932). The Brown et al., (1932) method determine the minimum reflux and stages in accordance with the binary McCabe-Thiele method. The temperature on each stage has to be calculated in order to determine the equilibrium composition on each stage when stepping off stages at

total reflux. The equilibrium points obtained from the stepping off stages at total reflux determine the equilibrium curve used to step off stages at finite reflux (Brown et al., 1932). Brown et al., (1932) used the graphical plot of one component – either light or heavy key component, depending on the type of separation – to determine the number of stages. Brown et al., (1932) reduced the multicomponent system to a pseudo-binary system of the light and heavy key components. Hence, the McCabe-Thiele method of stepping off stages to determine the number of stages required can be used. The method uses absorption and stripping factors to determine the compositions (distributions) of the other components in the mixture (Brown et al., 1932). Jenny (1939) used a trial-and-error method of calculating the minimum reflux. The reflux is increased whilst performing tray-by-tray calculations until a point where the reflux corresponds to a point where the compositions remain constant (pinch point is reached). This method requires many calculations as it is trial-and-error in nature. Jenny (1939) proposed determining the temperature at which the key components go through a maximum concentration, hence determining the distillate and bottoms product temperatures to set the extremities for both column sections. Stage by stage calculation are carried out to determine the temperature and compositions from the equilibrium relationship (Jenny, 1939). The methods by Jenny (1939), Cope & Lewis (1932) and Brown et al., (1932) require additional, tedious calculations in order to determine the number of stages and compositions of products, failing to capture the simplicity of the binary McCabe-Thiele method which determines the number of stages and compositions with minimal additional calculations.

The graphical techniques developed by Cope & Lewis (1932), Brown et al., (1932), Jenny (1939), Marek (1954) and Hengstebeck (1946) have started with the fundamentals of the binary McCabe-Thiele method, but have lost vital information inherent in their simplifying assumptions. The proposed graphical method in this thesis is not limited by simplifying assumptions, and retains the simplicity and inherent elements of the binary McCabe-Thiele method as well as visually depicting the behaviour of all the components in the system. The determination of minimum stages, number of theoretical stages and feed stage location requires the

representation of the contours of VLE once, after which all the design parameters can be determined from a single plot, with minimal additional calculations, using the proposed graphical method. The proposed graphical method, presented in this thesis, for minimum reflux does not require trial-and-error calculations and uses simple graphical calculations to determine minimum reflux.

2.5.5 Traditional Graphical Methods for Reactive Multicomponent Systems

Jantharasuk et al., (2011), Sánchez-Daza et al., (2003), Flores-Estrella et al., (2016) and Marek (1954) have presented graphical methods for reactive multicomponent systems using the McCabe-Thiele method. The Jantharasuk et al., (2011) method is based on the assumption made by Hengstebeck (1946) of reducing multicomponent systems to a pseudo-binary system such that components in the system are represented as elements. With the addition of a reactive driving force diagram (Gani & Bek-Pederson, 2000) into the 2D plot conventional design parameters similar to the McCabe-Thiele method are determined (Jantharasuk et al., 2011). The method presented by Sánchez-Daza et al., (2003) for the reactive Ponchon-Savarit method is applicable to the McCabe-Thiele method without the considerations of heat effects. The equivalent x-y plot of the 'element' VLE curve (without non-key consideration) is used to perform the McCabe-Thiele method (Sánchez-Daza et al., 2003). Both methods can only be applied if the intermediate components can be neglected. Flores-Estrella et al., (2016) plotted the VLE represented by the transformed variables (Ung & Doherty, 1995) and the operating lines for the reactive McCabe-Thiele method such that the McCabe-Thiele diagram is plotted for one component (Flores-Estrella et al., 2016). The method can determine all the conventional preliminary design parameters as the non-reactive McCabe-Thiele method but since the VLE is approximated by a linear correlation it cannot correctly predict pinch points and reactive azeotropes (Flores-Estrella et al., 2016). Marek (1954) plotted the VLE in untransformed variables with the reactive operating lines defined for chemical reactions on an x-y plot for the heavy

and light key. The method developed by Marek (1954) is a combined numerical-graphical method in order to calculate the number of stages. The method is limited to ideal systems and fully reactive columns (Marek, 1954).

Although several graphical methods based on the McCabe-Thiele method have been developed for reactive distillation systems, these methods are limited in at least one aspect. The Jantharasuk et al., (2011), Flores-Estrella et al., (2016) and Sánchez-Daza et al., (2003) methods rely on transformed variables, fully reactive columns and reducing the system to pseudo-binary pairs. The Marek (1954) method is restricted to ideal systems, fully reactive columns and requires numerical calculation to aid the graphical method. Hence, a comprehensive purely graphical tool is lacking that is intuitive to the McCabe-Thiele method.

The proposed graphical method, presented in this thesis, will be applicable to ideal and non-ideal systems, as well as hybrid columns, and will not require transformed composition variables or reduction to a pseudo-binary system.

2.5.6 Closing Remarks

The McCabe-Thiele method is a powerful visual and preliminary design tool for binary distillation processes. Many graphical techniques have been proposed for the design of multicomponent distillation systems. These methods have started with the fundamentals of the binary McCabe-Thiele method but have lost vital information inherent in their simplifying assumptions. Hence, the graphical representation of these methods has lost the powerful impact and simplicity of the binary McCabe-Thiele method. The proposed graphical method, in this thesis, for reactive and non-reactive processes, through the depiction of the contours of VLE, retains the simplicity and inherent visual elements of the binary McCabe-Thiele method.

2.6 RCM Based Graphical Methods

The most developed and researched graphical methods, apart from the traditional graphical methods, are based on the concept of residue curve maps (RCMs). The literature on RCMs, and the applications thereof to conceptual and preliminary design tools, is extensive. The task of reviewing all the literature pertaining to RCM graphical methods is formidable. The most important RCM graphical tools for conceptual, total reflux, minimum reflux, finite reflux and reactive distillation design will be discussed in order to provide the fundamental insights to the topics covered in this thesis.

Shreinemakers (1901) first defined and applied RCMs. A multicomponent liquid mixture with a given initial composition is allowed to boil until the boiling point, such that the vapour produced is rich in the light key component and is in equilibrium with the liquid (Pham & Doherty, 1990). The vapour is removed as it is produced, such that the liquid composition will move from the initial composition towards a point close to the pure heavy key component (Doherty & Malone, 2001). The trajectory of the change in liquid composition from the initial concentration is termed as a residue curve (Doherty & Malone, 2001). An RCM is composed of a collection of residue curves obtained from a simple experimental setup depicted on a mass balance triangle (MBT) (Fien & Liu, 1994). Residue curve maps (RCMs) are used as conceptual and preliminary design graphical tools that can theoretically be applied to any number of components, but can only be visually depicted for up to four components (Fien & Liu, 1994).

RCMs are recommended as a conceptual design tool for engineers to quickly determine the behaviour and feasibility of different distillation processes (Doherty & Caldarola, 1985). RCMs provide visual insights of azeotropes (Doherty & Perkin, 1978; van Dongen & Doherty, 1985; Wahnschafft et al., 1992; Levy et al., 1985a), feasible splits, and selection of entrainers (Wahnschafft & Westerberg, 1993) and analyse possible column operability problems (Wasylkiewicz et al., 2000; Doherty & Caldarola, 1985). RCMs also depict distillation regions as a series

of residue curves that connect an unstable node and a stable node (Rooks et al., 1998). In addition, RCMs display the shape of the separation space, azeotropic distillation boundaries and distillation regions (Wasylkiewicz et al., 2000).

Distillation lines are classified as discrete points (not represented by a continuous line) that represent the composition of the liquid on each stage of a staged column at total reflux (Castillo & Towler, 1998; Thong et al., 2000). A collection of distillation lines represented on a MBT is defined as a distillation curve map (DCM). Whereas residue curves are defined as liquid composition profiles in a packed column at total reflux (Thong et al., 2000), distillation lines are less popular than residue curves but are equally as useful for synthesis and design of distillation columns (Castillo & Towler, 1998). DCMs have the same graphical limitations of RCMs and can only plot systems with a maximum of four components (Thong et al., 2000). RCMs and DCMs are quantitatively identical and predict the same properties at a singular point (predict the same behaviour of systems) (Thong et al., 2000; Castillo & Towler, 1998). Plotting the liquid compositions on each stage obtained – using the proposed graphical method in this thesis – for several separations will produce a series of distillation lines in the composition space.

RCMs and DCMs are applicable to both ideal and non-ideal systems and can incorporate the appropriate thermodynamic model. The proposed graphical method can also predict the behaviour of non-ideal systems on a 2D plane in accordance with the behaviour predicted by RCMs (a well-established visual tool). RCMs can be adapted from simple processes to azeotropic, reactive and extractive distillation (Fien & Liu, 1994). Many graphical methods for total reflux, minimum reflux, total reflux and reactive distillation use RCMs as the visual depiction of the VLE required for the application of the methods.

2.6.1 Total Reflux

Castillo et al., (1998) proposed methods of calculating the minimum number of stages at total reflux using DCMs. A stage composition line is defined as the locus

of liquid compositions on a given stage at different reflux or boil up ratio (Thong et al., 2000). The liquid stage composition lines are plotted for the rectifying and stripping section at varying reflux and boil up ratios respectively (Thong et al., 2000). If the stage composition line of the rectifying and stripping sections intersect, the separation is feasible (Thong et al., 2000). Additionally, the liquid composition lines must also pass through the product compositions. The minimum number of stages required is determined by counting the lines up to the point of intersection (Thong et al., 2000). According to Thong & Jobson (2001), a reliable design method to determine the theoretical minimum number of stages for non-ideal systems is limited. The proposed graphical method, in this thesis, presents a simple graphical technique which can be likened to binary McCabe-Thiele diagrams for calculating the minimum number of stages for ideal and non-ideal systems.

2.6.2 Minimum reflux

The boundary value method (BVM) is one of the most established graphical methods for minimum reflux calculations. The BVM is a geometric based graphical method presented by Levy et al. (1985a, 1985b). Under the assumption of CMO, the rectifying and bottoms profiles from stipulated product specifications are depicted on a MBT for ternary systems. Levy et al. (1985a, 1985b) express that minimum reflux can be visually identified when the rectifying and bottoms profiles intersect, but do not cross over. The reflux ratio is determined by trial-and-error until the minimum reflux is reached, such that the rectifying and bottoms profiles just intersect (Worms et al., 2017). The BVM has been applied to ideal, non-ideal and homogeneous systems by Levy et al. (1985a, 1985b) and extended further to complex columns (Nawaz & Jobson, 2011) and reactive distillation (Barbosa & Doherty, 1988).

The Shortest Stripping Line Method (SSLM) proposed by Lucia & Taylor (2006), plots the bottoms profile first, from the bottoms product, and then the rectifying profile is plotted from the last tray of the bottoms profile to the distillate product. The minimum reflux is shown to correlate to the column with the shortest geometric

bottoms profile for a feasible separation (Lucia & Taylor, 2006). The SSLM requires several profiles to be plotted by nonlinear programming to determine minimum reflux which is a computationally intensive process. Hence the method also requires trial-and-error calculations.

Stichlmair (2005) showed graphically on a DCM for sharp direct splits that when the heavy key (HK) component is reduced to almost zero in the distillate product (system reduces to binary of component light key (LK) and intermediate key (IK)), the internal liquid concentration profiles passes through transition points (saddle pinch). On a binary McCabe-Thiele diagram, the intersection of the operating line (for LK component) and the binary equilibrium curve of the LK and IK components, represent the transition point (saddle pinch). Likewise, for a sharp indirect split the LK is reduced to zero in the bottoms product (system reduces to binary of HK and IK). The intersection of the operating line (for HK component) and the binary equilibrium curve of component HK and IK represents the transition point. Stichlmair et al. (1993) determines the transition points using analytical equations and hence minimum reflux. A similar graphical method for determining minimum reflux using McCabe-Thiele diagrams and hence locating the transition point has not been provided for ternary systems. The proposed graphical method in this thesis of calculating the minimum reflux will be based on the observations of Stichlmair (2005) using the contours of VLE and McCabe-Thiele plots.

There is an exhaustive list of additional methods in literature that calculate minimum reflux, both numerical and graphical in nature. These methods do not use the concepts of RCMs and DCMs, and hence fall outside of the scope of this review. A full review of these methods is provided by Lucia & Taylor, (2008).

2.6.3 Finite Reflux

The BVM can also be used to determine the number of stages required at finite reflux, as presented by (Doherty & Malone, 2001). The feed, bottoms and distillate compositions are plotted on a MBT. The rectifying and stripping operating lines

(defined by Doherty & Malone, 2001), and an appropriate VLE model, is required. Performing stage by stage calculation from the liquid distillate or bottoms compositions (for sharp indirect and indirect respectively) results in the depiction of the liquid rectifying and stripping profiles on the MBT, at a specified finite reflux and reboil. The changeover from one operating line to the next is determined using the feed stage location method by Doherty & Malone (2001), explained in Section 2.6.4. Once the rectifying and stripping profiles are determined, the total number of stages is calculated by the sum of stages in the rectifying and stripping profiles. The proposed graphical method determines the composition on each stage and hence can be used to depict the rectifying and stripping profiles on a MBT.

2.6.4 Feed Stage Location

Methods of determining the feed stage location for multicomponent systems have been presented by Doherty & Malone (2001) and Vogelpohl (2015). The feed stage location using the Vogelpohl, (2015) method is determined by plotting the rectifying and stripping profiles for both the liquid and vapour compositions at finite reflux on a mass balance triangle (MBT). For a saturated liquid feed, a material balance line is drawn from the distillate product composition to the intersection of the vapour rectifying and stripping profiles. At this point the vapour compositions in the rectifying and stripping sections are equal ($y_R = y_S$) at the introduction of the feed (no vapour in the feed). If the same material balance line is extended to intersect the rectifying liquid profile then the rectifying liquid composition is in equilibrium with the feed (x_R). Another material balance is plotted from the bottoms product composition to the intersection of the vapour rectifying and stripping products. The intersection of the material balance line and the liquid bottoms profile yields the composition of the liquid (x_S) in equilibrium with the feed in the stripping section, and hence the feed stage location. The rectifying (x_R) and stripping (x_S) liquid compositions in equilibrium with the feed will lie on a straight line with the feed (x_F). The method by Vogelpohl (2015) does not take into consideration an actual tray but a point on a MBT. Hence, the feed stage will be taken as the stage

closest to that point. The proposed graphical method provides the designer with the stage number at which the feed should enter the column.

Doherty & Malone (2001) proposed determining a region on the stripping profile between the point, x^0, (yields the saddle pinch rectifying profile) and $\hat{x}^{1,s}$ the node pinch on the stripping profile (the point at which the stripping profile terminates). The method aims at identifying the region of feasible rectifying profiles. The fixed point method or the bisection method can be used to find x^0. The rectifying profile can start at any point between x^0 and $\hat{x}^{1,s}$ to achieve a feasible rectifying profile. If the rectifying profile begins before x^0, the rectifying profile will turn away from the distillate and the required distillate product cannot be attained.

Both methods, by Doherty & Malone (2001) and Vogelpohl (2015) require additional calculations on residue curve maps (RCMs) in order to determine the feed stage location. The proposed graphical method, presented in this thesis requires no additional calculations as the feed stage location is determined visually whilst determining the number of stages required.

2.6.5 Reactive Distillation

According to Dragomir (2004), graphical methods can be classified as conventional graphical methods or in the group of methods based on the Boundary Value Method (BVM) using residue curve maps (RCM). The reactive graphical methods for conventional methods were discussed in Section 2.5. Barbosa & Doherty, (1987) presented a set of transformed composition variables such that the mass balance equations can be represented without the reaction term analogous to non-reactive distillation systems (Barbosa & Doherty, 1988a). The transformed composition variables laid the foundation of many conceptual/preliminary graphical design methods for reactive distillation. Barbosa & Doherty (1988a) presented the mass balance equations, and hence differential equations, used to plot RCMs for reactive systems, in order to identify feasible designs by identifying distillation boundaries for ideal and non-ideal ternary and quaternary systems. Barbosa & Doherty (1988b)

and Barbosa & Doherty (1988c) used the foundations of transformed variables and derived a new set of differential equations to extend the BVM of Levy et al., (1985a) to reactive distillation processes for single-feed and double-feed columns respectively. Additionally, Barbosa & Doherty (1988b) and Barbosa & Doherty (1988c) presented a method of calculating minimum reflux for reactive distillation based on the Levy et al., (1985b) method for conventional distillation.

Ung & Doherty (1995) extended the method by Barbosa & Doherty (1988b) to multiple reactions. Doherty & Buzard, (1994) and Buzard & Doherty, (1994, 1995) applied the Barbosa & Doherty (1988b) method to kinetically controlled reactions by incorporating the fixed point method and the Damköhler number. Espinosa et al., (1995, 1996) extended the method developed by Barbosa & Doherty (1988b) to systems containing inert (non-reacting) components and show that inert components play a vital role in the design of reactive distillation processes. Dragomir & Jobson (2005) presented a method with reactive zones in different column sections (either stripping, core or rectifying) using stage composition lines and the BVM. All the above-mentioned methods use the transformed compositions and assume reaction on every stage in the column (except Dragomir & Jobson (2005)) and hence are not applicable to columns with non-reacting stages (Taylor & Krishna, 2000).

2.6.6 Closing remarks

RCMs and DCMs are well-established and widely used graphical methods used in the conceptual and preliminary design processes. Although RCMs and DCMs are powerful visual tools, the methods of determining preliminary design parameters are complex and require several calculations. Once the contours of VLE are represented on the x-y diagram for a ternary system, various design parameters can be determined from a single plot. The methods developed for the design of reactive systems using RCMs require the transformation of composition variables, thus losing the visual impact of non-reactive RCMs in the normal composition space.

The proposed graphical method, presented in this thesis, does not require the transformation of composition variables for reactive distillation processes, hence retaining the visual impact of binary McCabe-Thiele diagrams.

2.7 Concluding Remarks

It has been established that distillation is at the forefront of all separation technologies in industry and require large amounts of energy to achieve the desired separations. Thus, the need for optimally designed distillation columns is of utmost importance. The usefulness and impact of graphical techniques as conceptual and preliminary design tools has been highlighted. Graphical techniques complement and ensure the competent use of rigorous simulators. The McCabe-Thiele method is arguably the most well-known, simple and effective graphical design method to date for the design of binary distillation processes (Kong & Maravelias, 2019). Many authors have presented graphical methods for the design of multicomponent reactive and non-reactive systems, starting with the fundamentals of the binary McCabe-Thiele method. These graphical methods have lost vital visual information inherent in their simplifying assumptions. There is a need for a graphical method for reactive and non-reactive multicomponent systems that retains the simplicity and inherent visual elements of the binary McCabe-Thiele method. The proposed graphical techniques, developed in this thesis, provides a comprehensive yet simple graphical method retaining the basis of the binary McCabe-Thiele method. The need for a graphical preliminary design tool of such a nature is to ensure the efficient initialization of rigorous simulators for detailed design calculations.

REFERENCES

Almeida-Rivera, C.P., Swinkels, P.L.J., Grievink, J., **2004**. Designing reactive distillation processes: present and future. *Comp. Chem. Eng*. 28(10), pp. 1997-2020.

Bahadori, A., & Vuthaluru, H.B., **2010**. Simple equations to correlate theoretical stages and operating reflux in fractionators. *Energy*. 35(3), pp. 1439–1446.

Barbosa, D. & Doherty, M.F., **1987**. A new set of transformed variables for the representation of reactive-phase diagrams. *Proc. R. Soc. Lond*. 413(1845), pp. 459-464.

Barbosa, D. & Doherty, M.F., **1988a**. The simple distillation of homogeneous reactive mixtures. *Chem. Eng. Sci*. 43(3), pp. 541-550.

Barbosa, D. & Doherty, M.F., **1988b**. Design and minimum-reflux calculations for single-feed multicomponent reactive distillation columns. *Chem. Eng. Sci*. 43(7), pp. 1523-1537.

Barbosa, D. & Doherty, M.F. **1988c**. Design and minimum-reflux calculations for double-feed multicomponent reactive distillation columns. *Chem. Eng. Sci*. 43(9), pp. 2377-2389.

Barnes, F. J., Hanson, D. N., King, C. J. **1971**. Calculation of Minimum Reflux for Distillation Columns with Multiple Feeds. *Ind. Eng. Chem. Process. Des. Develop.* 11(1), pp. 136 -140.

Bausa, J., v. Watzdorf, R., Marquardt, W. **1998**. Shortcut Methods for Nonideal Multicomponent Distillation: 1. Simple Columns. *AIChE J*. 44(10), pp. 2181-2198.

Brown, G.G., & Martin, H. Z., **1939**. An empirical relationship between reflux ratio and the number of equilibrium plates in fractionating columns. *AIChE J*. 35, pp. 679-708.

Brown, G.G., Sauders, M., Nyland, H.V., **1932**. V. Fundamental Design of Fractionating Columns for Complex Mixtures. *Ind. Eng. Chem.* 24(5), pp. 522-527.

Brüggemann, S. & Marquardt, W., **2004**. Shortcut methods for nonideal multicomponent distillation: 3. Extractive distillation columns. *AIChE J*. 50(6), pp. 1129-1149.

Buzard, G. & Doherty, M.F., **1994**. Design of three-component kinetically controlled reactive distillation systems using fixed-point methods. *Chem. Eng. Sci*. 49(12), pp. 1947-1963.

Buzard, G. & Doherty, M.F., **1995**. New tools for the design of kinetically controlled reactive distillation columns for ternary mixtures. *Comp. Chem. Eng*. 19(4), p. 395-408.

Cao, R., Fu, G., Guo, H., Liu, Y., Tang, Y., Wu, Y., Zhang, X., **2014**. Exponential Function Shortcut Method for the Calculation of the Number of Theoretical Plates in a Distillation Column. *Ind. Eng. Chem. Res*. 53(38), pp. 14830-14840.

Castillo, F.J.L., Thong, D.Y.C., Towler, G.P., **1998**. Homogeneous Azeotropic Distillation. 1. Design Procedure for Single-Feed Columns at Nontotal Reflux. *Ind. Eng. Chem. Res.* 37(3), pp. 987-997.

Castillo, F.J.L. & Towler, G.P., **1998**. Influence of multicomponent mass transfer on homogeneous azeotropic distillation. *Chem. Eng. Sci.* 53(5), pp. 963-976.

Colburn, A.P. **1941**. The Calculation of Minimum Reflux Ratio in the Distillation of Multicomponent Mixtures. *Trans. Am. Inst. Chem. Engrs. 37*, pp. 805-825.

Cope, J.Q. & Lewis, W.K., **1932**. Studies in Distillation-Graphical Method of Computation for Rectifying Complex Hydrocarbon Mixtures. *Ind. Eng. Chem.* 24(5), pp. 498-501.

Doherty, M.F. & Buzard, G., **1994**. New tools for the design of kinetically controlled reactive distillation columns. *Comp. Chem. Eng.* 18(1), pp. S1-S13.

Doherty, M.F. & Caldarola, G.A., **1985**. Design and Synthesis of Homogeneous Azeotropic Distillation. 3. The Sequencing of Columns for Azeotropic and Extractive Distillation. *Ind. Eng. Chem. Fundam.* 24(4), pp. 474-485.

Doherty, M.F. & Malone, M.F., **2001.** Conceptual Design of Distillation Systems. *McGraw-Hill, Inc:* New York.

Doherty, M.F. & Perkin, J.D., **1979**. On the dynamics of distillation processes- III: The topological structure of ternary residue curves. *Chem. Eng. Sci*. 34(12), pp. 1401-1414.

Dragomir, R.M., **2004**. Synthesis and Design of Reactive Distillation Columns. PHD Thesis, UMIST, UK.

Dragomir, R.M & Jobson, M., **2005**. Conceptual design of single-feed hybrid reactive distillation columns. *Chem. Eng. Sci.* 60(16), pp. 4377-4395.

Erbar, J.H., & Maddox, R.N., **1961**. Latest score: reflux vs. Trays. *Petroleum Refiner*. 40 (5), pp. 183-188.

Espinosa, J., Scenna, N., Pérez, G., **1993**. Graphical procedure for reactive distillation systems. *Chem. Eng. Com.* 119(1), pp. 109-124.

Espinosa, J., Aguirre, P.A., Pérez, G.A, **1995**. Some aspects in the design of multicomponent reactive distillation columns including nonreactive species. *Chem. Eng. Sci.* 50(3), pp. 469-484.

Espinosa, J., Aguirre, P.A., Pérez, G., **1996**. Some Aspects in the Design of Multicomponent Reactive Distillation Columns with a Reacting Core: Mixtures Containing Inerts. *Ind. Eng. Chem. Res.* 35(12), pp. 4537-4549.

Fenske, M.R., **1932**. Fractionation of Straight-Run Pennsylvania Gasoline. *Ind. Eng. Chem*. 24(5), pp. 482–485.

Fien, G.J.A. & Liu Y.A., **1994**. Heuristic Synthesis and Shortcut Design of Separation Processes using Residue Curve Maps: A Review. *Ind. Eng. Chem. Res*. 33(11), pp. 2505–2522.

Flores-Estrella, R.A. & Iglesias-Silva, G.A., **2016**. Reactive McCabe-Thiele: Short-cut method including reactive vapor-liquid efficiency. *Rev. Mex. Ing. Quim.* 15(1), pp. 193-207.

Gani, R. & Bek-Pedersen, E., **2000**. Simple New Algorithm for Distillation Column Design. *AIChE J*. 46(6), pp. 1271-1274.

Gilliland, E.R. **1940**. Multicomponent rectification. Estimation of the Number of Theoretical Plates as a Function of the Reflux Ratio. *Ind. Eng. Chem.* 32(9), pp. 1220-1223.

Górak, A. & Sorensen, E., **2014**. Distillation: Fundamentals and Principles. *Elsevier: Academic Press*: London

Harmsen, G.J., **2007**. Reactive distillation: The front-runner of industrial process intensification: A full review of commercial applications, research, scale-up, design and operation. *Chem. Eng. Proc.* 46(9), pp. 774-780.

Hengstebeck, R.J., **1946**. A Simplified Method for Solving Multicomponent Distillation Problems. *Trans. AIChE.* 42, pp. 309-329.

Hengstebeck, R.J., **1961**. Distillation: Principles and Design Procedures. *Reinhold Publishing Corp:* New York.

Ho, T.J., Huang, C.T., Lee, L.S., Chen, C.T, **2010**. Extended Ponchon-Savarit Method for Graphically Analyzing and Designing Internally Heat-Integrated Distillation Columns. *Ind. Eng. Chem. Res*. 49(1), pp. 350-358.

Hauan, S., Westerberg, A.W., Lien, K.M., **1999**. Phenomena-based analysis of fixed point in reactive separation systems. *Chem. Eng. Sci*. 55(6), pp. 1053-1075.

Hauan, S., Ciric, A.R., Westerberg, A.W., Lien, K.M., **2000**. Difference points in extractive and reactive cascades. I. Basic properties and analysis. *Chem. Eng. Sci*. 55(16), pp. 3145-3159.

Jantharasuk, A., Gani, R., Górak, A., & Assabumrungrat, S. **2011**. Methodology for design and analysis of reactive distillation involving multielement systems. Chem. Eng. Res. Des. 89(8), pp. 1295-1307.

Jenny, F.J., **1939**. Graphical solution of problems in multicomponent fractionation. *Trans. Am. Inst. Chem. Eng.* 35, pp. 635-677.

Kiss, A.A., Jobson, M., Goa, X., **2019**. Reactive Distillation: Stepping Up to the Next Level of Process Intensification. *Ind. Eng. Chem. Res.* 58(15), pp. 5909−5918.

Kister, H.Z., **1992**. Distillation Design. *McGraw-Hill, Inc: USA.*

Kirkbride, G.G. **1944**. Process Design Procedure for Multicomponent Fractionators. *Pet. Refin*, 23(9), pp. 23-87.

Koehler, J., Poellmann, P., Blass E., **1995**. A Review on Minimum Energy Calculations for Ideal and Nonideal Distillations. *Ind. Eng. Chem. Res*. 34(4), pp. 1003-1020.

Kong, L. & Maravelias, C.T., **2019**. From graphical to model-based distillation column design: A McCabe-Thiele-inspired mathematical programming approach. *AIChE J*. 65(11), p.e16731.

Lee, J.W., Hauan, S., Lien, K.M., Westerberg, A.W., **2000a**. Difference points in extractive and reactive cascades. II—Generating design alternatives by the lever rule for reactive systems. *Chem. Eng. Sci*. 55(16), pp. 3161-3174.

Lee, J.W., Hauan, S., Lien, K.M., Westerberg, A.W., **2000b**. A graphical method for designing reactive distillation columns. I. The Ponchon-Savarit method. P*roceedings of the Royal Society of London*. 456(2000), pp. 1953-1964.

Lee, J.W., Hauan, S., Lien, K.M., Westerberg, A.W., **2000c**. A graphical method for designing reactive distillation columns. II. The McCabe-Thiele method. P*roceedings of the Royal Society of London*. 456(2000), pp. 1965-1978.

Lee, J.W., Hauan, S., Westerberg, A.W., **2000d**. Graphical Methods for Reaction Distribution in a Reactive Distillation Column. *AIChE J*. 46(6), pp. 1218-1233.

Levy, S.G., Van Dongen, D.B., Doherty, M.F., **1985a**. Design and Synthesis of Homogeneous Azeotropic Distillations. 1. Problem Formulation for a Single Column. *Ind. Eng. Chem. Fundam*. 24(4), pp. 454–463.

Levy, S.G., Van Dongen, D.B., Doherty, M.F., **1985b**. Design and Synthesis of Homogeneous Azeotropic Distillations. 2. Minimum Reflux calculations for Nonideal and Azeotropic Columns. *Ind. Eng. Chem. Fundam*. 24(4), pp. 463–474.

Lucia, A., Amale, A., Taylor, R., **2006**. Energy Efficient Hybrid Separation Processes. *Ind. End. Chem*. 45(6), pp. 8319-8328.

Lucia, A. & Taylor, R., **2008**. Distillation pinch point and more. *Comp. Chem. Eng*. 32(6), pp. 1342-1364.

Marek, J., **1954**. Rectification with a chemical reaction. I. Calculation of the number of theoretical plates for continuous plate columns. *Collection of Czechoslovak Chemical Communications*. 19(6), pp. 1055-1073.

Mathias, P.M., **2009**. Visualizing the McCabe-Thiele Diagram. *Chem. Eng. Prog*. 105(12), pp. 36-44.

McCabe, W.L. & Thiele, E.W., **1925**. Graphical Design of Fractionating Columns. *Ind. Eng. Chem.* 17(6), pp. 605-611.

Nawaz, M. & Jobson, M., **2011**. A boundary value design method for complex demethaniser distillation columns. *Chem. Eng. Res. Des*. 89(8), pp. 1333-1347.

Neri, B., Mazzotti, M., Storti, G., Morbidelli, M., **1998**. Multicomponent Distillation Design through Equilibrium Theory. *Ind. Eng. Chem. Res*. 37(6), pp. 2250-2270.

Orjuela A., Santaella M.A., Molano P.A., **2016**. Process Intensification by Reactive Distillation. In: Segovia-Hernández J., Bonilla-Petriciolet A. (eds) Process Intensification in Chemical Engineering. *Springer International Publishing*, Cham. pp. 131-181.

Partin, L.R., **1993**. Use Graphical Techniques to Improve Process Analysis. *Chem. Eng. Prog*. 89(1), pp. 43-48.

Pérez-Cisneros, E.S. **1997**. Modelling, Design and Analysis of Reactive Separation Process. Technical Univ. of Denmark.

Perry, R.H. & Green, D.W., **1999**. Perry's Chemical Engineers' Handbook, Seventh Edition. *McGraw-Hill, Inc: New York.*

Pham, H.N. & Doherty, M.F., **1990**. Design and synthesis of heterogenous azeotropic distillation-II: Residue curve maps. *Chem. Eng, Sci.* 45(7), pp. 1837-1843.

Reyes, J.A., Gomez, A., Marcilla, A., **2000**. Graphical Concepts to Orient the Minimum Reflux Ratio Calculation on Ternary Mixtures in Distillation. *Ind. Eng. Chem. Res*. 39(10), pp. 3912-3919.

Rooks, R.E., Julka, V., Doherty, M.F., Malone, M.F., **1998**. Structure of distillation regions for multicomponent azeotropic mixtures. *AIChE J*. 44(6), pp. 1382-1391.

Ryan, J.M., **2001**. Replotting the McCabe-Thiele Diagram. *Chem. Eng.* 108(5), pp. 109-113.

Sánchez-Daza, O., Pérez-Cisneros, E.S., Bek-Pedersen, E., Gani, R., **2003**. Graphical and stage-to-stage methods for reactive distillation column design. *AIChE J*. 49(11), pp. 2822-2841.

Schreinemakers, F.A.H. **1901**. Dampfdrücke Ternärer Gemische. *Z. Phys. Chem.* 36, pp. 257–289.

Smoker, E., **1938**. Analytical Determination of Plates in Fractionating columns. *Trans. Am. Inst. Chem. Eng*. 34, pp.165.

Soliman, M.A., **2009**. A Shortcut Method for Binary Distillation Column Design. *J. King Saud Univ*. 21(1), pp. 1-4.

Stichlmair, J., Offers, H., Potthoff, R.W., **1993**. Minimum Reflux and Minimum Reboil in Ternary Distillation. *Ind. Eng. Chem. Res*. 32(1), pp. 2438-2445.

Stichlmair, J., **2005**. Distillation and Rectification. In Ullmann's Encyclopaedia of Industrial chemistry. *Wiley-VCH Verlag GmbH & Co: Weinheim.*

Stichlmair, J.G., Klein, H., Rehfeldt, S., **2021**. Distillation: Principles and Practice. *John Wiley & Sons*: New Jersey.

Sundmacher, K. & Qi, Z., **2003**. Conceptual design aspects of reactive distillation processes for ideal binary mixtures. *Chem. Eng. Proc*. 42(3), pp. 191-200.

Taylor, R. & Krishna, R., **2000**. Modelling reactive distillation. *Chem. Eng. Sci*. 55(22), pp. 5183-5229.

Thong, D.Y.C., Castillo, F.J.L., Towler, G.P., **2000**. Distillation design and retrofit using stage-composition lines. *Chem. Eng. Sci*. 55(3), pp. 625–640.

Thong, D.Y.C. & Jobson, M., **2001**. Multicomponent homogeneous azeotropic distillation. 2. Column design. *Chem. Eng. Sci*. 56(14), pp. 4393-4416.

Underwood, A.J.V. **1948**. Fractional Distillation of Multicomponent Mixtures. *Chem. Eng. Prog*. 44(8), pp. 603-614.

Ung, D. & Doherty, M.F., **1995**. Synthesis of Reactive Distillation Systems with Multiple Equilibrium Chemical Reactions. *Ind. Eng. Chem. Res*. 34(8), pp. 2555-2565.

Van Dongen, D & Doherty, M., **1985**. Design and Synthesis of Homogeneous Azeotropic Distillations. 1. Problem Formulation for a Single Column. *Ind. Eng. Chem. Fundam*. 24(4), pp. 454–463.

Van Winkle, M., **1967**. Distillation. *McGraw-Hill, Inc: USA*.

Vogelpohl, A., **2015**. Distillation. *Walter De Gruyter*: Berlin/Munich/Boston.

von Watzdorf, R., Bausa, J., Marquardt, W., **1999**. Shortcut Methods for Nonideal Multicomponent Distillation: 2. Complex Columns. *AIChE J*. 45(8), pp. 1615-1628.

Wahnschafft, O.M., Koehler, J.M., Blass, E., Westerberg, A.W., **1992**. The Product Composition Regions of Single-Deed Azeotropic Distillation Columns. *Ind. Eng. Chem. Res.* 31(10), pp. 2345-2362.

Wahnschafft, O.M. & Westerberg, A.W., **1993**. The Product Composition Regions of Azeotropic Distillation Columns. 2. Separation in Two-Feed Columns and Entrainer Selection. *Ind. Eng. Chem. Res*. 32(6), pp. 1108-1120.

Wasylkiewicz, S.K., Kobylka, L.C., Castillo, F.J.L., **2000**. Optimal design of complex azeotropic distillation columns. *Chem. Eng. J*. 79(3), pp. 219-227.

Widago, S. & Seider, W.D., **1996**. Azeotropic Distillation. *AIChE J*. 42(1), pp. 96-130.

Winn, F.W. **1958**. New relative volatility method for distillation calculations. *Petrol. Refin*. 37(5), pp. 216–218.

Yaws, C.L., Li, K.Y., Fang, C.S., **1981**. How to Find the Minimum Reflux for Binary Systems in Multiple-Feed Columns. *Chem. Eng*. 88(10), pp. 153-156.

Chapter 3

Novel Representation of VLE and Analysis of System Behaviour

The work in this chapter has been published in**:** Seedat, N., Kauchali, S., Patel, B., **2020**. Novel representation of vapour-liquid equilibrium curves for multicomponent systems: design of total reflux distillation columns. *Chem. Eng. Res. Des*. 155, p. 22-39.
The work is a reproduction based on the journal publication, although some changes have been made in the addition of Section 3.2.2.2 for the purpose of adhering to the standards of this thesis, as well as simplifying the work for clarity and easy understanding. The reproduction was done with permission. (**Copyright © 2021 Elsevier)**

Abstract

McCabe-Thiele diagrams were developed as a graphical tool for designing binary distillation columns. In this chapter, the method to construct the novel contours of vapour-liquid equilibrium (VLE) for the generation of McCabe-Thiele diagrams for ternary systems is presented. A variety of examples is used to depict the novel representation of the (VLE) in two-dimensional space (2D) as contours of VLE for the generation of the x-y diagram for ideal and non-ideal mixtures. Through these examples, it is shown that the depiction of the contours of VLE is a powerful visual tool to identify the type of separation (difficult or simple separation), binary and ternary azeotropes and tangent pinch points. Additionally, the method can be applied to any thermodynamic model for ideal and non-ideal systems. Hence, the proposed graphical method retains the authenticity, simplicity and versatility of the binary McCabe-Thiele method.

3.1 Introduction

Separation processes are an integral and essential part of all chemical processes. Multicomponent azeotropic and non-ideal close boiling mixtures are often encountered in industrial practice (Wahnschafft et al, 1992). It is imperative to design efficient and feasible distillation processes for the separation of azeotropic and close boiling distillation mixtures to meet product specifications. (Skibrowski et al., 2018; Kister, 1995). Distillation processes are amongst the most frequently used methods for the separation of non-ideal and azeotropic mixtures (Wahnschafft et al, 1992).

Current practice for distillation design is for designers to synthesise process flowsheets, set the operating parameters and input the information into a rigorous equilibrium tray simulation (Partin, 1993). Rigorous simulators, such as the RadFrac model using Aspen Plus^{TM} software, are generally used for distillation design (Skibrowski et al., 2018). The simulator then performs a rating calculation at the operating parameters for the process (Partin, 1993). It can be challenging to determine the required operating parameters to initialize the process specifications in a simulator and the designer is not guaranteed that the design is feasible (Partin. 1993). Preliminary design tools, such as shortcut and graphical methods, are used to determine design variables such as minimum reflux, minimum number of stages at total reflux and feed stage location (Gani & Bek-Pedersen, 2000). Once determined using a preliminary design tool, the above-listed operating parameters are used to initialize a rigorous simulator to perform detailed design and optimization simulations (Fidkowski et al., 1991). Essentially, the preliminary design procedure should serve as a precursor to the rigorous simulation process. This ensures the competent use of the simulation tools. Hence, both procedures play an important role in the overall distillation design procedure (Mathias, 2009).

Graphical methods are powerful visual tools that produce ‘pictures’ that enable the capturing of the fundamentals of distillation and provide insight into the separation process (Mathias, 2009). The designer can visually identify problems and the effects of making changes easily from a graphical representation, rather than from

data generated from a simulator. There are many advantages of using graphical methods as a preliminary design tool. Graphical methods are comprehensive preliminary design tools providing engineers, not only with results, but also insights and understanding, of a particular system. With this understanding, designers have the ability to identify and resolve possible operational issues as well as develop quality designs (Mathias, 2009). Graphical methods provide the designer with a visual understanding of the behaviour of non-ideal, azeotropic and close boiling mixtures as well as the capabilities over the entire composition for the components (Partin, 1993). In addition, through the visual depiction of the behaviour of the vapour-liquid equilibrium (VLE), design problems in the form of composition pinches (inflection points) and steep peaks (compositions change drastically from one stage to another), and in composition profiles of one or more components in a multicomponent mixture can be detected and overcome in the preliminary design phase (Mathias, 2009). In addition, through understanding the interrelationships of the process variables for a specific process, insights can be gained by engineers to assess the qualitative impact of making a change to the design of a separation process (Lee at al., 2000a).

McCabe and Thiele developed the McCabe-Thiele diagram, a graphical preliminary design tool, to gain behavioural insights as well as the design of binary distillation columns, and which is based on Lewis's method (McCabe & Thiele, 1925; Lee et al., 2000b). For decades, when computers were not at the forefront for designing distillation processes, the McCabe-Thiele diagram provided engineers with a quick tool which enabled effective design and operational analysis of binary distillation processes (Lee et al., 2000b). The McCabe-Thiele method has been taught to generations of chemical engineers to design and troubleshoot binary distillation processes (Mathias, 2009). Kister (1995) highlights the importance of using McCabe-Thiele diagrams as a troubleshooting tool to determine if a simulation would achieve design specifications as well as design problems. Although, the availability of rigorous computer software for distillation design has become so widespread, textbooks and journal papers have stressed the importance of using McCabe-Thiele diagrams as an essential preliminary design tool (Mathias, 2009). According to Kister (1995), both rigorous simulators and graphical methods must

coexist to benefit from the accuracy and flexibility of rigorous simulators and the understanding gained by visualization obtained from the McCabe-Thiele method. Although the McCabe-Thiele method is encouraged to be incorporated in the distillation design process, it has been limited mainly to binary processes which are rarely encountered in industry.

Several adaptations of McCabe-Thiele diagrams have been made for applicability to multicomponent systems. Cope & Lewis (1932), Brown et al., (1932) and Jenny (1939) presented graphical methods for complex hydrocarbon mixtures. Cope & Lewis (1932) applied Raoult's law to relate the vapour (y) and liquid (x) composition, whereas Brown et al., (1932) and Jenny (1939) used the equilibrium constant, K, to generate the equilibrium curves. The methods proposed by Jenny (1939), Cope & Lewis (1932) and Brown et al., (1932) have not been applied to other equilibrium relationships, other than the ideal equilibrium model presented in their respective work. The Cope & Lewis (1932) and Brown et al., (1932) methods plots the equilibrium curves for all components. The method proposed by Jenny (1939) plots the equilibrium curves for one component in the rectifying section (heavy key) and one component in the stripping section (light key), hence prior knowledge of the key components is essential. Plotting the VLE of all components graphically, as proposed by Cope & Lewis (1932), provides insights into the behaviour of all the components in the system, rather than two components as proposed by Jenny (1939). Gaining insight into the behaviour of all the components provides the designers with an idea, if one or more components will present composition pinches or steep peaks in composition, which would not be detected if that component is not plotted.

The Cope & Lewis (1932) method requires the determination of the temperature profile in the column in order to determine the distribution of components in the product streams. The temperature on each stage is determined by graphical trial-and-error from the equilibrium curves (Cope & Lewis 1932). The Brown et al., (1932) method uses absorption and stripping factors to determine the compositions of the other components in the mixture. Jenny (1939) proposed the determination of the temperature at which the key components go through a maximum

concentration, hence determining the distillate and bottoms product temperatures to set the extremities for both column sections. Stage by stage calculation are carried out to determine the temperature and compositions from the equilibrium relationship (Jenny, 1936). The methods proposed by Jenny (1939), Cope & Lewis (1932) and Brown et al., (1932) require additional, tedious calculations in order to determine the number of stages and compositions of products, failing to capture the simplicity of the binary McCabe-Thiele method of calculating the number of stages and compositions with minimal calculations (Cope & Lewis, 1932; Brown et al., 1932; Jenny, 1939).

Hengstebeck (1946) developed the most well-known adaptation of the McCabe-Thiele diagram to multicomponent distillation. The Hengstebeck method assumes no intermediate components between the key components, hence treating the systems as pseudo-binary mixtures of the key components (or 'effective' key components) (Hengstebeck, 1946). This resulted in the depiction of an equivalent McCabe-Thiele plot as the compositions plotted as the novel pseudo component from which the number of stages and feed location could be determined at specified reflux ratio (Hengstebeck, 1961). However, the accuracy of the method relies on the assumption of the pseudo-binary system (Hengstebeck, 1946). Errors will result if intermediate components between the key components cannot be neglected (Kister, 1992). In addition, the plots are presented as transformed mole fractions of the pseudo-binary systems, hence the designer cannot simply read off compositions from the plot as with the binary McCabe-Thiele method.

The graphical techniques developed by Cope & Lewis (1932), Brown et al., (1932), Jenny (1939) and Hengstebeck (1946) have started with the fundamentals of the binary McCabe-Thiele method but have lost vital information inherent in their simplifying assumptions. A graphical technique is required that would not be limited by simplifying assumptions, but would retain the simplicity and inherent elements of the binary McCabe-Thiele method, as well as visually depict the behaviour of all the components in the system. The proposed graphical technique solves the above-mentioned issues by the novel representation of the equilibrium relationship between x and y as a series of contours of VLE for each component

over the composition space on individual x-y 2D plots. By plotting the contours of VLE of each component, the designer can visually analyse the behaviour of the system. The data required to generate the unique contours of VLE are not restricted to a specific thermodynamic model and can be applied to any model appropriate for both ideal and non-ideal systems, without any simplifying assumptions. Once the novel contours of VLE are plotted, the fundamental McCabe-Thiele design method is retained. The proposed graphical method can be used by designers, as well as students, to analyse the behaviour of ideal and non-ideal mixtures. Design parameters (number of stages, feed stage location and minimum reflux) obtained from the binary McCabe-Thiele method can be determined from the generated multicomponent plot with minimal additional calculations. In addition, the liquid and vapour compositions are plotted for each component in untransformed coordinates, hence compositions can be read off directly from the McCabe-Thiele diagram. Hence, the proposed graphical technique retains the simplicity and flexibility of the binary McCabe-Thiele method as well as overcoming the limitations of the traditional methods proposed thus far. The proposed graphical method can also be used to visually analyse the results obtained from a rigorous simulation for non-ideal multicomponent systems (more effectively than Hengstebeck diagrams).

This chapter postulates a novel approach to calculating and depicting the equilibrium relationship between x and y as a series of contours of VLE. Ternary ideal and non-ideal systems will be considered from which the applicability will be generalised to higher dimension systems. In section 3.2 the basis for the generation of the contours of VLE will be explained. Section 3.3 will present the different VLE characteristics that can be identified visually for ternary ideal and non-ideal systems. It will be shown that important behavioural characteristics of simple and difficult separations, azeotropes and tangent pinch points can be identified visually in different systems. It will also be shown that the method of representing the contours of VLE can be applied to different thermodynamic models.

3.2 Novel Representation of Vapour-Liquid Equilibrium (VLE)

The starting point of the McCabe-Thiele method (1925) is the graphical representation of the VLE on an x-y diagram. Graphical representation of VLE on the McCabe-Thiele diagram is a powerful visual tool that allows a designer to identify and interpret the behaviour of distillation systems. For binary mixtures, the correct depiction of VLE on an x-y diagram allows designers to visually identify non-ideal behaviour in the form of binary azeotropes, tangent pinches and close boiling mixtures (McCabe &Thiele, 1925; Fidkowski et al., 1991). In accordance with the McCabe-Thiele method each tray in a distillation column is considered to be an equilibrium stage. The representation of the equilibrium curve will determine the equilibrium composition of vapour (y) and liquid (x) leaving the same tray (Jenny, 1939). For binary mixtures VLE is represented by the composition of a single component in the liquid and vapour phases (Cope & Lewis, 1932). Hence, the representation of the VLE is fairly simple as there is a direct relationship between x and y for a single component and this is represented as a single unique equilibrium curve (Mathias, 2009). Unlike binary systems, the VLE of a component in a multicomponent mixture is also influenced by the other components present in the mixture, and complexity arises as the equilibrium curve cannot be represented by a single curve (Cope & Lewis, 1932). An appropriate representation of the VLE for a component in a multicomponent mixture requires the influence of the other components present in the liquid and vapour phase to be accounted for in the depiction of a component's VLE. The method proposed for the representation of the VLE for ternary systems accounts for the interactions of the other two components in a system by defining a component's VLE as a series of ratios of the other components present in the system. The binary McCabe-Thiele method has generally been stipulated by stepping off stages from the distillate to the bottoms composition for a specified separation, although the stepping can be done from the bottoms to the distillate composition. The graphical method, proposed in this thesis, will show the method of stepping off stages in either direction. The method of generating the contours of VLE by stepping off stages in either direction is the same, with the only difference being in the definition of the ratios at which each VLE contour is plotted.

Consider a three-component system. At constant relative volatility (α) the vapour compositions for component *i* can be defined by Equation 3.1 (The full derivation can be found in Appendix A):

$$y_i = \frac{\alpha_{ik}\left(\frac{x_i}{1-x_i}\right)(CR_{jk}+1)}{1+\alpha_{ik}\left(\frac{x_i}{1-x_i}\right)(CR_{jk}+1)+\frac{\alpha_{ik}}{\alpha_{ij}}CR_{jk}} \tag{3.1}$$

Where:

$$CR_{jk} = \frac{x_j}{x_k} \tag{3.1a}$$

$$CR_{jk} = \frac{y_j}{y_k} \tag{3.1b}$$

It is noted that for a fixed ratio (CR_{jk}) the vapour fraction (y_i) is only dependent on the liquid mole fraction (x_i). Hence, the contours of VLE can be plotted at different ratios using Equation 3.1 required to apply the graphical method presented in this thesis.

Likewise, the vapour composition for component *j* and *k* can be determined from Equations 3.2 and 3.3 respectively:

$$y_j = \frac{\alpha_{jk}\left(\frac{x_j}{1-x_j}\right)(CR_{ik}+1)}{1+\alpha_{jk}\left(\frac{x_j}{1-x_j}\right)(CR_{ik}+1)+\frac{\alpha_{jk}}{\alpha_{ji}}CR_{ik}} \tag{3.2}$$

Where:

$$CR_{ik} = \frac{x_i}{x_k} \tag{3.2a}$$

$$CR_{ik} = \frac{y_i}{y_k} \tag{3.2b}$$

$$y_k = \frac{\alpha_{kj}\left(\frac{x_k}{1-x_k}\right)(CR_{ij}+1)}{1+\alpha_{kj}\left(\frac{x_k}{1-x_k}\right)(CR_{ij}+1)+\frac{\alpha_{kj}}{\alpha_{ki}}CR_{ij}} \tag{3.3}$$

Where:

$$CR_{ij} = \frac{x_i}{x_j} \tag{3.3a}$$

$$CR_{ij} = \frac{y_i}{y_j} \tag{3.3b}$$

Equations 3.1 – 3.3 present the equilibrium relationship between x and y for a ternary ideal system used to generate the contours of VLE. For stepping off stages from the bottoms composition, the ratios for component *i* are defined in terms of the liquid compositions of component *j* and *k* (Equation 3.1a, 3.2a, 3.3a). Whereas,

for stepping off stages from the distillate composition, the ratios for component *i* are defined in terms of the vapour compositions of component *j* and *k* (Equation 3.1b, 3.2b, 3.3b). The VLE contours plotted from Equation 3.1 and incorporating either equation 3.1a and 3.1b will be identical, and only the ratios that represent each contour will differ. It should be noted that Equations 3.1, 3.2 and 3.3 must be rearranged to solve for x_i as a function of y_i such that Equation 3.1b, 3.2b and 3.3b can be incorporated to plot the contours of VLE.

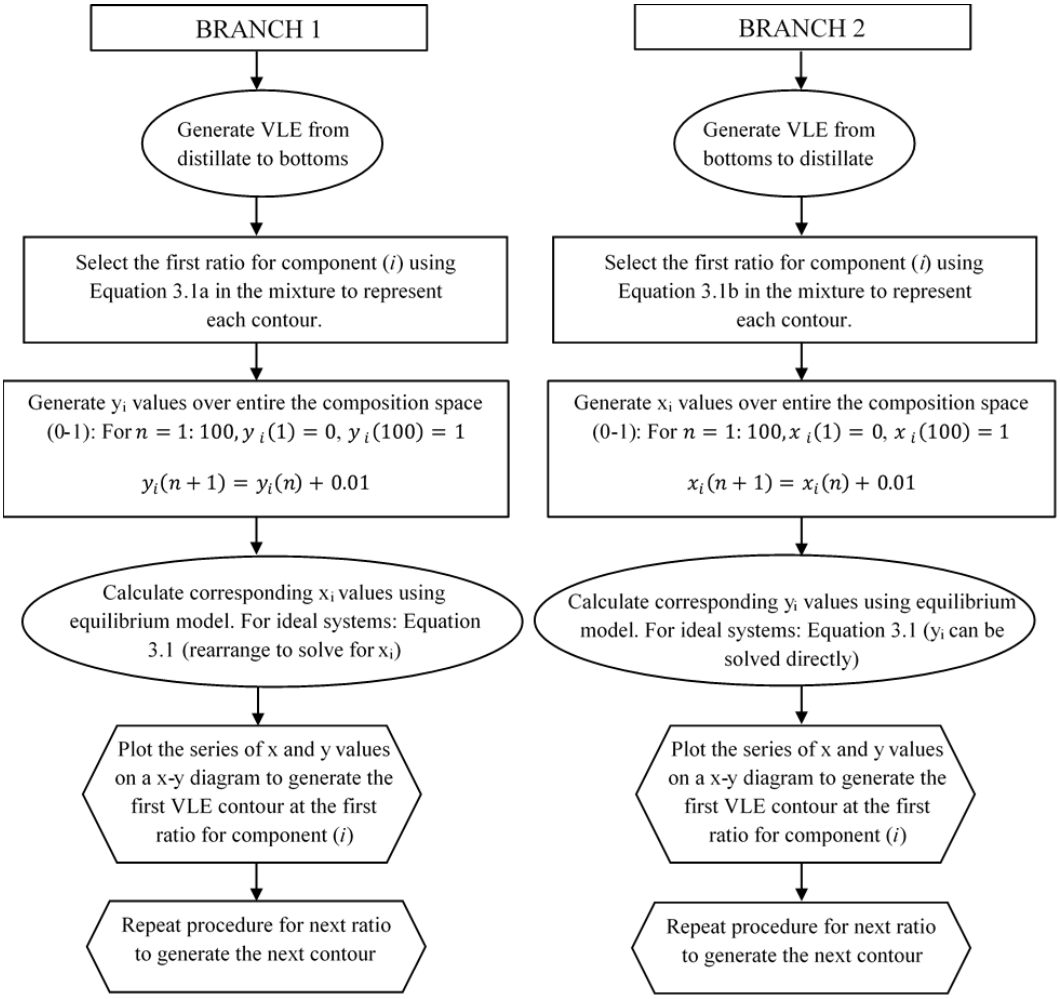

Figure 3.1: Flow chart for the generation of the contours of VLE for component *i* in multicomponent mixtures. (The Same procedure repeated for component *j* and *k*)

Although Equation 3.1 – 3.3 applies to ideal systems, a more general method is presented in Figure 3.1. The method plots contours of VLE where the ratios are varied instead of one unique VLE curve. A series of contours is plotted from

different ratios of component *j* and *k* over the entire composition space for component *i*. Likewise, the contours of VLE for component *j* and *k* are plotted as ratios of component *i* and *k* and *i* and *j* respectively. Each component will have its own contours of VLE plotted on an x-y diagram taking into consideration the influence of all the interactions of the components in the system. Hence the procedure depicted in Figure 3.1 will be performed separately for components *j* and *k* to obtain the x-y plot for components *j* and *k.*

The method proposed in this thesis for the representation of the contours of VLE is generic in nature and can be applied to any type of components (not limited to hydrocarbons) present in a mixture provided data for the equilibrium relationship can be generated. The method of using ratios can be incorporated into any thermodynamic model to plot the contours of VLE for non-ideal systems as stipulated in Figure 3.1. Furthermore, it is only required to plot the contours of VLE once for subsequent analysis.

3.3 Characteristics of Novel VLE Representation

In this section it will be demonstrated how the visual representation of the contours of VLE, on an x-y diagram of all the components in a mixture, is an invaluable visual tool for distillation design. The VLE can provide designers with insights to identify ideal and non-ideal behaviour, close boiling mixtures, tangent pinches and, most importantly, azeotropes.

3.3.1 Ideal Systems

The distillation design process is essentially oriented around achieving the correct product specification as well as achieving the theoretically possible product composition (Wahnschafft & Westerberg, 1993). For ideal systems, it is sufficient to have quantitative knowledge of the order of the normal boiling points or relative volatilities to determine feasible design splits (Wahnschafft & Westerberg, 1993).

In this section, the aspect of the boiling points and volatilities of components in an ideal mixture will be considered. The volatilities of components are essential to the design of an ideal distillation column as this will dictate which product will be richer in the distillate and bottoms product. Two different ideal systems will be depicted to differentiate visually between a simple and difficult separation. In a simple separation the relative volatilities (boiling points) of the components differ considerably from one another. The driving force for the separation would be high due to the difference in the relative volatilities (Gani & Bek-Pedersen, 2000). Hence, the light key component with the lower boiling point will vaporize first and report to the distillate product. The heavy key with a boiling point considerably higher than the light key will report to the bottoms product. If the components of a mixture have boiling points which are in close proximity to each other, the relative volatilities would be close to each other and close to 1. The driving force for the separation will be low due to all the relative volatilities being close to 1 (Ryan, 2001). This mixture is referred to as a close-boiling mixture and would represent a difficult separation. For simplification and illustrative purposes of an ideal system, constant relative volatility is assumed for all components (Hengstebeck, 1946). The equilibrium equations used to relate the liquid mole fraction (x) to the vapour mole fraction (y) for components *i*, *j* and *k* can be found in Equations 3.1 – 3.3 respectively.

3.3.1.1 Example 3.1: Simple Separation (n-hexane, n-heptane and n-nonane)

An ideal system of n-hexane, n-heptane and n-nonane will be considered for a simple separation. N-hexane is the most volatile component (normal boiling point (nbpt) – 68.9°C), n-heptane (nbpt – 98.4°C) is the intermediate volatile component and n-nonane is the least volatile component (nbpt – 150.78°C) (Wahnschafft & Westerberg, 1993; Gamba et al., 2009). The relative volatilities (relative to the light key) of the components were used to determine the equilibrium data for the contours of VLE (Equations 3.1 – 3.3). The relative volatilities of the components are calculated using K-values which are dependent on temperature and pressure. The De-Priester chart was used to determine the K-values for n-hexane, n-heptane and n-nonane at 373 K and 600 kPa. The values obtained are given in Table 3.1:

Table 3.1: K-values and relative volatilities for n-hexane, n-heptane and n-nonane

Component	K value	Relative volatility (α)
n-hexane	0.450	7.03
n-heptane	0.220	3.44
n-nonane	0.064	1.00

The contours of VLE for n-hexane (x_{C6}, y_{C6}), n-heptane (x_{C7}, y_{C7}) and n-nonane (x_{C9}, y_{C9}) at constant pressure were generated using the method presented in Figure 3.1. The results are shown in Figures 3.2 - 3.4. The x-y diagram for each component is represented as several contours of VLE. Figures 3.2 - 3.4 depict 5 contours to show the general behaviour of the system, but allow for visual clarity as well. Each contour is represented by two ratios. The vapour mole fraction ratios (Equations 3.1b, 3.2b and 3.3b), represented by the first element in the vector, are used if the number of stages will be determined from the distillate to bottoms composition. The liquid mole fraction ratios (Equations 3.1a, 3.2a and 3.3a), represented by the second element in the vector, are used if the number of stages will be determined from the bottoms to distillate composition.

Consider Figure 3.2 for n-hexane. If the number of stages is to be determined from the distillate to bottoms compositions, Branch 1 of Figure 3.1 will be followed. For a vapour mole fraction ratio (calculated using Equation 3.1b) of n-heptane and n-nonane (y_{C7}/y_{C9}), the composition space of an x-y diagram is divided into discrete values of y_{C6} from 0 to 1. Equation 3.1 should be rearranged to determine the corresponding liquid compositions x_{C6}. The x_{C6} and y_{C6} values generated for the specified ratio are plotted on the x-y plot to produce a single contour in the composition space. The procedure is repeated to generate additional contours of VLE at different vapour mole fraction ratios and at different liquid mole fraction ratios by varying the vapour mole fractions of n-heptane and n-nonane.

A detailed explanation to generate the x and y values for n-hexane to plot a contour of VLE will be presented. By following the calculation the contours of VLE can be generated effortlessly. A detailed calculation to represent a contour of VLE for n-

hexane at a liquid molar ratio of n-heptane and n-nonane (x_{C7}/x_{C9}) of 5.00 will be presented.

The primary code to plot one contour for n-hexane at a ratio 5.00 is provided below:

```
K(C6) = 0.450;      K(C7) = 0.220;      K(C9) = 0.064;
α(C6/C7) = K(C6) / K(C7);
α(C6/C9) = K(C6) / K(C9);
CRC7/C9 = 5.00;

xC6 (1) = 0.00;
yC6 (1) = ( α (C6/C9) *( xC6(1)/(1- xC6(1)))*( CRC7/C9 +1))/(1+( α (C6/C9))*(
xC6(1)/(1- xC6(1)))*( CRC7/C9 +1))+ ((α(C6/C9) / α(C6/C7))* CRC7/C9);

for n=1:10
xC6 (n+1) = xC6 (n) + 0.100;
yC6 (n+1) = ( α (C6/C9) *( xC6 (n+1)/(1- xC6 (n+1)))*( CRC7/C9 +1))/(1+( α(C6/C9)
*( xC6 (n+1)/(1- xC6 (n+1)))*( CRC7/C9 +1)) + ((α (C6/C9)) / α (C6/C7)) * CRC7/C9))
end`
```

Detailed calculation for one value of x:

The relative volatilities (α) and ratio of n-heptane and n-nonane (x_{C7}/x_{C9}) are required to calculate the x and y values that represent the specific contour of VLE as shown in Equation 3.1.

α(*C6*/*C7*) = 2.05

α(*C6*/*C9*) = 7.03

$CR_{C7/C9}$ = 5.00

For the first x value of 0 for n-hexane, the corresponding y value is calculated to be 0, as shown in Equation 3.4.

$x_{C6}\ (1) = 0.00$

$$y_{C6}(2) = \frac{\left[7.03 \quad \left(\frac{0.00}{1.00-0.00}\right)(5.00+1.00)\right]}{1.00+\left[7.03 \quad \left(\frac{0.00}{1.00-0.00}\right)(5.00+1.00)\right]+\left(\frac{7.03}{2.05}\times 5.00\right)} = 0.00 \tag{3.4}$$

The second value of x can be calculated at any interval. In this depiction, the interval is chosen to be 0.1, hence the next x value is 0.1 (Equation 3.5). The corresponding y value is calculated to be 0.205 as portrayed in Equation 3.6.

$$x_{C6}(2) = 0.00 + 0.100 = 0.1 \tag{3.5}$$

$$y_{C6}(2) = \frac{\left[7.03 \quad \left(\frac{0.1}{1-0.1}\right)(5.00+1.00)\right]}{1.00+\left[7.03 \quad \left(\frac{0.100}{1.00-0.100}\right)(5.00+1.00)\right]+\left(\frac{7.03}{2.05}\times 5\right)} = 0.205 \tag{3.6}$$

The iterations continue until an x value of 1, such that the liquid and corresponding vapour compositions are obtained as illustrated in Table 3.2.

Table 3.2: Vapour and liquid composition for n-hexane at a ratio of n-heptane / n-nonane (C7/C9) of 5.00.

x	0.0	0.10	0.20	0.30	0.40	0.50	0.60	0.70	0.80	0.90	1.00
y	0.00	0.21	0.37	0.499	0.61	0.70	0.78	0.84	0.90	0.95	1.00

The x-y values generated in Table 3.2 are used to plot a contour of VLE represented by the curve labelled 5.00 in Figure 3.2.

If the number of stages is to be determined from the bottoms to distillate compositions, branch 2 of Figure 3.1 will be followed. For a liquid mole fraction ratio (calculated using Equation 3.1a) of n-heptane and n-nonane (x_{C7}/x_{C9}), the composition space of an x-y diagram is divided into discrete values of x_i from 0 to 1. The corresponding vapour compositions (y_{C6} values) are determined using Equation 3.1. The generated x_{C6} and y_{C6} values are plotted on an x-y diagram to represent a contour of VLE. The procedure is repeated to generate additional contours of VLE at different liquid mole fraction ratios by varying the liquid mole fractions of n-heptane and n-nonane.

The method presented in this thesis to represent the contours of VLE and the method proposed by Cope & Lewis (1932) represent each component's VLE as a unique plot. The Cope & Lewis (1932) method uses Raoult's law and plots straight lines at the operating pressure and the temperatures at each stage. Unlike the Cope & Lewis (1932) method, the proposed graphical method is more robust, as it can be applied to any equilibrium relationship and is not restricted to Raoult's law. In addition, once the contours of VLE are plotted for a specified system, different design calculations can be investigated using the generated plot. The proposed graphical method is not dependent on the temperature profile of a column at a specific design specification, as proposed by Cope & Lewis (1932).

The contours of VLE for n-hexane (Figure 3.2) form a leaf above the 45 degree line which is expected as n-hexane is the light key component. The conventional binary McCabe-Thiele method plots the most volatile component to graphically solve for design variables and is very similar to Figure 3.2. Figure 3.3 depicts the contours of VLE for n-heptane which is the intermediate key component, and hence the contours of VLE form a leaf on either side of the 45 degree line. The representation of VLE on either side of the 45 degree line has not yet been seen in the field of distillation design as the intermediate component has not been plotted, and displays one aspect of the novelty of the work. Figure 3.4 depicts the contours of VLE for n-nonane. Since n-nonane is the heavy key component, the contours of VLE are depicted as a leaf below the 45 degree line. Such behaviour of VLE has been seen in the method presented by Jenny (1939). Jenny (1939) plots the VLE for the heavy key but in the rectifying section of the column. Jenny (1939) performed a rigorous stage-by-stage calculation to confirm the behaviour of the heavy key as a VLE curve below the 45 degree line. The method proposed to represent VLE in this thesis provides insights of the behaviour of all components in a mixture in both the rectifying and stripping sections. Jenny (1939) plotted the VLE of the key components in the rectifying and stripping section. Hence, the method by Jenny (1939) provides no insights into the behaviour of the intermediate components in either the stripping or rectifying section.

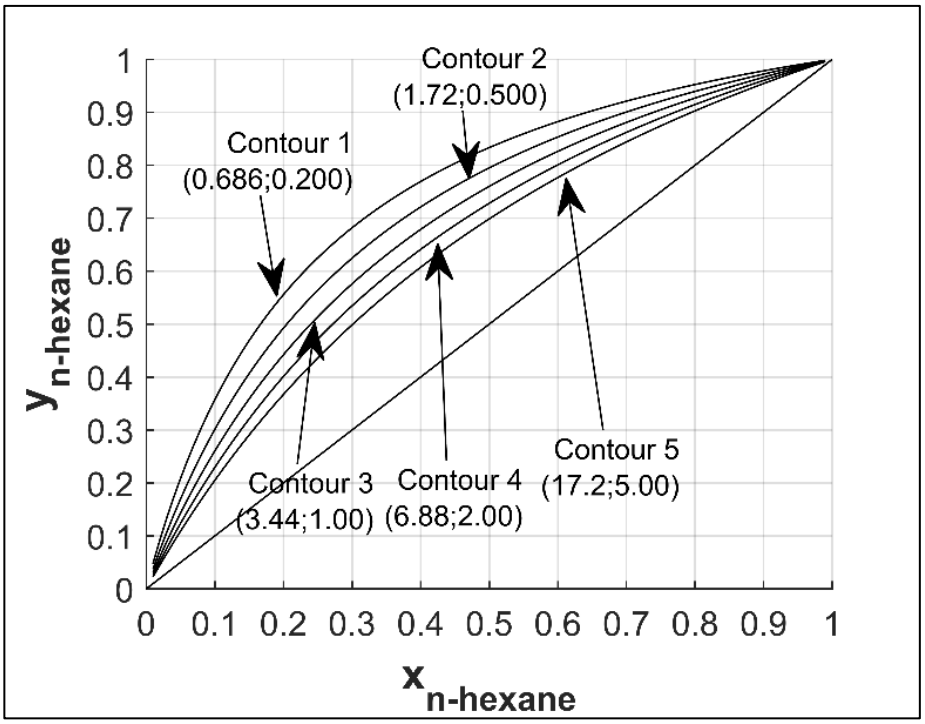

Figure 3.2: Contours of VLE for the most volatile component (n-hexane) at different vapour ratios of n-heptane / n-nonane for calculating the number of stages from distillate and different liquid ratios of n-heptane / n-nonane for calculating the number of stages from the bottoms

From Figures 3.2 and 3.4, it can be seen that each contour lies in a fair proximity from each other and far from the 45 degree line thus the depicting a simple separation with relative volatilities varying from 7.03 – 1. Since the mixture is not a close boiling mixture and the relative volatilities differ considerably, the light key and heavy key will have a high tendency to separate into the distillate and bottoms product respectively.

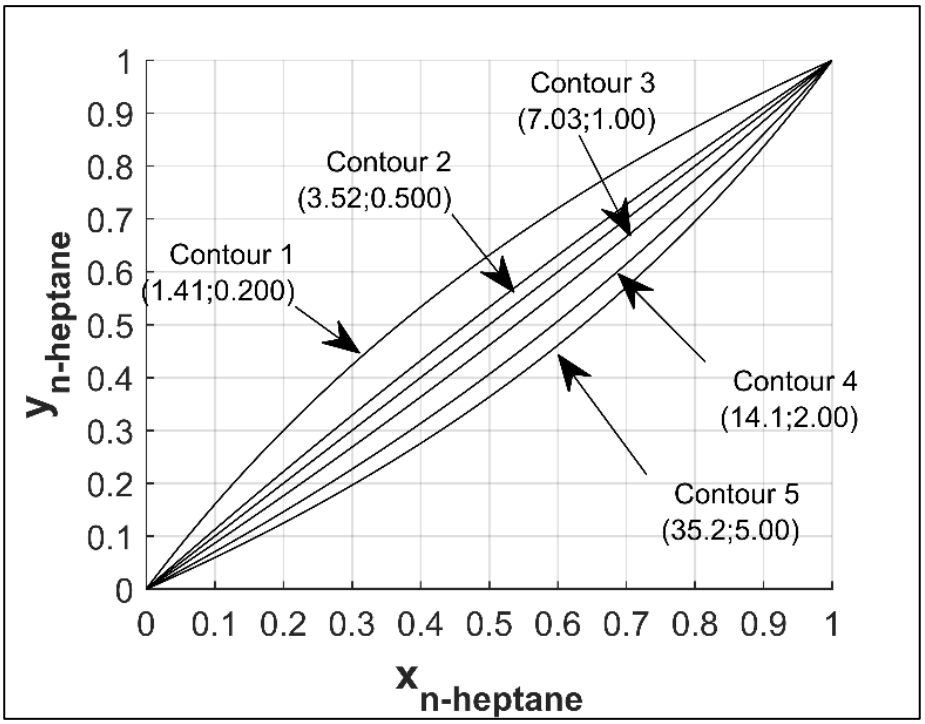

Figure 3.3: Contours of VLE for the intermediate volatile component (n-heptane) at different vapour ratios of n-hexane / n-nonane for calculating the number of stages from distillate and different liquid ratios of n-hexane / n-nonane for calculating the number of stages from the bottoms

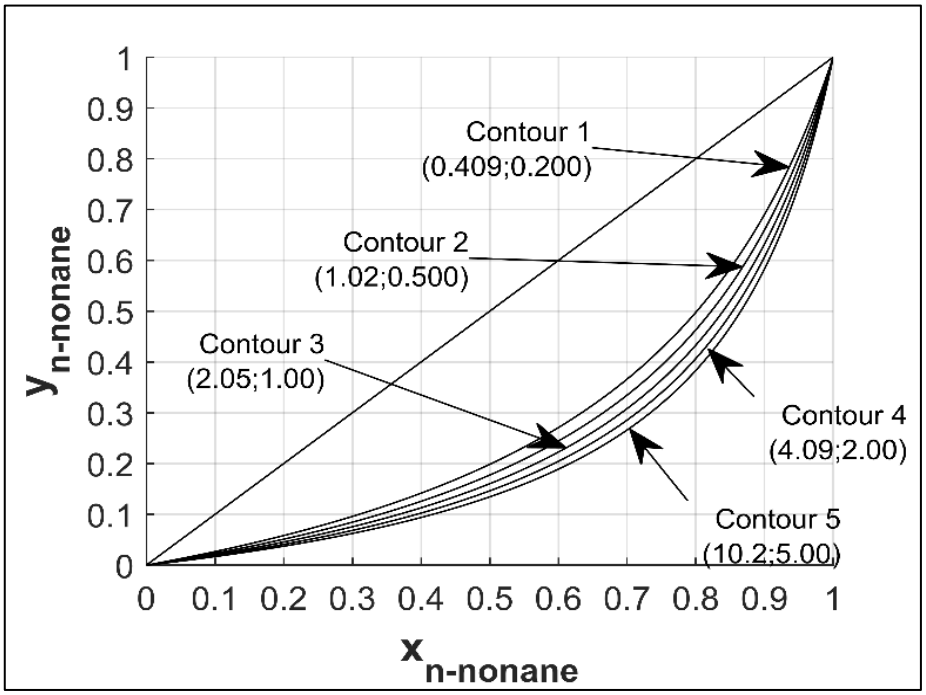

Figure 3.4: Contours of VLE for the least volatile component (n-nonane) at different vapour ratios of n-hexane / n-heptane for calculating number of stages from distillate and different liquid ratios of n-hexane / n-heptane for calculating number of stages from the bottoms

3.3.1.2 Example 3.2: Difficult (close boiling) Separation (fictitious system)

Difficult separations can be classified as close-boiling mixtures. This means that the mixture contains two or more components with close-boiling points (Hengstebeck, 1946). Difficult separations are frequently found in de-isobutanizers in butylene alkylation units in refineries (Ryan, 2001). Consider three fictitious components, namely A, B and C, for the depiction of the VLE for a ternary system in which the tendency to separate is low. The contours of VLE were plotted using the method presented in Figure 3.1, for stepping from bottoms and distillate (ratios of liquid mole fractions). The K-values of these components were chosen such that the relative volatilities (relative to the least volatile component C) of B and C are close to each other and to unity. The K-values and relative volatilities are given in Table 3.3 below:

Table 3.3: K-values and relative volatilities for component A, B and C

Component	K value	Relative volatility (α)
A	0.870	1.38
B	0.700	1.11
C	0.630	1.00

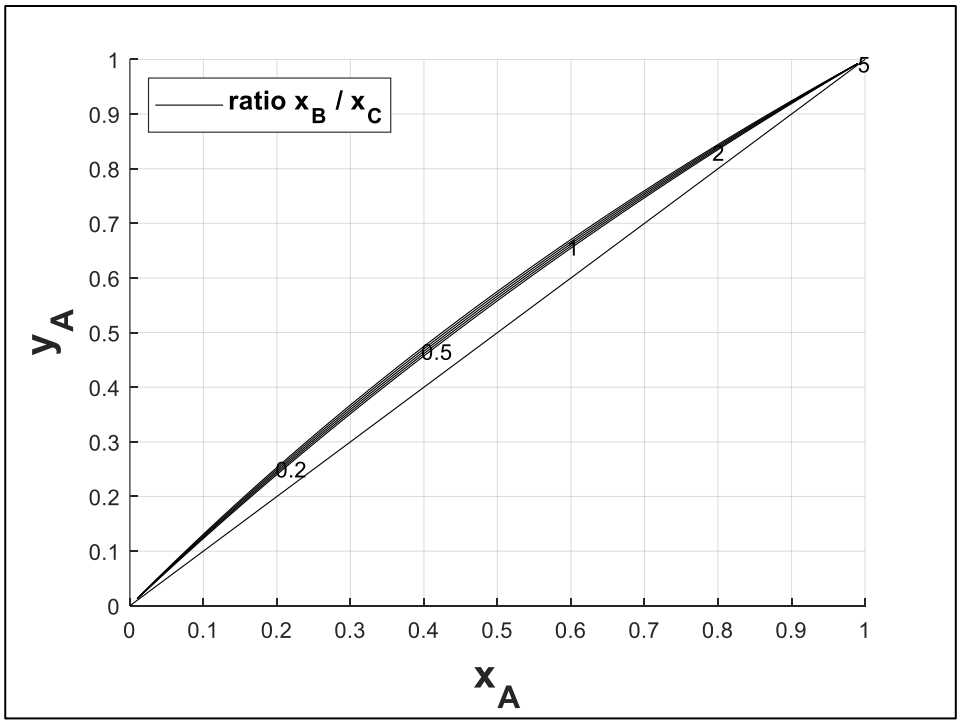

Figure 3.5: Contours of VLE for fictitious component A at different ratios of B / C

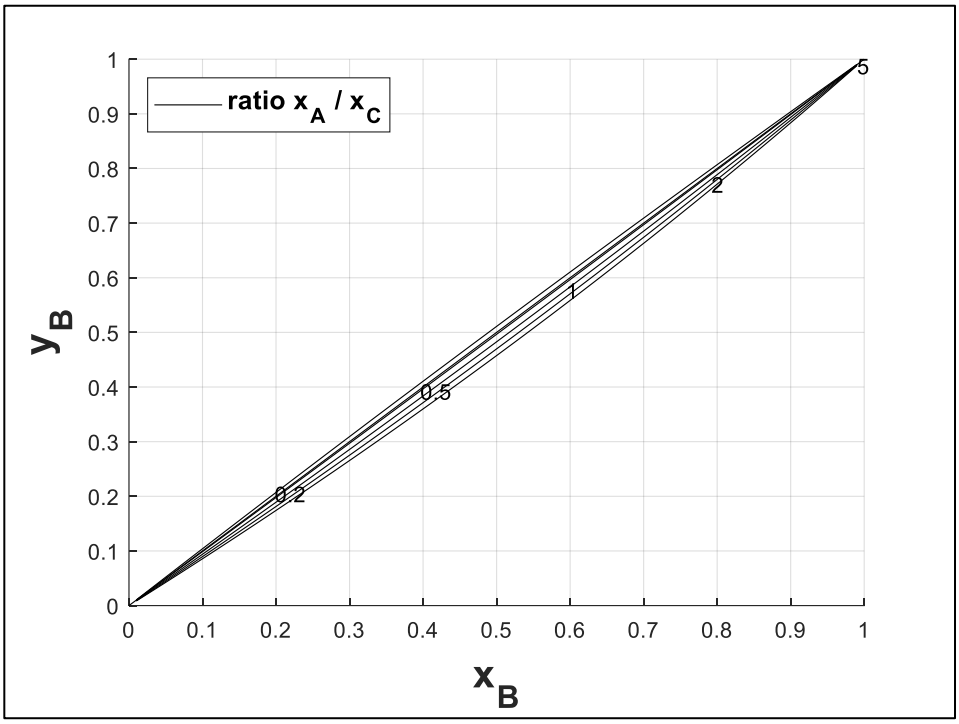

Figure 3.6: Contours of VLE for fictitious component B at different ratios of A / C

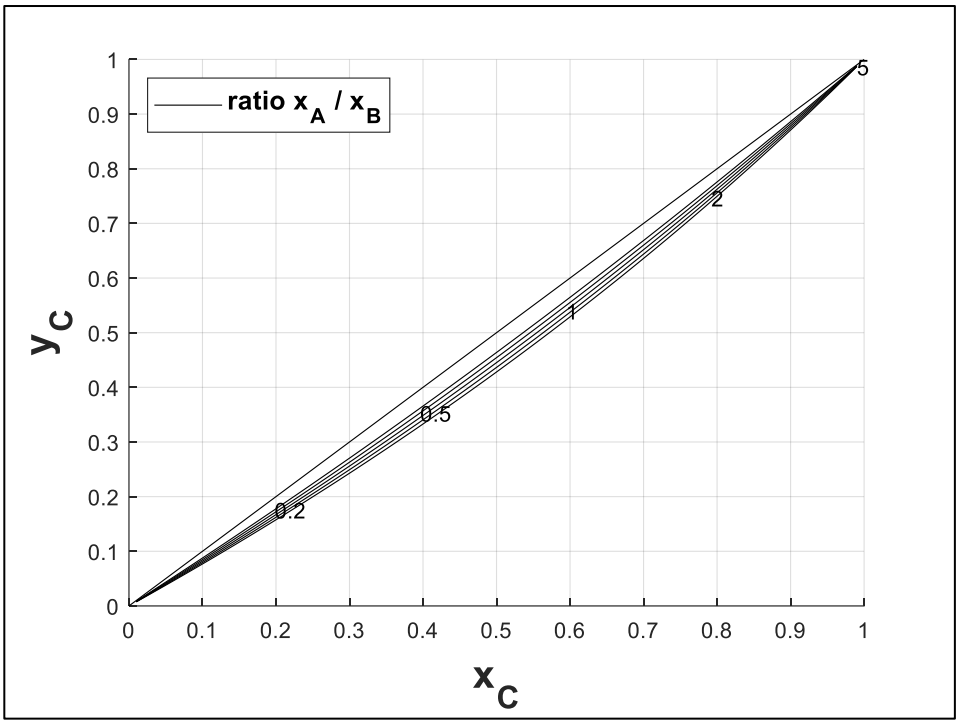

Figure 3.7: Contours of VLE for fictitious component C at different ratios of A / B

Unlike Example 3.1, the VLE of all the components in Example 3.2, depicted in Figures 3.5 - 3.7, do not display a simple separation. The individual contours are very close together and lie in very close proximity to the 45 degree line. The relative volatilities vary from 1.38 – 1, and are in close proximity to 1 and each other. The separation in Example 3.2 shows a close-boiling mixture which will have a low tendency to separate into the distillate and bottoms product respectively. Many more stages will be required to achieve the desired products in comparison with Example 3.1 due to the contours close proximity to the 45 degree line, hence rendering this a 'difficult separation'.

3.3.2 Non-Ideal Systems

Components very seldom behave ideally, hence non-ideal systems are frequently encountered in design problems. Unlike ideal systems, non-ideal systems cannot be approximated by relative volatilities and require a more accurate analysis to determine non-ideal behaviour, such as azeotropes (Wahnschafft & Westerberg, 1993). Azeotropes and tangent pinches can be visualized for ternary systems from the contours of VLE, as proposed in this thesis. For examples in this section, the vapour pressure of pure components was determined using the extended Antoine equation (refer to Appendix B) and the Wilson / NRTL activity coefficient models (refer to Appendix B) have been used to predict the activity coefficients of the species in the non-ideal mixtures. The thermodynamic parameters were extracted from Aspen Plus^{TM} (refer to Appendix B). Contours of VLE for the components are plotted as the ratio of the other components in accordance with the flow chart in Figure 3.1.

A detailed explanation to generate the x and y values for acetone in order to plot a contour of VLE will be presented. A detailed calculation to represent a contour of VLE at a liquid molar ratio of benzene and chloroform ($x_{Benzene}/x_{Chloroform}$) of 5.00 will be presented. The contour of VLE at a ratio of 5.00 is graphically depicted in Figure 3.10.

The primary code to plot one contour for acetone at a ratio 5.00 is provided below:

$$CR_{Benzene/Chloroform} = \frac{x_B}{x_C} = 5.00$$

$For\ p = 1{:}10$

$$x_{Acetone}(p+1) = x_{Acetone}(p) + 0.100 \quad (3.7)$$

$$x_{Benzene}(p+1) = \left(\frac{CR_{\frac{Benzene}{Chlorofrom}}}{CR_{\frac{Benzene}{Chlorofrom}}+1}\right)\left(1 - x_A(p+1)\right) \quad (3.8)$$

$$x_{Chloroform}(p+1) = 1 - x_{Acetone}(p+1) - x_{Benzene}(p+1) \quad (3.9)$$

$For\ p = 1$

$x_{Acetone}(1) = 0.000$

$x_{Benzene}(1) = 0.833$

$x_{Chloroform}(1) = 0.167$

$For\ p = 2$

$x_{Acetone}(2) = 0.100$

$x_{Benzene}(2) = 0.750$

$x_{Chloroform}(2) = 0.150$

For non-ideal systems that require a thermodynamic model to correctly depict the behaviour of a system, Equations 3.1 - 3.3 cannot be implemented. Nevertheless, the method is still applicable with a slightly more complex calculation. The value of x for acetone begins at 0 and increases in increments of 0.1 to a value of 1 (Equation 3.7). At each x value of acetone, the x values of benzene and chloroform are calculated using Equations 3.8 and 3.9 such that the ratio of the two compositions is 5. The x values are then computed into the thermodynamic model to yield the corresponding y value for acetone as shown in Figure 3.8.

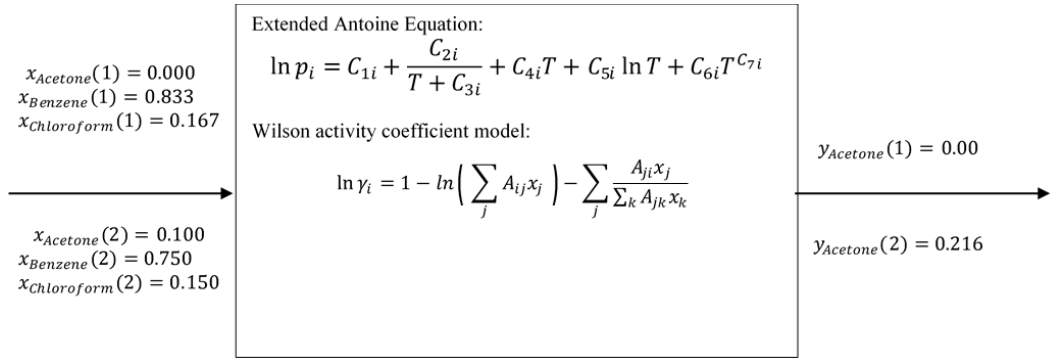

Figure 3.8: Figure depicting the incorporation of the thermodynamic model to generate corresponding vapour and liquid pairs used to plot contours of VLE

The iterations from x values of 0 to 1 and the corresponding y values calculated from the method above are illustrated in Table 3.4. The x and y values are plotted on the 2D plot for acetone in Figure 3.9 and is represented by the curve labelled 5. The specific contour of VLE represented by a certain ratio can be plotted in the same manner. The method was repeated and contours representing ratios of 0, 0.2, 0.5, 1 and 2 are plotted in Figure 3.9.

Table 3.4: Vapour and liquid composition for acetone at a ratio of benzene / chloroform of 5.00

$x_{acetone}$	0.00	0.10	0.20	0.30	0.40	0.50	0.60	0.70	0.80	0.90	1.0
$y_{acetone}$	0.00	0.22	0.37	0.50	0.59	0.68	0.75	0.81	0.87	0.94	1.0

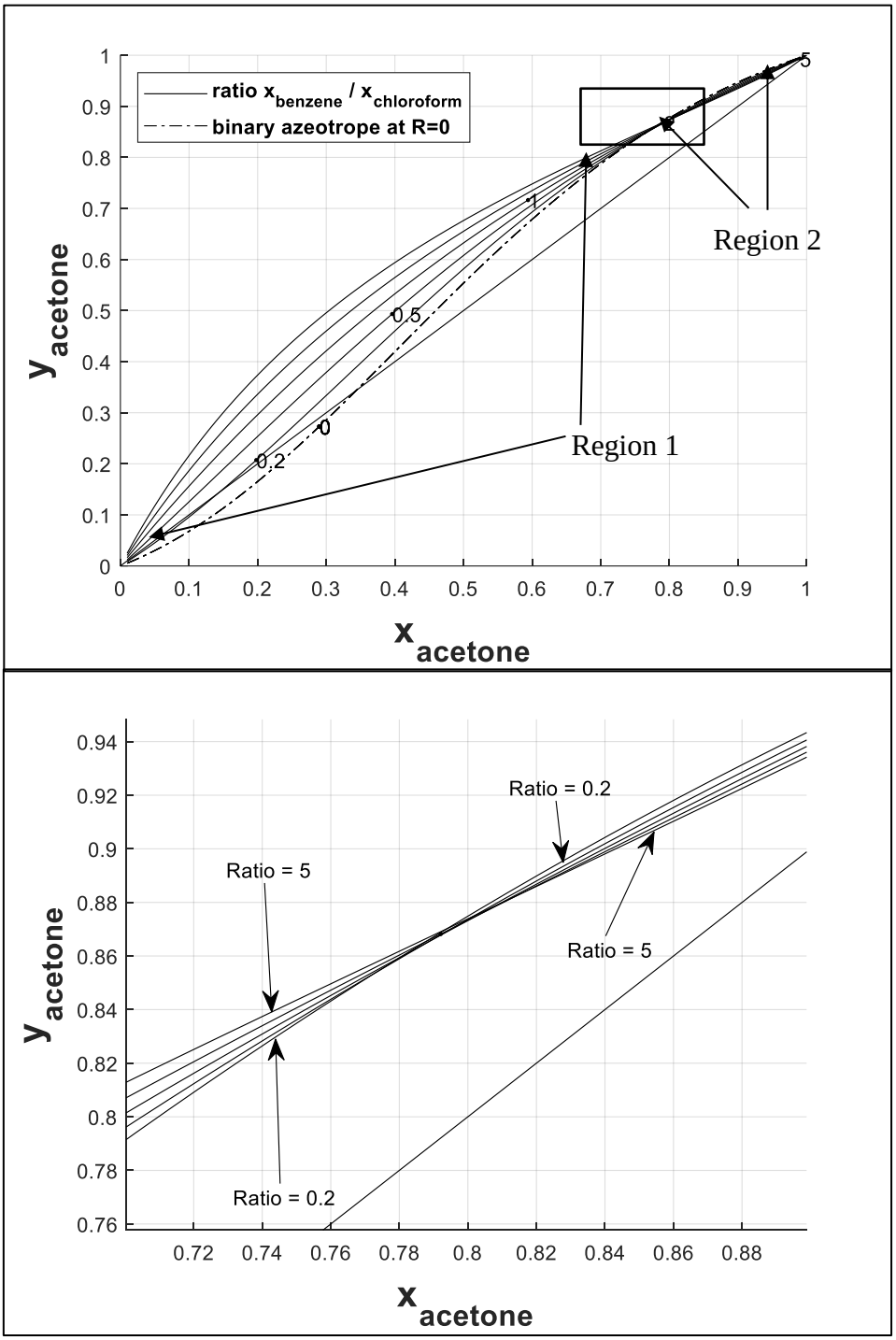

(a)

(b)

Figure 3.9: (a) Contours of VLE for acetone at different ratios of benzene / chloroform using the Wilson activity coefficient model, (b) enlargement of a portion of graph 3.10a

3.3.2.1 Example 3.3: Azeotropic system (acetone, benzene and chloroform)

An azeotrope is also known as a constant boiling mixture and behaves like a pure component (McCabe & Thiele, 1925). An infinite number of stages would be required to reach the concentration of the azeotrope by distillation alone (McCabe & Thiele, 1925). Azeotropes can therefore pose a distillation design problem. The importance of the VLE for azeotropes shown graphically is to understand and identify all the physiochemical restrictions which the nature of a mixture has on a separation process (Hilmen, 2000). An advantage of the McCabe-Thiele method for binary distillation is that azeotropes are shown visually as the intersection of the equilibrium curve with the 45 degree line (Anderson & Doherty, 1983). At this point of intersection, the liquid and vapour compositions are equal (x=y). By plotting the contours of VLE for a ternary mixture on the x-y axis using the method proposed in this thesis the designer would be able to qualitatively identify binary azeotropes and gain the necessary understanding in order to identify feasible and infeasible design specifications.

A mixture of acetone (nbpt – 56.5°C), benzene (nbpt – 80.1°C) and chloroform (nbpt – 61.2°C) will be considered to depict a system with a single maximum-boiling binary azeotrope (bpt – 64.4°C) between acetone (34.09 mol%) and chloroform (65.19 mol%) at 1 bar (Luyben, 2008; Wahnschafft & Westerberg, 1993). The extended Antoine equation and the Wilson activity coefficient model were used to model the equilibrium data. The Wilson model was used to model the VLE for the system as it correlated accurately with experimental data (Kojima et al., 1991).

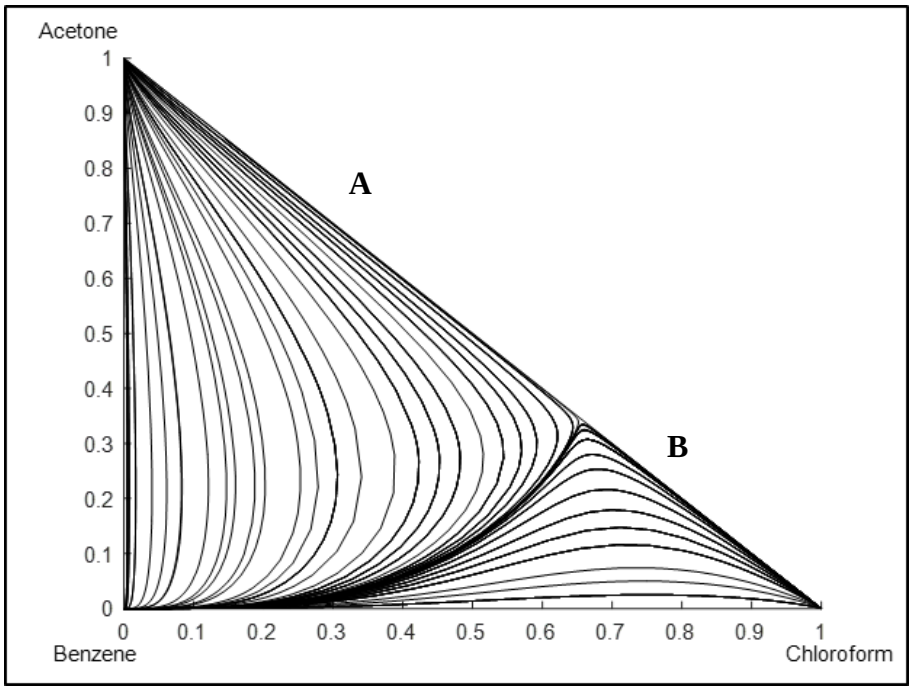

Figure 3.10: RCM for acetone-benzene-chloroform system

Residue curve maps (RCMs) are graphical tools that are useful to study ternary systems. RCMs are also used to determine azeotropes, feasible splits, select entrainers and analyse possible column operability problems (Wasylkiewicz et al., 2000; Doherty & Caldarola, 1985). RCMs depict distillation regions as a series of residue curves that connect an unstable node and a stable node (Rooks et al., 1998). RCMs display the shape of the separation space, azeotropic distillation boundaries and distillation regions (Wasylkiewicz et al., 2000). Figure 3.10 depicts the RCM for the acetone, benzene and chloroform system. Due to the binary azeotrope that forms in the mixture between acetone and chloroform, there are two distillation regions (A and B) for separation, separated by a single distillation boundary. The boundary between the distillation regions restricts the products that can be obtained from a simple distillation column (one feed and two products) (Wasylkiewicz et al., 2000). Distillation boundaries can be crossed by mixing streams, recycles and pressure-swing operations (Wasylkiewicz et al., 2000).

Figures 3.9a and 3.11 show that more than one of the contours of VLE intersect the 45 degree line for acetone and chloroform respectively. In order to determine the composition of the azeotrope, the liquid or vapour composition of benzene would

have to be 0. For chloroform, the ratio would be infinity and hence depicted in Figure 3.11 as a ratio of infinity. For acetone this would result in the azeotrope being depicted by the contour that represents a ratio of 0 (Figure 3.9a). These contours predict the composition of the azeotrope to be approximately 34% acetone which correlated with literature and the RCM for the system (Luyben, 2008). Unidistribution lines in the composition space of a RCM join points where the equilibrium constant of component *i* is 1 ($K_i = 1$) and hence has the same liquid and vapour mole fractions ($x_i = y_i$) at each point (Kiva et al., 2003). The points that represent $x_i = y_i$ are classified as the turning points of that component. On a multicomponent x-y plot, the points of $x_i = y_i$ (turning points) would be represented by multiple contours intersecting the 45 degree line in addition to the azeotrope. Binary azeotropes will exhibit two unidistribution curves ($K_{acetone} = 1$ and $K_{chloroform} = 1$) (Kiva et al., 2003). Hence, both figures 3.9 a and 3.11 for acetone and chloroform respectively, exhibit multiple contours intersecting the 45 degree line. The contours of VLE for benzene in Figure 3.12 do not cross the 45 degree line and hence depict no azeotropes or unidistribution lines.

Figure 3.9b depicts an enlargement of a section of Figure 3.9a for acetone. The VLE contours seem to be represented by a single contour but this is not the case. At this point, the binary equilibrium curves of acetone-benzene and acetone-chloroform intersect and the order of the contours of VLE changes. Below the intersection point, the binary VLE curve of acetone and chloroform lies above the binary VLE curve of acetone chloroform. After the intersection, the binary VLE curve of acetone and chloroform lies above the binary acetone benzene curve, hence changing the order of the contours of VLE.

Stepping towards a specific ratio, although on the same curve, will lie at different positions on either side of this point. Below the intersection point (Region 1), the binary VLE curves lie in greater proximity due to a greater difference in the volatilities of acetone compared with benzene and chloroform. Above the intersection (Region 2) of the binary VLE, the contours of VLE lie very close together as the difference in the volatilities of acetone compared with benzene and

chloroform is much smaller. The contours of VLE below the intersections point have a wider leaf of operation than above the intersection. In non-ideal systems, such as the acetone, benzene and chloroform system, the volatilities change with composition, unlike ideal systems of constant relative volatilities, as depicted in Examples 3.1 and 3.2. Figure 3.12, for benzene, depicts the same behaviour as acetone where the binary equilibrium curves for benzene and acetone and benzene and chloroform intersect, hence changing the order of the contours below the intersection.

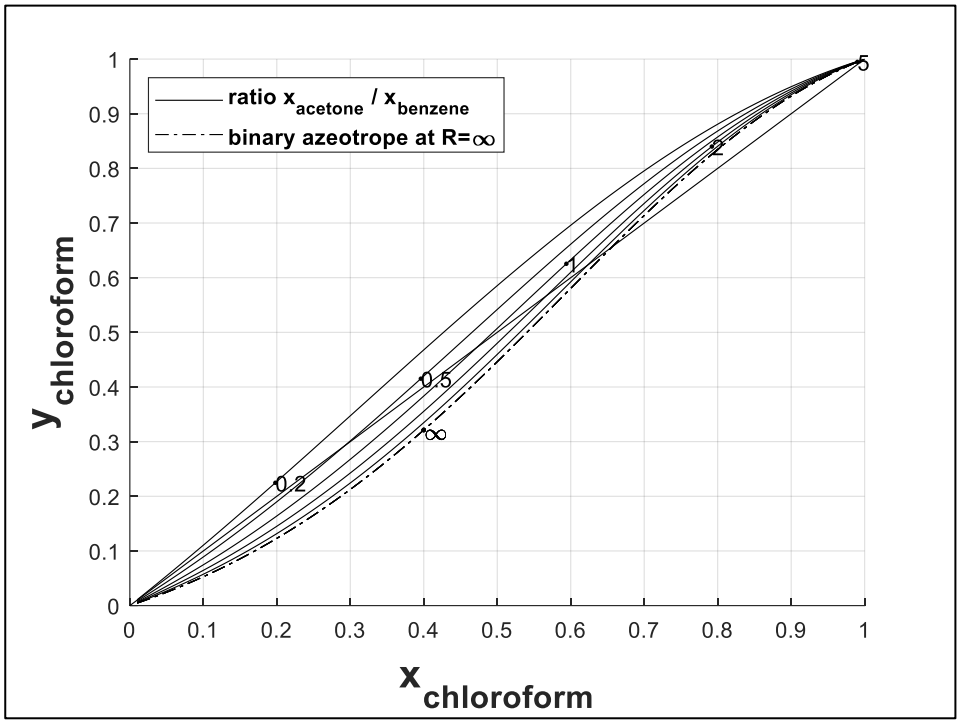

Figure 3.11: Contours of VLE for chloroform at different ratios of acetone / benzene using the Wilson activity coefficient model

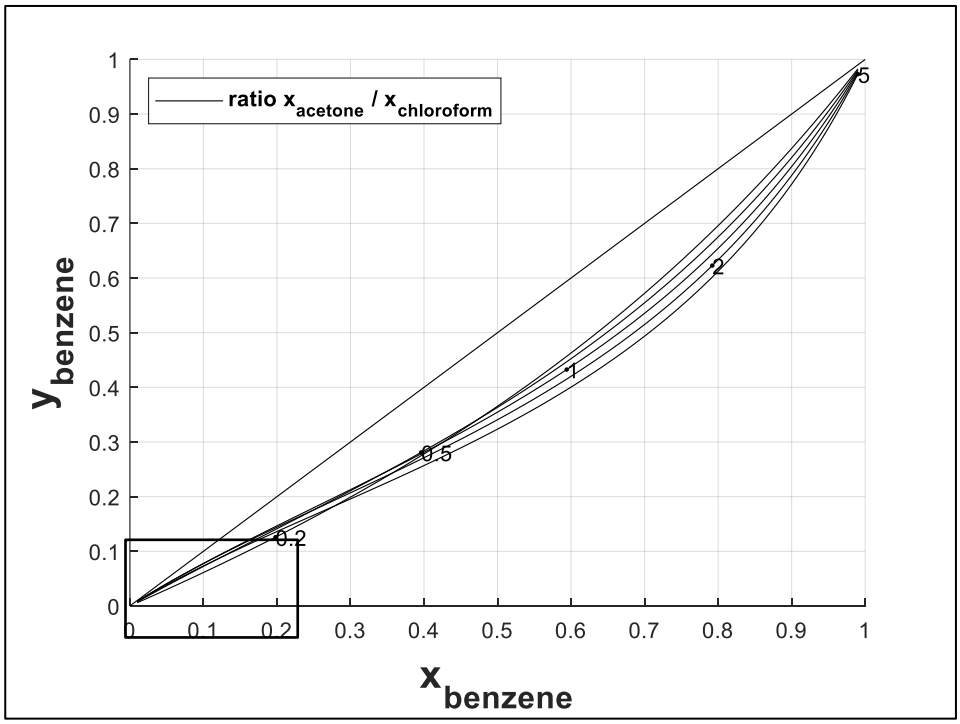

Figure 3.12: Contours of VLE for benzene at different ratios of acetone / chloroform using the Wilson activity coefficient model

3.3.2.2 Depiction of contours of VLE for acetone-benzene-chloroform system using NRTL thermodynamic model

As stated in the introduction to this chapter, the novel representation of the contours of VLE is not restricted to a specific thermodynamic model and can be applied to any model appropriate for the system under investigation. According to Mathias (2016), the experimental data for acetone-benzene-chloroform produced by Kojima et al., (1991) can also be accurately modelled using the NRTL activity coefficient model. Hence, it can be predicted that the contours of VLE produced using the Wilson and NRTL models should correlate. In addition, the contours of VLE produced using the NRTL model should correctly depict the behaviour of the systems as well as the azeotrope formed between acetone and chloroform.

The extended Antoine equation and the NRTL activity coefficient model were used to model the equilibrium data. The parameters were taken from Aspen Plus^{TM} and can be found in Appendix B.

Figures 3.13-3.14 depict the contours of VLE for acetone, benzene and chloroform respectively, predicted using the NRTL activity coefficient model. It can be seen that contours of VLE correlate with the contours of VLE predicted by the Wilson model (Figures 3.10-3.12). Figures 3.13 and 3.15, for acetone and chloroform, show the binary azeotrope at a composition of approximately 34% acetone which correlates with literature and the Wilson model.

Hence, it can be concluded that the representation of the contours of VLE are applicable to any thermodynamic model suitable for the system under investigation.

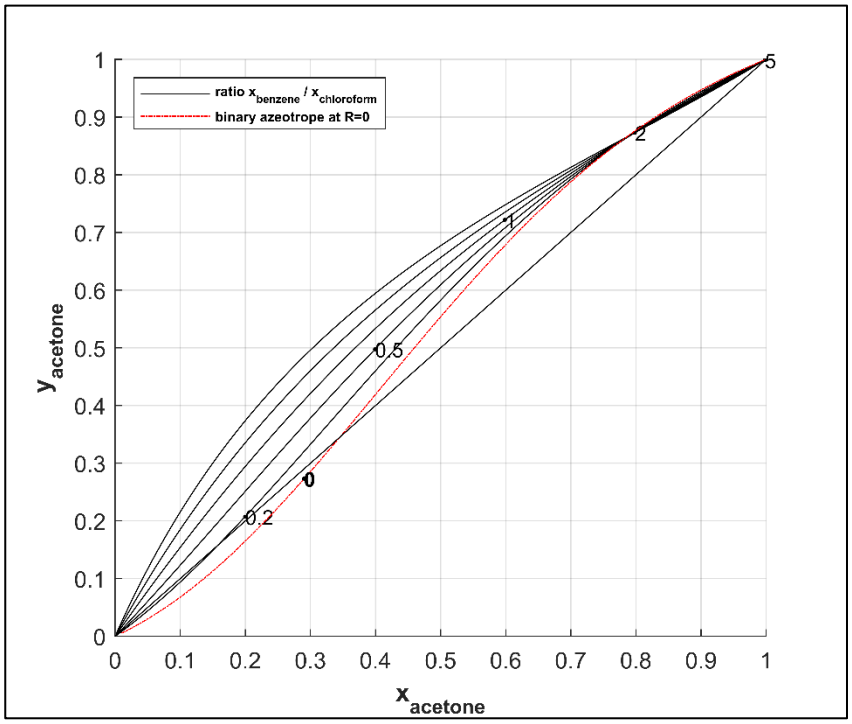

Figure 3.13: Contours of VLE for acetone at different ratios of benzene / chloroform using the NRTL activity coefficient model

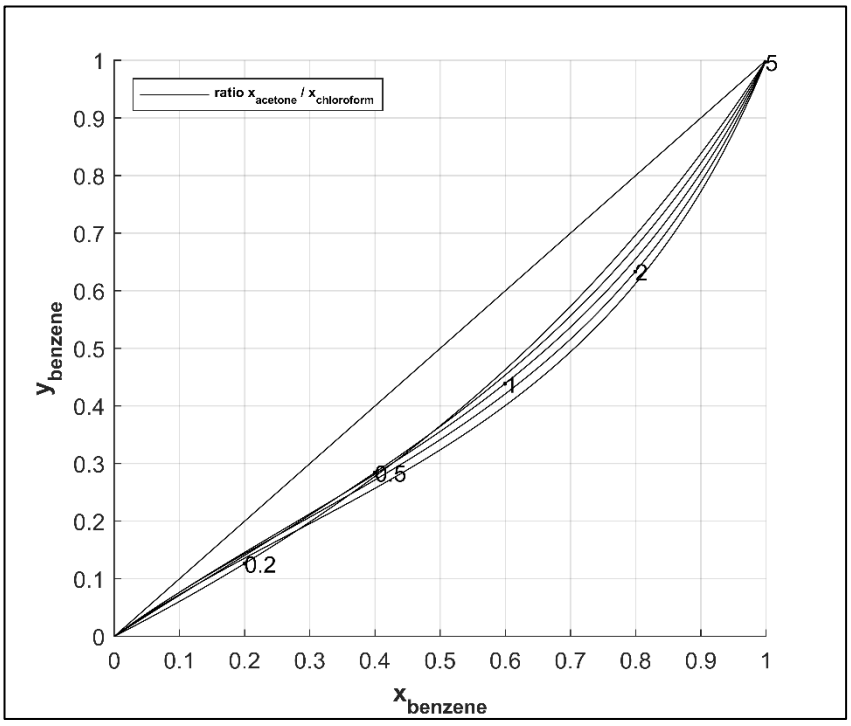

Figure 3.14: Contours of VLE for benzene at different ratios of acetone / chloroform using the NRTL activity coefficient model

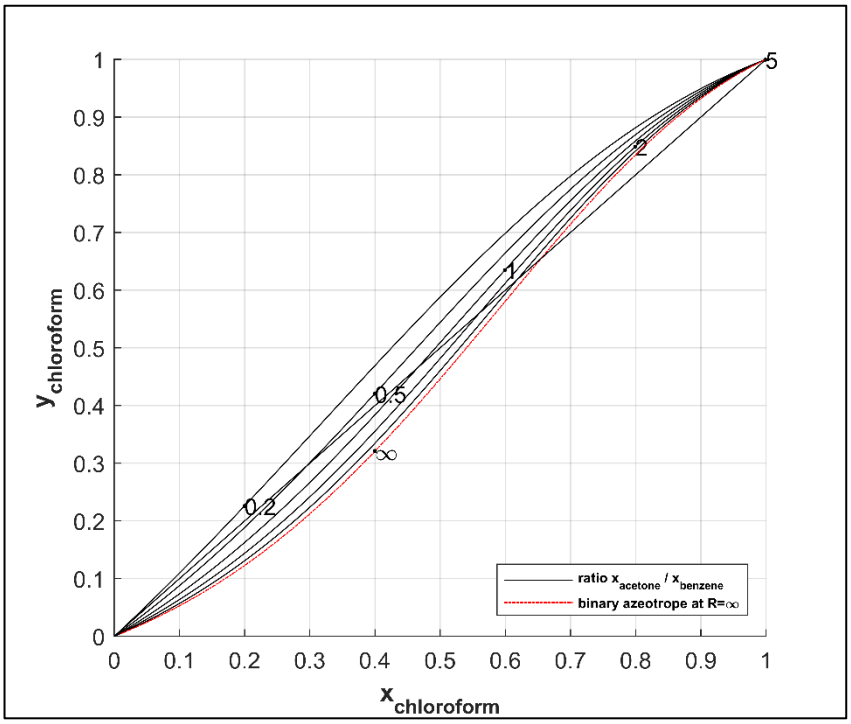

Figure 3.15: Contours of VLE for chloroform at different ratios of acetone / benzene using the NRTL activity coefficient model

3.3.2.3 Example 3.4: Ternary Azeotrope system (acetone, chloroform and methanol)

A mixture of acetone (nbpt – 56.5°C), chloroform (nbpt – 61.2°C) and methanol (nbpt – 64.5°C) will be investigated to depict a mixture with three binary azeotropes (one in each binary pair) and one ternary azeotrope (Castillo & Towler, 1998; Wahnschafft & Westerberg, 1993). A minimum-boiling azeotrope between acetone (79%) and methanol (21%) (bpt – 55.4°C), a minimum-boiling azeotrope between methanol (34%) and chloroform (66%) (bpt – 53.9°C) and a maximum-boiling azeotrope between acetone (34%) and chloroform (66%) (bpt – 64.5°C) are present in the system (Ewell & Welch, 1945; Castillo & Towler, 1998). Figure 3.16 depicts the RCM for the acetone, chloroform and methanol system. From Figure 3.13, the composition of the ternary azeotrope is 33% acetone, 24% chloroform and 43% methanol. It is classified as a saddle point azeotrope as the azeotrope boils at 57.5°C and this temperature is neither a minimum nor a maximum boiling temperature of the system (Ewell & Welch, 1945; Castillo & Towler, 1998).

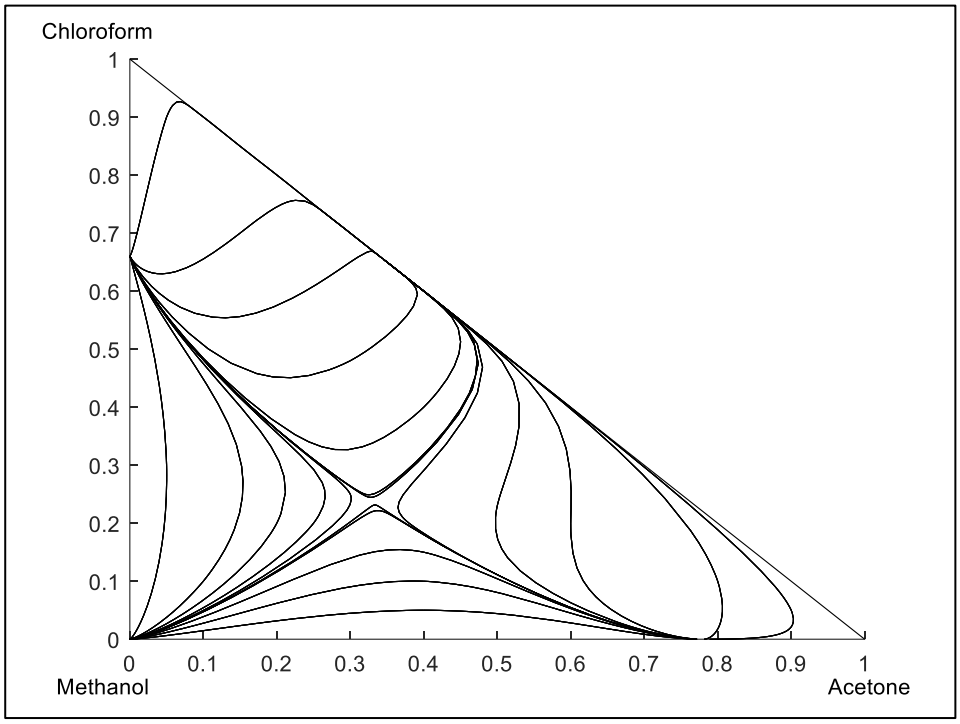

Figure 3.16: RCM for acetone-methanol-chloroform system

Ternary azeotropes exhibit unidistribution curves ($K_{acetone} = 1$, $K_{methanol} = 1$ and $K_{chloroform} = 1$) (Kiva et al., 2003). Hence the contours of VLE will exhibit turning points for all three components in the mixture. Consider Figures 3.17a – 3.19a, in which more than one set of contours of VLE intersect the 45 degree line for all the components. Hence, each component will exhibit a unidistribution line. Figures 3.17b - 3.19b show the binary and ternary azeotropes for each component. Figure 3.17b, for acetone, shows that the binary azeotrope of acetone-chloroform is represented by a ratio of infinity. According to Figure 3.17a, the composition of the azeotrope is approximately 34% acetone which is in agreement with Figure 3.10a in Example 3.3 and literature (Luyben, 2008). In addition, the binary azeotrope of acetone-methanol would be represented by a ratio of 0 containing 78.5% acetone. Once again, the composition correlates to literature and the RCM for the mixture in Figure 3.16 (Castillo & Towler, 1998). Figure 3.19b, for chloroform, shows that both binary azeotropes (acetone-chloroform and chloroform-methanol) have the same composition of approximately 66% chloroform. Hence, both binary azeotrope contours ($r = 0$ and $r = \infty$) intersect at a 66% chloroform. The ternary azeotrope is

represented by the contours of ratio 0.5503, 0.7656 and 1.391 for acetone, chloroform and methanol respectively.

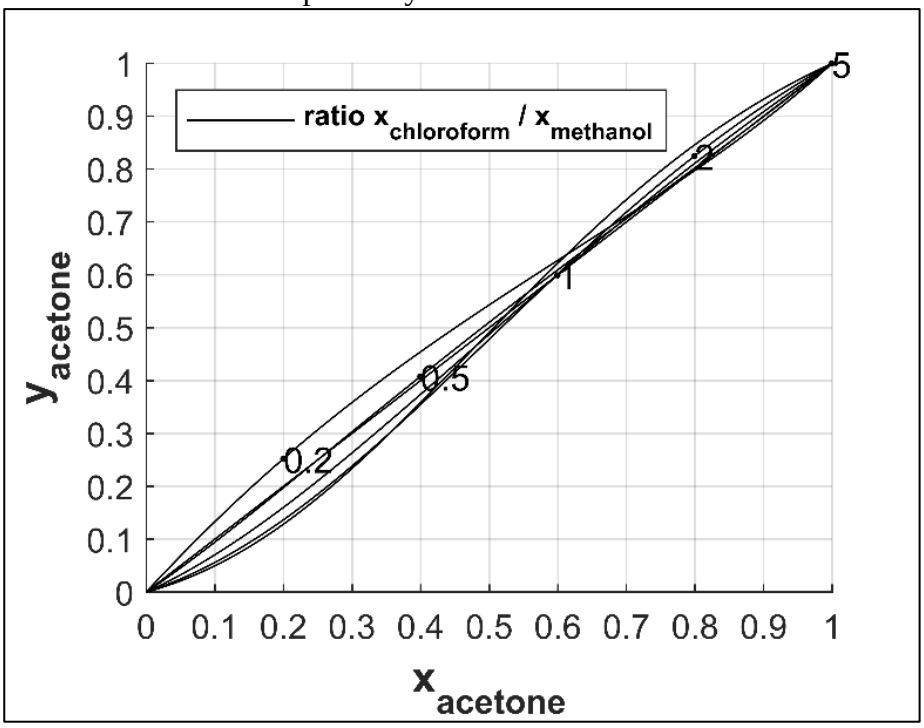

(a)

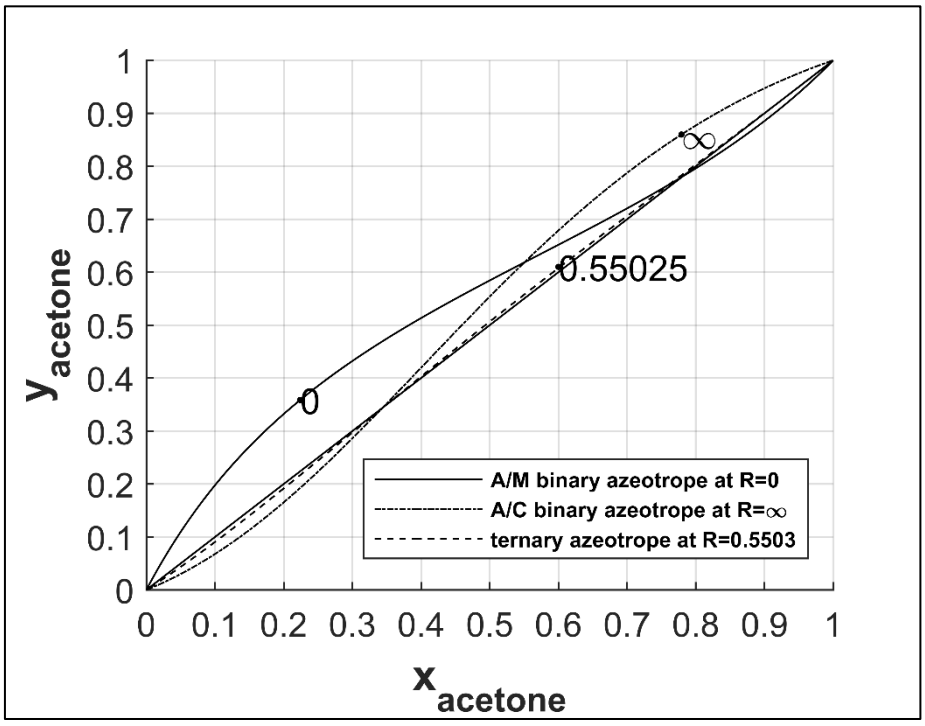

(b)

Figure 3.17: (a) Contours of VLE for acetone at different ratios of chloroform / methanol, (b) Contours of VLE representing the binary and ternary azeotropes for acetone and the corresponding ratios

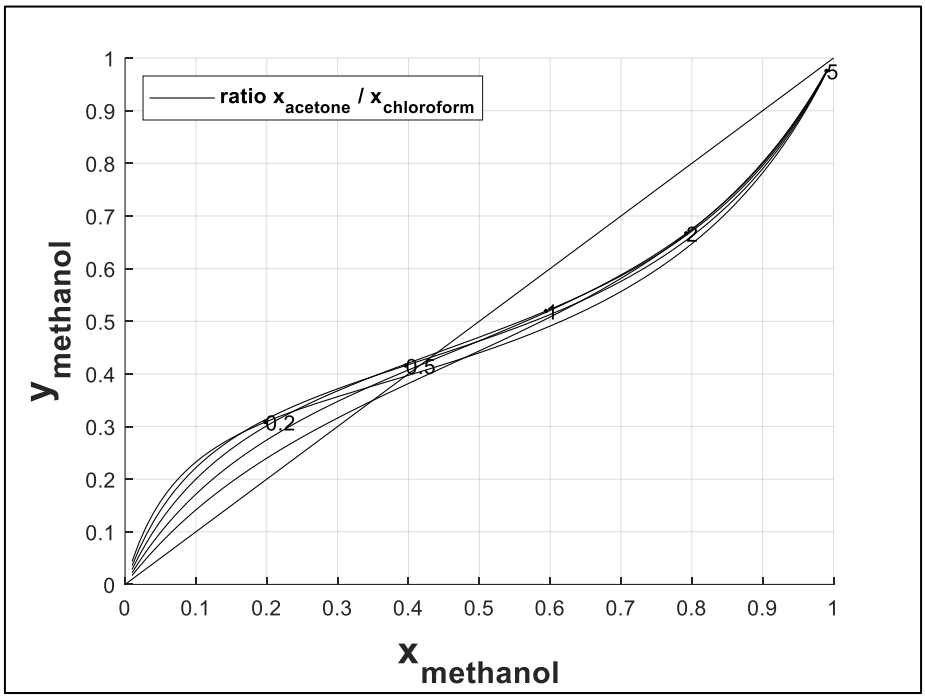

(a)

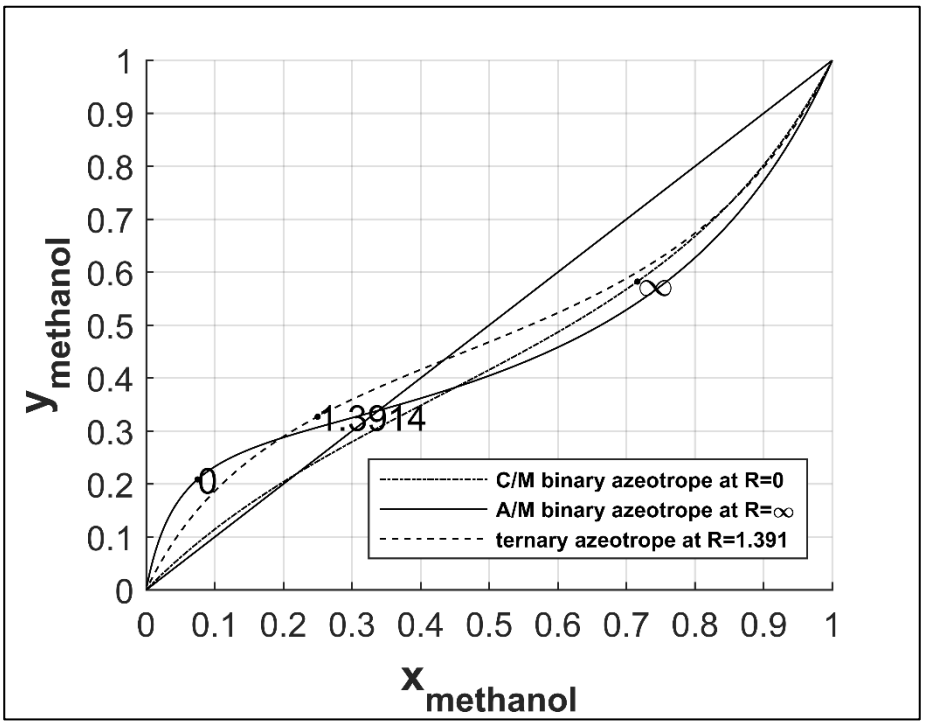

(b)

Figure 3.18: (a) Contours of VLE for methanol at different ratios of acetone / chloroform, (b) Contours of VLE representing the binary and ternary azeotropes for methanol and the corresponding ratios

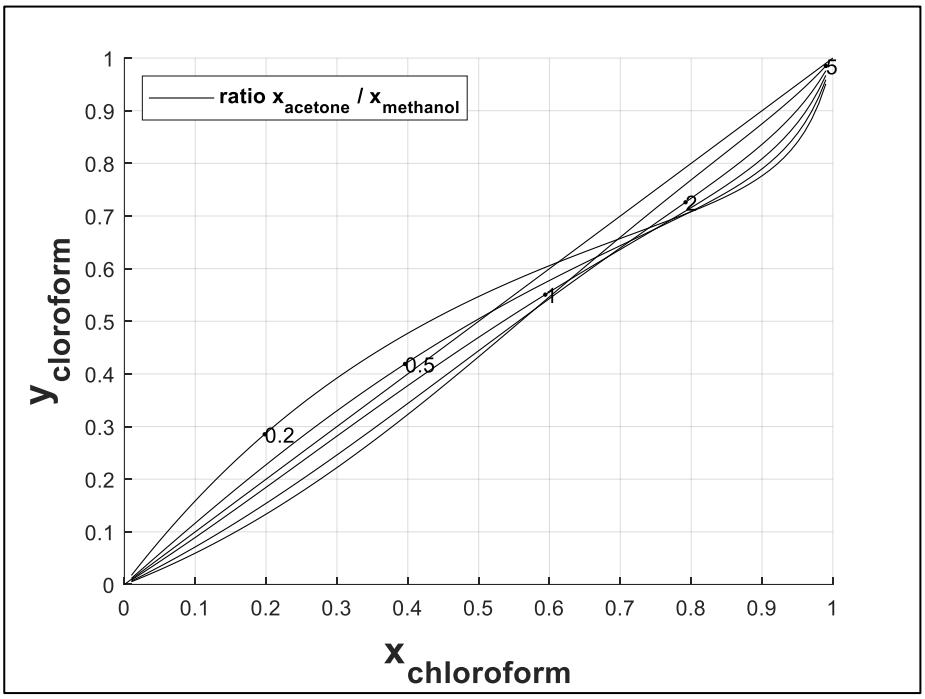

(a)

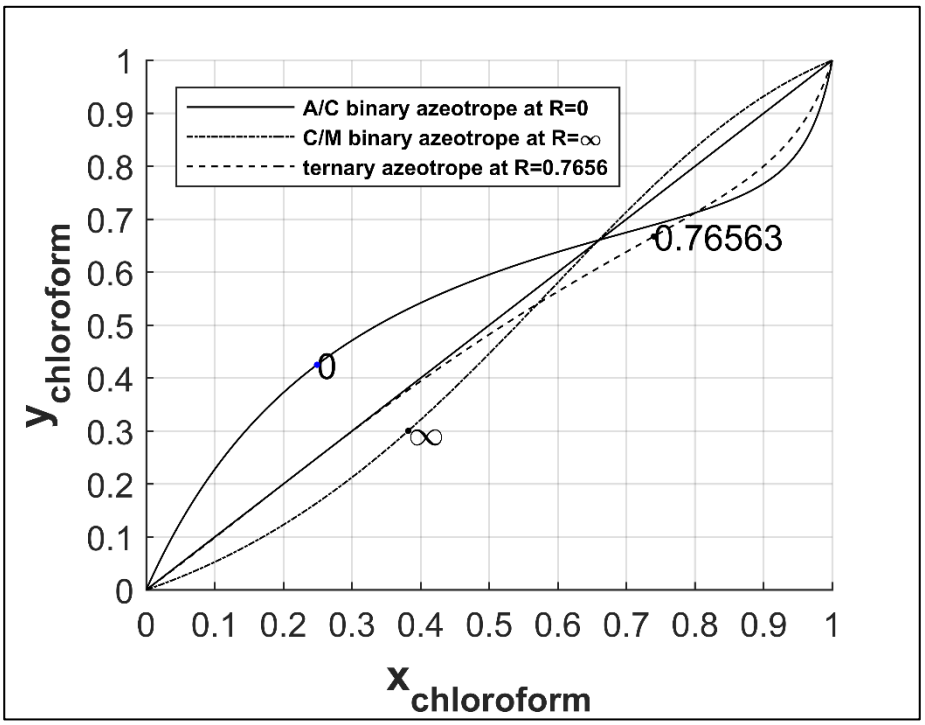

(b)

Figure 3.19: (a) Contours of VLE for chloroform at different ratios of acetone / methanol, (b) Contours of VLE representing the binary and ternary azeotropes for chloroform and the corresponding ratios

3.3.2.4 Example 3.5: Tangent pinch system (acetone, ethanol and water)

Tangent pinches often occur in non-ideal binary and multicomponent mixtures. A tangent pinch can only exist if there is an inflection in the equilibrium x-y relationship and which can be identified visually from a McCabe-Thiele diagram for binary systems (Górak & Sorensen, 2014). For binary systems, a tangent pinch is depicted by multiple intersections of the equilibrium curve and operating line (Górak & Sorensen, 2014). Tangent pinch points are of interest because they may cause severe changes in minimum energy requirements and impact distillation design (as with azeotropic distillation) (Koehler et al., 1995; Levy & Doherty, 1986).

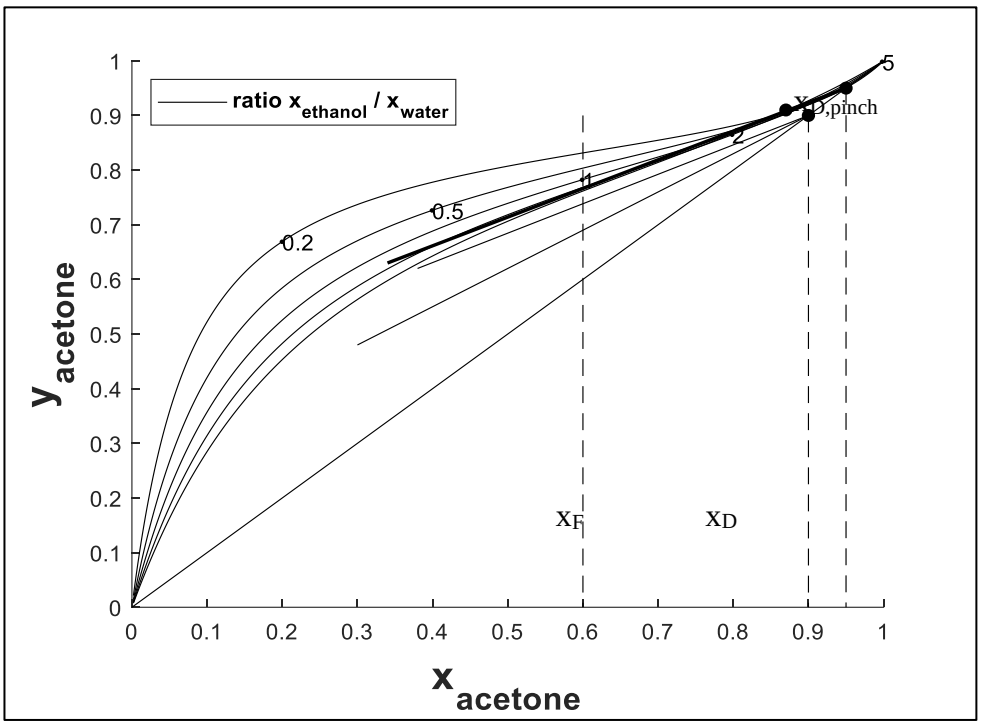

Figure 3.20: Illustration of a tangent pinch in acetone for the ternary system acetone, ethanol, water

Example 3.5 sows that, analogous to binary McCabe-Thiele diagrams, tangent pinch points can be identified visually for ternary mixtures on an x-y plot using the method of plotting contours of VLE presented in this chapter. A system of acetone-ethanol-water yields a tangent pinch for acetone in the rectifying section. In considering Figure 3.20, for a given separation and specified feed composition, there is a critical distillate product ($x_{D,\ pinch}$) for acetone below which no tangent pinch can occur, regardless of the reflux ratio. Likewise, if a tangent pinch exists in the stripping section there is a critical bottoms product ($x_{B,\ pinch}$) above which no tangent will occur. Binary VLE is represented as a single unique equilibrium curve and a single unique $x_{D,\ pinch}$ exists. For ternary mixtures, the contours of VLE are represented as many equilibrium curves as a function of the other components in the system. Depending on the nature of the contours of VLE, the $x_{D,\ pinch}$ will change.

3.4 Conclusion

This chapter postulates a novel approach to calculating and depicting the vapour-liquid equilibrium (VLE) for ternary ideal and non-ideal systems as contours on a 2D x-y plot. The method for determining the contours of VLE is generic and uses any thermodynamic model or experimental data. Illustrative examples show that the representation of contours of VLE provide the designer with an insight into the behaviour (simple or difficult separation, azeotropes and tangent pinches) of all the components in the system. With the visual picture of the behaviour of a system, the designer is able to determine if the type of separation is simple or difficult, and can take the necessary design decisions to determine the correct operating parameters for a distillation column. Non-ideal behaviour in the form of azeotropes and inflection points can also be visualised and taken into consideration to achieve product specifications.

REFERENCES

Almeida-Rivera, C.P., Swinkels, P.L.J., Grievink, J., **2004**. Designing reactive distillation processes: present and future. *Comp. Chem. Eng*. 28(10), pp. 1997-2020.

Brown, G.G., Sauders, M., Nyland, H.V., **1932**. V. Fundamental Design of Fractionating Columns for Complex Mixtures. *Ind. Eng. Chem.* 24(5), pp. 522-527.

Castillo, F.J.L. & Towler, G.P., **1998**. Influence of multicomponent mass transfer on homogeneous azeotropic distillation. *Chem. Eng. Sci*. 53(5), pp. 963-976.

Cope, J.Q. & Lewis, W.K., **1932**. Studies in Distillation-Graphical Method of Computation for Rectifying Complex Hydrocarbon Mixtures. *Ind. Eng. Chem.* 24(5), pp. 498-501.

Doherty, M.F. & Caldarola, G.A., **1985**. Design and Synthesis of Homogeneous Azeotropic Distillation. 3. The Sequencing of Columns for Azeotropic and Extractive Distillation. *Ind. Eng. Chem. Fundam.* 24(4), pp. 474-485.

Ewell, R.H. & Welch, L.M., **1945**. Rectification in Ternary Systems Containing Binary Azeotropes. *Ind. Eng. Chem.* 37(12), pp. 1224-1231.

Fidkowski, Z.T., Malone, M.F., Doherty, M.F., **1991**. Nonideal Multicomponent Distillation: Use of Bifurcation Theory for Design. *AIChE J*. 37(12), pp. 1761-1779.

Gamba, S., Soave, G.D., Pellegrini, L.A., **2009**. Use of normal boiling point correlations for predicting critical parameters of paraffins for vapour-liquid equilibrium calculations with the SRK equation of state. *Fluid Phase Equilib*. 276(2), pp. 133-141.

Gani, R. & Bek-Pedersen, E., **2000**. Simple New Algorithm for Distillation Column Design. *AIChE J*. 46(6), pp. 1271-1274.

Górak, A. & Sorensen, E., **2014**. Distillation: Fundamentals and Principles. *Elsevier: Academic Press*: London.

Hengstebeck, R.J., **1946**. A Simplified Method for Solving Multicomponent Distillation Problems. *Trans. AIChE*. 42, pp. 309-329.

Hengstebeck, R.J., **1961**. Distillation: Principles and Design Procedures. *Reinhold Publishing Corp:* New York.

Hilmen, E.K., **2000**. Separation of Azeotropic Mixtures: Tools for Analysis and Studies in Batch Distillation Operation. Dr. Ing. Thesis. Norwegian University of Science and Technology. Trondheim.

Ho, T.J., Huang, C.T., Lee, L.S., Chen, C.T, **2010**. Extended Ponchon-Savarit Method for Graphically Analyzing and Designing Internally Heat-Integrated Distillation Columns. *Ind. Eng. Chem. Res*. 49(1), pp. 350-358.

Jenny, F.J., **1939**. Graphical solution of problems in multicomponent fractionation. *Trans. Am. Inst. Chem. Eng.* 35, pp. 635-677.

Kister, H.Z., **1992**. Distillation Design. *McGraw-Hill, Inc: USA.*

Kister, H.Z., **1995**. Troubleshoot Distillation Simulations. *Chem. Eng. Prog*. 91(6) pp. 63-75.

Kiva, V.N., Hilem, E.K., Skogestad, S., **2003**. Azeotropic phase equilibrium diagrams: a survey. *Chem. Eng. Sci*. 58(10), pp. 1903-1953.

Koehler, J., Poellmann, P., Blass E., **1995**. A Review on Minimum Energy Calculations for Ideal and Nonideal Distillations. *Ind. Eng. Chem. Res*. 34(4), pp. 1003-1020.

Kojima, K., Katsumi, T., Kiyofumi, K., Mikiyoshi, N., **1991**. Isobaric vapor-liquid equilibria for acetone+benzene+chloroform and the three constituent binary systems. J. *Chem. Eng. Data.* 36(3), pp. 343-345.

Lee, J.W., Hauan, S., Lien, K.M., Westerberg, A.W., **2000a**. A graphical method for designing reactive distillation columns. I. The Ponchon-Savarit method. P*roceedings of the Royal Society of London*. 456(2000), pp. 1953-1964.

Lee, J.W., Hauan, S., Lien, K.M., Westerberg, A.W., **2000b**. A graphical method for designing reactive distillation columns. II. The McCabe-Thiele method. P*roceedings of the Royal Society of London*. 456(2000), pp. 1965-1978.

Levy, S.G. & Doherty, M.F., **1986**. A simple exact method for calculating tangent pinch points in multicomponent nonideal mixtures by bifurcation theory. *Chem. Eng. Sci*. 41(12), pp. 3155-3160.

Luyben, W.L., **2008**. Control of the Maximum-Boiling Acetone/Chloroform Azeotropic Distillation. *Ind. Eng. Chem. Res*. 47(16), pp. 6140-6149.

Mathias, P.M., **2009**. Visualizing the McCabe-Thiele Diagram. *Chem. Eng. Prog*. 105(12), pp. 36-44.

Mathias, P.M., **2016**. Effect of VLE uncertainties on the design of separation sequences by distillation-Study of the benzene-chloroform-acetone system. *Fluid Phase Equilib*. 408, pp. 265-272.

McCabe, W.L. & Thiele, E.W., **1925**. Graphical Design of Fractionating Columns. *Ind. Eng. Chem.* 17(6), pp. 605-611.

Partin, L.R., **1993**. Use Graphical Techniques to Improve Process Analysis. *Chem. Eng. Prog*. 89(1), pp. 43-48.

Rooks, R.E., Julka, V., Doherty, M.F., Malone, M.F., **1998**. Structure of distillation regions for multicomponent azeotropic mixtures. *AIChE J*. 44(6), pp. 1382-1391.

Ryan, J.M., **2001**. Replotting the McCabe-Thiele Diagram. *Chem. Eng.* 108(5), pp. 109-113.

Skiborowski, M., Recker, S., Marquardt, W., **2018**. Shortcut-based optimization of distillation-based processes by a novel reformulation of the feed angle method. *Chem. Eng. Res. Des*. 132, pp. 135-148.

Wahnschafft, O.M., Koehler, J.M., Blass, E., Westerberg, A.W., **1992**. The Product Composition Regions of Single-Deed Azeotropic Distillation Columns. *Ind. Eng. Chem. Res.* 31(10), pp. 2345-2362.

Wahnschafft, O.M. & Westerberg, A.W., **1993**. The Product Composition Regions of Azeotropic Distillation Columns. 2. Separation in Two-Feed Columns and Entrainer Selection. *Ind. Eng. Chem. Res*. 32(6), pp. 1108-1120.

Wasylkiewicz, S.K., Kobylka, L.C., Castillo, F.J.L., **2000**. Optimal design of complex azeotropic distillation columns. *Chem. Eng. J.* 79(3), pp. 219-227.

Chapter 4

Minimum Number of Stages at Total Reflux for Distillation Design

The work in this chapter has been published in**:** Seedat, N., Kauchali, S., Patel, B., **2020**. Novel representation of vapour-liquid equilibrium curves for multicomponent systems: design of total reflux distillation columns. *Chem. Eng. Res. Des*. 155, pP. 22-39

The work is a reproduction of the journal publication although some formatting changes have been made for the purpose of adhering to the standards of this thesis as well as simplifying the work for clarity and easy understanding. The reproduction was done with permission.

Abstract

The method of plotting the novel contours of vapour-liquid equilibrium (VLE) for a ternary ideal and for non-ideal systems is presented in Chapter 3. Chapter 4 introduces the procedure for calculating the minimum number of stages at total reflux for ideal and non-ideal ternary systems. The minimum number of stages obtained from the graphical method correlates with the Fenske Equation for ideal systems. Several simulations for non-ideal systems of acetone, benzene and chloroform are generated using Aspen Plus^{TM} to validate the proposed graphical method. It is shown that the proposed graphical method correlates more closely with rigorous simulations than traditional methods. Lastly, it is shown that the proposed graphical method correlates more closely with rigorous simulations than the method proposed by Hengstebeck (1946).

4.1 Introduction

Wankat (2012) emphasises the usefulness of looking at limiting conditions in separation processes. For distillation, there are two limiting conditions: total reflux and minimum reflux. Minimum reflux will be presented in Chapter 5. Knowledge of operation at total reflux is particularly important in the following situations (Wankat, 2012):

- Start- up of columns
- When certain sections of the plant are shut down or under maintenance total reflux allows the distillation column to continue operating
- For testing column efficiency

The maximum separation that can be obtained with a given number of stages, but with no throughput, is determined at total reflux (Wankat, 2012). Additionally, at total reflux, the minimum number of stages to obtain the required product specification is determined. Hence, if a column is designed with a reduced number of stages, the product specification will not be achieved.

Short-cut methods and graphical methods are frequently used by designers to determine preliminary design parameters. Short-cut empirical methods make use of limiting assumptions, such as constant relative volatility (CRV) and constant molar overflow (CMO) (Reyes et al., 2000). The Fenske-Underwood-Gilliland (FUG) method is a popular short-cut method for the design of ideal liquid mixtures (Thong & Jobson, 2001). The FUG method is extensively used to determine the effect of reflux ratio on the investment and operational costs with simple calculations, although these values produce inaccuracies and uncertainties (Van Winkle, 1967; Kister, 1992). The main reasons for these inaccuracies are the limiting assumptions of CRV and CMO. Even though short-cut methods are limited by the above-stated assumptions, they are still used in industry as the designer is provided with initial estimates (which may not be very accurate but could suffice as a good starting point) from performing fairly simple calculations quickly.

The Fenske (1932) and Winn (1958) equations calculate the minimum number of stages for ideal binary and multicomponent systems. The Fenske (1932) equation assumes constant relative volatilities, (α), whereas the Winn (1958) equation uses the vapour−liquid equilibrium constant, (K). The Winn equation is deemed more robust than the Fenske equation for systems in which the relative volatility is strongly dependent on temperature (Cao et al., 2014). Nevertheless, both equations are limited to ideal systems.

Castillo et al., (1998) proposed the stage composition line method that is an extension of the residue curve and distillation line methods. The stage composition line method is applicable to ternary systems and can be used to determine the feasible separation, minimum reflux and minimum number of stages. A stage composition line is defined as the locus of liquid compositions on a given stage, at any reflux or boil up ratio (Thong et al., 2000). The stage composition lines are plotted for the rectifying and stripping section at the specified reflux and boil up ratio respectively (Thong et al., 2000). If the stage composition lines of the rectifying and stripping sections intersect, the separation is feasible (Thong et al., 2000). The minimum number of stages required is obtained by counting the lines up to the point of intersection respectively (Thong et al., 2000). According to Thong & Jobson (2001) a reliable design method to determine the theoretical minimum number of stages for non-ideal systems is limited.

The McCabe-Thiele method for determining the minimum number of stages for a binary separation is simple and effective. A similar graphical method for higher order systems is lacking. With the establishment of the novel method of plotting the contours of VLE in Chapter 3, students and designers alike can now determine the minimum number of stages effectively with minimal calculations using a slightly modified method of the original McCabe-Thiele method.

This chapter presents the procedure for preliminary distillation design at total reflux for both ternary ideal and non-ideal systems. The method has been extended to higher order systems in Chapter 6. The number of stages and product compositions

can be read off directly from the produced diagrams. A comparison and validation of the results obtained using the proposed graphical method at total reflux to a rigorous simulation method using the RadFrac column in Aspen Plus^{TM} is presented. In addition, it will be shown that once the novel contours of VLE have been generated and plotted, a manual calculation can be performed on the plot to obtain accurate values in comparison to computer generated solutions. Lastly, a comparison of the proposed graphical method, proposed in this thesis, with the method by Hengstebeck (1946), for a non-ideal system, is established.

4.2 McCabe-Thiele Method at Total Reflux

Operation of a single adiabatic distillation column, such that all the vapour leaving the top stage is condensed and returned back to the column as a liquid reflux, is said to be operating at the limiting condition of total reflux (Wahnschafft et al., 1992). Since no product is withdrawn from the column, the internal streams and their corresponding composition profiles are not affected by the feed stream, hence the entire column can be considered as a single section (Górak & Sorensen, 2014). At total reflux, the operating lines in both the rectifying and stripping sections approach unity and coincide with the 45 degree line (McCabe & Thiele, 1925). At the limiting condition of total reflux, the number of stages is determined by stepping between the equilibrium curve and the 45 degree line. The number of stages determined in this manner yields the minimum number of stages required for a specified separation (Mathias, 2009). For simplification, the same assumptions are made in accordance with the assumptions made for the binary McCabe-Thiele method namely (Kister, 1992):

- Constant molal overflow (CMO)
- Vapour and liquid on a tray are in equilibrium
- Tray efficiency is 100%
- Constant heat of vaporization
- Sensible heat and heat of mixing effects is negligible
- Heat losses to surroundings are negligible

- Constant pressure.

The McCabe-Thiele method, using the novel representation of the contours of VLE proposed in this thesis, will be presented in several examples for ideal and non-ideal mixtures. The objective of these examples is to show that the application of the traditional McCabe-Thiele method for practical use has been retained by applying the proposed method of representing the VLE data.

4.2.1 Example 4.1: Total Reflux - Ideal System (n-hexane, n-heptane and n-nonane)

Consider the following design problem: a mixture of n-hexane, n-heptane and n-nonane is fed into a total reflux column at constant pressure (1 bar). The bottoms product composition (mole fraction) is specified in Table 4.1. It is required to achieve a minimum distillate product composition for n-hexane of 0.9 (mole fraction). The minimum number of stages and the distillate product composition for the specified separation is to be determined. Since the bottoms composition is specified, the number of stages will be determined from the bottoms composition to the distillate composition.

Table 4.1: The liquid bottom product composition for n-hexane, n-heptane and n-nonane

Component	x_B (mole fraction)	x_D (mole fraction)	Relative volatility (α)
n-hexane	0.100	0.922	7.03
n-heptane	0.300	0.0773	3.44
n-nonane	0.600	0.000322	1.00

The computational solution involves the following algorithm:

1. Consider the first component, n-hexane. Calculate the first ratio for n-hexane (defined in Equation 3.1a) using the given liquid bottoms product composition. $CR_{1,C7/C9} = x_{C7}/ x_{C9} = 0.3/0.6 = 0.500$.

2. Calculate the first ratio for n-heptane (defined in Equation 3.2a) using the given liquid bottoms product composition. $CR_{1,C6/C9} = x_{C6} / x_{C9} = 0.1/0.6 = 0.167$.
3. Using the ratios calculated in steps 1-2, determine the VLE contour that represents the ratio using the method from bottoms to distillate compositions presented in Figure 3.1 for all components.
4. Move vertically towards the VLE contour determined in step 3 to determine the equilibrium composition of the vapour (y_{eqm}) at x_B.
5. Move horizontally towards the 45 degree line. Determine the new liquid composition from $x_1 = y_{eqm}$.
6. Calculate the second ratio (steps 1-2) using the new composition obtained in step 6 for all the components, and repeat steps 3-5.

For the simple separation in this example, the relative volatilities in Table 4.1 were used to plot the VLE curves for the ideal components. Figures 4.1 – 4.3 depict the McCabe-Thiele diagrams for n-hexane, n-heptane and n-nonane respectively, at total reflux.

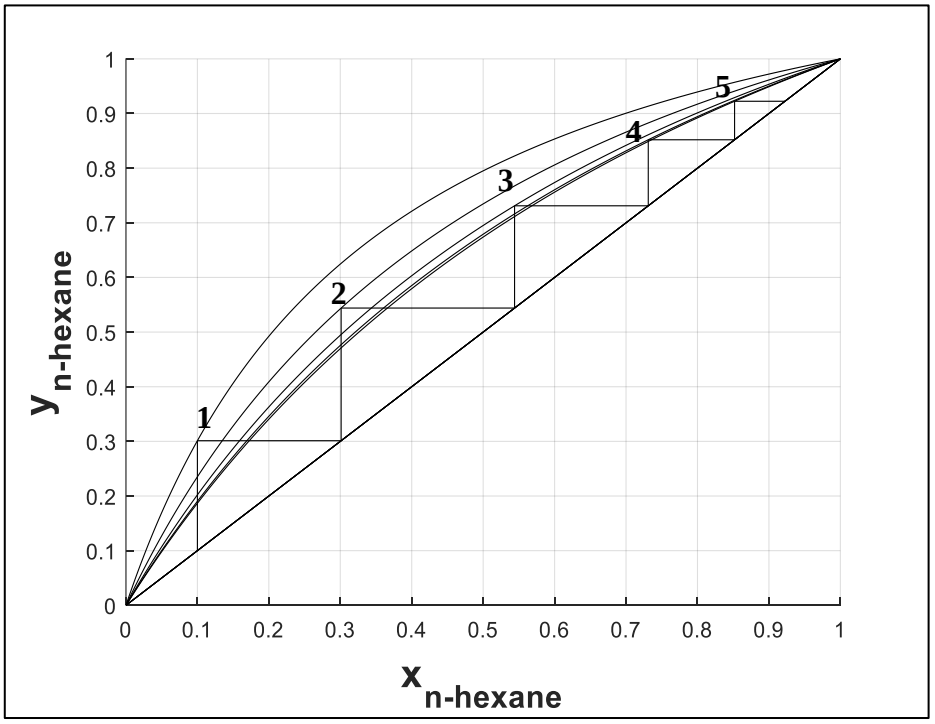

Figure 4.1: Minimum number of stages determined from stepping from the bottoms to distillate composition at total reflux using the McCabe-Thiele method for n-hexane

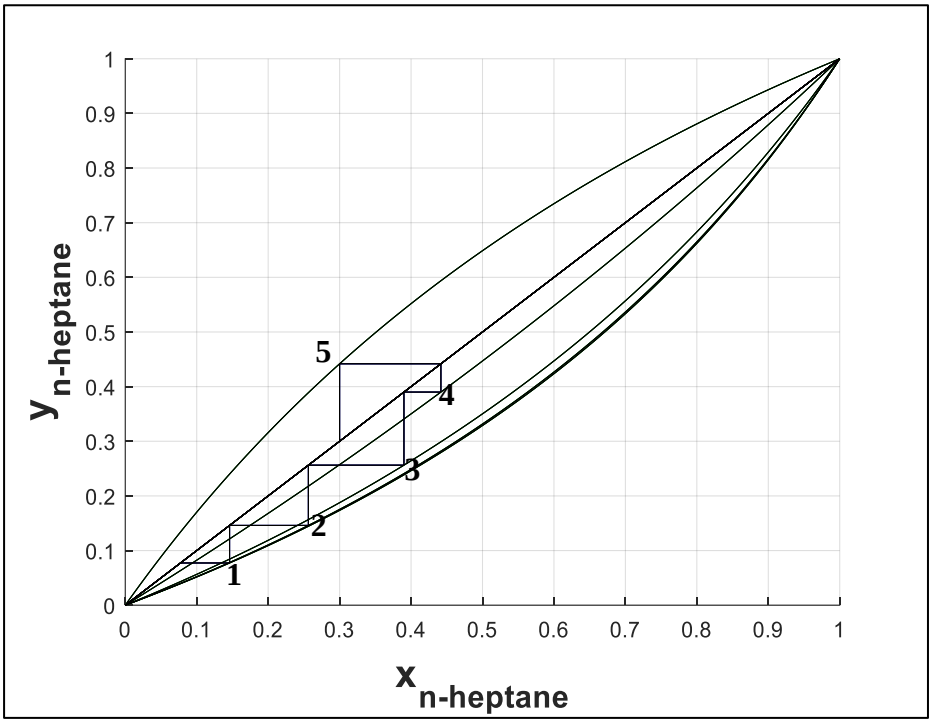

Figure 4.2: Minimum number of stages from stepping from the bottoms to distillate composition at total reflux using the McCabe-Thiele method for n-heptane

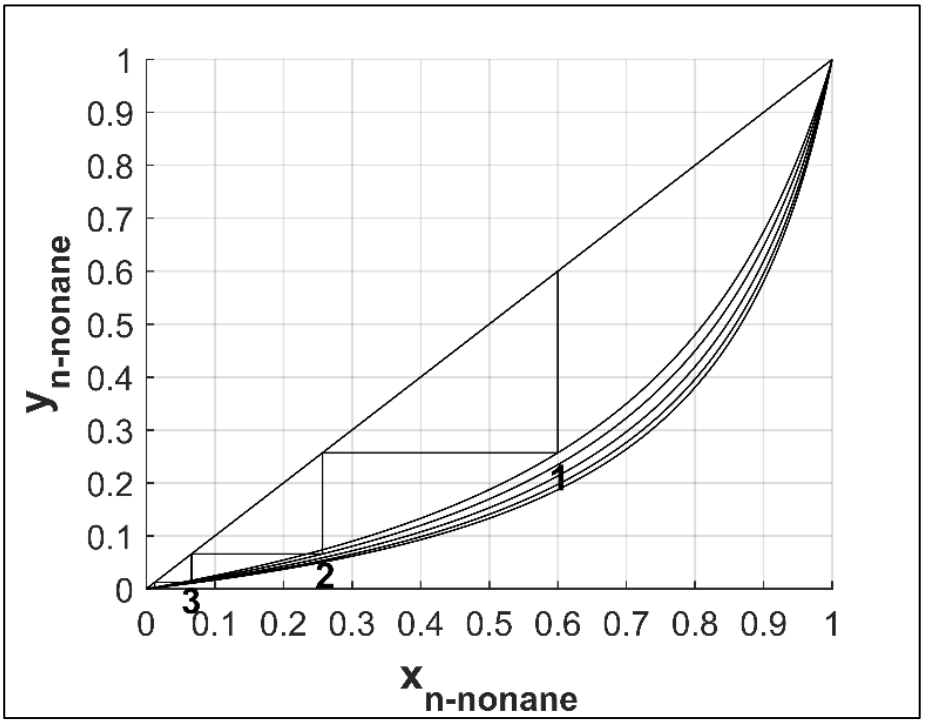

(a)

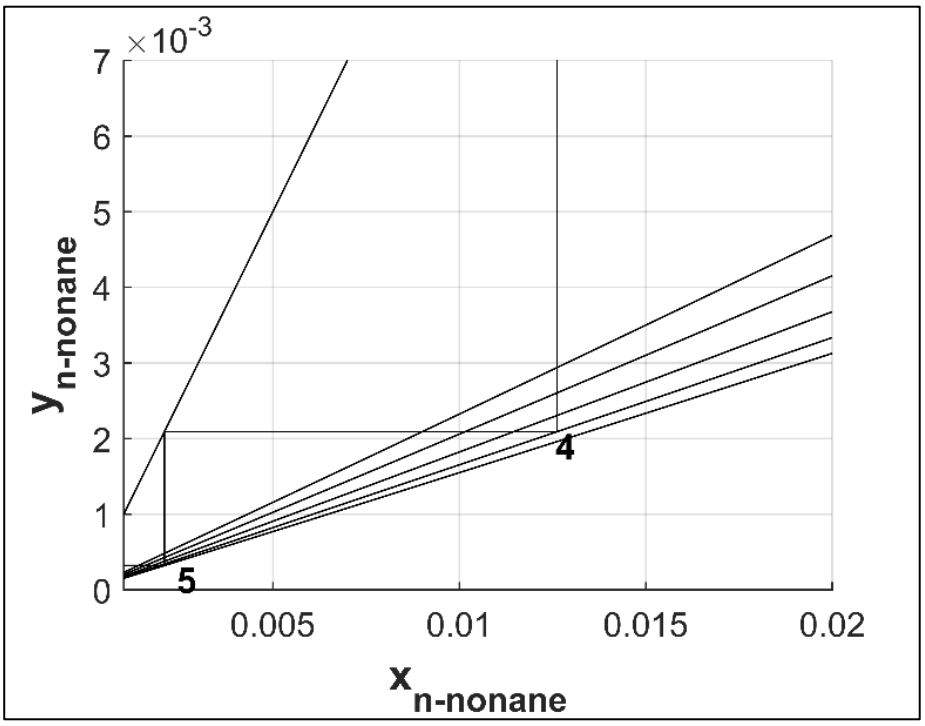

(b)

Figure 4.3: (a) Minimum number of stages from stepping from the bottoms to distillate composition at total reflux using the McCabe-Thiele method for n-nonane, (b) enlargement to show the last two stages of the simulation

The minimum number of stages required to achieve a distillate product of 0.9224 for n-hexane is 5 stages. The final liquid distillate composition is presented in Table 4.1. Since the system is nearly ideal and constant relative volatility is assumed, the Fenske (1932) equation can be applied to determine the minimum number of stages for the specified simulation. The Fenske equation yields 5.0 stages including a partial reboiler (The full calculation can be found in Appendix C). The minimum number of stages determined using the Fenske equation is consistent with the 5 stages required using the McCabe-Thiele method and the algorithm of plotting the contours of VLE. The distillate product is rich in n-hexane and contains very little of the other components and represents a simple, sharp separation. In this example, the method of determining the number of stages from the bottoms product composition towards the set distillate composition is shown. The method of determining the number of stages from a specified distillate product to the bottoms product composition will be shown in Example 4.2.

4.2.2 Example 4.2: Total Reflux - Non-Ideal System (acetone, benzene, chloroform)

Design problem: A mixture of acetone, benzene and chloroform is fed to a total reflux column at constant pressure (1 bar). The distillate product composition (mole fraction) is specified in Table 4.2. It is required to achieve a minimum bottoms product composition for acetone of 0.250 (mole fraction). Determine the minimum number of stages and the distillate product composition for the specified separation.

Table 4.2: The vapour distillate product composition for acetone, benzene and chloroform

Component	y_D (mole fraction)	x_B (mole fraction)
Acetone	0.952	0.250
Benzene	0.0230	0.300
Chloroform	0.0250	0.450

In this example the algorithm for determining the number of stages from a specified distillate composition to the bottoms composition we will demonstrated. This is the manner in which calculating the number of stages has been adopted for the binary McCabe-Thiele method. In addition, the results from determining the number of stages from the distillate to bottoms will be compared with the number of stages determined from the bottoms to distillate.

The solution for determining the number of stages from the distillate product to the bottoms product involves the following algorithm:

1. Consider the first component, acetone. Calculate the first ratio (defined in Equation 3.1b) for acetone, using the given distillate vapour product composition. $CR_{1,\,(benzene/acetone)} = y_{benzene} / y_{chloroform} = 0.0230/0.250 = 0.920$.
2. Calculate the first ratio for benzene (defined in Equation 3.2b) using the given bottoms product composition. $CR_{1,\,(acetone/chloroform)} = y_{acetone} / y_{chloroform} = 0.952/0.0250 = 38.1$.
3. Using the ratios calculated in steps 1-2, generate the VLE contour that represents the ratio using the method from distillate to bottoms compositions presented in Figure 3.1 for all components.
4. Move horizontally towards the VLE contour determined in step 3 to determine the equilibrium composition of the liquid (x_{eqm}) at x_D.
5. Move vertically towards the 45 degree line. Determine the composition of the new vapour composition from $y_1 = x_{eqm}$.
6. Calculate the second ratio (steps 1-2) using the new vapour composition obtained in step 6 for all the components and repeat steps 3-5.

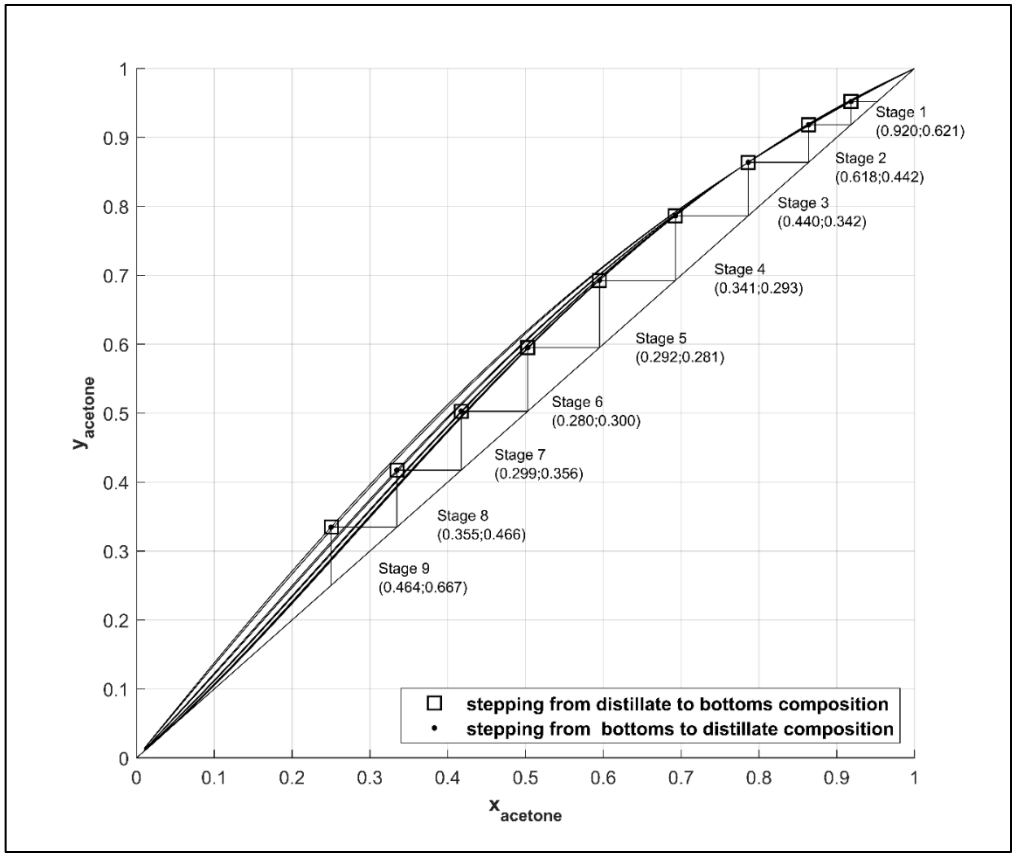

Figure 4.4: McCabe-Thiele diagram for acetone comparing the number of stages determined from distillate to bottoms composition and from bottoms to distillate composition

The minimum number of stages required to achieve a bottoms product of 0.250 for acetone is 9 stages. The final liquid distillate composition is presented in Table 4.2. The results obtained from calculating the number of stages from the bottoms compositions to the distillate composition was solved using the algorithm presented in Example 4.1. The bottoms product given in Table 4.2, and limiting the acetone composition in the distillate to 0.952 (Table 4.2), was used as the design specification. Figure 4.4 depicts the comparison of the equilibrium compositions on each stage for determining the number of stages from the distillate to bottoms and from the bottoms to the distillate. Each equilibrium point, from moving in either direction, is the same and lies on the same VLE contour at each stage. Hence, both methods of determining the number of stages produce the same results. Figure 4.2 shows that each contour represents two ratios (defined in Example 4.1). The element of the first vector represents the vapour mole fraction ratios, used to

determine the number of stages from the distillate composition. The second element in the vector represents the liquid mole fraction ratio, used to calculate the number of stages from the bottoms composition.

4.3 Rigorous Simulations

In this section, a rigorous stage by stage Aspen Plus™ simulation will be implemented in order to validate the accuracy of the results obtained from the proposed graphical method for ternary systems. The RadFrac column was used in Aspen Plus™ in order to obtain the closest simulation to total reflux. The RadFrac column also provides the compositions of the components on each stage. A comparison of the Aspen Plus™ compositions to the proposed graphical method compositions on each stage will be made. The composition on each stage obtained from Aspen Plus™ will be compared to the value obtained from the proposed graphical method by two representations. The first representation will plot the Aspen Plus™ and the proposed graphical method compositions on a McCabe-Thiele diagram as validation that the behaviour of the components is correctly predicted by the novel method for representing the contours of VLE. The second representation plots the compositions obtained from the proposed graphical method and Aspen Plus™ compositions on a residue curve map (RCM) for a ternary system. A simulation in each distillation region will be analysed to determine operation in both regions.

4.3.1 Example 4.3: Total Reflux - Rigorous Simulation

Rigorous simulations were generated in each distillation region for a ternary system of acetone, benzene and chloroform at total reflux. The feed compositions for both distillation regions in Table 4.3 were used as inputs to initialise the rigorous simulations in Aspen Plus™. The distillate and bottoms compositions obtained from the rigorous simulations were used as inputs to determine the compositions on each stage using the proposed graphical method.

Rigorous simulation configuration: The equilibrium column is set up as follows: the number of stages is required as an input and the feed is introduced at the bottom of the column on the stage above the reboiler. A high reboil rate is set whilst the distillate flowrate is set to almost zero. The pressure of all the streams and the column were set at 1 bar.

Table 4.3: Feed compositions and results for simulations in both distillation regions using Aspen Plus™

	Region A			Region B		
Component	x_F	x_B	x_D	x_F	x_B	x_D
Acetone	0.1	0.0991	0.999	0.04984	0.0499	0.000867
Benzene	0.7	0.701	0.000739	0.52516	0.526	1.33E-05
Chloroform	0.2	0.200	5.39E-07	0.425	0.424	0.999

The converged rigorous simulation results for the distillate and bottoms compositions are given in Table 4.3. For simplification of convergence of the proposed graphical method, the distillate compositions are limited to 0.999 for acetone and chloroform in regions A and B respectively. The converged values are entered into the proposed graphical method to obtain the compositions on each tray. Figures 4.6a and 4.6b plot the comparisons of the Aspen Plus™ and proposed graphical method for acetone in region A and region B (Figure 4.5) on an x-y diagram respectively. It is clear that the results of both methods produce the same compositions on each stage. The correlation validates the proposed graphical method and establishes the use of the method as a preliminary design tool in conjunction with a rigorous simulation for detailed design and optimization procedures.

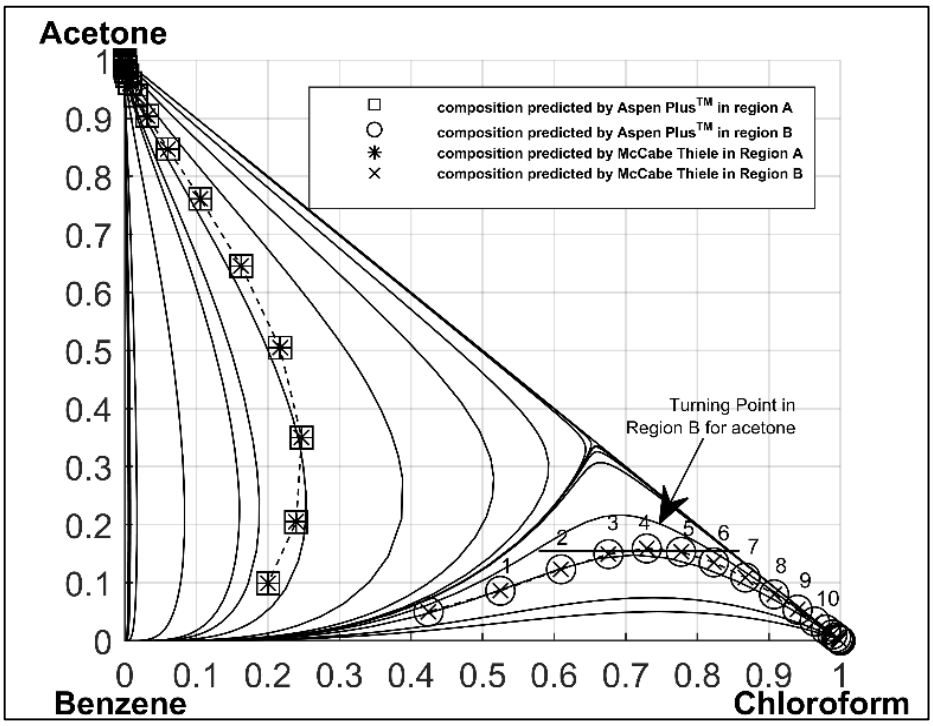

Figure 4.5: RCM depicting the results of the Aspen Plus™ simulation and the proposed graphical method

Figure 4.5 depicts the Aspen Plus™ and the proposed graphical method in this chapter, results from the simulations solved in Example 4.3 on an RCM. The liquid compositions on each stage for the Aspen Plus™ simulations, as well as the proposed graphical method, follow a 'curve' in each region and do not cross the distillation boundary. It should also be noted that the 'curve' that the results follow does not follow a residue curve as depicted in Figure 4.5, the RCM for acetone, benzene and chloroform. This 'curve' is defined as the distillation line. Residue curves and distillation lines differ as they represent the composition profiles in packed and staged columns at total reflux respectively (Górak & Sorensen, 2014). Distillation lines are less popular than residue curves but are equally useful for synthesis and design of distillation columns (Castillo & Towler, 1998). Distillation lines are classified as discrete points (not represented by a solid line) that represent the composition of the liquid on each stage of a column at total reflux (Castillo & Towler, 1998). Plotting the liquid compositions on each stage, obtained using the

proposed graphical method for several separations, will produce a series of distillation lines in the composition space.

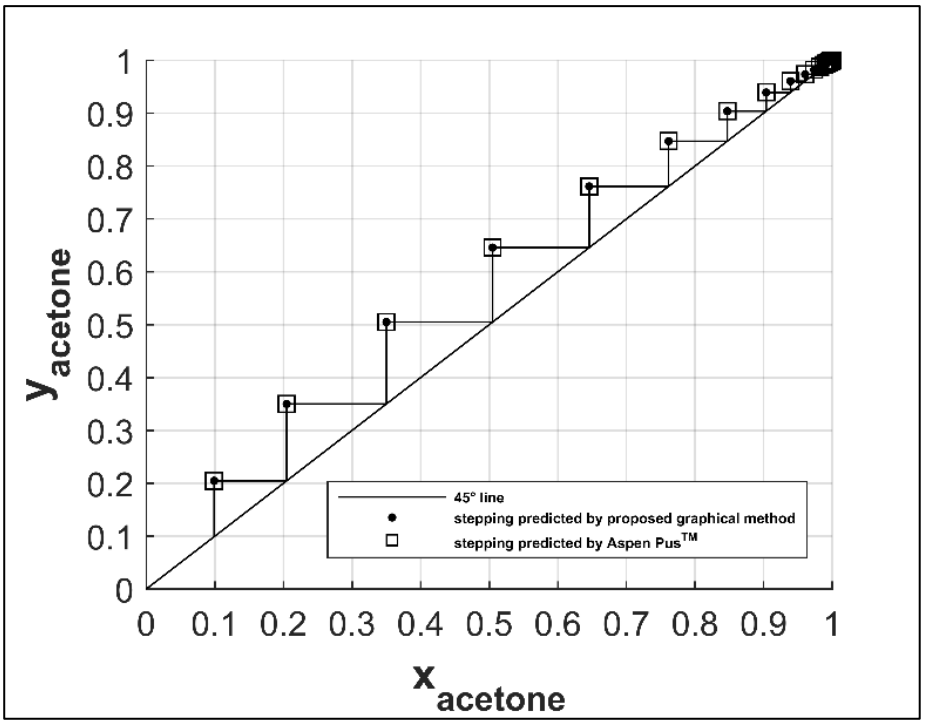

(a)

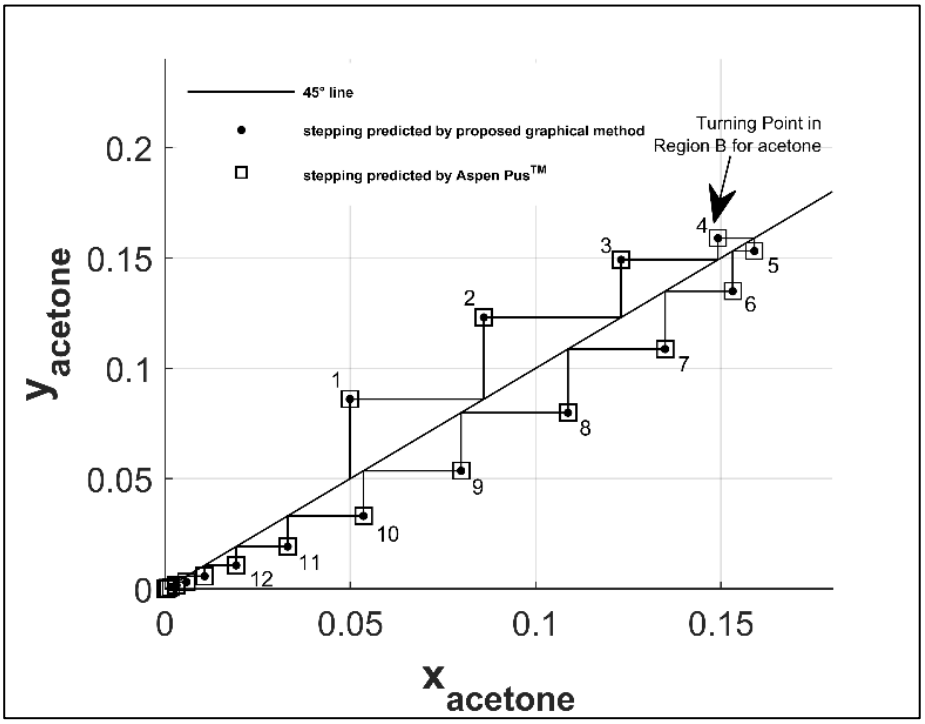

(b)

Figure 4.6: (a) Comparison of Aspen Plus™ simulation and the McCabe-Thiele method for acetone in distillation region A, (b) Comparison of Aspen Plus™ simulation and the McCabe-Thiele method for acetone in distillation region B

Hence the proposed graphical method would be very useful in the generation of distillation line maps. In distillation region B (Figure 4.6b), the mole fraction of acetone increases until stage 4 (the point at which the VLE contour crosses the 45 degree line). Stage 4 represents the maximum mole fraction reached on the distillation line (Figure 4.5) which the simulation is following. The point that represents the maximum mole fraction is the turning point, after which the mole fraction of acetone decreases until the bottoms composition of 0.000867 is reached.

4.4 Manual Simulation

McCabe & Thiele (1925) stated that, for any binary combination, the VLE curve is required to be plotted only once. Thereafter, any number of specified simulations can be investigated using the x-y equilibrium plot. In the 1920's, McCabe & Thiele (1925) proposed plotting the curves manually by hand, but, with the advent of computers, equilibrium curves are generated within seconds. Likewise, for any ternary system, the contours of VLE are only plotted once using the computational method presented in Figure 3.1. Once the contours of VLE are generated, students and designers can quickly investigate, by hand, various distillation design options in order to obtain design parameters such as the minimum number of stages and minimum reflux.

4.4.1 Example 4.4: Total Reflux – Manual Simulation

Example 4.4 will look at manually simulating the design problem specified in Example 4.3, for a separation in distillation region A (Table 4.3). The distillate concentration was limited to 0.96. The vapour and liquid compositions on each stage determined from the manual simulation will be compared to the values obtained using the computational method presented in Example 4.1 (number of stages determined from the bottoms composition).

The manual solution involves the following algorithm:

1. Plot the contours of VLE for at least two components in the ternary mixture using the method presented in Figure 3.1 for determining the number of stages from the bottoms composition.
2. Consider the first component, acetone. Calculate the first ratio for n-hexane (defined in Equation 3.1a) using the given liquid bottoms product composition. $CR_{1,(benzene/chloroform,)} = x_{benzene} / x_{chloroform} = 0.701/0.200 = 3.50$.
3. Calculate the first ratio for benzene (defined in Equation 3.2a) using the given liquid bottoms product composition. $CR_{1,(acetone/chloroform)} = x_{acetone} / x_{chloroform} = 0.0991/0.200 = 0.496$.
4. Using the contours of VLE plotted in step 1, and by interpolation locate the VLE contour that represents the ratio calculated in steps 2-3 for each component on the x-y plot.
5. Move vertically towards the VLE contour determined in step 5 to determine the equilibrium composition of the vapour (y_{eqm}) at x_B.
6. Move horizontally towards the 45 degree line. Determine the new liquid composition from $x_1 = y_{eqm}$.
7. Calculate the second ratio (step 2-3) using the new composition obtained in step 6 for all the components, and repeat steps 4-6.

Figure 4.7 shows the generic contours of VLE plotted on 2D from a ratio of 0.1 to 10. In a similar manner to the binary McCabe-Thiele method, once the contours of VLE are plotted on 2D, different design scenarios can be investigated using the generated plot. Figure 4.7 shows the compositions predicted on each stage by manually calculating the ratio of the compositions on the previous stage, and locating the ratio on the contours of VLE already plotted. The ratio calculated for acetone from the bottoms composition of benzene and chloroform is 3.50. An approximate position of the contour of VLE that represents a ratio of 3.5 will lie between the curves represented by a ratio of 2.667 and 4.5, as depicted in Figure 4.7. Table 4.4 provides the acetone vapour and liquid compositions for each stage comparing the manual simulation and the computational simulation (Example 4.3). The manual simulation provides a good approximation to the computational

method, as well as the rigorous Aspen Plus™ simulation. The manual simulation would be effective, for both students and designers, to perform quick calculations to investigate and identify the qualitative behaviour of ternary mixtures for separations at specified conditions.

Table 4.4: Comparison of acetone liquid and vapour composition on each stage for the manual and computational simulation

	Manual simulation			Computational simulation		
Stage	Ratio	vapour (x)	liquid (y)	Ratio	vapour (x)	liquid (y)
1	2.753	0.96	0.940	2.972	0.9604	0.9391
2	1.930	0.94	0.900	2.067	0.9391	0.9038
3	1.451	0.90	0.850	1.538	0.9038	0.8469
4	1.224	0.85	0.760	1.262	0.8469	0.7615
5	1.172	0.76	0.640	1.180	0.7615	0.6457
6	1.286	0.64	0.500	1.286	0.6457	0.5050
7	1.605	0.51	0.350	1.630	0.5050	0.3502
8	2.327	0.35	0.210	2.320	0.3502	0.2048
9	3.500	0.21	0.099	3.500	0.2048	0.0991

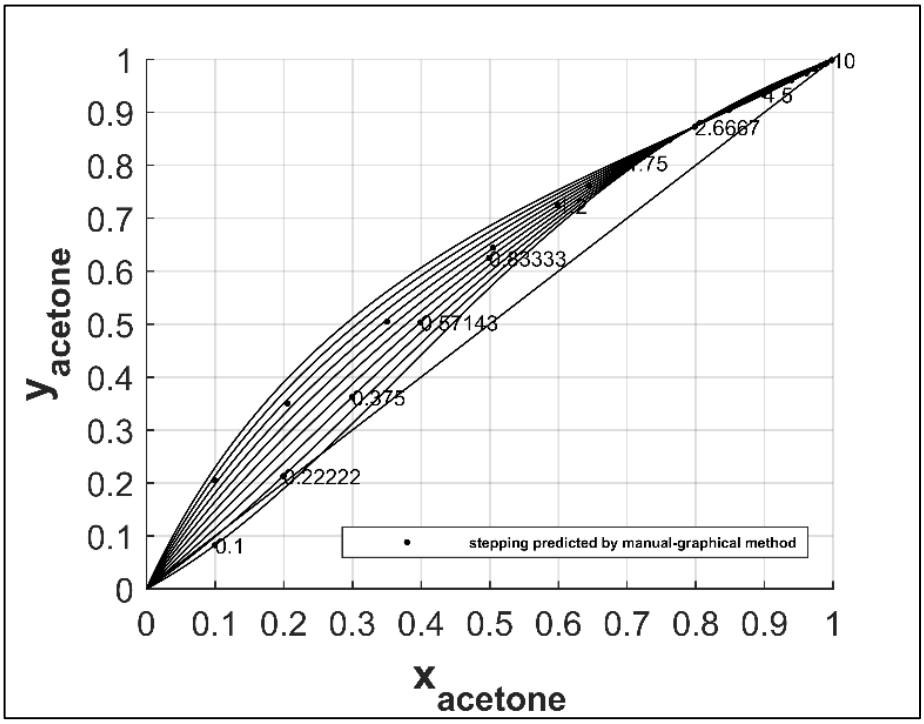

Figure 4.7: The generic contours of VLE from a ratio of 0.1 to 10 and compositions on each stage predicted from manually determining the ratio to move towards, in accordance with the binary McCabe-Thiele method

4.5 Hengstebeck Correlation

The Hengstebeck method has been widely used for the graphical representation and design of multicomponent mixtures. Hengstebeck extended the binary McCabe-Thiele method to multicomponent mixtures by introducing the novel concept of representing the separation as a pseudo-binary mixture of the key components (Reyes, 2000). The simplifying assumption of a pseudo-binary system results in errors if the intermediate volatile components are considered (Hengstebeck, 1946). Hengstebeck (1946) showed a comparison of the Hengstebeck method and rigorous stage by stage method (Hummel method) for five different separations. Hengstebeck (1946) categorised separations into sharp separations (key components with constant relative volatility), difficult separations (key components are close boiling materials), sloppy separations and separations with variable volatility. The Hengstebeck method displays a more accurate prediction of the number of stages (deviation of between 0.5-0.9 stages) in comparison with the rigorous stage by stage method, for separations that the key components were correctly identified (Hengstebeck, 1946). If the key components were not correctly selected, the split would be incorrect and hence the number of stages predicted would be incorrect (Hengstebeck, 1946). For non-ideal systems, it can be challenging to determine the key components in order to reduce a system to a pseudo-binary system. Kister (1995) proposed a trial-and-error method of plotting different key component pairs. The graph that depicts the closest component pair that is actually being separated is considered to be the key components (Kister, 1995). Kister (1995) also mentioned that the key components in the rectifying section may not coincide with the key in the stripping section, hence posing a challenge in determining the key components. The proposed graphical method does not require a trial-and-error method to determine key components, and will simplify the number of calculations involved to produce the graphical plots.

In this thesis, the proposed graphical method for ternary systems includes all components in the simulation. Hence, the proposed graphical method results provide an accurate correlation to a rigorous stage by stage simulation (Aspen Plus^{TM}). Lee et al., (2000) stressed the importance and simplicity of graphical

methods that present untransformed mole fraction coordinates as compositions which can be directly determined from these plots. Unlike the Hengstebeck method, the mole fractions are represented as untransformed coordinates in the proposed graphical method. The proposed graphical method produces an x-y diagram for ternary systems to provide a simpler visual figure for determining compositions directly from the plot.

4.5.1 Example 4.5: Pseudo-binary System

The acetone, benzene and chloroform system is reduced to a pseudo-binary system of acetone and benzene, as done by Hengstebeck for the simulation in Example 4.3 for distillation region A. Figure 4.8a plots the VLE as an 'average' single equilibrium curve, using the proposed method, to generate contours of VLE (Chapter 3, Section 3.2). Figure 4.8a shows the calculation of the number of stages using the average equilibrium curve. The average equilibrium curve is obtained by finding the average compositions of x and y from the multiple contours of VLE.

Figure 4.8b plots the contours of VLE by the method in Chapter 3, using the rigorous simulation results (Aspen Plus^{TM}) reduced to a pseudo-binary system of acetone and benzene. Figures 4.8a and 4.8b both show that the VLE cannot be approximated by a single curve when compared to the proposed graphical method and rigorous simulation (Aspen Plus^{TM}) respectively. It can be deduced that, even if a system is reduced to a pseudo-binary system, the VLE is accurately represented by a series of contours of VLE and cannot be approximated by a single curve. This validates the dependence of the VLE of a component in multicomponent mixtures on the other components present in the mixture (Cope & Lewis, 1932). In conclusion, the Hengstebeck method should not be used as a preliminary design tool for non-ideal systems such as the acetone-benzene-chloroform system.

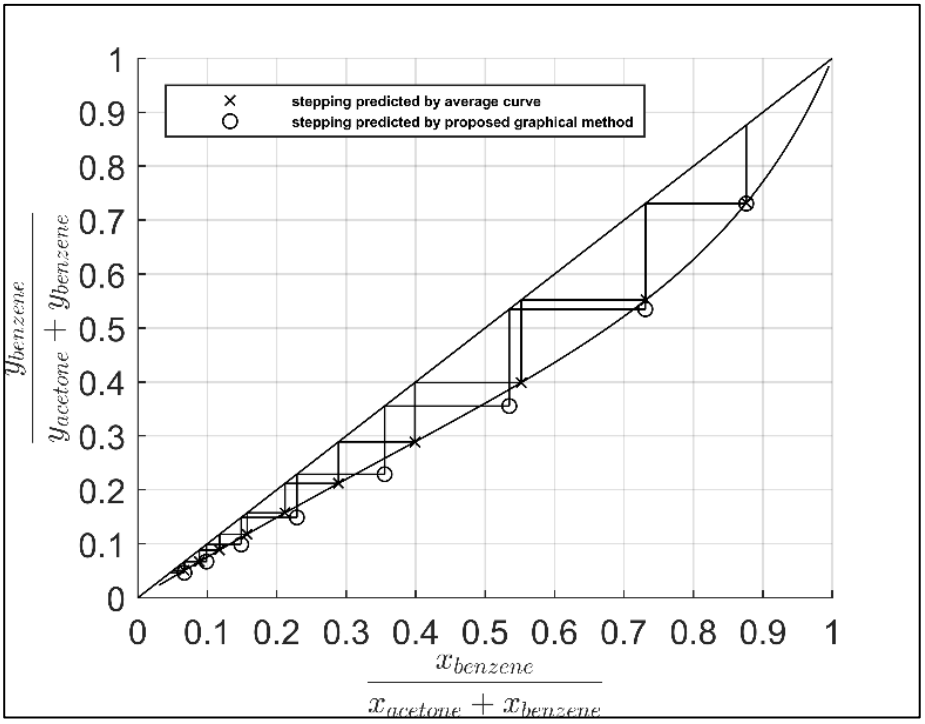

(a)

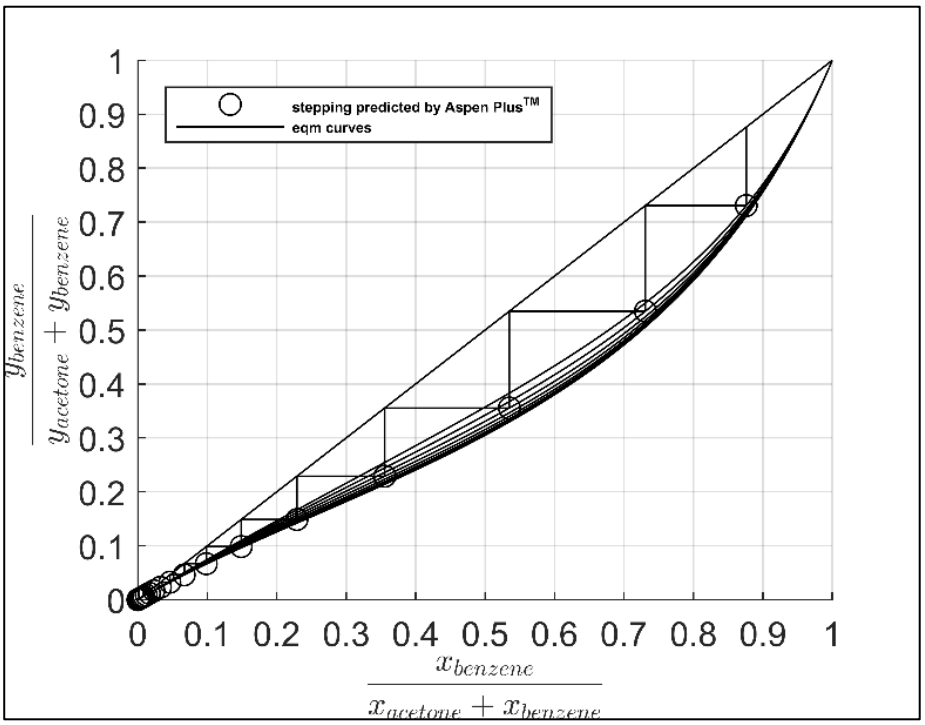

(b)

Figure 4.8: (a) Proposed graphical method plotted as a pseudo-binary pair of benzene and acetone using contours of VLE and average VLE curve, (b) Aspen Plus™ results plotted as a pseudo-binary pair of benzene and acetone

4.6 Conclusion

A graphical method based on the McCabe-Thiele method was proposed for ideal and azeotropic ternary systems at total reflux. The minimum number of stages for an ideal system obtained using the proposed graphical method correlated to the minimum number of stages using the Fenske equation. The results of several rigorous simulations using Aspen Plus™ for a non-ideal, azeotropic system validated the results obtained from the proposed graphical method at total reflux.

The algorithm to determine the minimum number of stages at total reflux for the proposed graphical method was presented by both computational and manual simulations. Both computational and manual simulation require minimal calculations, and designers can quickly generate the x-y diagram to use as preliminary design tool. Finally, it was shown that the VLE of non-ideal multicomponent systems cannot be represented as a single curve on an x-y plot.

Hence, the proposed graphical method correlated more closely to rigorous simulations than the method proposed by Hengstebeck (1946) of reducing multicomponent systems to a pseudo-binary system. Overall, the method will not only provide the designer with an understanding of the behaviour of the system, but proves to be a quick and simple preliminary design tool at total reflux.

REFERENCES

Cao, R., Fu, G., Guo, H., Liu, Y., Tang, Y., Wu, Y., Zhang, X., **2014**. Exponential Function Shortcut Method for the Calculation of the Number of Theoretical Plates in a Distillation Column. *Ind. Eng. Chem. Res*. 53(38), pp. 14830-14840.

Castillo, F.J.L. & Towler, G.P., **1998**. Influence of multicomponent mass transfer on homogeneous azeotropic distillation. *Chem. Eng. Sci.* 53(5), pp. 963-976.

Cope, J.Q. & Lewis, W.K., **1932**. Studies in Distillation-Graphical Method of Computation for Rectifying Complex Hydrocarbon Mixtures. *Ind. Eng. Chem.* 24(5), pp. 498-501.

Fenske, M.R., **1932**. Fractionation of Straight-Run Pennsylvania Gasoline. *Ind. Eng. Chem*. 24(5), pp. 482–485.

Górak, A. & Sorensen, E., **2014**. Distillation: Fundamentals and Principles. *Elsevier: Academic Press*: London.

Hengstebeck, R.J., **1946**. A Simplified Method for Solving Multicomponent Distillation Problems. *Trans. AIChE*. 42, pp. 309-329.

Kister, H.Z., **1992**. Distillation Design. *McGraw-Hill, Inc: USA.*

Kister, H.Z., **1995**. Troubleshoot distillation simulations. *Chem. Eng. Prog*. 91(6) pp. 63-75.

Lee, J.W., Hauan, S., Lien, K.M., Westerberg, A.W., **2000**. A graphical method for designing reactive distillation columns. I. The Ponchon-Savarit method. P*roceedings of the Royal Society of London*. 456(2000), pp. 1953-1964.

Mathias, P.M., **2009**. Visualizing the McCabe-Thiele Diagram. *Chem. Eng. Prog*. 105(12), pp. 36-44.

McCabe, W.L. & Thiele, E.W., **1925**. Graphical Design of Fractionating Columns. *Ind. Eng. Chem.* 17(6), pp. 605-611.

Reyes, J.A., Gomez, A., Marcilla, A., **2000**. Graphical Concepts to Orient the Minimum Reflux Ratio Calculation on Ternary Mixtures in Distillation. *Ind. Eng. Chem. Res*. 39(10), pp. 3912-3919.

Thong, D.Y.C., Castillo, F.J.L., Towler, G.P., **2000**. Distillation design and retrofit using stage-composition lines. *Chem. Eng. Sci*. 55(3), pp. 625–640.

Thong, D.Y.C. & Jobson, M., **2001**. Multicomponent homogeneous azeotropic distillation. 2. Column design. *Chem. Eng. Sci*. 56(14), pp. 4393-4416.

Van Winkle, M., **1967**. Distillation. *McGraw-Hill, Inc: USA.*

Wahnschafft, O.M., Koehler, J.M., Blass, E., Westerberg, A.W., **1992**. The Product Composition Regions of Single-Deed Azeotropic Distillation Columns. *Ind. Eng. Chem. Res.* 31(10), pp. 2345-2362.

Wankat, P.C., **2012**. Separation Process Engineering, Third edition. *Pearson: Upper Saddle River*, NJ.

Winn, F.W. **1958**. New relative volatility method for distillation calculations. *Petrol. Refin.* 37(5), pp. 216–218.

Chapter 5

Minimum Reflux and Reboil for Distillation Design

The work in this chapter has been published as**:** The work in this chapter has been published as: Seedat, N., Kauchali, S., Patel, B., **2021**. A graphical method for the preliminary design of ternary simple distillation columns at finite reflux. *SAJCE*. 37, pp. 99-109 as supplementary material. The work is a reproduction of the journal publication although section 5.3.2.1 Part B has been added for the purpose of adhering to the standards of this thesis, as well as simplifying the work for clarity and easy understanding. The reproduction was done with permission from the publisher. (**Copyright © 2021 Elsevier)**

Abstract

A simple and quick graphical method to determine minimum reflux for transition, sharp direct and indirect splits for ideal and non-ideal systems is illustrated. The method requires the calculation of the minimum reflux ratio at the double feed pinch, and hence the graphical location of the transition point for the desired separation. Finally, the minimum reflux and reboil ratios are calculated for the sharp split using the desired product specification. For ideal systems, the proposed graphical method is consistent with the Underwood method in predicting the minimum reflux for all classifications of splits. The proposed graphical method provides sufficient estimates of minimum reflux for highly, non-ideal azeotropic systems with deviations of less than 2%. In conclusion, the proposed graphical method is an efficient and effective conceptual and preliminary design tool which retains the simplicity of the original McCabe-Thiele method, but is limited to sharp direct and indirect splits.

5.1 Introduction

Distillation processes are extremely energy intensive and account for up to 50% of operational and capital costs in the chemical and petrochemical industries (Górak & Sorensen, 2014). Government regulations for environmental conservation and increasing energy costs have shifted focus to designing energy-efficient distillation processes (Koehler et al., 1995). The minimum reflux and reboil ratios primarily determine the minimum energy requirements of a distillation process (Stichlmair et al., 1993). Minimum reflux and reboil ratios represent a lower, thermodynamically defined operating limit which corresponds to an infinite number of stages (Koehler et al, 1995; Górak & Sorensen, 2014). Hence, at minimum reflux and reboil the investment cost would also reach infinity and represents an infeasible operating point (Koehler et al., 1995). Once the minimum reflux and reboil ratios are determined, the actual operating reflux is chosen to be slightly higher than the minimum values (Stichlmair et al., 1993). Minimum reflux impacts both the operating and capital costs (Górak & Sorensen, 2014). In practice, the optimum operating reflux ratio is chosen in a range of 1.1 to 1.5 times the minimum reflux (Koehler et al., 1995). This range represents the optimum operating point for a distillation column, taking into considerations the operational and capital costs (Koehler et al., 1995).

At minimum reflux/reboil, a distillation column exhibits a pinch point (unless a tangent pinch controls the minimum reflux/reboil). At a pinch point, the vapour and liquid are in equilibrium, hence mass transfer stops between the two phases. On a McCabe-Thiele diagram for binary distillation, pinch points can be identified visually on a 2D plane. At a pinch point, the compositions of the vapour and liquid remain constant. Hence, approaching a pinch point requires an infinite number of stages (Stichlmair et al., 1993). In binary distillation, a double pinch occurs above and below the feed stage (only if no tangent pinch exists) (Stichlmair et al., 1993). This can be seen visually as the rectifying and bottoms operating line intersect each other and the equilibrium curve on the feed lines of the light key (LK) component for binary systems.

The McCabe-Thiele and Underwood methods are the best-known short-cut methods to determine minimum reflux (Górak & Sorensen, 2014). The McCabe-Thiele method is the simplest available short-cut method but it is restricted to binary systems. Underwood (1948) used the notion of 'pinches' proposed by McCabe & Thiele (1925) to develop an empirical equation to calculate minimum reflux for multicomponent mixtures, but which are limited to constant molar overflow (CMO) and constant relative volatility (CRV) (Lee & Wong, 2008). Numerous publications have modified the Underwood equation for non-ideal, multicomponent systems (Bausa et al., 1998), multicomponent complex columns (Barnes et al., 1972; von Watzdorf et al., 1999; Yaws et al., 1981) and extractive distillation (Brüggemann & Marquardt, 2004). In recent years, many methods have used the Underwood method or tray to tray calculations (concentration profiles) similar to the McCabe-Thiele method to determine minimum reflux (Górak & Sorensen, 2014).

A broader group of graphical methods uses the depiction of concentration profiles on a mass balance triangle (MBT) to solve for the minimum reflux. The boundary value method (BVM) and shortest stripping line method (SSLM) are based on concentration profile calculations to calculate minimum reflux (Górak & Sorensen, 2014). BVM is one of the most established geometric methods for minimum reflux calculation. BVM presented by Levy et al. (1985a, 1985b) plots the rectifying and bottoms profiles from stipulated product specifications under CMO conditions. The reflux ratio is lowered by trial-and-error, until the minimum reflux is reached and the rectifying and bottoms profiles touch but do not cross (Worms et al., 2017). The BVM has been applied to ideal, non-ideal and homogeneous systems by Levy et al. (1985a, 1985b) and extended further to complex columns (Nawaz & Jobson, 2011) and reactive distillation (Barbosa & Doherty, 1988).

Lucia & Taylor (2006) proposed the Shortest Stripping Line Method (SSLM) which plots only the bottoms profile first from the bottoms product, and then the rectifying profile is plotted from the last tray of the bottoms profile to the distillate product. The minimum reflux is shown to correlate with the column which has the shortest geometric bottoms profile for a feasible separation (Lucia & Taylor, 2006). The

SSLM requires several profiles to be plotted by nonlinear programming to determine minimum reflux which is a computationally intensive process.

V_{min} diagrams were developed by Halvorsen & Skogestad (2003a) to determine minimum energy demands for all possible separations for a stipulated multicomponent feed. V_{min} diagrams use either the Underwood equation or rigorous simulations to visually represent the energy demand of a reversible column and hence, the minimum energy demand – which corresponds to the minimum reflux– can be identified (Górak & Sorensen, 2014; Halvorsen & Skogestad, 2003a). V_{min} diagrams are found to be particularly useful in determining the minimum energy requirements in Petlyuk columns (Halvorsen & Skogestad, 2003b).

A simple graphical method for determining minimum reflux or reboil ratios for transition, sharp and non-sharp splits is presented. The methods of determining minimum reflux and reboil are not suitable for non-sharp and sloppy separations. The proposed graphical method for minimum reflux does not require trial-and-error calculations, and uses simple graphical calculations to determine minimum reflux. Firstly, the graphical method is used to calculate the minimum reflux and reboil ratio that satisfies the double feed pinch, using the contours of VLE which represent the feed composition (Chapter 3) and McCabe-Thiele diagrams for multicomponent systems. Secondly, the graphical method uses the minimum reflux at the feed pinch to graphically locate the transition point for the defined sharp separation. Finally, the minimum reflux and reboil ratios, using the transition point and the required product specifications for the specified sharp direct or indirect split are calculated. Once the minimum reflux and reboil ratios are determined, the designer chooses an operating reflux and reboil ratio slightly above the minimum values.

The chapter opens with explaining the type of splits for which the method can be used, such that the method is only applied to transition, sharp direct and indirect splits. The algebraic method of calculating minimum reflux for the three classifications of splits is defined. The method for determining minimum reflux and reboil ratios for transition splits (double feed pinch) is applied to both ideal and

non-ideal systems. This is followed by the method for determining minimum reflux which is illustrated for both a sharp direct and an indirect split for an ideal system of methanol, ethanol, and n-propanol. Lastly, the minimum reflux and reboil ratios for a sharp indirect split for an azeotropic non-ideal system of acetone, benzene and chloroform is solved. The proposed graphical method will be compared to the traditional Fenske-Underwood-Gilliland (FUG) method for ideal systems and BVM for non-ideal splits. In all simulations, the BVM will be used to confirm that the minimum refluxes obtained are indeed the correct values. Through the illustrated examples, it will be demonstrated that the method is indeed simple and effective in adherence to the binary McCabe-Thiele method, with minimal additional calculations to determine minimum reflux and reboil ratios.

5.2 Types of Splits in Ternary Distillation Systems

Ternary separations can be categorised into the following groups of separations: sharp direct, indirect, and transition splits, as depicted in Figure 5.1. A sharp direct split is characterised as a separation in which the distillate will contain very small quantities of the heavy key component (C), and higher recovery of the light key component (A) in the distillate (Doherty & Malone, 2001). An indirect split produces a high recovery of the heavy key component (C) in the bottoms product. Very small quantities of the heavy key (C) will be present in the distillate product. Transition splits are identified when the node pinch points of both the rectifying and bottoms profiles meet at the feed composition of the system and the intermediate key (B) distributes between the distillate and bottoms compositions.

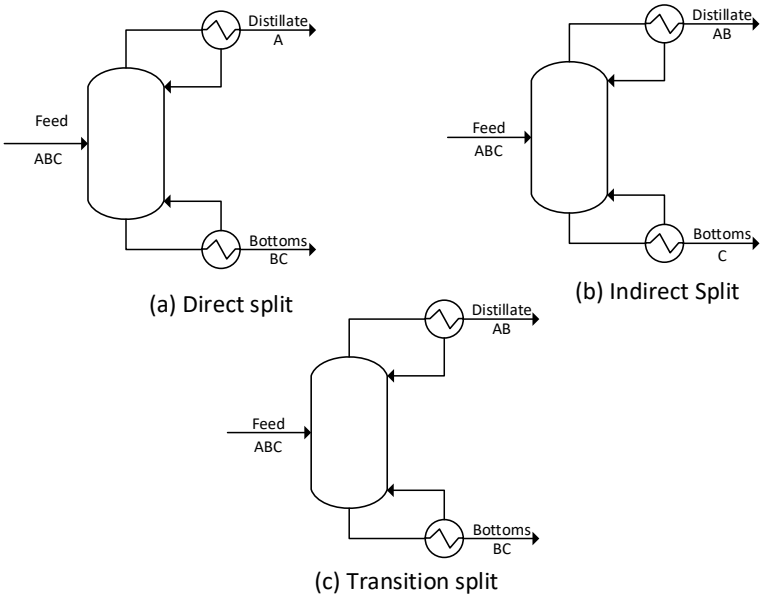

Figure 5.1: Ternary separations (a) direct, (b) indirect and (c) transition splits

A simple graphical method of determining minimum reflux for transition splits, sharp direct and indirect splits, for an ideal system, will be presented. The method for minimum reflux will first be illustrated algebraically, followed by worked examples. The method of determining the minimum reflux for a direct split will be depicted for an ideal system of methanol, ethanol and n-propanol. In addition, the method of determining the minimum reflux ratio for an indirect split for the non-ideal acetone-benzene-chloroform system will be explained.

5.3 Algebraic Derivation of the Method of Determining Minimum Reflux ratio for Transition, Sharp Direct and Indirect Splits

This section presents the full algebraic derivation of the graphical method for determining the minimum reflux ratio for transition, sharp direct and indirect splits.

5.3.1 Transition Split

Step 1

The graphical approach is rather intuitive. The basis is to determine the VLE contours that represent the feed composition for each component in the system.
For a ternary system, the ratio that represents the VLE contours for the feed composition for component *i* is calculated using Equation (5.1):

$$CR_{F,jk} = \frac{x_{F,j}}{x_{F,k}} \tag{5.1}$$

Similarly, the contours of VLE that represent the feed composition for component *j* and *k* can be calculated using Equation (5.2) and (5.3).

$$CR_{F,ik} = \frac{x_{F,i}}{x_{F,k}} \tag{5.2}$$

$$CR_{F,ij} = \frac{x_{F,i}}{x_{F,j}} \tag{5.3}$$

The operating line, feed line and the VLE contours that represent the feed will need to intersect to determine the minimum reflux. The designer will select the component which is required to meet the product specification defined in the design question. For illustrating the method, component *i* will be the component selected. The VLE contours that represent the feed composition (Equation 5.1) and the feed line will be plotted for component *i* on an x-y diagram.

Step 2

A line beginning at the distillate composition on the 45 degree line, and progressing towards the intercept of the contours of VLE representing the feed and the feed line is constructed. The gradient of the straight line which is plotted can be equated to the gradient of the rectifying operating line, such that the minimum reflux ratio can be determined as depicted in Equation 5.4. Likewise, the same method can be followed to determine the minimum reboil ratio by equating the gradient of the minimum reboil line to the gradient of the bottoms operating line, and using Equation 5.5.

$$R_{min} = \frac{R_{gradient}}{(1-R_{gradient})} \quad (5.4)$$

Where

$$R_{gradient} = \frac{y_{D,i}-y_{F,i}^{*}}{x_{D,i}-x_{F,i}} \quad (5.4a)$$

$$S_{min} = \frac{-1}{(1-S_{gradient})} \quad (5.5)$$

Where

$$S_{gradient} = \frac{y_{B,i}-y_{F,i}^{*}}{x_{B,i}-x_{F,i}} \quad (5.5a)$$

Where:

$y_{D,i}$ is the vapour distillate composition of component *i*,

$x_{D,i}$ is the liquid distillate composition of component *i*,

$y_{B,i}$ is the vapour bottoms composition of component *i*,

$x_{B,i}$ is the liquid bottoms composition of component *i*,

$x_{F,i}$ is the feed composition of component *i*,

$y_{F,i}^{*}$is the liquid equilibrium composition corresponding to the liquid feed composition, $x_{F,i}$, for component *i*.

Step 3

Once the gradient of the minimum reflux line is determined, and hence the minimum reflux ratio, the distillate compositions of the other components (*j* and *k*) have to be adjusted as follows:

a. Plot the VLE contour representing the feed composition for component *j* and *k*
b. Plot the feed lines for the components.
c. Draw a line from the intercept of the contours of VLE representing the feed and the feed line for component *j* and k towards the 45 degree line, using the gradient calculated in step 2.
d. The intercept of the line with the 45 degree line represents the adjusted distillate composition.

5.3.2 Sharp Direct and Indirect Splits

Step 1

The first step in the graphical method is to determine the minimum reflux ratio for a transition split, given a specified feed. The method for determining the minimum reflux ratio for a transition split is presented in section 5.2.1.

Step 2

If the split is direct, the binary equilibrium curve for Components A and B and the operating line for Component A (light key-LK) is plotted on the x-y diagram. For an indirect split, the binary equilibrium curve for Components B and C and the operating line for Component C (heavy key- HK) is plotted on the x-y plot. The intersection of the rectifying operating line and binary equilibrium curve (Components A and B) represents the transition point in the rectifying section for a direct split. Similarly, the intersection of the bottoms operating line and the binary equilibrium curve (Components B and C) represents the transition point in the bottoms section for an indirect split.

Step 3

Once the transition point is located, the minimum reflux/reboil ratio can be determined for any distillate or bottoms composition, provided the feed composition is the kept the same. In order to determine the minimum reflux/reboil ratio, the slope of the rectifying (direct split) and bottoms (indirect split) operating line needs to be determined respectively. The transition point $({x_{TR,i}}^*, {y_{TR,i}}^*)$/ $({x_{TB,i}}^*, {y_{TB,i}}^*)$ and the distillate/bottoms composition provide two points on the straight line to determine the slope and hence the minimum reflux/reboil ratio. Equations 5.6 and 5.7 are used to calculate the gradient of the rectifying (direct split) and bottoms (indirect split) operating lines. Equations 5.4 and 5.5 can then be used to determine the minimum reflux and reboil ratios respectively.

$$R_{gradient} = \frac{y_{D,A} - y_{TR,A^*}}{x_{D,A} - x_{TR,A^*}} \quad (5.6)$$

$$S_{gradient} = \frac{y_{B,C} - y_{TB,C^*}}{x_{B,C} - x_{TB,C^*}} \quad (5.7)$$

Step 4

Once the minimum reflux ratio is determined for a direct split the corresponding reboil ratio can be calculated using Equation 5.8 (Julka & Doherty, 1990). Likewise, the reflux ratio for an indirect split can be determined by rearranging Equation 5.8, once the minimum reboil ratio is determined.

$$S = (R + q)\left[\frac{x_{B,i} - x_{F,i}}{x_{F,i} - x_{D,i}}\right] + q - 1 \quad (5.8)$$

5.4 Graphical Method for Calculating the Minimum Reflux Ratio

5.4.1 Transition Split (double feed pinch)

Transition splits are special cases of separation in which the intermediate key distributes between the distillate and bottoms compositions (similar to a binary system). Transition splits are identified when the node pinch points of both the rectifying and bottoms profiles meet at the feed composition of the system (Doherty & Malone, 2001). Hence, a double pinch point is observed above and below the feed stage (Doherty & Malone, 2001). The reflux and reboil ratios for a certain feed, distillate and bottoms composition are at the lowest value in a transition split, in comparison with any other type of split (Stichlmair et al., 1993). A graphical method for determining minimum reflux and reboil ratios is presented below, in the form of an example.

5.4.1.1 Example 5.1: Ideal system (methanol, ethanol, n-propanol)

Consider the following design problem, using data sourced from Doherty & Malone (2001): A mixture of methanol (M), ethanol (E) and n-propanol (P) is fed into a simple distillation column at constant pressure (1 bar). The composition of the saturated liquid (q=1) feed to the column is presented in Table 5.1. The design specification is to achieve a maximum distillate product composition for methanol of 0.730 (mole fraction) and a bottoms product composition of 0.01 (mole fraction). Determine the minimum reflux and reboil ratios for the specified separation.

Table 5.1: Relative volatilities, feed, distillate and bottoms compositions for a methanol, ethanol and n-propanol system in a sharp direct and indirect split (Doherty & Malone (2001))

	Relative Volatilities		**Direct Split**		**Indirect Split**	
Component		x_F	x_B	x_D	x_B	x_D
methanol	3.25	0.300	0.005	0.980	5.00×10^{-11}	0.550
ethanol	1.71	0.250	0.350	0.020	0.022	0.440
n-propanol	1.00	0.450	0.645	5.00×10^{-11}	0.978	0.010

Step 1

The first step is to determine the minimum reflux and reboil ratios at the transition split, as discussed in section 5.2.1. The detailed calculation for the method for determining minimum reflux and reboil ratios for a transition split will be demonstrated. A detailed explanation to generate the x and y values for methanol to plot a contour of VLE, which represents the feed, will then be presented.

Generation of the feed contour of VLE

The ratio representing the contour of VLE (for methanol) for the feed composition of ethanol/n-propanol is calculated to be 0.556 (Equation 5.9):

$$CR_{F,E/P} = \frac{x_{F,M}}{x_{F,P}} = \frac{0.25}{0.45} = 0.556 \quad (5.9)$$

The relative volatilities and feed compositions are required to calculate the x and y values that represent the feed contour of VLE as shown in Equation 5.10.

$\alpha_{(\frac{M}{P})}$ = 3.25
$\alpha_{(\frac{M}{E})} = 1.71$

$$y_M = \frac{\alpha_{(\frac{M}{P})}\left(\frac{x_M}{1-x_M}\right)(CR_{F,E/P}+1)}{1+\alpha_{(\frac{M}{P})}\left(\frac{x_M}{1-x_M}\right)(CR_{F,E/P}+1)+\frac{\alpha_{(\frac{M}{P})}}{\alpha_{(\frac{M}{E})}}CR_{F,E/P}} \quad (5.10)$$

The first point of the contour of VLE is calculated at a liquid mole fraction of 0 for methanol, as shown in Equation 5.11, and the corresponding vapour composition of methanol is 0.

At $x_M(1) = 0$;

$$y_M = \frac{\alpha_{(\frac{M}{P})}\left(\frac{x_M}{1-x_M}\right)\left(CR_{F,\frac{E}{P}}+1\right)}{1+\alpha_{(\frac{M}{P})}\left(\frac{x_M}{1-x_M}\right)\left(CR_{F,\frac{E}{P}}+1\right)+\frac{\alpha_{(\frac{M}{P})}}{\alpha_{(\frac{M}{E})}}CR_{F,\frac{E}{P}}} = \frac{3.25\left(\frac{0}{1-0}\right)(0.556+1)}{1+3.25\left(\frac{0}{1-0}\right)(0.556+1)+\frac{3.25}{1.71}\times 0.556} = 0 \quad (5.11)$$

Subsequent points are calculated at liquid compositions in intervals of 0.1 (Equation 4.12). The next x and y pair is represented by 0.1 and 0.215 respectively. The calculations are continues until an x value of 1 and the resultant x and y pairs that are used to plot the feed contour of VLE are found, as in Table 5.2.

$for\ n = 1{:}10$

$$x_M\ (n+1) = x_M(n) + 0.1; \quad (5.12)$$

$$y_M = \frac{\alpha_{\left(\frac{M}{P}\right)}\left(\frac{x_M}{1-x_M}\right)\left(CR_{F,\frac{E}{P}}+1\right)}{1+\alpha_{\left(\frac{M}{P}\right)}\left(\frac{x_M}{1-x_M}\right)\left(CR_{F,\frac{E}{P}}+1\right)+\frac{\alpha_{\left(\frac{M}{P}\right)}}{\alpha_{\left(\frac{M}{E}\right)}}CR_{F,\frac{E}{P}}} = \frac{3.25\left(\frac{0.1}{1-0.1}\right)(0.556+1)}{1+3.25\left(\frac{0.1}{1-0.1}\right)(0.556+1)+\frac{3.25}{1.71}\times 0.556} = 0.215 \quad (5.13)$$

Table 5.2: Vapour and liquid composition for methanol at a ratio of ethanol / n-propanol of 0.556

x	0.00	0.10	0.20	0.30	0.40	0.50	0.60	0.70	0.80	0.90	1.00
y	0.00	0.22	0.38	0.51	0.62	0.71	0.79	0.85	0.91	0.96	1.00

The same procedure is followed for ethanol and n-propanol, to plot the unique feed contour of VLE for each component. The ratio for ethanol and n-propanol defining the VLE contour representing the feed composition is 0.667 ($CR_{F,M/P}$) and 1.20 ($CR_{F,M/E}$) respectively. The ratios defining the vapour liquid equilibrium (VLE) contours representing the feed are depicted in Figures 5.2 - 5.3 for the light key (LK- ethanol) and heavy key (HK- n-propanol) components. The intersection of the feed line and the contours of VLE for all the components represents the feed pinch concentration. At this point, the vapour composition in equilibrium with the feed can be read off the x-y plot for all the components. The feed vapour compositions for methanol, ethanol and n-propanol are 0.513, 0.250 and 0.237 respectively.

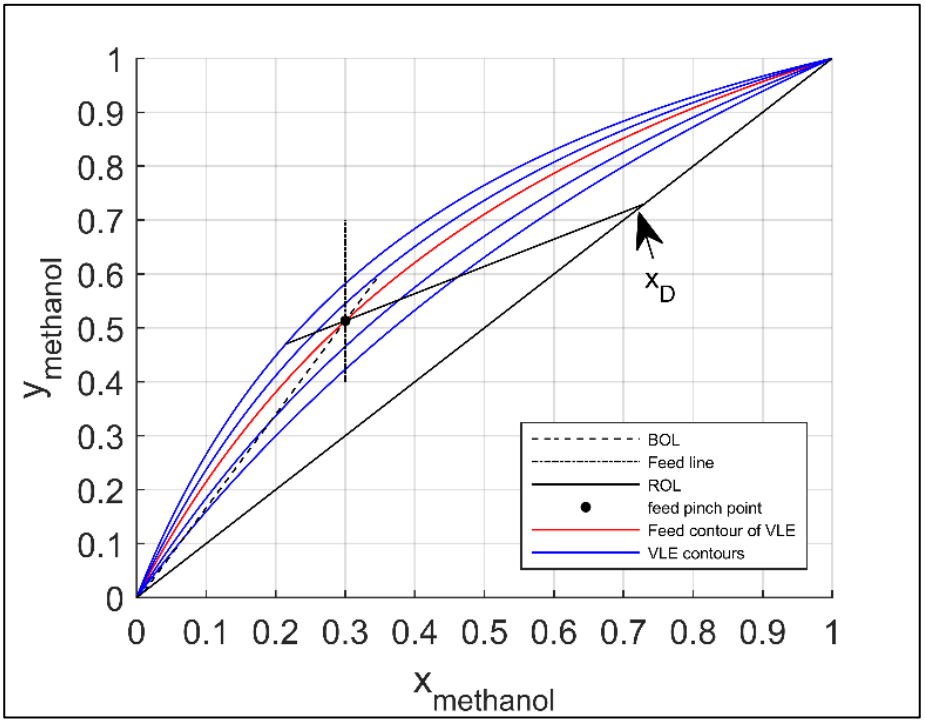

Figure 5.2: McCabe-Thiele diagram for methanol (LK), plotting the rectifying (ROL) and bottoms (BOL) operating lines to determine the adjusted bottoms and distillate compositions from minimum reflux and reboil calculations

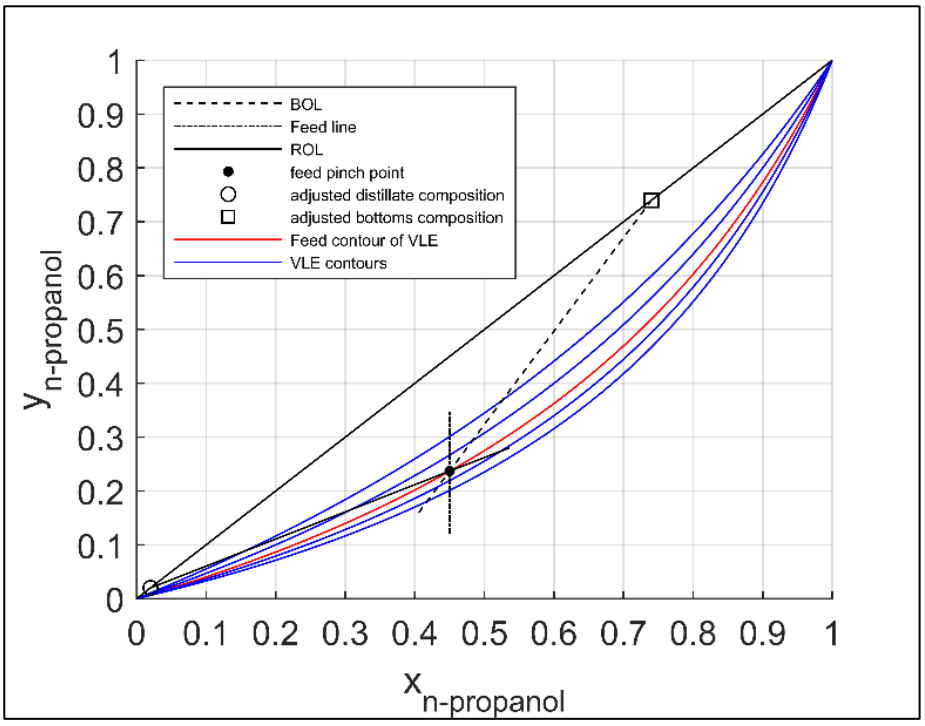

Figure 5.3: McCabe-Thiele diagram for n-propanol (HK), plotting the rectifying (ROL) and bottoms (BOL) operating lines to determine the adjusted bottoms and distillate compositions from minimum reflux and reboil calculations

Step 2

To determine the minimum reflux and reboil ratios, the gradient of the straight line representing the rectifying and stripping operating lines must be calculated. Using the product specification for methanol in the design problem, the distillate and bottoms compositions are fixed for methanol. Two straight lines are extended from the distillate and bottoms compositions of methanol towards the feed pinch point, determined in step 1 (Figure 5.2). The gradient of the rectifying and stripping operating lines is determined in Equations 5.12 and 5.14 as 0.505 and 1.73 respectively. Hence, the minimum reflux and reboil ratios are calculated using Equation 5.13 and 5.15 and found to be 1.02 and 1.30 respectively.

$$R_{gradient} = \frac{y_{D,i} - y_{F,i}^{*}}{x_{D,i} - x_{F,i}} = \frac{0.730 - 0.513}{0.730 - 0.300} = 0.505 \quad (5.12)$$

$$R_{min} = \frac{R_{gradient}}{(1 - R_{gradient})} = \frac{0.505}{1 - 0.505} = 1.02 \quad (5.13)$$

$$S_{gradient} = \frac{y_{B,i} - y_{F,i}^{*}}{x_{B,i} - x_{F,i}} = \frac{0.01 - 0.513}{0.01 - 0.300} = 1.73 \quad (5.14)$$

$$S_{min} = \frac{-1}{(1 - 1.73)} = 1.36 \quad (5.15)$$

Step 3

Once the gradient has been established, straight lines are plotted from the feed pinch points, as determined in step 1, with the gradient of the rectifying and stripping operating lines calculated in step 2 for one component (HK is recommended), in order to determine the adjusted bottoms and distillate composition. The intermediate key (IK) does not distribute into the two products, hence it is recommended that HK be graphically analysed to find the adjusted bottoms and distillate compositions. Thereafter, by mass balance the third component's (IK) adjusted distillate and bottoms compositions are determined. The adjusted distillate and bottoms compositions of the heavy key component (n-propanol) are determined by reading off the intersection of the rectifying and bottoms operating lines with

the 45 degree line in Figure 5.3. The intersection point is (0.450, 0.237) for n-propanol. Using Equation (5.16) and the rectifying and stripping operating lines' gradients of 0.505 and 1.73, as calculated in Equations 5.12 and 5.14, the intercept (c) of the straight line can be determined and plotted on the x-y diagram. The intercept for both the rectifying and stripping operating lines is calculated below. The equation for the rectifying and stripping operating lines are represented by Equations 5.17 and 5.18 respectively. From the plotted straight lines, the intersection of the straight operating lines with the 45 degree line will be the adjusted bottoms/distillate compositions.

Equation of a straight line:

$$y = mx + c \tag{5.16}$$

For n-propanol rectifying operating line:

$$0.237 = (0.45 \times 0.505) + c$$

$$c = 0.00975$$

$$y = 0.505x + 0.00975 \tag{5.17}$$

For n-propanol bottoms operating line:

$$0.237 = (0.45 \times 1.73) + c$$

$$c = -0.542$$

$$y = 1.73x - 0.542 \tag{5.18}$$

The adjusted distillate and bottoms compositions are read off Figure 5.2 and are found to be 0.02 and 0.74 respectively. By mass balance, the adjusted distillate and bottoms compositions of ethanol are 0.250 and 0.250 respectively (refer to Table 5.3). The adjusted distillate and bottoms compositions have to be determined in order to satisfy mass balance requirements for the ternary system.

Table 5.3: Comparison of distillate and bottoms compositions determined by the proposed graphical method and Doherty & Malone (2001)

	x_B		x_D	
Component	graphical method	Doherty & Malone (2001)	graphical method	Doherty & Malone (2001)
methanol	0.010	0.010	0.730	0.730
ethanol	0.250	0.250	0.250	0.250
n-propanol	0.740	0.740	0.020	0.020

The proposed graphical method for determining the minimum reflux and reboil ratios retains the simplicity of the binary McCabe-Thiele method. The method does not require excessive computation time and requires few calculations once the contours of VLE have been plotted. The distillate and bottoms compositions for the transition split correspond to those predicted by Doherty & Malone (2001) (using the Boundary Value Method) as shown in Table 5.3. In addition, the minimum reflux and reboil ratios of 1.02 and 1.30 correlate with those calculated by Doherty & Malone (2001). The Underwood method requires the adjusted distillate and bottoms compositions as well as the feed composition to be specified in order to calculate the minimum reflux. The Underwood method does not provide a method of calculating these adjusted bottoms and distillate compositions. Nevertheless, if the adjusted distillate and bottoms compositions are used in the Underwood method, the minimum reflux and reboil ratio are calculated to be 1.02 and 1.30 respectively. The minimum reflux and reboil ratios calculated from the graphical method correlated with those predicted by the Underwood method (The detailed calculation of the Underwood method can be found in Appendix D).

5.4.2 Sharp Direct and Indirect Split

For a sharp direct split, at minimum reflux, the node pinch in the bottoms profile must be collinear with the feed composition and the saddle pinch in the rectifying profile, on a mass balance triangle (MBT). Hence, the node pinch in the bottoms

profile controls the separation (Doherty & Malone, 2001). On the other hand, in sharp indirect splits, the node pinch in the rectifying section controls, hence the node pinch in the rectifying profile must be collinear with the feed and the saddle pinch in the bottoms profile on a MBT (Doherty & Malone, 2001).

Stichlmair et al. (1993) observed that for sharp splits, with nearly pure products, the internal liquid concentration profiles are characterized by 'transition points'. Stichlmair et al. (1993) determined the pinch points using analytical equations and hence the minimum reflux ratio. Consider a sharp indirect split of component A= LK, B = IK and C = HK. Stichlmair (2005) observed that when the HK (C) is reduced to almost zero in the distillate product (the system reduces to binary of Components A and B), the intersection of the operating line (for Component A) and the binary equilibrium curve of the Components A and B, represent the transition point (saddle pinch). Likewise, for a sharp indirect split the LK is reduced to zero in the bottoms product (the system reduces to binary of Components B and C). The intersection of the operating line (for component C) and the binary equilibrium curve of Components B and C represents the transition point. The Underwood method is an empirical correlation based on the same observations, but requires the feed, distillate and/or bottoms product compositions to be specified for all components in order to calculate the minimum reflux. Using the observations made by Stichlmair (2005), a graphical method for determining the transition point for a specified feed, and hence the minimum reflux ratio will be presented.

5.4.2.1 Example 5.2: Ideal system (methanol, ethanol, n-propanol)

Part A: Sharp direct split

Design problem: The mixture of methanol (M), ethanol (E) and n-propanol (P) is fed into a finite reflux column at constant pressure (1 bar). The composition of the saturated liquid (q=1) feed to the column, the distillate product and bottoms product for the direct split can be found in Table 5.1. The compositions data were sourced from Doherty & Malone (2001). Determine the minimum reflux and reboil ratios to achieve a minimum recovery of methanol of 0.980 in the distillate product.

Table 5.4: Feed, distillate and bottoms compositions for methanol, ethanol and n-propanol system in a transition split

Component	x_F	y_F^*	x_B	x_D
methanol	0.300	0.513	1.00×10^{-10}	0.750
ethanol	0.250	0.250	0.250	0.250
n-propanol	0.450	0.237	0.750	1.00×10^{-10}

Step 1

Stichlmair et al. (1993) stated that, for sharp direct and indirect splits the internal liquid profile does not reach the feed composition, unlike transition splits (double feed pinch). More importantly, Stichlmair et al. (1993) stated that in a direct split the internal liquid profile above the feed (rectifying section) is identical to the profile of the transition feed. Likewise, in an indirect split, the internal liquid profile below the feed (bottoms section) is identical to the profile of the transition split. Hence, it can be concluded that for a specified feed, the transition point for both the transition split and the sharp direct/indirect split are the same.

Step 1 in the graphical method is to determine the minimum reflux for a transition split, given a specified feed. Direct splits produce a distillate product rich in the light key, methanol, and contain very little of the heavy component, n-propanol. Hence once the transition point in the rectifying section is reached, the system can be approximated as a binary mixture of methanol and ethanol. In order to determine the transition point in the rectifying section, the transition split, in which very little n-propanol is present in the distillate product, must be determined. To determine the minimum reflux ratio of the transition split for a direct split the distillate composition of n-propanol is set to 1.00×10^{-10} in the distillate product (Figure 5.4). The minimum reflux ratio is found to be 1.11 and the resulting adjusted distillate composition of methanol to be 0.750 (Figure 5.5). The distillate product to obtain the pinch at the feed can be found in Table 5.4.

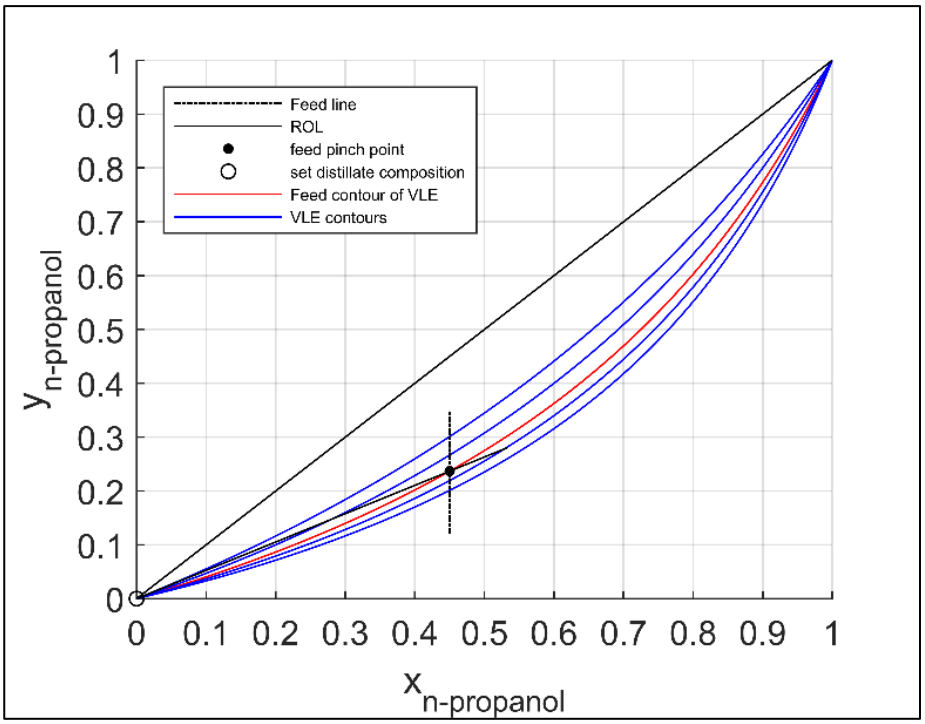

Figure 5.4: McCabe-Thiele diagram for n-propanol (HK), plotting the rectifying operating line (ROL) to determine the minimum reflux for the transition split in direct split

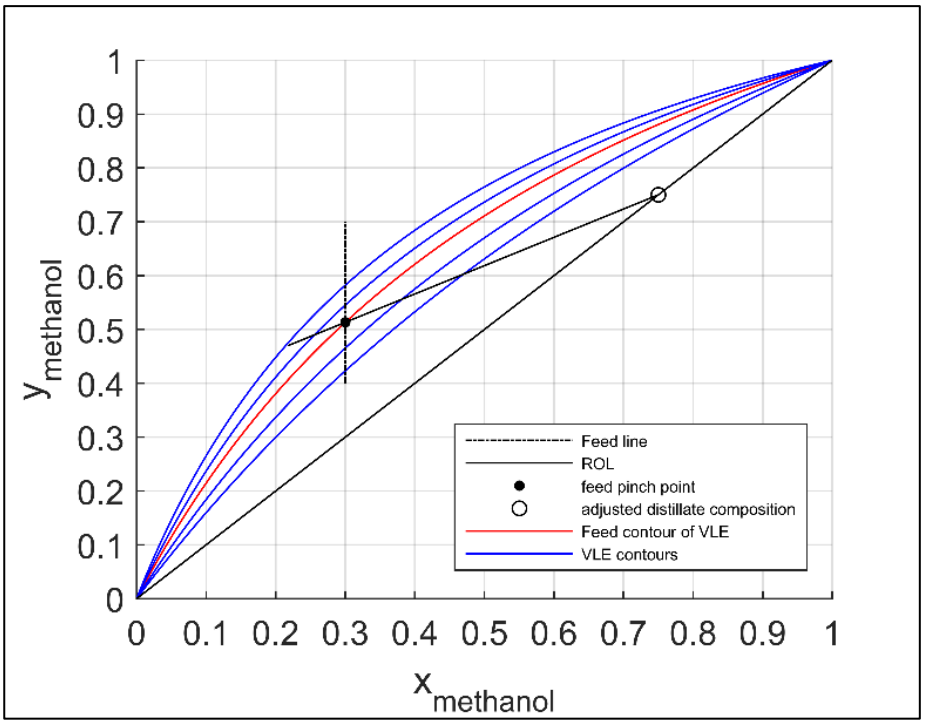

Figure 5.5: McCabe-Thiele diagram for methanol (LK), showing the adjusted distillate composition and plots the rectifying operating line (ROL) to determine the minimum reflux for transition split in direct split

Step 2

For the general case, if the split is direct, the binary equilibrium curve for Components A (LK) and B (IK) and the operating line for component A (LK) are plotted on the x-y diagram. For an indirect split, the binary equilibrium curve for Components B (IK) and C (HK) and the operating line for Component C (HK) are plotted on the x-y plot. The intersection of the rectifying operating line and binary equilibrium curve (Components A and B) represents the transition point in the rectifying section for a direct split. Similarly, the intersection of the bottoms operating line and the binary equilibrium curve (Components B and C) represents the transition point in the bottoms section for an indirect split.

For Example 5.2, using the estimated minimum reflux ratio of 1.11 (Step 1), the rectifying operating line for methanol (LK) for the transition split can be plotted from the calculated adjusted distillate composition (0.75), calculated from the transition split depicted in Figure 5.5. The rectifying operating line is plotted on the same x-y diagram with the binary equilibrium curve of methanol (LK) and ethanol (IK) (α_{ME}). Figure 4.6 depicts the rectifying operating line and binary equilibrium curve on the x-y plot for methanol (LK). The transition point ($x_{TR,i}{}^{*}$, $y_{TR,i}{}^{*}$) is read off Figure 5.6 at the intersection of the binary equilibrium curve and the rectifying operating line for the transition split. The transition point for the specified feed is (0.470, 0.602).

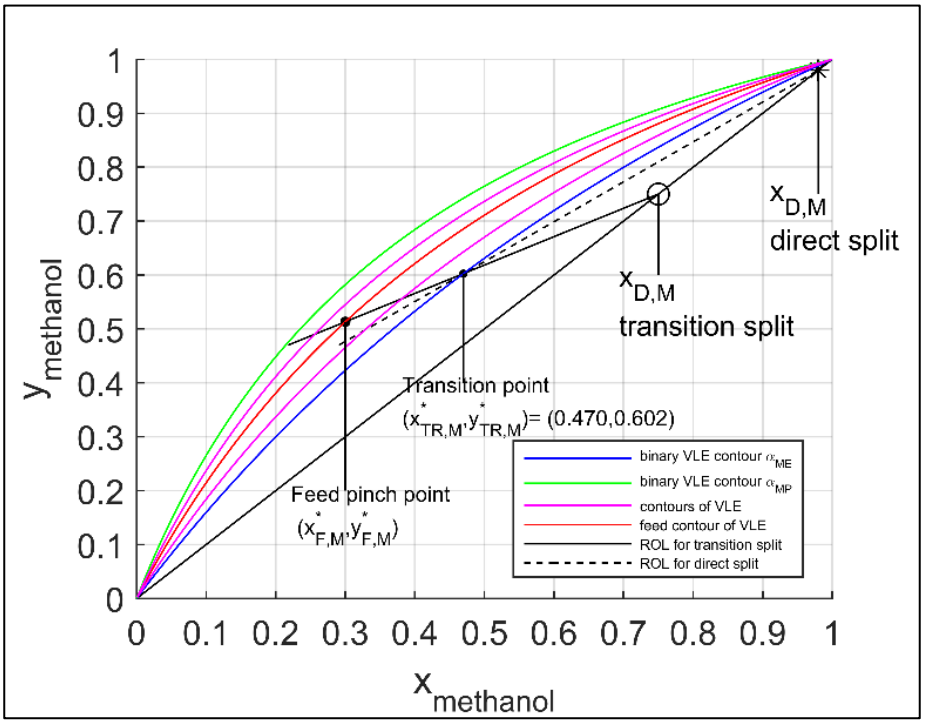

Figure 5.6: McCabe-Thiele plot for methanol to determine the transition point and hence the minimum reflux ratio for a direct split

Step 3

Given the desired distillate product for methanol (LK= 0.980) and the calculated transition point in Step 2, the gradient of the new rectifying operating line at the desired split can be calculated using Equation 5.6. The gradient is found to be 0.740 and hence the minimum reflux ratio is found to be 2.85 (Figure 5.6). A minimum reflux ratio of 2.70 and 2.84 is predicted by the boundary value method (BVM) (Doherty & Malone, 2001) and Underwood (1948) methods respectively. The distillate product compositions obtained by Doherty & Malone (2001), presented in Table 5.3 were used to calculate the minimum reflux ratio using the Underwood (1948) method. The proposed graphical method correlated closer to the reflux ratio predicted by Underwood (1948) (0.112 % deviation) than Doherty & Malone (2001).

The estimate of the minimum reflux ratio of 2.85 can be used to plot McCabe-Thiele diagrams for the three components to determine the equilibrium compositions on each stage. The compositions on each stage can be plotted on a

MBT for methanol (x) and ethanol (y). The BVM can be used to determine if the rectifying and bottoms profiles just intersect, which correlates with the minimum reflux. Figure 5.7 depicts the rectifying and bottoms composition profiles for the direct split analysed above, using the distillate product compositions in Table 5.1. It can be seen that both profiles just intersect, indicating that the estimate is sufficient. Hence the proposed method of plotting the VLE contours can be used to determine if the calculated minimum is a good estimate of the actual minimum reflux ratio.

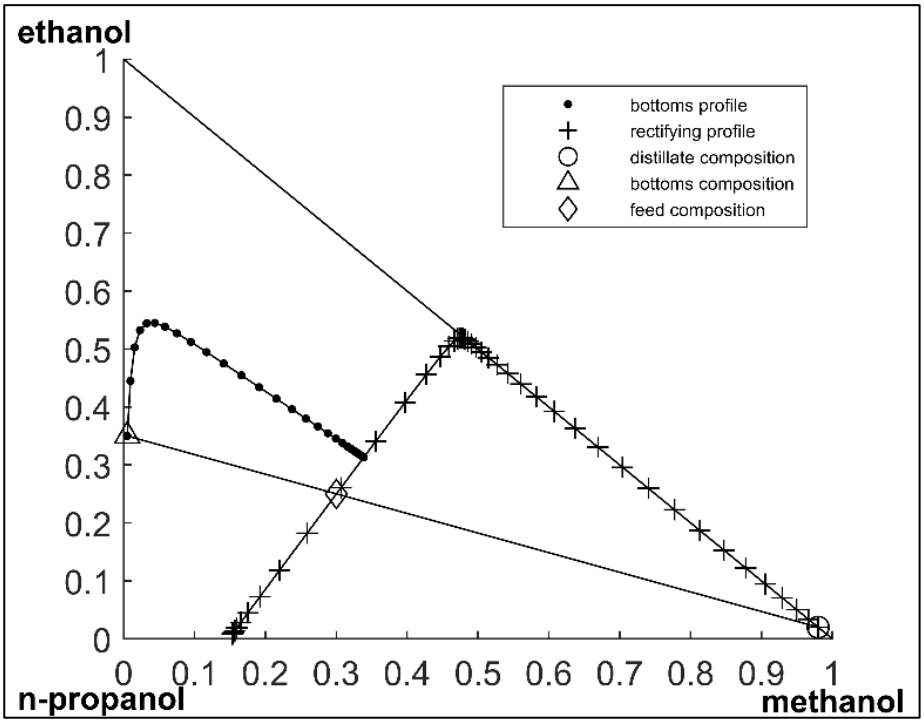

Figure 5.7: Mass balance triangle (MBT) depicting the rectifying and operating profiles at the minimum reflux predicted by the proposed graphical method for direct split

Part B: Sharp indirect split

The mixture of methanol (M), ethanol (E) and n-propanol (P) in Example 5.2 is fed into a finite reflux column at constant pressure (1 bar). The composition of the saturated liquid (q=1) feed to the column, the distillate product and bottoms product for the indirect split can be found in Table 5.1. Determine the minimum reflux and reboil ratios to achieve a minimum recovery of n-propanol of 0.978 in the bottoms product.

Step 1

The first step is to determine the minimum reboil ratio for the transition split, given a specified feed. A bottoms product rich in the heavy key, n-propanol, is achievable in an indirect split, and hence contains very little to none of the light key component, methanol. The minimum reboil ratio can be obtained in two ways:

1. Using Equation 5.8 and the minimum reflux of 1.11 calculated in Step 1 of Example 5.2.
2. Determine the minimum reboil ratio using the method illustrated for transition splits in Step 1 of Part A, but setting the bottoms composition of methanol (LK) to 1×10^{-10} in the bottoms product (Figure 5.8).

Both methods estimate a minimum reboil ratio of 1.41. If the second method is chosen, the resulting bottoms product composition can be found in Table 5.3 for the transition split. The adjusted bottoms composition (n-propanol (HK)) was determined using Figure 5.9.

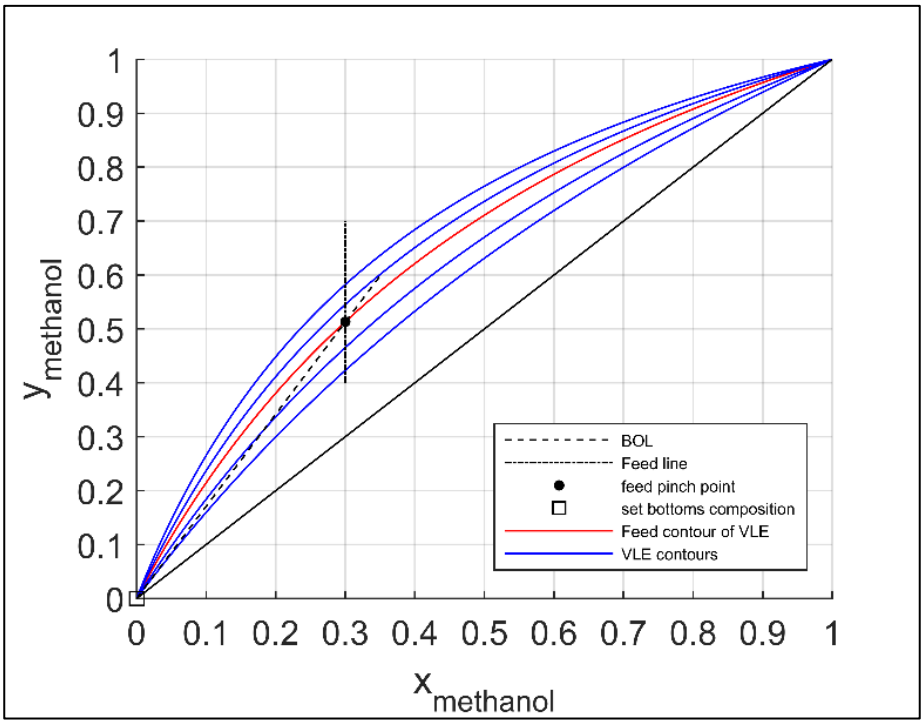

Figure 5.8: McCabe-Thiele diagram for methanol (LK), plotting the bottoms operating line (BOL) to determine the minimum reboil ratio for the transition split in an indirect split

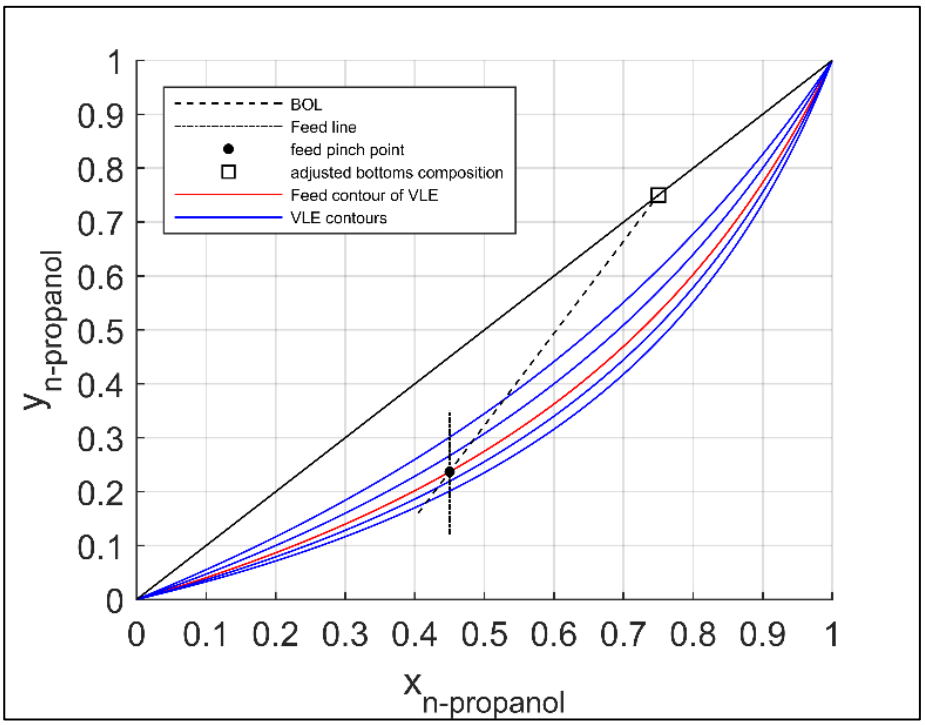

Figure 5.9: McCabe-Thiele diagram for n-propanol (HK), depicting the adjusted bottoms composition and plotting the bottoms operating line (BOL) to determine the minimum reboil ratio for transition split in an indirect split

Step 2

This required plotting the binary VLE curve of n-propanol and ethanol (α_{PE}) and the bottoms operating line (using the calculated minimum reboil ratio), on the x-y diagram for n-propanol. The transition point ($x_{TB,i}^{*}$, $y_{TB,i}^{*}$) is then read off Figure 5.10 at the intersection of the binary equilibrium curve and the bottoms operating line for the transition split. The transition point for the specified feed is (0.528, 0.371).

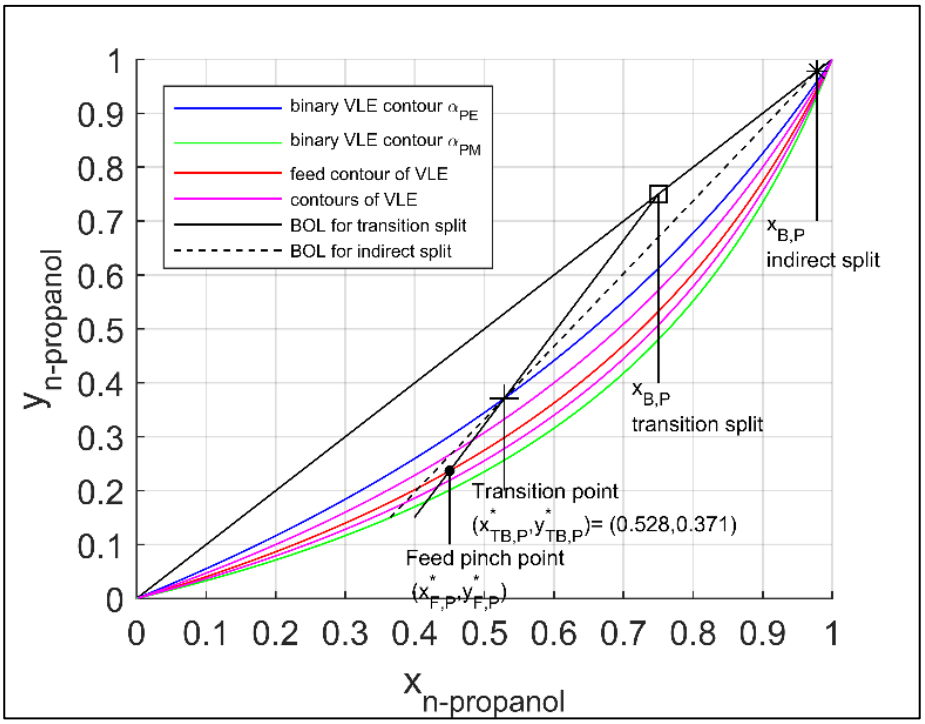

Figure 5.10: McCabe-Thiele plot for n-propanol to determine the transition point and hence the minimum reboil ratio for an indirect split

Step 3

Using the target bottoms composition for n-propanol of 0.978 and the calculated transition point in Step 2, the gradient of the new stripping operating line at the desired split can be calculated. The gradient is found to be 1.35 and hence the minimum reboil ratio is found to be 2.85 (Figure 5.10).

Step 4

Rearranging Equation 5.8, the corresponding minimum reflux ratio is calculated to be 1.38. The minimum reflux ratio calculated using BVM by Doherty & Malone (2001) is 1.35 and Underwood (1948) (using the bottoms compositions by Doherty & Malone (2001) in Table 5.3) is 1.38. Once again, the proposed graphical method predicts the minimum reflux ratio closer to that of Underwood (1948) (0.0580% deviation) in comparison with Doherty & Malone (2001) for indirect splits as well. Figure 5.11 depicts the rectifying and stripping composition profiles for the

calculated minimum reflux and reboil ratios using the bottoms and distillate product compositions in Table 5.1. Figure 5.11 shows that both profiles just intersect symbolising a sufficiently accurate estimate.

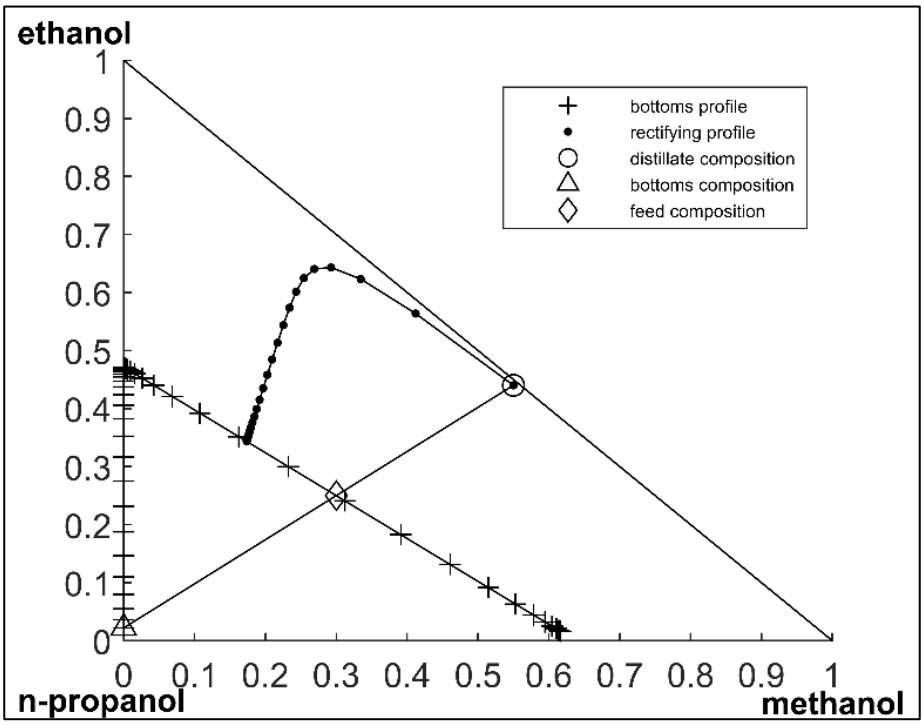

Figure 5.11: Mass balance triangle (MBT) depicting the rectifying and operating profiles at the minimum reflux predicted by the proposed graphical method for indirect split

Underwood (1948), and the proposed graphical method based on Stichlmair (2005) observations, hold only if the distillate product for a direct split is close to a binary mixture. The bottoms product can lie in the interior of the MBT. Similarly, the bottoms product must be close to a binary mixture for an indirect split (distillate product can be a ternary mixture) for Underwood (1948) and the proposed graphical method to produce correct minimum reflux ratio values. Figure 5.12 (a) depicts an indirect split of a binary bottoms product and a ternary distillate product. The minimum reflux ratio predicted by Underwood (1948) and the proposed graphical method are 1.17 and represents the true minimum reflux, which is depicted as the profiles just touch in Figure 5.12a. Figure 5.12b, depicts a ternary distillate and bottoms product (for an indirect split) and in such a case the minimum reflux predicted by Underwood (1948) and the proposed graphical method are 1.12 and

1.10 respectively. Figure 5.12b shows the minimum reflux ratio predicted by the proposed graphical method. It can be seen that the minimum reflux ratio predicted by both methods is too low compared to the actual minimum reflux ratio required of 4.17 (Figure 5.12c). It can be deduced that two factors have to hold for the correct prediction of minimum reflux ratio:

(1) The separation must reach the saddle pinch where the system reduces to a binary mixture, such that

(2) The node pinch is aligned with the feed and saddle pinch (Levy et al., 1985b).

Figure 5.12 (c) depicts the rectifying and stripping profiles on a MBT at the actual reflux ratio of 4.17 (determined using BVM). It can be seen on Figure 5.12 (c) that the node pinch in the rectifying profile is not aligned with the feed, as the saddle pinch is absent.

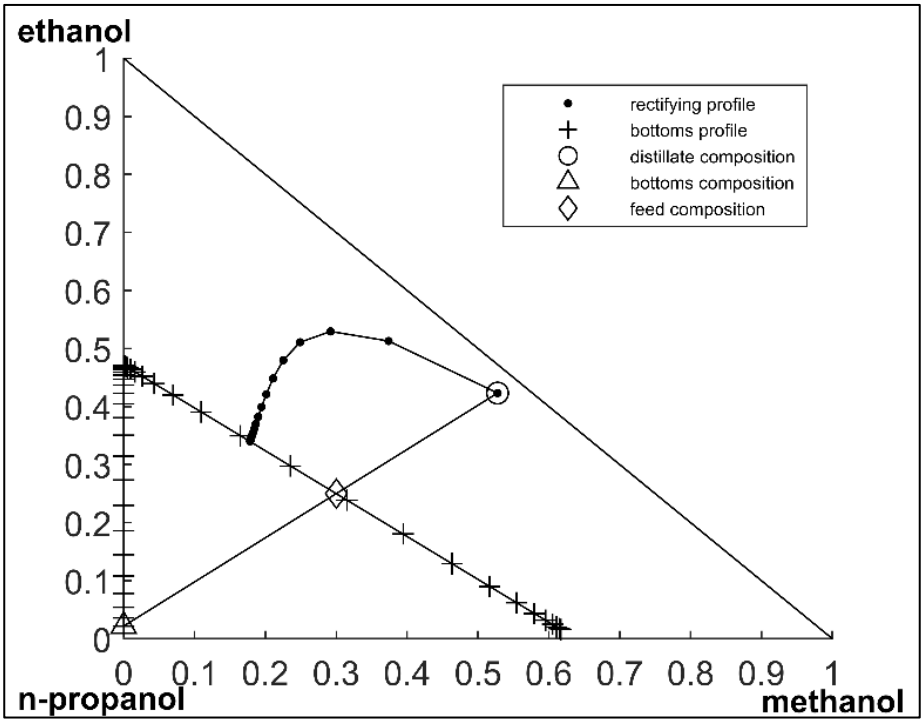

(a)

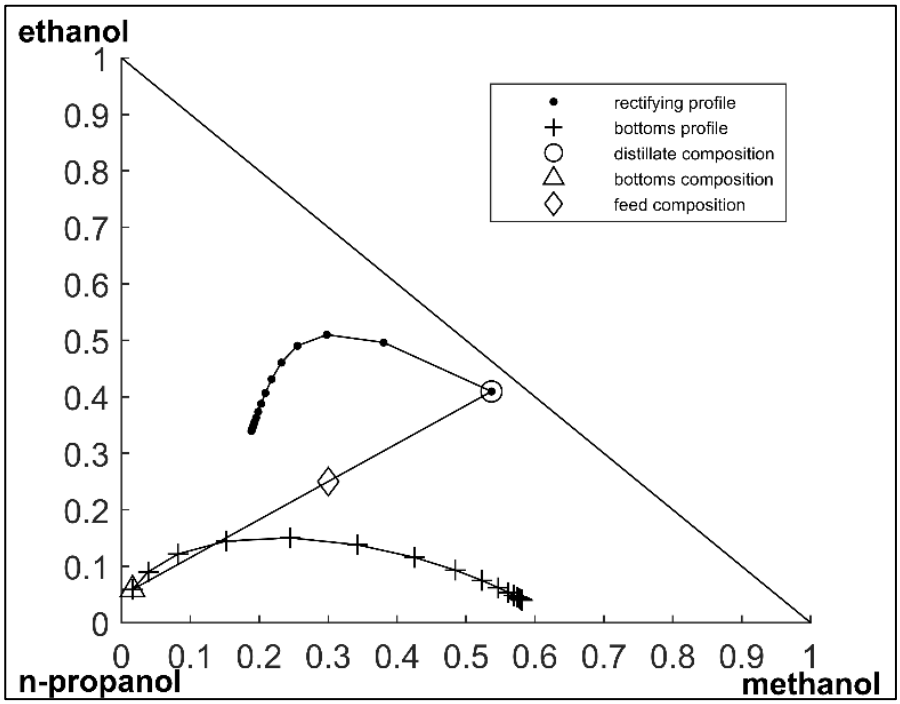

(b)

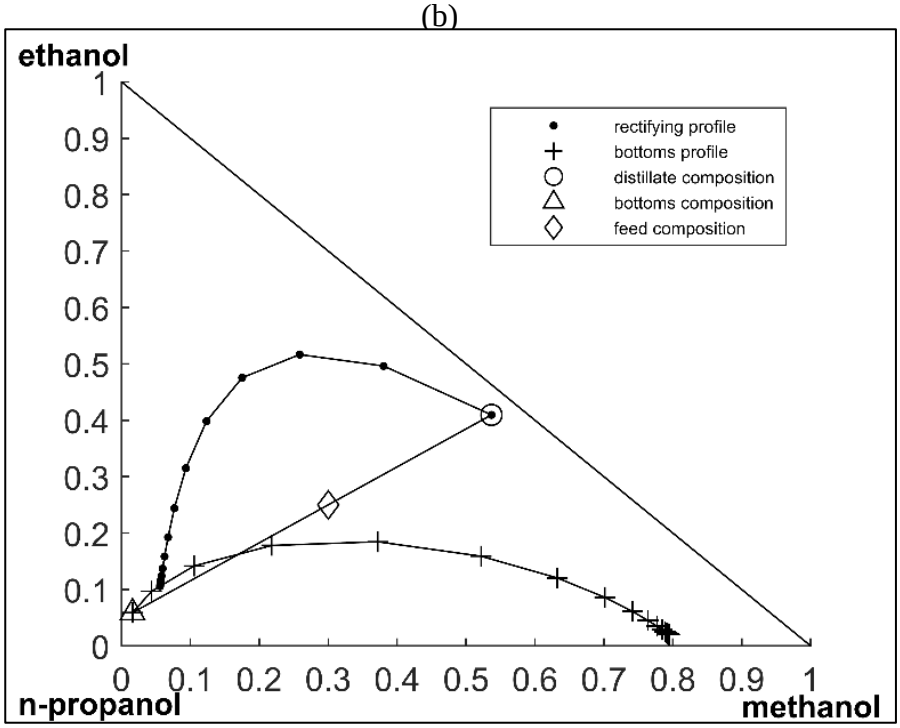

(c)

Figure 5.12: (a) Mass balance triangle (MBT) depicting the rectifying and operating profiles at the minimum reflux ratio predicted by the proposed graphical method for an indirect split, with a binary bottoms product and ternary distillate product, (b) Mass balance triangle (MBT) depicting the rectifying and operating profiles at the minimum reflux ratio predicted by the proposed graphical/Underwood methods for an indirect split, with ternary bottoms product and distillate products, (c) Mass balance triangle (MBT) depicting the rectifying and operating profiles at the actual minimum reflux ratio of 4.17

5.4.2.2 Example 5.3: Non-ideal simple separation (acetone, benzene, chloroform)

Design problem: A mixture of acetone (A), chloroform (B), and benzene (C) feeds into a finite reflux column at constant pressure (1 bar). The composition of the saturated liquid (q=1) feed, distillate and bottoms products for the transition split is presented in Table 5.5. The aim of the separation is to achieve a mole fraction of 0.978 of benzene recovered in the bottoms product. Determine the minimum reflux and reboil ratios.

Table 5.5: Feed, distillate and bottoms compositions for the acetone, benzene and chloroform system for a transition split.

Component	x_F	y_F^*	x_B	x_D
acetone	0.213	0.4059	5.00×10^{-10}	0.9224
benzene	0.7094	0.5165	0.9224	5.00×10^{-10}
chloroform	0.0776	0.0776	0.0776	0.0776

Step 1 and Step 2

The design problem illustrates an indirect split as the bottoms product is almost pure benzene and contains very little acetone. For azeotropic systems, the type of split is dependent on the distillation region of operation. Hence, the graphical method presented in Section 5.3.2.1 for indirect splits will be followed to calculate the minimum reflux and reboil ratios. The first step is to determine the minimum reboil ratio for the transition split. The method presented for indirect splits and transition splits is used to determine the values in Table 5.5 and the minimum reflux and reboil ratios for the transition split. The minimum reflux and reboil ratios are found to be 2.68 and 1.10 respectively for the transition split.

On the same x-y diagram, the binary equilibrium curve of benzene and chloroform (α_{BC}) and the bottoms operating line (using the minimum reboil ratio calculated for transition split) for benzene is plotted. The transition point ($x_{TB,B}{}^*$, $y_{TB,B}{}^*$) is read

off Figure 5.13 at the intersection of the binary equilibrium curve (α_{BC}) and the bottoms operating line for the transition split. The transition point for the feed is (0.849, 0.783).

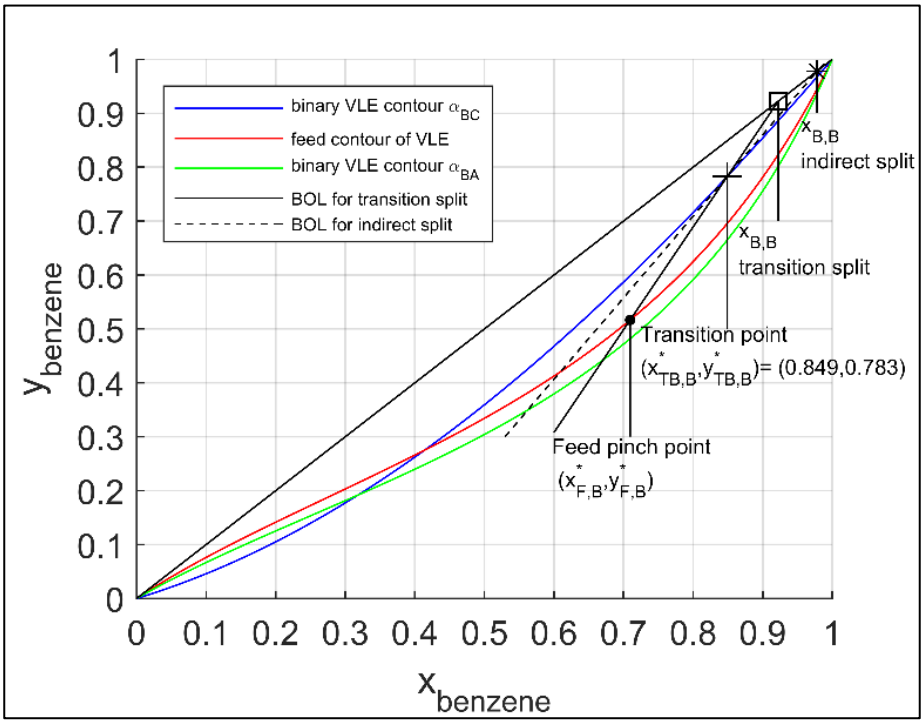

Figure 5.13: McCabe-Thiele plot for benzene to determine the transition point and hence the minimum reboil ratio for an indirect split

Step 3

The target bottoms composition for benzene of 0.978 and the calculated transition point in Step 2 are used to determine the gradient of the new bottoms operating line. The gradient is found to be 1.51 and hence the minimum reboil ratio is found to be 1.95 (Figure 5.13).

Step 4

Rearranging Equation 5.8, the corresponding minimum reflux ratio is calculated to be 4.089. Using the proposed graphical method of calculating the composition on each stage and the BVM, the minimum reflux is found by trial-and-error to be 4.17. The fairly simple method only deviates from the actual minimum reflux of 1.93% and would be a sufficiently accurate estimate for preliminary design calculations.

The distillation curves for the acetone-benzene-chloroform system display a high degree of curvature, unlike other non-ideal and azeotropic systems which are more linear (Levy et al., 1985b). Hence, the proposed graphical method would be appropriate for use in preliminary design calculation for non-ideal and azeotropic systems of high curvature as well as linear distillation curves.

The limitation of this method is that it applies only to direct and indirect splits. In addition, the feed compositions must align with the composition on the feed stage of the column. This assumption is also made by Underwood and for the boundary value method.

5.5 Conclusion

In this chapter, a simple graphical method is presented to find the minimum reflux and reboil ratios for ternary ideal and non-ideal systems. The method is only applicable to three classifications of splits namely: transition, sharp direct and indirect splits. In addition, the method also assumes that feed compositions must align with the composition on the feed stage of the column. This assumption is also made by Underwood and for the boundary value method. Firstly, an algebraic explanation is presented for the method of determining the minimum reflux ratio for the three classifications of splits. Secondly, the method for transition splits is applied to both ideal and non-ideal systems. Thirdly, the method is depicted for both a sharp direct and indirect split for an ideal system of methanol, ethanol, and n-propanol. Lastly, a method for a sharp indirect split for an azeotropic non-ideal system of acetone, benzene and chloroform is presented. Although not shown, the method for sharp direct splits can be applied to non-ideal systems as well. The proposed graphical method for ideal systems is consistent with the Underwood method in predicting the minimum reflux for all classifications of splits. The proposed graphical method provides sufficiently accurate estimates of minimum reflux ratio for highly non-ideal azeotropic systems with deviations of less than 2%.The method is simple and effective in adherence to the binary McCabe-Thiele method.

REFERENCES

Barbosa, D. & Doherty, M.F., **1988**. Design and minimum-reflux calculations for single-feed multicomponent reactive distillation columns. *Chem. Eng. Sci*. 43(7), pp. 1523-1537.

Barnes, F. J., Hanson, D. N., King, C. J. **1971**. Calculation of Minimum Reflux for Distillation Columns with Multiple Feeds. *Ind. Eng. Chem. Process. Des. Develop.* 11(1), pp. 136 -140.

Bausa, J., von Watzdorf, R., Marquardt, W. **1998**. Shortcut Methods for Nonideal Multicomponent Distillation: 1. Simple Columns. *AIChE J*. 44(10), pp. 2181-2198.

Brüggemann, S. & Marquardt, W., **2004**. Shortcut methods for nonideal multicomponent distillation: 3. Extractive distillation columns. *AIChE J*. 50(6), pp. 1129-1149.

Doherty, M.F. & Malone, M.F., **2001.** Conceptual Design of Distillation Systems. *McGraw-Hill, Inc:* New York.

Górak, A. & Sorensen, E., **2014**. Distillation: Fundamentals and Principles. *Elsevier: Academic Press*: London.

Halvorsen, I.J. & Skogestad, S., **2003a**. Minimum Energy Consumption in Multicomponent Distillation. 1. V_{min} Diagram for a Two-Product Column. *Ind. Eng. Chem. Res.* 42(3), pp. 596-604.

Halvorsen, I.J. & Skogestad, S., **2003b**. Minimum Energy Consumption in Multicomponent Distillation. 2. Three-Product Petlyuk Arrangements. *Ind. Eng. Chem. Res*. 42(3), pp. 605-615.

Julka, V, & Doherty, M.F., 1990. Geometric behavior and minimum flows for nonideal multicomponent distillation. *Chem. Eng. Sci*. 45(7), pp.1801-1822.

Koehler, J., Poellmann, P., Blass E., **1995**. A Review on Minimum Energy Calculations for Ideal and Nonideal Distillations. *Ind. Eng. Chem. Res*. 34(4), pp. 1003-1020.

Lee, E.K. & Wong, D.S.H., **2008**. Shortcut design of complex distillation Part 1. Basic theory and applications to multi-feed columns. *J. Chin. Inst. Chem. Eng*. 39(5), pp. 519–527.

Levy, S.G., Van Dongen, D.B., Doherty, M.F., **1985a**. Design and Synthesis of Homogeneous Azeotropic Distillations. 1. Problem Formulation for a Single Column. *Ind. Eng. Chem. Fundam.* 24 (4), pp. 454–463.

Levy, S.G., Van Dongen, D.B., Doherty, M.F., **1985b**. Design and Synthesis of Homogeneous Azeotropic Distillations. 2. Minimum Reflux calculations for Nonideal and Azeotropic Columns. *Ind. Eng. Chem. Fundam*. 24(4), pp. 463–474.

Lucia, A., Amale, A., Taylor, R., **2006**. Energy Efficient Hybrid Separation Processes. *Ind. End. Chem*. 45(6), pp. 8319-8328.

McCabe, W.L. & Thiele, E.W., **1925**. Graphical Design of Fractionating Columns. *Ind. Eng. Chem.* 17(6), pp. 605-611.

Nawaz, M. & Jobson, M., **2011**. A boundary value design method for complex demethaniser distillation columns. *Chem. Eng. Res. Des*. 89(8), pp. 1333-1347.

Stichlmair, J., Offers, H., Potthoff, R.W., **1993**. Minimum Reflux and Minimum Reboil in Ternary Distillation. *Ind. Eng. Chem. Res*. 32(1), pp. 2438-2445.

Stichlmair, J., **2005**. Distillation and Rectification. In Ullmann's Encyclopaedia of Industrial chemistry. *Wiley-VCH Verlag GmbH & Co: Weinheim.*

Underwood, A.J.V. **1948**. Fractional Distillation of Multicomponent Mixtures. *Chem. Eng. Prog*. 44(8), pp. 603-614.

von Watzdorf, R., Bausa, J., Marquardt, W., **1999**. Shortcut Methods for Nonideal Multicomponent Distillation: 2. Complex Columns. *AIChE J*. 45(8), pp. 1615-1628.

Worms, G., Meyer, M., Rouzineau, D., Brehelin, M., **2017**. Production Zone Method: a Non-ideal Shortcut Method for Distillation Column Design. *Comp. Aid. Chem. Engin*. 40, pp. 745-750.

Yaws, C.L., Li, K.Y., Fang, C.S., **1981**. How to Find the Minimum Reflux for Binary Systems in Multiple-Feed Columns. *Chem. Eng*. 88(10), pp. 153-156.

Chapter 6

The Number of Theoretical Stages and Feed stage Location at Finite Reflux for Distillation Design

The work in this chapter has been published as**:** The work in this chapter has been published as: Seedat, N., Kauchali, S., Patel, B., **2021**. A graphical method for the preliminary design of ternary simple distillation columns at finite reflux. *SAJCE*. 37, p. 99-109. The work is a reproduction of the journal publication although Section 6.2.2, 6.4 and 6.5 have been added for the purpose of clarity and easy understanding and extension of the work published in the paper. The reproduction was done with permission from the publisher. (**Copyright © 2021 Elsevier)**

Abstract

A graphical method for the design of multicomponent distillation systems at finite reflux is presented. Here, key design parameters are determined, in particular feed stage location and the number of theoretical stages required for separation at finite reflux, for ideal and non-ideal systems in simple columns. A general procedure for ternary and quaternary systems is presented and can be applied to higher order systems. The procedure provides designers with a visual tool to determine the design parameters simultaneously and no additional calculations are required, unlike current approaches. The proposed graphical method correlates with the Fenske-Underwood-Gilliland (FUG) method for ideal systems. The parameters obtained from the proposed graphical method allow for implementation in rigorous simulators as starting values to achieve a converged column with the first simulation and with less computational difficulty.

6.1 Introduction

The distillation design procedure consists of three crucial stages namely conceptual, preliminary and detailed/optimization design phase. In the conceptual design stage, graphical methods are invaluable tools as they provide crucial visual insights into the behaviour of systems. Residue curve maps (RCMs) and distillation curve maps (DCMs) have been used frequently in the conceptual design of multicomponent zeotropic and azeotropic distillation systems (Widago & Seider, 1996). Feasible and infeasible designs can be identified prior to preliminary and detailed design calculations, saving the designer time and preventing convergence issues. In distillation design, preliminary design tools are used to determine key design parameters such as minimum reflux ratio, theoretical number of stages at finite reflux ratio and feed stage location (Gani & Bek-Pedersen, 2000). The above-listed parameters are used to initialise rigorous simulators to perform detailed design and optimization simulations (Fidkowski et al., 1991). Essentially, the conceptual and preliminary design procedures serve as a precursor to the rigorous simulation process. Preliminary design tools can be categorised into two main methods: short-cut/empirical methods and graphical methods (Kister, 1992).

Short-cut methods are fairly simple empirical correlations to determine design parameters. Short-cut methods to determine the minimum reflux ratio were proposed by Brown & Martin (1939), Colburn (1941), and Underwood (1948). Smoker (1938), Gilliland (1940) and Erbar and Maddox, (1961) provided an empirical correlation to determine the number of theoretical separation units at finite reflux for multicomponent systems. The Kirkbride (1944) equation is an empirical correlation that determines the feed stage location for multicomponent systems. Short-cut methods rely on making several assumptions such as constant relative volatility (CRV) and constant molar overflow (CMO), key limitations, and hence are not applicable to non-ideal and azeotropic systems (Reyes et al., 2000; Wasylkiewicz et al., 2000). According to Kong & Maravelias (2019) short-cut methods do not take into consideration the combined effect of reflux ratio on the

number of stages, hence energy and capital requirements are not considered as interlinked variables.

Graphical methods are essential tools in both the conceptual and preliminary design phases. Graphical methods depict mass and energy balances as well as vapour-liquid equilibrium (VLE) in a 'picture'. The depiction of VLE provides the designer with visual insights into identifying feasible designs, pinch point (minimum energy requirements) and possible operational issues (Mathias, 2009). In addition, graphical methods can be used to determine preliminary design parameters. The Ponchon & Savarit and McCabe & Thiele methods are two dimensional (2D) graphical methods presented in the 1920s for binary distillation processes, and have remained prominent in the discussion of distillation design for almost a century (Ho et al., 2010; Lee et al., 2000a; Lee et al., 2000b).

The mathematical theory for the design of binary distillation was first presented by Sorel (1889) (Hengstebeck, 1961). Sorel (1889) assumed equilibrium of the vapour and liquid on each stage, such that the mass and energy leaving and entering a stage could be determined (Lewis, 1922). The method proposed by Sorel (1889) is iterative in nature and requires calculating mass and energy balances on each stage, and hence lacks the visual impact of understanding the separation (Lewis, 1922). Lewis (1922) adapted the method by Sorel (1889) with simplified computation by neglecting energy balances. McCabe & Thiele (1925) developed the McCabe-Thiele diagram and method for the conceptual and preliminary design of binary distillation systems which is based on Lewis's method. McCabe & Thiele (1925) represented the simplified equations proposed by Lewis (1922) on a 2D, vapour (x) and liquid (y) plane for binary mixtures. The McCabe-Thiele method also graphically solves the mass and equilibrium equations to calculate the minimum number of stages, the theoretical number of stages, the feed stage location and minimum reflux ratio (McCabe & Thiele, 1925).

The McCabe-Thiele diagram is arguably the most well-known, simple and effective graphical design method to date (Kong & Maravelias, 2019). The popularity and effectiveness of using McCabe-Thiele diagrams as a binary distillation design tool

is the powerful pictorial understanding of the behaviour of a system in addition to quantitatively determining design parameters (Neri et al., 1998). Every chemical engineer has been taught and has drawn a McCabe-Thiele diagram to design or troubleshoot binary distillation processes (Mathias, 2009). The generation of a McCabe-Thiele diagram requires the representation of vapour-liquid equilibrium (VLE) on a 2D plot. Once the VLE has been plotted, as the initial step, the designer is equipped to visually analyse the behaviour of systems by incorporating mass balance equations as operational lines. Although the McCabe-Thiele method is an efficient design method, it is limited mainly to binary systems due to the difficulty in depicting the multivariant behaviour of VLE for multicomponent systems (Neri et al., 1998). Cope & Lewis (1932), Brown et al., (1932), Jenny (1939) and Hengstebeck (1946) presented adaptations of McCabe-Thiele diagrams for multicomponent systems. The methods presented by the above authors have started with the fundamentals of the binary McCabe-Thiele method but have lost vital information inherent in their simplifying assumptions. Assumptions such as Raoult's law, (Cope & Lewis, 1932), equilibrium constant, K (Brown et al., 1932 and Jenny, 1939) and pseudo-binary mixtures of key components, (Hengstebeck, 1946), are applied to calculate and represent VLE.

Methods of determining feed stage location for multicomponent systems have been presented by Doherty & Malone (2001) and Vogelpohl (2015). Both methods require additional calculations on residue curve maps (RCM) in order to determine the feed stage, unlike the original McCabe-Thiele method, where the feed stage is determined visually while determining the number of stages required.

According to Neri et al., (1998), no graphical method is available for designers to (1) determine design parameters and (2) visualize the behaviour of multicomponent systems at finite and infinite reflux. To overcome these limitations, a novel method of representing the contours of VLE for ternary systems has recently been established, as discussed in Chapter 3. Chapter 4 presented a robust and simple graphical method to design simple infinite reflux columns. In this Chapter, the novel method of representing the contours of VLE is used to provide a graphical

insight based approach to determine the design parameters at finite reflux for ternary distillation column design. The design parameters obtained are used to complement the efficient use of rigorous simulators. The theoretical number of stages and the feed stage location are determined simultaneously, whilst carrying out the graphical method once the VLE has been plotted as an initial step. Thereafter, different design options can be investigated on the plotted VLE curves with minimal calculations.

In this Chapter, firstly, the original McCabe-Thiele method is extended to ternary mixtures, illustrating that the proposed graphical method retains the simplicity of the original method. Secondly, using the contours of VLE, the method of determining the theoretical number of stages at finite reflux and feed stage location is presented for sharp direct and indirect splits. A general procedure for higher order systems is explained and illustrated with an example of a quaternary system. Finally, the graphical method to determine the number of theoretical stages and feed stage location can be extended to non-ideal mixtures and systems in which CMO is not valid. A straightforward derivation is presented which can be applied to non-CMO systems. The proposed graphical method, in this chapter, will be compared to the traditional Fenske-Underwood-Gilliland (FUG) method for ideal systems. For non-ideal systems, the graphical method will be used to initialise a rigorous simulator, Aspen Plus^{TM}, to achieve a converged preliminary design for further detailed design calculations. Using the minimum reflux and reboil ratios, as determined in Chapter 5, the designer chooses operating reflux and reboil ratios slightly above the minimum values. The discussion of this chapter will focus mainly on the design of finite reflux ternary and quaternary distillation systems. In addition, the proposed graphical method is not restricted to the systems depicted in this work, but applies to systems with all types of chemical components (ideal and non-ideal).

6.2 The McCabe-Thiele Method for Ternary Systems

The mathematical theory for the design of binary distillation was first presented by Sorel in 1889 (Lewis, 1922; Hengstebeck, 1961). Sorel assumed equilibrium of the

vapour and liquid on each stage, such that the mass and energy leaving and entering a stage could be equated (Lewis, 1922). The method proposed by Sorel is iterative in nature and requires calculating mass and energy balances on each stage and hence lacks the visual impact of understanding the separation (Lewis, 1922). Lewis (1922), adapted the method by Sorel with simplified computation by neglecting energy balances (Lewis, 1922; Hengstebeck, 1961). McCabe & Thiele (1925) represented the simplified equations proposed by Lewis (1922) on a 2D, vapour (x) and liquid (y) plane for binary mixtures. The McCabe-Thiele method graphically solves the mass and equilibrium equations to calculate the minimum number of stages, theoretical number of stages and minimum reflux (McCabe & Thiele, 1925; Hengstebeck, 1961).

The proposed graphical method will apply the same assumptions made in the original McCabe-Thiele method, as listed below (Kister, 1992; Lewis, 1922; Wankat, 2012):

- Constant molar overflow (CMO)
- Heat losses to surroundings are negligible (adiabatic) in comparison to heat carried by vapour in the column
- Boiling points of all the components must not be significantly different and do not change at any point in the column (temperature range of column must not be substantial)
- Molar latent heat of vaporization of all the components must not be considerably different and be constant at all conditions of the column
- Sensible heat and heat of mixing effects are negligible in comparison to latent heat changes
- On each stage the vapour and liquid are in equilibrium
- 100% tray efficiency
- Constant pressure

The equations derived by Lewis (1992), and hence the McCabe-Thiele method, are based on the very important assumption of constant molar overflow (CMO)

(McCabe & Thiele, 1925). CMO assumes that the liquid and vapour flowrates in a column section are constant (Lee et al., 2000b). According to Kong & Maravelias (2019) the assumptions of CMO hold in general as (1) heat losses to the surroundings are negligible as most distillation columns are insulated, and (2) the need for distillation arises because it is required to separate components of similar nature (similar boiling points and latent heats). Nevertheless, if heat losses are not negligible and boiling points vary over the column, a new mass balance would have to be constructed for each stage (McCabe & Thiele, 1925). According to McCabe & Thiele (1925), this is a tedious procedure and the effects are small and cancel out, hence rarely requiring special attention. According to Górak & Sorensen (2014), CMO is least valid when the latent heats of vaporizations are substantially different. In Section 6.5, it will be shown how the proposed graphical method can be extended to non-CMO conditions using the method presented by Fischer (1963).

The construction of the McCabe-Thiele diagram requires the representation of the VLE and operating lines. The binary McCabe-Thiele method is well known in the field of distillation design, and hence a brief outline of the ternary systems will be presented.

6.2.1 Representation of VLE

For ternary systems, the depiction of VLE on a 2D (x-y) plane is not as simple as binary mixtures. Chapter 3 provided the derivation and explanation of a novel method of representing the VLE of ternary mixtures as contours of VLE (multiple unique contours) for both ideal and non-ideal systems. The proposed method overcomes the difficulty of representing VLE for ternary mixtures in 2D by defining a component's VLE as a series of ratios of the other components present in the system. In this way, the vapour composition in equilibrium with a known liquid composition can be read off from the diagram. The method can incorporate any thermodynamic model to plot the contours of VLE for ideal and non-ideal systems. Applying the same principles used to derive the equations and ratios required to plot the contours of VLE for a ternary system, the equations and ratios

for higher order systems can be derived and are presented in Section 6.4. A brief recap is provided below, for ternary systems. The proposed method overcomes the difficulty of representing VLE for multicomponent mixtures in 2D by defining a component's VLE as a series of ratios of the other components present in the system.

Consider an ideal three-component system (*i, j* and *k*). At constant relative volatility (α) the vapour compositions for component i can be defined by Equation 6.1:

$$y_i = \frac{\alpha_{ik}\left(\frac{x_i}{1-x_i}\right)(CR_{jk}+1)}{1+\alpha_{ik}\left(\frac{x_i}{1-x_i}\right)(CR_{jk}+1)+\frac{\alpha_{ik}}{\alpha_{ij}}CR_{jk}} \tag{6.1}$$

Where

$$CR_{jk} = \frac{x_j}{x_k} \tag{6.1a}$$

$$CR_{jk} = \frac{y_j}{y_k} \tag{6.1b}$$

It is noted that for a fixed ratio (CR_{jk}) the vapour fraction (y_i) is only dependent on the liquid mole fraction (x_i). Hence, the contours of VLE can be plotted at different ratios. Equation 6.1a is applied to calculate ratios for determining the number of stages from the bottoms composition, while Equation 6.1b is applied for calculating the number of stages from the distillate composition (Equation 6.1 would have to be rearranged to solve for x_i). Similarly, the contours of VLE can be plotted for component *j* and *k.* The proposed method for the representation of the contours of VLE is generic in nature, and can be applied to any type of components present in a mixture, provided data for the equilibrium relationship can be generated. The method of using ratios can be incorporated into any thermodynamic model to plot the contours of VLE for non-ideal systems. Furthermore, it is only required to plot the contours of VLE once for subsequent analysis. Hence, the proposed method will be used to generate the equilibrium relationship required in this thesis to calculate the minimum reflux, the theoretical number of stages and the feed stage location.

6.2.2 Feed line, Rectifying and Bottoms Operating Lines for Ternary Systems

The mass balance lines for a simple separation (one feed and two products) can be derived for ternary systems analogous to binary systems as presented by Lewis (1922) and (McCabe & Thiele, 1925). Detailed derivations are presented in this section.

6.2.2.1 Rectifying and Bottoms Operating Lines for Multicomponent Systems

For a simple separation (one feed and two products) depicted in Figure 6.1, the internal and external flowrates of the column at constant molar overflow (CMO) are depicted. All the balances derived from the column depicted in Figure 6.1 were presented by Sorel (1889), Lewis (1922) and McCabe & Thiele (1925).

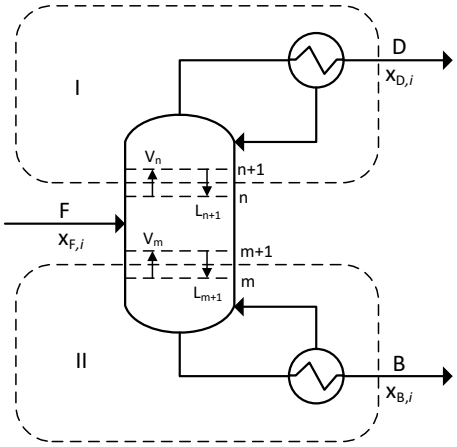

Figure 6.1: Depiction of internal and external flows in a simple distillation column for multicomponent mixtures

The overall and component mass balances over the column are defined in Equations 6.2 and 6.3 and adapted for multicomponent systems.

$$F = D + B \tag{6.2}$$

Where F, D and B are the molar flowrates of the feed, distillate and bottoms streams.

$$Fx_{F,i} = Dx_{D,i} + Bx_{B,i} \qquad for\ i = 1,2 \dots j \tag{6.3}$$

Where $x_{F,i}$, $x_{D,i}$, $x_{B,i}$ are the molar compositions of component *i* in the feed, distillate and bottoms streams respectively.

Generally, the light key component balance is derived for binary systems. For multicomponent systems, it would be required to perform *j-1* component balances to correctly represent and design a distillation system.

The rectifying operating lines (ROL) are derived from the overall mass balance (Equation 6.2) and component mass balances (Equation 6.5) over the upper (rectifying) column section (I), as defined in Equation 6.6.

Rectifying Operating Line:

$$V_n = L_{n+1} + D \tag{6.4}$$

$$V_{n,i}\ y_{n,i} = L_{n+1,i}\ x_{n+1,i} + Dx_{D,i} \quad for\ i = 1,2 \dots j \tag{6.5}$$

$$y_{n,i} = \frac{L_{n+1,i}}{V_{n,i}} x_{n+1,i} + \frac{D}{V_{n,i}} x_{D,i} \qquad for\ i = 1,2 \dots j \tag{6.6}$$

Under the assumption of CMO $L_{n+1,i} = L_n$, Equation 6.6 can hence be simplified as shown in Equation (6.7).

$$y_{n,i} = \frac{L_{n,i}}{V_{n,i}} x_{n+1,i} + \frac{D}{V_{n,i}} x_{D,i} \qquad for\ i = 1,2 \dots j \tag{6.7}$$

Reflux (L_n) is the amount of liquid returned to the column at the top of the column, and the separation efficiency is dependent on the reflux. The reflux ratio (R) is mathematically defined as $R = L_n/D$ and hence the rectifying operating line in Equation 6.7 can also be expressed in terms of the reflux ratio R. Equation 6.8 represents the rectifying operating line for multicomponent mixtures in terms of the reflux ratio, R.

$$y_{n,i} = \frac{R}{R+1} x_{n+1,i} + \frac{1}{R+1} x_{D,i} \quad for\ i = 1,2 \ldots j \tag{6.8}$$

Likewise, the bottoms operating lines (BOL) are derived from the overall mass balance (Equation 6.2) and component mass balances (Equation 6.10) over the lower (bottom) column section (II) as defined in Equation 6.11 for the assumption of CMO.

Bottoms Operating Line:

$$V_m = L_{m+1} - B \tag{6.9}$$

For CMO $L_{m+1} = L_m$

$$V_{m,i}\ y_{m,i} = L_{m,i} x_{m+1,i} - B x_{B,i} \quad for\ i = 1,2 \ldots j \tag{6.10}$$

$$y_{m,i} = \frac{L_{n,i}}{V_{m,i}} x_{m+1,i} - \frac{B}{V_{m,i}} x_{B,i} \quad for\ i = 1,2 \ldots j \tag{6.11}$$

The Reboil (V_m) is the amount of vapour returned to the column, at the bottoms of the column. Like the reflux ratio, the separation efficiency is also dependent on the reboil ratio. The reboil ratio (S) is mathematically defined as $S = V_m/B$. The bottoms operating line in Equation 6.11 can also be expressed in terms of the reflux ratio, S. Equation 6.12 represents the bottoms operating line for multicomponent mixtures in terms of the reboil ratio, S.

$$y_{m,i} = \frac{S+1}{S} x_{m+1,i} - \frac{1}{S} x_{B,i} \quad for\ i = 1,2 \ldots j \tag{6.12}$$

6.2.2.2 Feed Line for Multicomponent Systems

The intersection of the rectifying and bottoms operating lines on a binary McCabe-Thiele diagram yields the feed stage and is represented by the feed (q-line) (Wankat,

2012). The feed line is defined in Equation 6.13 which has been extended to multicomponent mixtures from the binary feed line (Wankat 2012).

$$y_{q,i} = \frac{q}{q+1} x_{q,i} - \frac{1}{q+1} x_{F,i} \quad for\ i = 1,2 \dots j \tag{6.13}$$

Where q is defined as the thermal state of the feed and represents the amount of liquid in the feed stream. For saturated liquid feeds, the typical value of q is 1 and for saturated vapours, the value of q is 0 (Hengstebeck, 1961). It is important to note that the feed line is dependent only on the value of q (determines the slope of the line only) and the mole fraction of the component in the feed. Hence, the feed line should pass through the feed composition on the McCabe-Thiele diagram.

The relationship between the reflux and reboil for multicomponent systems is the same as that for binary systems, and is represented in Equation 6.14 (Julka & Doherty, 1990).

$$S = (R + q)\left[\frac{x_{B,i} - x_{F,i}}{x_{F,i} - x_{D,i}}\right] + q - 1 \tag{6.14}$$

Table 6.1 represents the final mass balance equations required to construct the McCabe-Thiele diagrams for multicomponent systems.

Table 6.1: Summary of mass balance lines required to construct the McCabe-Thiele diagram

Mass Balance line	**Equation**
Rectifying Operating Line	$y_{n,i} = \frac{R}{R+1} x_{n+1,i} + \frac{1}{R+1} x_{D,i} \quad for\ i = 1,2 \dots j$ (6.8)
Bottoms Operating Line	$y_{m,i} = \frac{S+1}{S} x_{m+1,i} - \frac{1}{S} x_{B,i} \quad for\ i = 1,2 \dots j$ (6.12)
Feed line	$y_{q,i} = \frac{q}{q+1} x_{q,i} - \frac{1}{q+1} x_{F,i} \quad for\ i = 1,2 \dots j$ (6.13)

Relationship between reflux (R) and reboil ratio (S)	$S = (R + q)\left[\frac{x_{B,i} - x_{F,i}}{x_{F,i} - x_{D,i}}\right] + q - 1$	(6.14)

***$y_{q,i}$** and $x_{q,i}$ are the vapour and liquid composition of component *i* in the feed respectively

Equations (6.8), (6.12), (6.13) and (6.14) are valid for each component, *i*, in ternary mixtures. The mass balance equations (Equations 6.8, 6.12, 6.14) are represented on individual 2D x-y diagrams for each component after the contours of VLE have been plotted. The contours of VLE are plotted once, after which any combinations of reflux, (R), reboil (S), feed composition (x_F), thermal feed quality (q) and product compositions (x_D, x_B) can be analysed from a single VLE representation. The effectiveness and simplicity of the original McCabe-Thiele method is therefore retained.

6.3 The McCabe-Thiele Method at Finite Reflux

6.3.1 Ideal System

As mentioned in Chapter 5, ternary separations can be categorised into the following groups of separations: sharp direct and indirect splits, and transition splits. Several examples for ideal and non-ideal mixtures will be presented to highlight the application of the proposed method. These examples will demonstrate that the simplicity and effectiveness of the original McCabe-Thiele method has been retained. The method of calculating the number of theoretical stages and feed location is the same for transition and direct splits whilst for indirect splits there is a slight difference. The method for direct splits is explained and applied to an ideal system, and indirect splits for a non-ideal system.

6.3.1.1 Example 6.1: Sharp Direct Split of Ideal Simple Separation (methanol, ethanol, n-propanol)

In order to illustrate the application of the method to an ideal system, an example from Doherty & Malone (2001) will be considered. It should be noted that the design specifications (x_D, x_B, x_F, R and S) have been taken from Doherty & Malone (2001) without which the method cannot be applied as depicted in Figure 6.6. Figure 6.6 depicts the finite reflux method for ternary systems. This work does not present a method to determine the process specifications, but any appropriate method or simulation software can be used to determine these specifications. A system of methanol (normal boiling point (nbpt) – 64.5°C), ethanol (nbpt – 78.2°C), and n-propanol (nbpt – 97.15 °C) will be considered (Thong et al., 2000; Kubicek & Eubank, 1972). Methanol is the most volatile component or light key (LK), ethanol is the intermediate volatile component or intermediate key (IK) and n-propanol is the least volatile component or heavy key (HK). Relative volatilities of the components were assumed to be constant and used to determine the equilibrium data for the contours of VLE (Section 3.1).

Design problem: A mixture of methanol (M), ethanol (E) and n-propanol (P) is fed to a finite reflux column at constant pressure (1 bar). The composition of the saturated liquid (q=1) feed, distillate and bottoms compositions is provided in Table 6.2. The compositions were sourced from Doherty & Malone (2001). The target distillate composition for the light key component (methanol) should be a minimum of 0.980. The minimum reflux ratio was calculated to be 2.85 in Chapter 5 for the ideal direct split. The finite reflux to be 1.5 times the minimum reflux as previously calculated (4.27). The reboil ratio is calculated to be 2.29 using Equation 6.14.

Table 6.2: Relative volatilities, feed, distillate and bottoms compositions for a methanol, ethanol and n-propanol system in a sharp direct split (Doherty & Malone (2001))

Component	Relative volatility (α)	x_F	x_B	x_D
methanol	3.25	0.300	0.005	0.980
ethanol	1.90	0.250	0.350	0.020

n-propanol	1.00	0.450	0.645	5×10^{-11}

Consider Figure 6.2, a plot of the DCM depicting the rectifying and bottoms profiles from the distillate and bottoms liquid compositions set out in Table 6.2, for a direct split at the reflux and reboil values stated in the design problem. Figure 6.3 represents the reflux and reboil ratios in the form of the rectifying, bottoms and feed operating lines. The operating lines are plotted from the respective distillate, bottoms and feed compositions on an x-y diagram for methanol. The operating lines for ethanol and n-propanol can be depicted on their individual x-y diagrams. Once Figure 6.3 has been plotted it would be intuitive to start stepping off stages from the distillate composition towards the bottoms composition as in the binary McCabe-Thiele method. However, analysis of the behaviour of ternary systems on the DCM in Figure 6.2 provides insights as to the best practice for stepping off stages for direct splits.

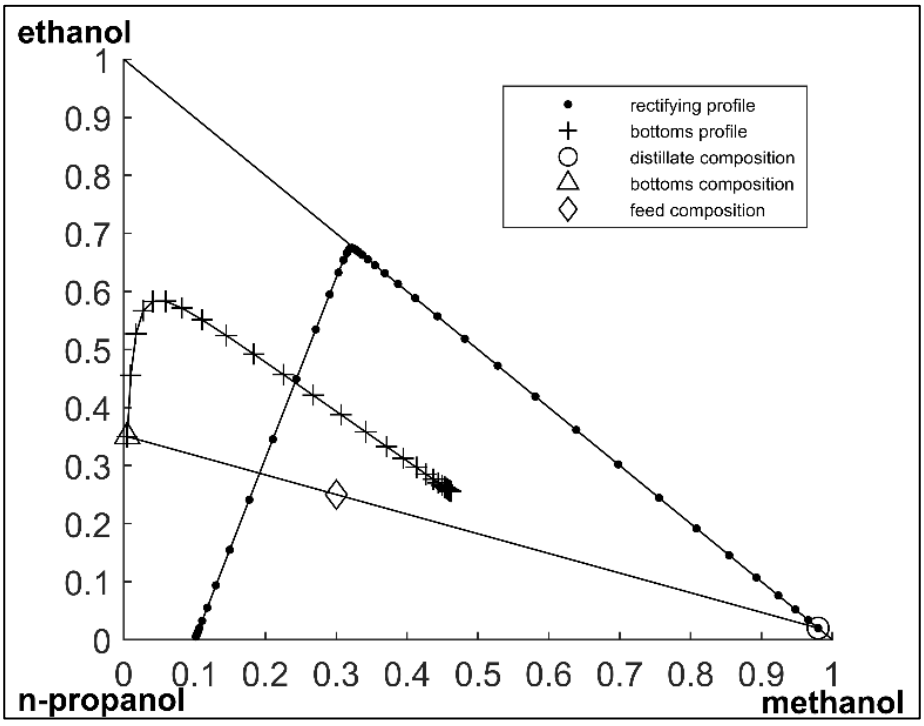

Figure 6.2: Distillation curve map (DCM) depicting the rectifying and bottoms operating profiles at finite reflux for a direct split

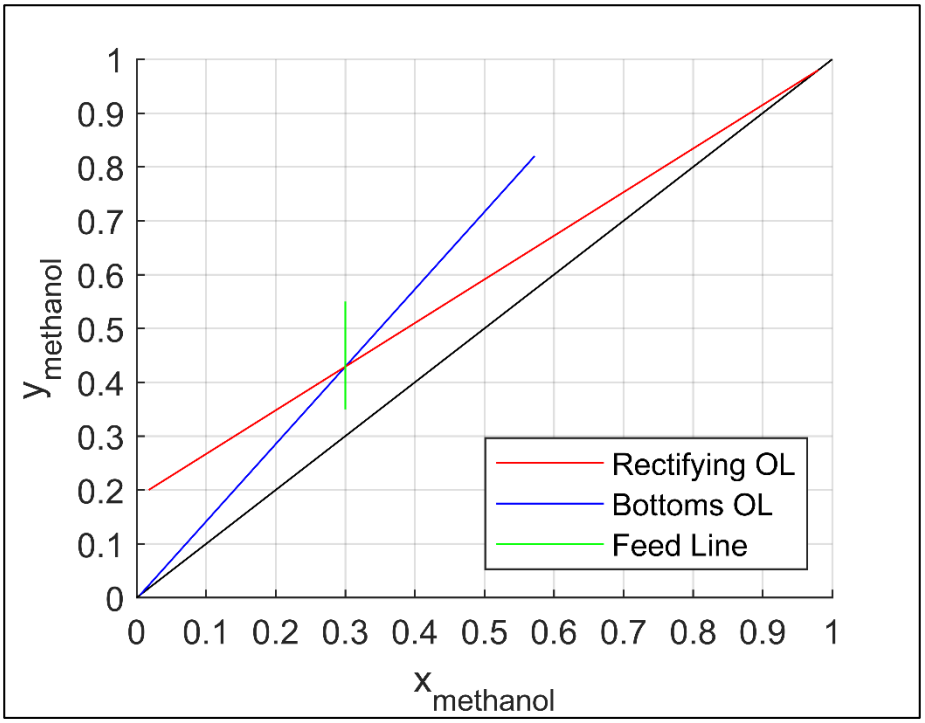

Figure 6.3: McCabe-Thiele diagram for methanol depicting the rectifying, bottoms and feed operating lines at finite reflux

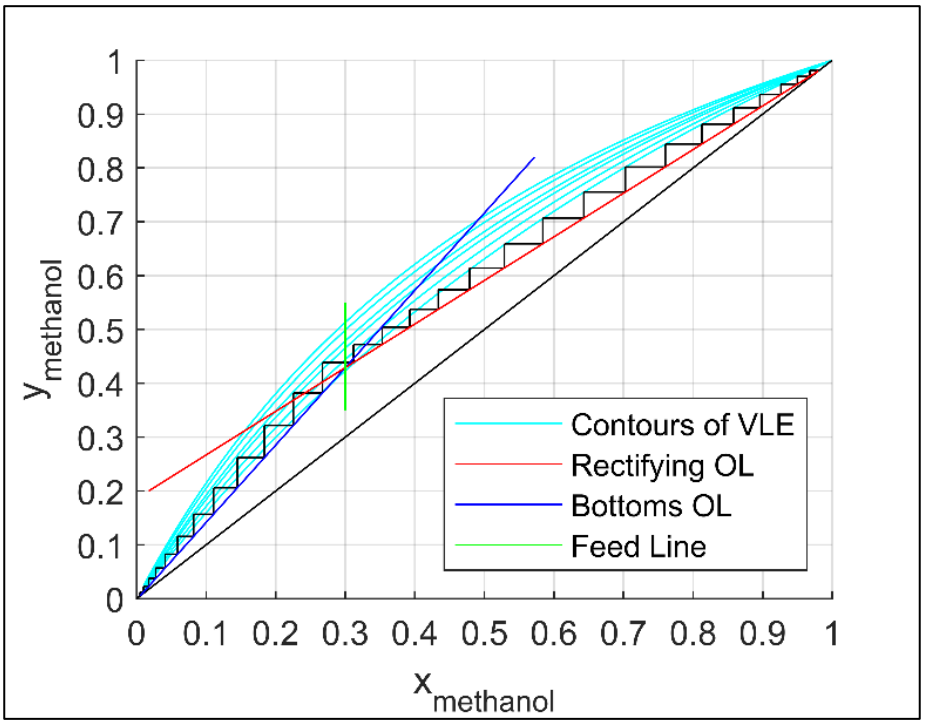

Figure 6.4: McCabe-Thiele diagram for methanol used to determine the number of theoretical stages at finite reflux and feed stage location for direct split

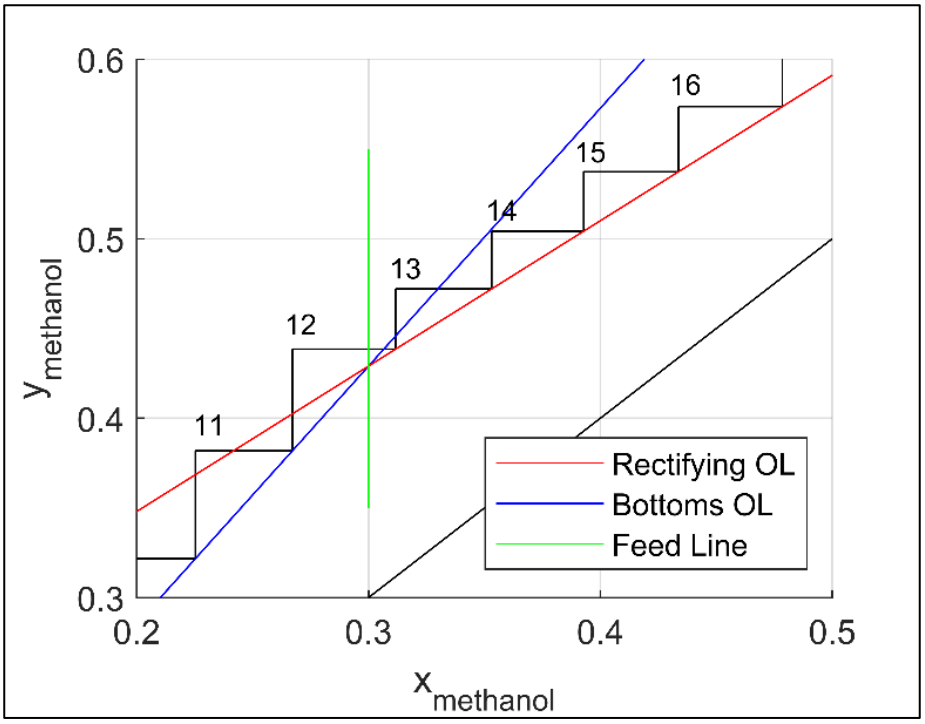

Figure 6.5: Enlargement of Figure 6.4 to show the changeover from the bottoms operating line to the rectifying operating line symbolising feed stage for a direct split.

In direct splits, the distillate purity dictates the shape of the rectifying profile. As the composition of the heavy component (n-propanol) decreases from the feed stage towards the distillate product, the profile approaches the saddle pinch in the rectifying profile (Figure 6.2). A saddle pinch is an unstable node: to move out of the pinch point requires many stages which is undesirable (Doherty & Malone, 2001). Hence, to avoid operation at saddle pinches the number of stages is determined from the bottoms composition and not from the distillate composition. The optimal feed stage is chosen on the bottoms profile, from which point the rectifying profile would start.

Figure 6.4 depicts the stepping off stages from the bottoms composition towards the distillate composition for methanol. It should be noted that only the VLE contours required for the separation have been represented and these have been

precisely determined using a computer. The same result would be produced if done by hand, if the contours of VLE were first plotted and then by stepping towards the VLE contour that represents the ratio of compositions. Chapter 4 showed the manual calculations for total reflux. This can be done in a similar manner for finite reflux, following the algorithm presented below.

The algorithm below is followed to determine the number of theoretical stages for a direct split.

1. To construct the McCabe-Thiele diagram, the 45 degree line, feed line, rectifying operating line and the bottoms operating line are plotted using Equations 6.13, 6.8 and 6.12 respectively, on x-y diagrams for the light key (methanol) and heavy key (n-propanol) component. It is only necessary to plot two components as the third component's composition can be calculated from a material balance.
2. Calculate the first ratio for methanol (LK) (Equation 6.1a), using the given liquid bottoms product composition. $CR_{1,(ethanol/propanol)} = x_{ethanol} / x_{n\text{-}propanol} = 0.350/0.645 = 0.543$.
3. Calculate the first ratio for n-propanol (HK) using the given liquid bottoms product composition. $CR_{1,(methanol/ethanol)} = x_{methanol} / x_{ethanol} = 0.005/0.350 = 0.0143$.
4. Using the ratios calculated in steps 2-3, determine the VLE contour that represents the ratio, using the method presented in Section 6.2.1 or in Chapter 3.
5. Move vertically from the bottoms product composition on the 45 degree line towards the VLE contour, determined in step 4, to determine the equilibrium composition of the vapour (y_{eqm}) at x_B. Interpolation may be required if the precise contour is not available.
6. Move horizontally from the VLE contour towards the bottoms operating line. Determine the new liquid composition for the light and heavy key components. The composition of the intermediate key can be calculated from material a balance.

7. Calculate the second ratio (steps 2-3) for the light and heavy key using the new composition obtained in step 6. Repeat steps 4-6 until the feed line of the light key is reached.
8. Once at the feed line for methanol (light key), swop over towards the rectifying operating line from the contour of VLE. Determine the new liquid composition from $x_1 = y_{eqm}$.
9. Repeat steps 7- 8 until the required distillate product is obtained.

The changeover from the bottoms operating line to the rectifying operating line takes place at the feed line of the LK for direct splits, which in this example is methanol. Figure 6.5 shows an enlargement of the changeover at the feed line for methanol.

Further explanation and analysis of the feed stage is presented in Analysis 6.1. The total number of stages required is 28, with the feed introduced at stage 12. The algorithm used to step off stages for both direct and indirect splits for ternary systems is presented in Figure 6.6. The method for direct splits (Figure 6.6b) was followed to produce Figures 6.2 – 6.5.

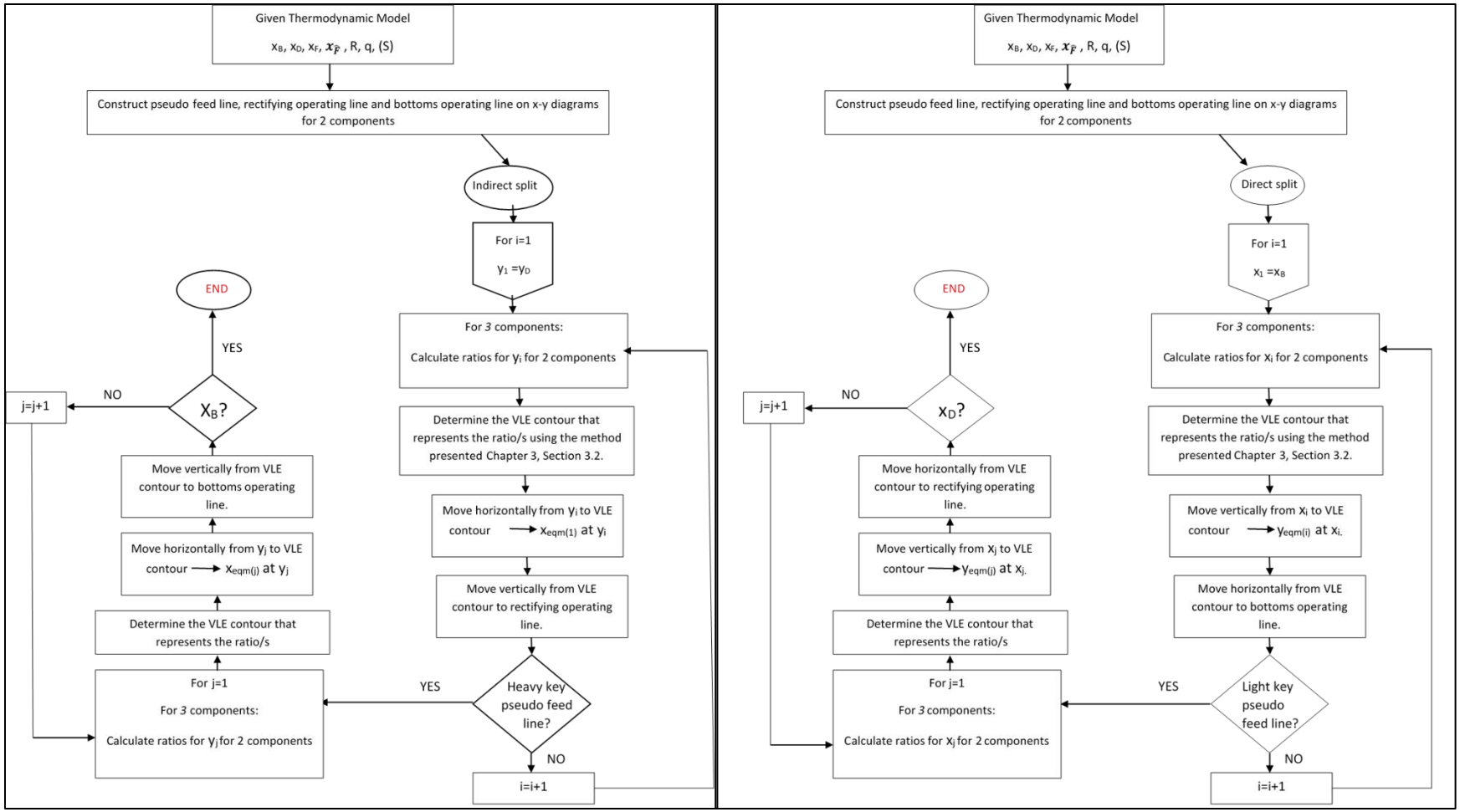

Figure 6.6: Method to determine the number of theoretical stages and feed stage location at finite reflux for 3 component systems for (a) indirect splits and (b) direct splits

The Fenske-Underwood-Gilliland method and the Kirkbride (1944) equation were also used to calculate the number of theoretical stages and the feed stage location respectively. The empirical correlations were used to compare the results obtained from the proposed graphical method. The minimum number of stages at total reflux to obtain a distillate composition of methanol of 0.980 is 16 stages using the method in Chapter 4. Using the distillate product determined from the graphical method (feed stage 12) and the bottoms composition in Table 6.2, the minimum number of stages required is 16.4 stages using the Fenske equation. The minimum reflux predicted by Underwood is 2.84 and the finite reflux will be taken to be 1.5 times (4.27) the minimum reflux. Using the Gilliland correlation, the number of theoretical stages at finite reflux is 27.7 ~ 28 stages which correlates closely with the 28 stages calculated from the proposed graphical method. It can be concluded that the proposed graphical method correlates with the FUG method for the ideal direct split.

Further calculations using Kirkbride or the FUG method are then required to calculate the feed stage. The Kirkbride (1944) equation predicted a feed stage of 11, which will be shown in Analysis 6.1 as an infeasible design. Hence, the proposed graphical method predicts the feed stage more accurately than the Kirkbride (1944) equation. The FUG method predicts the feed stage to be stage 21. This is far from that predicted by Kirkbride (1944) and the proposed graphical method. The FUG method works well for columns where the feed stage is close to the middle of the column which, however, is not the case in this design problem. The FUG method requires the minimum number of stages to be calculated as a prior step in order to determine the theoretical number of stages. In addition, numerous separate calculations have to be carried out in order to determine the number of theoretical stages and the feed stage location. The proposed graphical method does not require any additional calculations, once the VLE is plotted initially, the number of stages and feed stage are determined simultaneously.

Analysis 6.1: Effect of the feed stage location on distillation design

In the original McCabe-Thiele method, the starting point for determining the number of theoretical stages is typically the distillate composition, and the changeover from the rectifying operating line to the bottoms operating line occurs at the feed line for the light component. However, for direct splits, the number of theoretical stages is determined from the bottoms composition, and changeover from the bottoms operating line to the rectifying operating line occurs at the feed line (Figures 6.2- 6.5) of the light key component. Figure 6.5 depicts the changeover at the feed line of methanol (LK) which coincides with stage 12. If the changeover occurs below the feed line (stage 11) of the light key, the direction of the rectifying profile will turn away from the distillate composition (Figures 6.7-6.8) and the design will not be feasible.

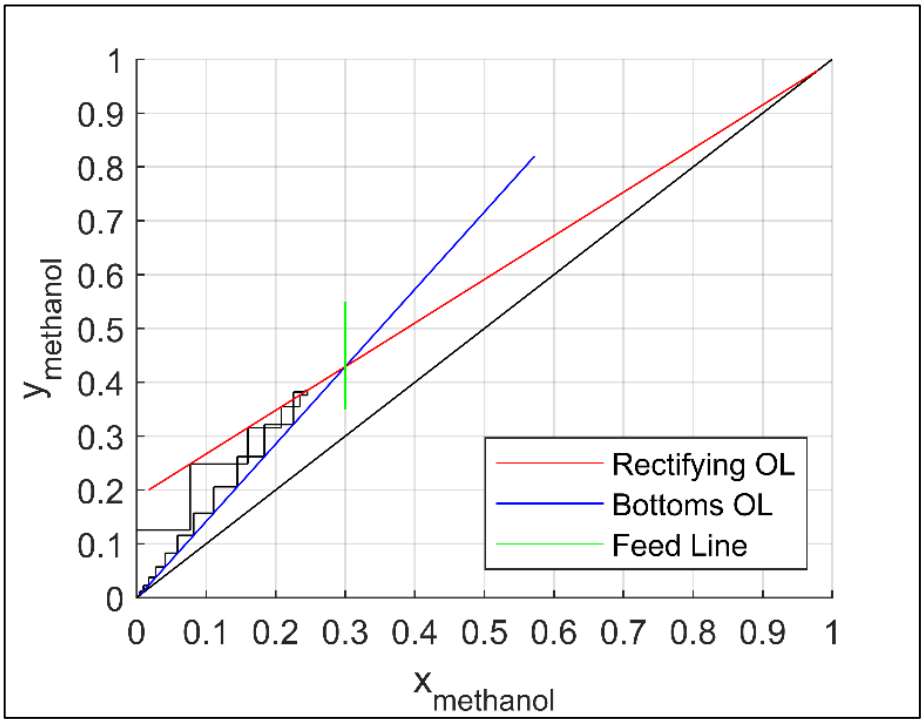

Figure 6.7: McCabe-Thiele diagram for methanol at feed stage location below the feed line for direct split

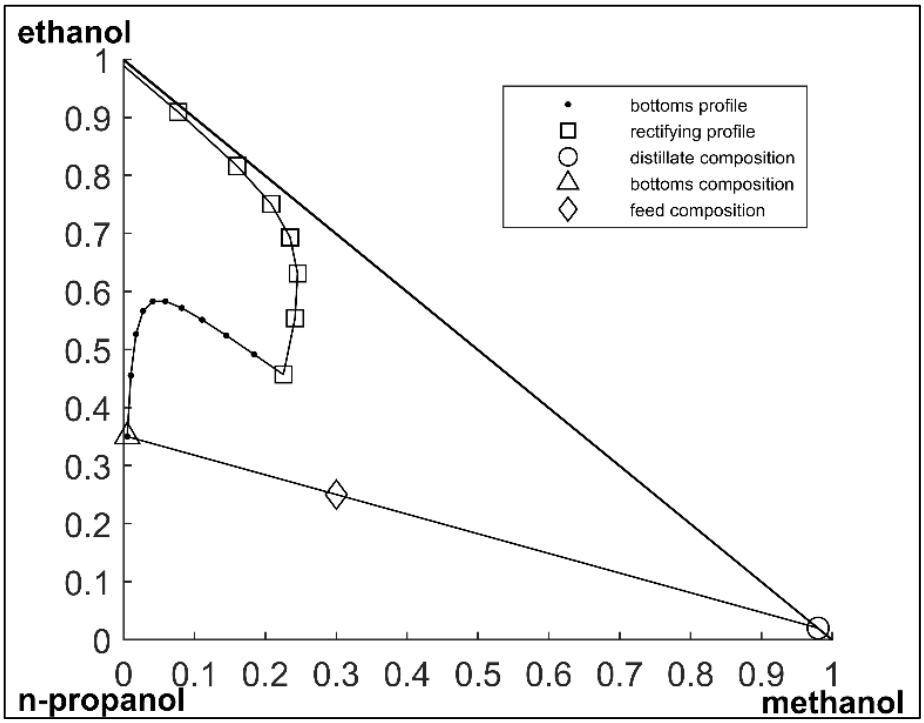

Figure 6.8: Distillation curve map (DCM) depicting the rectifying and operating profiles at the finite reflux and feed stage before the feed line for methanol as predicted by the proposed graphical method for a direct split

At the changeover of the operating lines corresponding to the feed line (stage 12- counted from the bottom of the column) for methanol, the distillate composition is 0.981, 0.0190 and 5.27×10^{-7} for methanol, ethanol and n-propanol respectively. From Figure 6.4, the total number of theoretical stages is 28 (including the partial reboiler), with 11 stages in the bottoms section and 17 in the rectifying section. If the changeover takes place above the feed line, with a set number of stages of 28, the number of stages in the bottoms section increases whilst the distillate decreases. In addition, the purity of the light key in the distillate will increase. If the total number of stages is kept at 28 and now moves over to the rectifying section at stage 12 (counting from the bottom), for example, the resulting distillate product will be 0.994, 0.00570 and 1.22×10^{-6} for methanol, ethanol and n-propanol respectively. In addition, the designer can change the feed stage location to any stage above stage

12, and calculate the number of stages and distillate composition of the IK and LK, whilst achieving the target distillate composition for LK, as recommended by Doherty & Malone (2001). The designer can thus perform a sensitivity analysis described above to determine where the optimal feed stage is located using a rigorous simulator such Aspen Plus^{TM}. But the rule of thumb is that the design will be feasible in terms of composition profiles if the changeover takes place at the feed composition of methanol (LK).

Doherty & Malone (2001) proposed determining a region on the stripping profile between the points, x^0, (which yields the saddle pinch rectifying profile) and $\hat{x}^{1,s}$ the node pinch on the stripping profile (the point at which the stripping profile terminates). The method aims at identifying the region of feasible rectifying profiles. The fixed point method, or the bisection method, can be used to find x^0. The rectifying profile can start at any point between x^0 and $\hat{x}^{1,s}$ to achieve a feasible rectifying profile. If the rectifying profile begins before x^0, the rectifying profile will turn away from the distillate product, as depicted in Figures 6.7 and 6.8. The proposed graphical method, in this chapter, does not require these additional calculations to determine a feasible region, as the designer can determine the feed stage location whilst determining the number of stages.

Analysis 6.2: Comparison of the Vogelpohl (2015) method and the proposed graphical method for feed stage location

Figure 6.9 represents the graphical method proposed by Vogelpohl (2015) to determine the feed location for the direct split in Example 6.1. The feed stage location is determined by plotting the rectifying and bottoms profiles for both the liquid and vapour compositions, at finite reflux on a mass balance triangle (MBT). For a saturated liquid feed, a material balance line is drawn from the distillate product composition to the intersection of the vapour rectifying and bottoms profiles. At this point, the vapour compositions in the rectifying and stripping sections are equal ($y_R = y_S$) at the introduction of the feed (no vapour in the feed).

If the same material balance line is extended to intersect the rectifying liquid profile, then the rectifying liquid composition will be in equilibrium with the feed (x_R). Another material balance line is plotted from the bottoms product composition to the intersection of the vapour rectifying and bottoms product compositions. The intersection of the material balance line and the liquid bottoms profile yields the composition of the liquid (x_S) in equilibrium with the feed in the bottoms section, and hence the feed stage location. The rectifying (x_R) and bottoms (x_S) liquid compositions in equilibrium with the feed will lie on a straight line with the feed (x_F), as depicted on Figure 6.9. Figure 6.10 plots the feed stage location predicted by Vogelpohl (2015) and by the proposed graphical method. It can be seen that the feed stage predicted by both methods correlate well. The method by Vogelpohl (2015) does not take into consideration an actual tray but a point on a MBT. Hence, the feed stage will be taken as the stage closest to that point. The proposed graphical method provides the designer with the feed stage number at which the feed should enter the column.

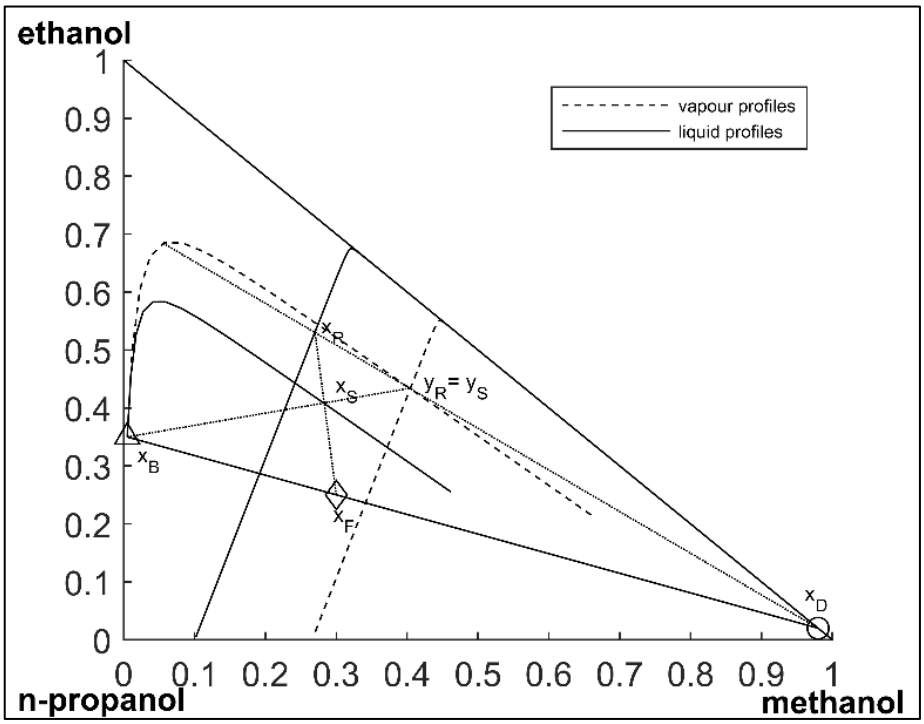

Figure 6.9: Plotting the method of feed stage location by Vogelpohl (2015)

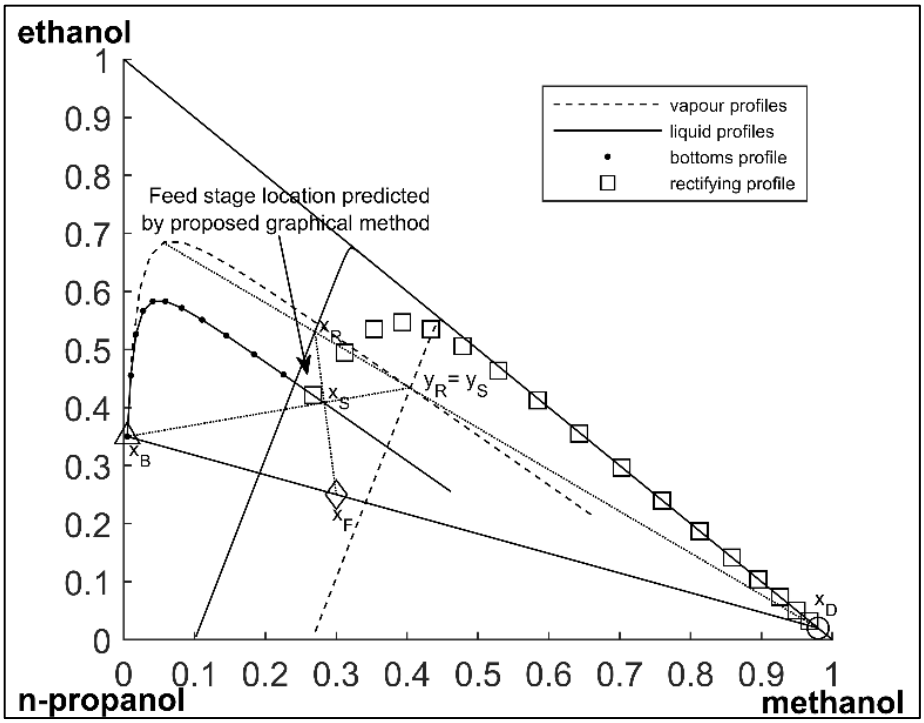

Figure 6.10: Depicts the feed stage location using the proposed graphical method and the method by Vogelpohl (2015)

The proposed graphical method does not require additional steps to determine feed stage location, in contrast to Vogelpohl (2015) and Doherty & Malone (2001). Whilst the designer is determining the total number of stages from the bottoms composition, and reaches the feed line, this is a visual indication of exactly where the changeover should take place for the first feasible rectifying profile, that moves towards the distillate product. In addition, regardless of the state of the feed (saturated vapour or liquid / partially vaporized) the method remains the same. The feed lines will differ only in the gradient of the line, but the changeover will take place at the feed line, as with the original McCabe-Thiele method. The method presented by Vogelpohl (2015) to find the feed stage location differs for different feed states.

6.3.1.2 Example 6.2: Sharp indirect split of ideal simple separation (methanol, ethanol, n-propanol)

Design problem: A mixture of methanol (M), ethanol (E) and n-propanol (P), as in Example 6.1, is fed to a finite reflux column at constant pressure (1 bar). The compositions of the saturated liquid feed, distillate and bottoms compositions are provided in Table 6.3 for an indirect split. The compositions data were sourced from Doherty & Malone (2001). The target composition for the heavy key component (n-propanol) in the bottoms stream should be a minimum of 0.978. For a reflux ratio of 2.08 and reboil ratio of 3.70, determine the number of theoretical stages required and the feed stage location to achieve the design specification.

Table 6.3: Relative volatilities, feed, distillate and bottoms compositions for methanol, ethanol and n-propanol system in a sharp indirect split (Doherty & Malone (2001))

	Relative volatility (α)	**Indirect Split**		
Component		x_F	x_B	x_D
methanol	3.25	0.300	5.00×10^{-11}	0.550
ethanol	1.90	0.250	0.0220	0.440
n-propanol	1.00	0.450	0.9780	0.010

Figure 6.11 depicts the rectifying and bottoms profiles plotted from the compositions in Table 6.3 for the indirect split, at the reflux and reboil ratio stipulated in the design problem for Example 6.2. The bottoms product purity dictates the shape of the bottoms profile in an indirect split, and the bottoms profile approaches a saddle pinch as the amount of the light component decreases towards the bottoms product (Figure 6.11). As with direct splits, operation at a saddle pinch is not feasible, hence the number of stages is determined from the distillate

composition, unlike direct splits. The optimal feed stage is chosen on the rectifying profile from which the bottoms profile would start.

Figure 6.12 plots the rectifying, bottoms and feed operating lines on an x-y diagram for n-propanol (LK) using the specified reflux and reboil ratios and compositions in Table 6.3. The method depicted in Figure 6.6a for indirect splits and 3 components is followed to determine the number of stages and feed stage location. Figure 6.13 depicts the graphical method of determining the number of theoretical stages and feed stage location, in an indirect split, for n-propanol. In accordance with the original McCabe-Thiele method, the starting point for determining the number of theoretical stages is from the distillate composition for indirect splits. The main difference in the method of indirect splits, compared to both the original McCabe-Thiele method and the method of direct splits, is that the heavy key component is analysed for the changeover of operating lines. The changeover from the rectifying operating line to the bottoms operating line occurs at the feed line for the heavy key component (Figures 6.13-6.14).

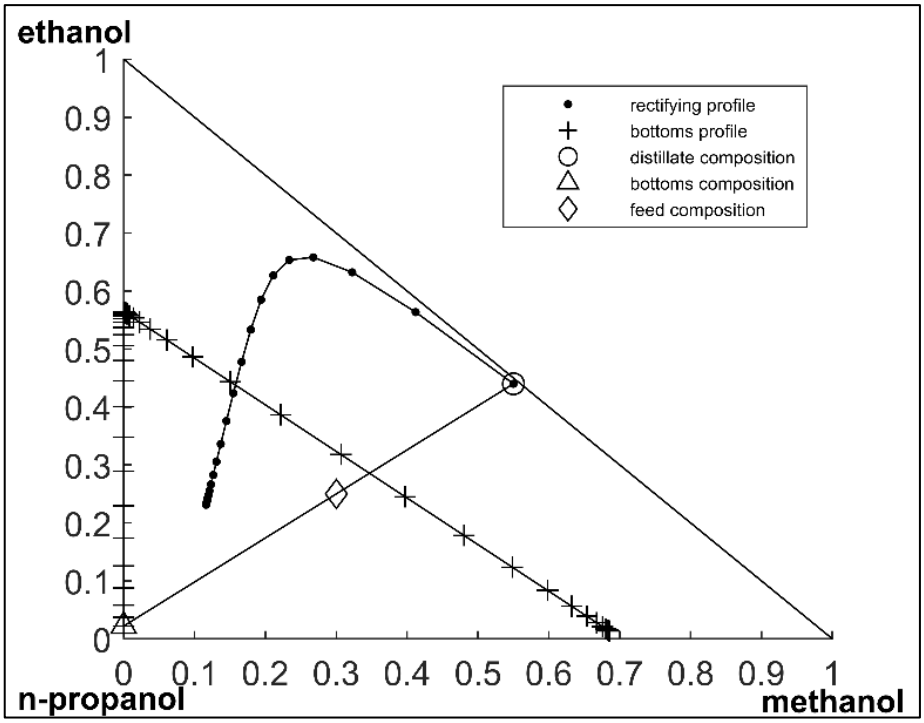

Figure 6.11: Distillation curve map (DCM) depicting the rectifying and bottoms operating profiles at finite reflux for an indirect split

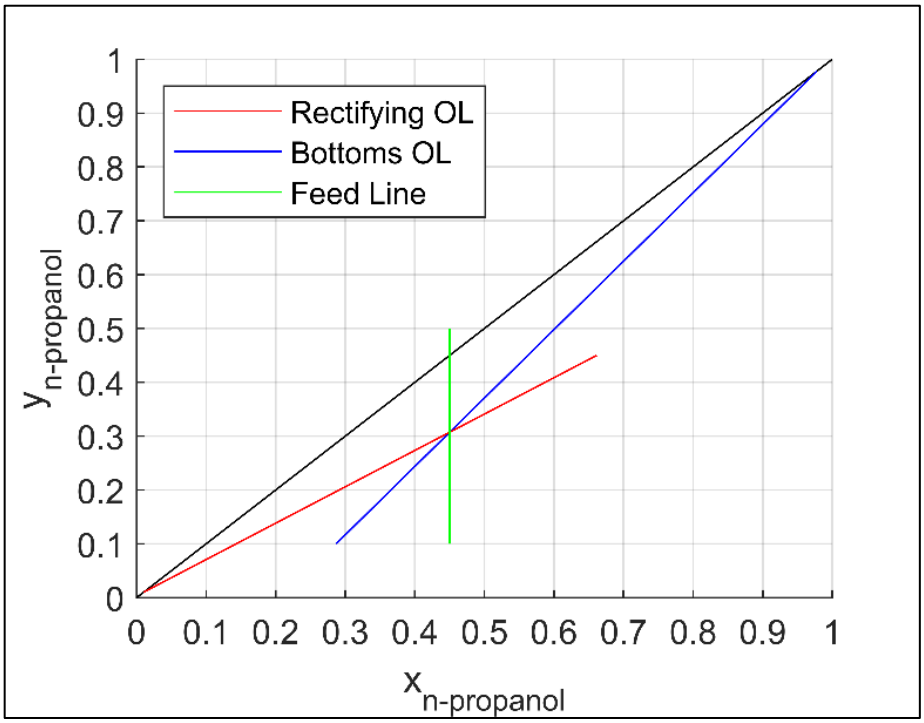

Figure 6.12: McCabe-Thiele diagram for n-propanol depicting the rectifying, bottoms and feed operating lines at finite reflux

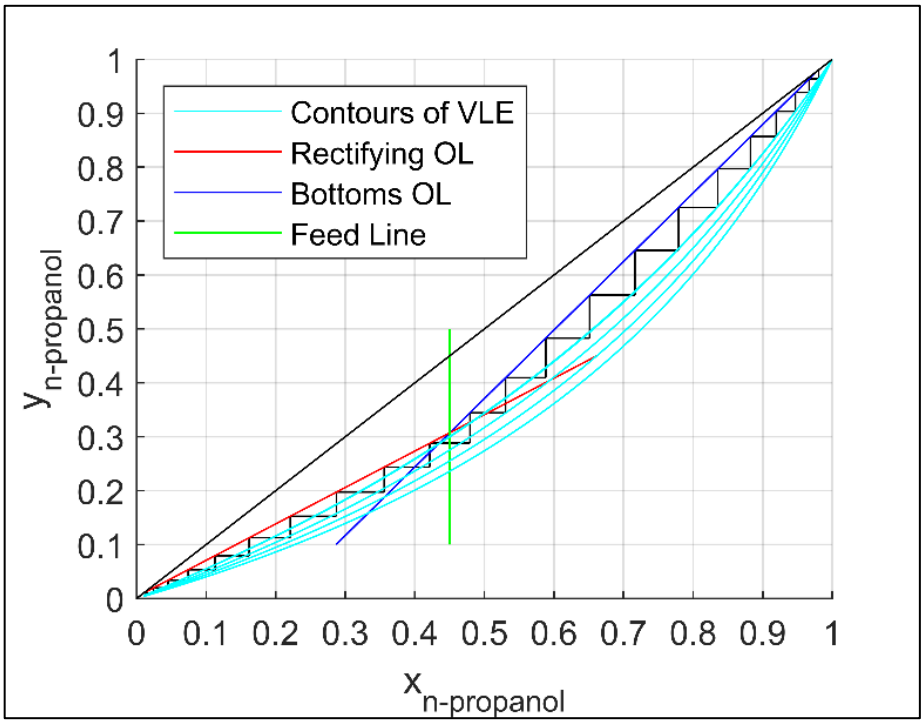

Figure 6.13: McCabe-Thiele diagram for n-propanol used to determine the number of theoretical stages at finite reflux and the feed stage location for an indirect split

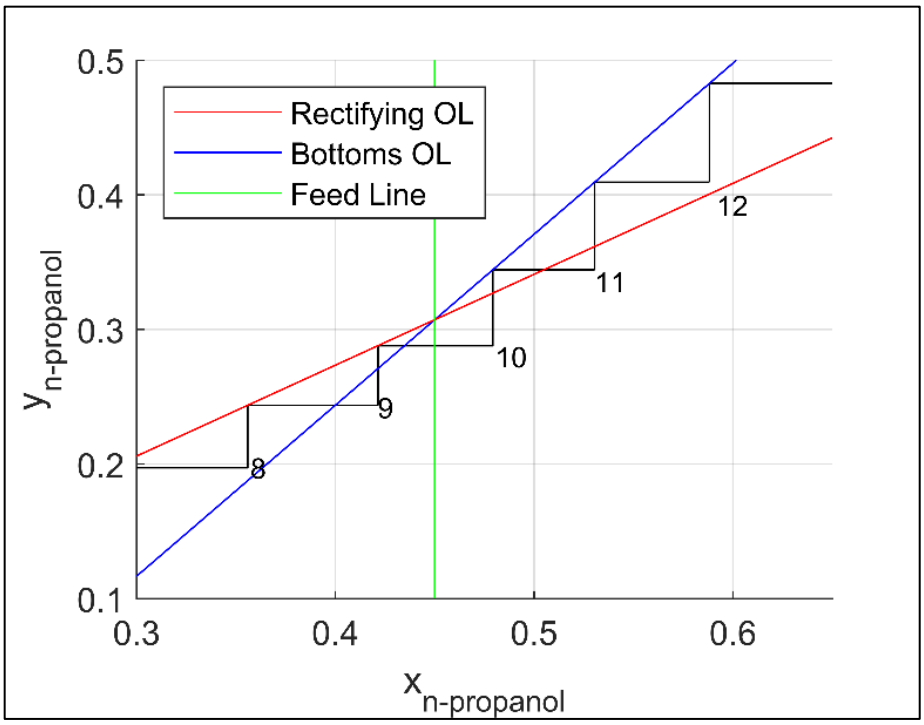

Figure 6.14: Enlargement of Figure 6.13 to show the changeover from the rectifying operating line to the bottoms operating line symbolising the feed stage for an indirect split

Figure 6.13 depicts that the total number of theoretical stages required (including the reboiler) is 21, of which 9 stages are required in the rectifying section and 12 in the bottoms section. The bottoms composition is 3.25×10^{-5}, 0.0194 and 0.981 for methanol, ethanol and n-propanol respectively. The feed stage is located on stage 10 (counted from the top of the column), as depicted in Figure 6.14. If the changeover takes place above the feed line (stage 11 or higher), the designer can perform a sensitivity analysis calculation by analysing the number of stages required, as well as the bottoms product for the LK and IK, and choose the optimal feed stage location. If the changeover occurs below the feed stage (stage 9 and below), the bottoms profile will turn away from the bottoms composition and the design will not be feasible, as seen with direct splits. Hence, the rule of thumb for indirect splits is that the changeover of the rectifying operating line to the bottoms

operating line will take place at the feed line for the heavy key component for all feed states.

6.3.2 Extension to Non-Ideal Systems

The proposed graphical method for distillation design at finite reflux is not limited to ideal systems and can be applied to non-ideal and non-ideal azeotropic systems. The method to determine the number of theoretical stages and feed stage location for direct splits, as illustrated for ideal systems, remains the same for non-ideal mixtures. For illustrative purposes, the theoretical stages and feed stage location for an indirect split will be presented, and this is applicable to ideal systems. The design parameters obtained from the proposed graphical method will be used to initialise a rigorous simulation using Aspen Plus™.

6.3.2.1 Example 6.2: Non-ideal Simple Separation (acetone, benzene, chloroform)

A mixture of acetone (nbpt – 56.5°C), chloroform (nbpt – 61.2°C) and benzene (nbpt – 80.1°C) will be considered to depict a non-ideal azeotropic system. For the non-ideal system in this section, the pure component vapour pressures were determined using the extended Antoine equation (refer to Appendix B) while the Wilson activity coefficient model (refer to Appendix B), while has been used to predict the activity coefficients of the species in the non-ideal mixtures. The Wilson model was used to model the VLE for the system as it correlated accurately with experimental data (Kojima et al., 1991). To provide a consistent basis for comparison of results of the rigorous Aspen Plus™ simulation and the proposed graphical method presented in this thesis, the thermodynamic parameters were taken from the rigorous simulator (Aspen Plus™). The method is, however, not dependent on taking the thermodynamic parameters from Aspen Plus™ and these can be taken from any other resource.

Design problem: A mixture of acetone (A), chloroform (B), and benzene (C) feeds into a finite reflux column at constant pressure (1 bar). The composition of the saturated liquid (q=1) feed is 0.213-acetone, 0.709-benzene and 0.0776-chloroform. The aim of the separation is to achieve a mole fraction of 0.978 of benzene recovered in the bottoms product and 0.01 mole fraction of benzene in the distillate product. Determine the number of theoretical stages required and the feed stage location to achieve a feasible separation, if the reflux and reboil ratios are 6.54 and 2.90 respectively.

The method presented in Figure 6.6 (a) for indirect splits will be followed to determine the number of theoretical stages at finite reflux for an indirect split. The split is classified as indirect, as the process recovers a high amount of benzene (HK) in the bottoms products in the operating distillation region. The design problem states that 0.978 and 0.01 mole fraction of benzene is to be obtained in the bottoms and distillate product respectively. In order to achieve an indirect split, the products needs to lie on the vertices of the MBT (Figure 6.19). In order to obtain a bottoms product close to the binary vertex of benzene and chloroform, a very small quantity of acetone in the bottoms composition is desirable. Hence, the composition of acetone in the bottoms product is set to 5.00×10^{-10}. Performing a mass balance over the column, the mole fraction of acetone in the distillate is found to be 0.768. The mole fractions of chloroform in the bottoms and distillate products are 0.0220 and 0.222 respectively. The feed line (Equation 6.13), rectifying (Equation 6.8) and bottoms (Equation 6.12) operating lines are plotted on x-y diagrams for at least two components. The third component's composition can be determined using mass balance.

For indirect splits, the number of stages is determined from the distillate product towards the bottoms product (Figure 6.6a). In addition the heavy key, benzene, is analysed for when the changeover from the rectifying to the bottoms operating line

takes place. The method followed to compute Figures 6.15 – 6.19 is provided below.

The algorithm provided below is used to determine the number of theoretical stages for an indirect split.

1. To construct the McCabe-Thiele diagram, the 45 degree line, feed line, rectifying operating line and bottoms operating line are plotted using Equations 6.13, 6.8 and 6.12 respectively on x-y diagrams for the light key (acetone) and heavy key (benzene). It is only necessary to plot two components, as the third component's composition can be calculated from a mass balance.
2. Calculate the first ratio for acetone (LK) (defined in Equation 6.1b) using the given vapour distillate product composition. $R_{1,(comp\ A/comp\ C)} = y_{comp\ A} / y_{comp\ C} = 0.0450/0.222 = 0.0450$.
3. Calculate the first ratio for benzene (HK) using the given liquid vapour distillate composition. $R_{1,(acetone/chloroform)} = y_{acetone} / y_{chloroform} = 0.768/0.222 = 3.46$.
4. Using the ratios calculated in steps 2-3, determine the VLE contour that represents the ratio using the method presented in Section 6.2.1 or in Chapter 3.
5. Move horizontally from the distillate product composition on the 45 degree line towards the VLE contour determined in step 4, to determine the equilibrium composition of the liquid (x_{eqm}) at y_D.
6. Move vertically from the VLE contour towards the rectifying operating line. Read off the new vapour composition on the rectifying operating line from for the light and heavy keys. The composition of the intermediate key can be calculated from a mass balance.
7. Calculate the second ratio (steps 2-3) using the new composition obtained in step 6 for the components. Repeat steps 4-6 until the feed line of the heavy key (benzene) is reached.

8. Once at the feed line for benzene (heavy key), swop over to moving vertically towards the bottoms operating line from the contour of VLE. Determine the new vapour composition by reading off on the bottoms operating line. (NOTE: the changeover can be done on any stage and analysis of the feasibility can carried out. See Figures 6.11 – 6. 14)
9. Repeat steps 7- 8 until the required bottoms product is obtained.

Figure 6.15 shows the changeover at the feed line for benzene (stage 31- A on Figure 6.15). Figure 6.16 shows this one stage below the feed line (stage 30- B on Figure 6.15). Figure 6.17 shoes this two stages below the feed line (stage 29- C on Figure 6.15) and in Figure 6.18 the changeover is three stages below the feed line (also show at stage 28- D on Figure 6.19). All feed stages are counted from the top of the column. The contours of VLE were omitted for Figures 6.15 – 6.18 and only a few contours of VLE were depicted in Figure 6.15 to improve the clarity of the number of stages required.

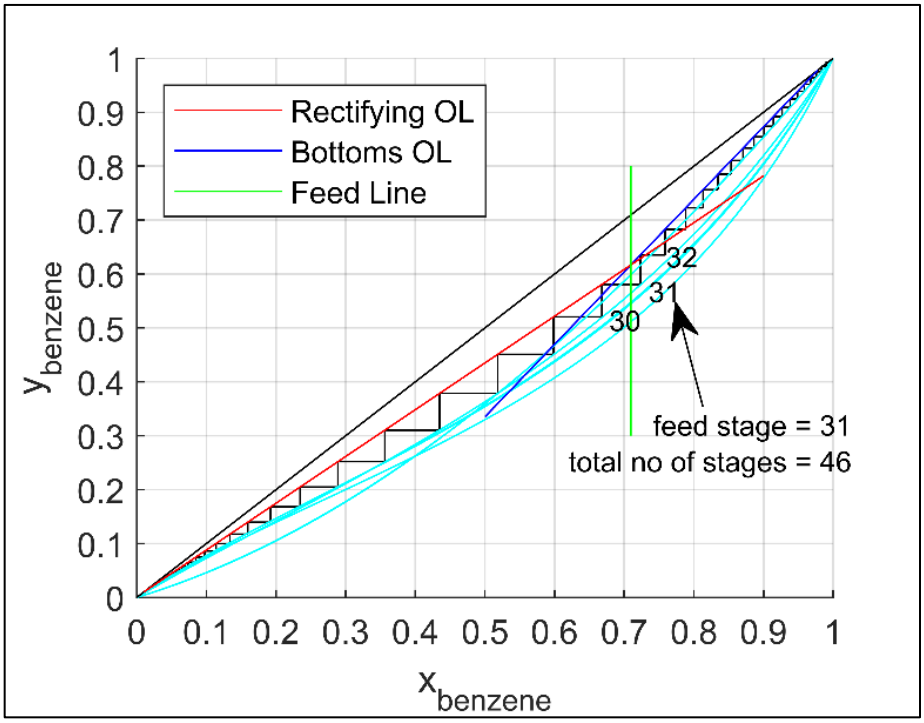

Figure 6.15: McCabe-Thiele diagram for benzene used to determine the number of theoretical stages at finite reflux and the feed stage location at stage 31

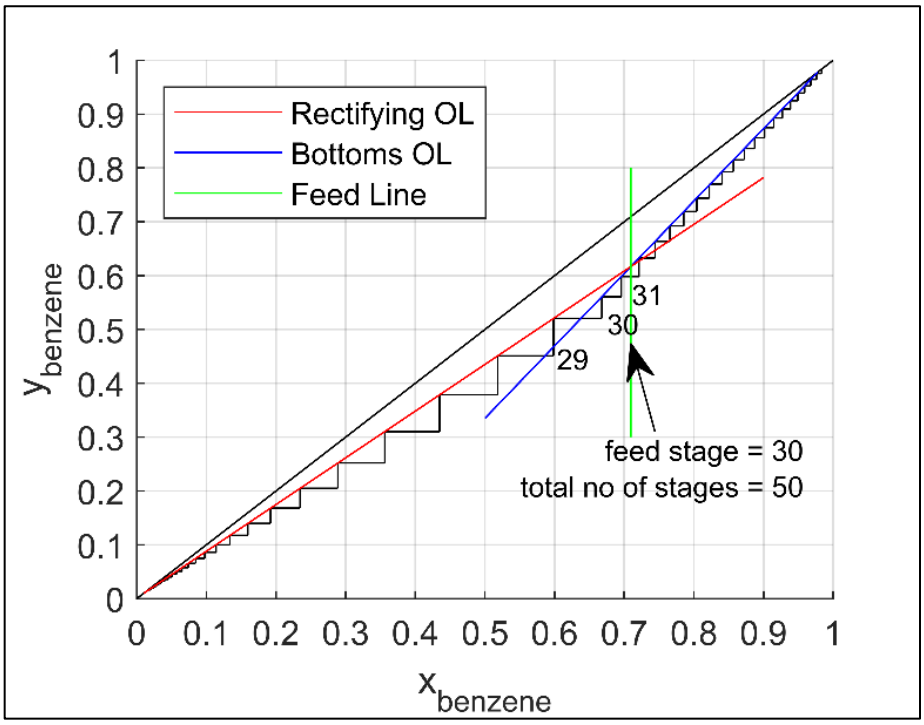

Figure 6.16: McCabe-Thiele diagram for benzene used to determine the number of theoretical stages at finite reflux and the feed stage location at stage 30

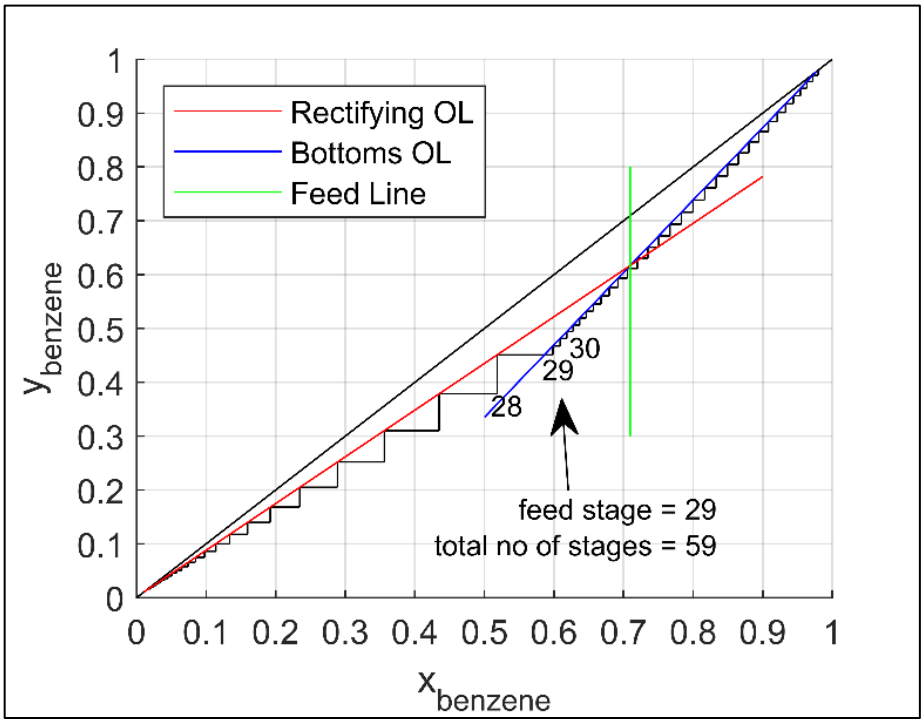

Figure 6.17: McCabe-Thiele diagram for benzene used to determine the number of theoretical stages at finite reflux and the feed stage location at stage 29

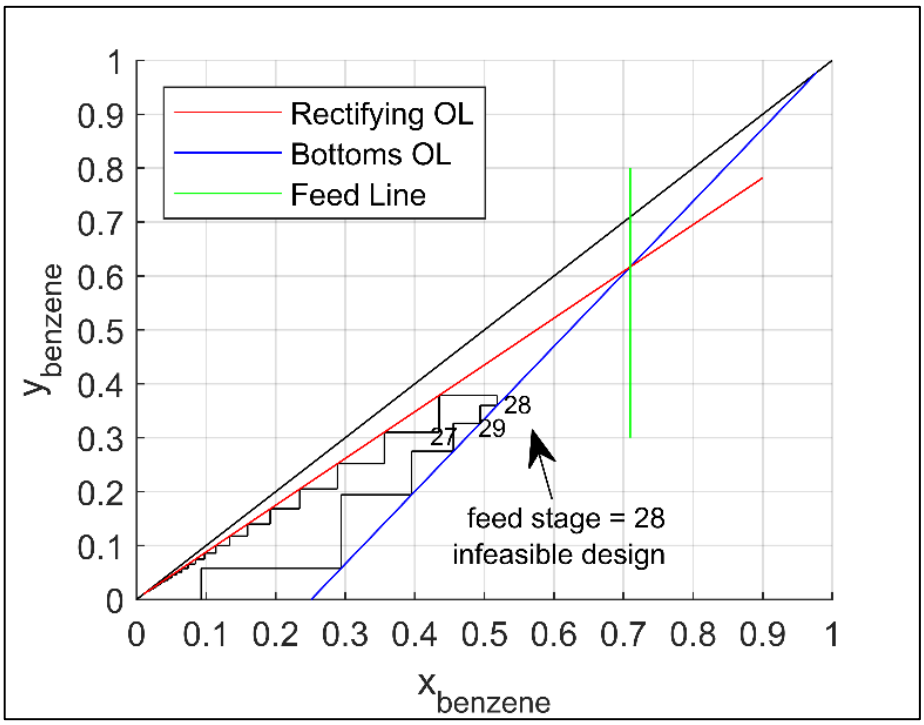

Figure 6.18: McCabe-Thiele diagram for benzene used to determine the number of theoretical stages at finite reflux and the feed stage location at stage 28

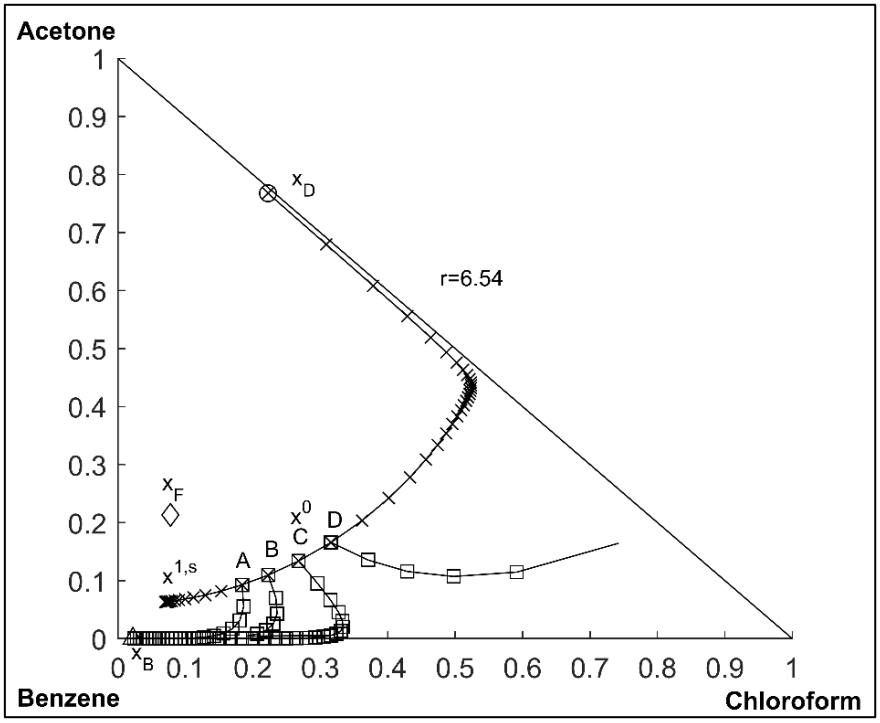

Figure 6.19: Showing several bottoms profiles at different feed stage location for an indirect split for the acetone-benzene-chloroform system

Figure 6.19 shows the visual representation of the feed stage location method presented by Doherty & Malone (2001), point A on Figure 6.19 and Figure 6.15 depicts a changeover at the feed line (stage 31) of benzene, and requires 46 stages (including the partial reboiler). Point D on Figure 6.19 and Figure 6.18 clearly shows that any change over, or at and below stage 28 will result in an infeasible design as the direction of the bottoms profile moves away from the bottoms product composition. Hence, the stage lies before the x^0 (saddle pinch) is reached and operation below x^0 is not feasible. The bottoms profile for Case D in Figure 6.19 can be visually identified by a designer when determining the number of stages on an x-y diagram, as the stepping moves in the opposite direction to the bottoms composition (Figure 6.18). The designer will immediately be able to change the feed stage location to a higher stage. Case C on Figure 6.17 represents the bottoms profile that passes closest to the saddle pinch (x^0). At a saddle pinch, the number of stages required to move out of the pinch is large (require 59 stages are required to reach the bottoms product composition).

Figure 6.17 shows that each step becomes smaller in the saddle pinch, and many more stages (13 additional stages) are required to achieve the bottoms product composition than depicted by changeover at the feed line in Figure 6.15. Lastly, changeover at stage 30 requires 50 stages (including the partial reboiler), which is 4 stages in excess of changeover at the feed stage of benzene. It can be seen on Figure 6.19 that case B lies between x^0 and $\hat{x}^{1,s}$ and this would be a feasible design, as shown by Doherty & Malone (2001). It is, however, recommended to change over from the rectifying line to the bottoms operating lines at the feed line for the heavy key for indirect splits. This rule will simplify calculations and be feasible in terms of the number of stages, as well as obtaining the correct product specification. This can be the first conceptual design iteration, after which the designer can perform further calculations to judge whether it would be more feasible to change over after the feed line (as described for the ideal system).

The design which changes over from the rectifying to the bottoms operating line at the feed line for benzene (stage 31) will be used to initialise a rigorous simulator. The aim of preliminary design calculations is to obtain initial design parameters that can be used to initialise more detailed design calculations using rigorous simulators. Thereafter, the designer can perform detailed design and optimization calculations.

Analysis 6.3: Rigorous simulation (Aspen Plus™) using design parameters from graphical method

The design parameters obtained from the preliminary design graphical method depicted in Figure 6.15 are as follows:

The total number of theoretical stages required is 46 stages (including the reboiler), 31 in the rectifying sections and 15 in the bottoms section. The feed stage is 31, and the reflux and reboil ratios are 6.54 and 2.90 respectively.

The Radfrac column in Aspen Plus™ was used. For pure components, vapour pressures were determined using the extended Antoine equation and the Wilson activity coefficient model. An Aspen Plus™ simulation was initialised with these parameters, including the feed composition in the design problem. The liquid compositions on each stage obtained from the Aspen Plus™ simulation and the proposed graphical method are depicted on MBT for the system, in Figure 6.20.

The first Aspen Plus™ simulation converged with the design parameters predicted by the proposed graphical method. Hence, the graphical method will save the designer time in trying to produce a converged design from which detailed calculations can be done. The final compositions of the graphical method correlated well with the rigorous simulation. Hence, it can be concluded that the proposed

graphical method proves to be a beneficial preliminary design tool that can be used in the conceptual and preliminary design phase of the distillation design procedure.

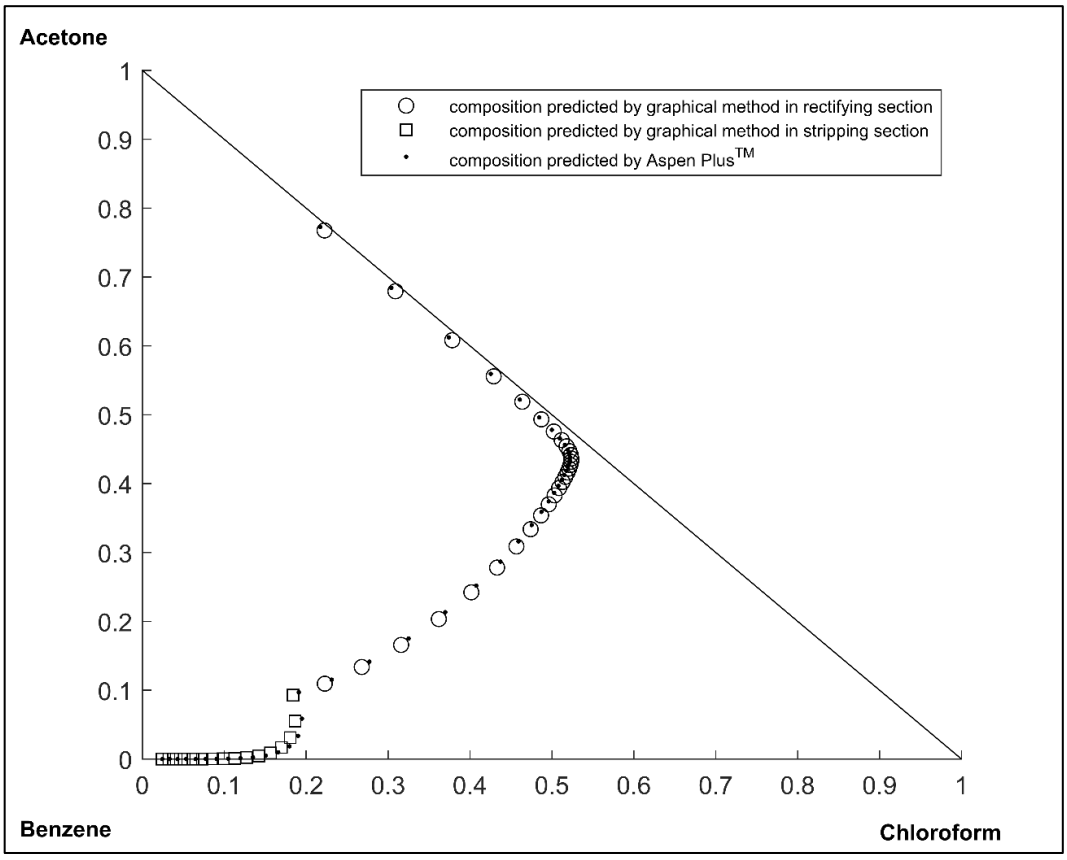

Figure 6.20: Distillation curve map (DCM) depicting the compositions on each stage for the proposed graphical method and Aspen Plus™

6.4 Extension to Quaternary Systems and the General Method for Higher Order Systems

Applying the same principles used to derive the equations and ratios required to plot the contours of VLE for a ternary system in Chapter 3, the equations and ratios for a quaternary system can be derived. Consider a four-component system (*i, j, k*

and *l*). At constant relative volatility (α) the vapour compositions for component *i* can be defined by Equation 6.15:

$$y_i = \frac{\propto_{ik}\left(\frac{x_i}{1-x_i}\right)(1+ CR_{jk}+ CR_{lk})}{1 + \propto_{ik}\left(\frac{x_i}{1-x_i}\right)(1+ CR_{jk}+ CR_{lk}) + \propto_{jk}(CR_{jk}) + \propto_{lk}(CR_{lk})} \quad (6.15)$$

Where:

$$CR_{jk} = \frac{x_j}{x_k} \quad (6.15a)$$

or

$$CR_{ki} = \frac{y_k}{y_i} \quad (6.15b)$$

$$CR_{lk} = \frac{x_l}{x_k} \quad (6.15c)$$

or

$$CR_{li} = \frac{y_l}{y_i} \quad (6.15d)$$

Likewise, the vapour composition for components *j*, *k* and l can be determined from Equations 6.16, 6.17 and 6.18 respectively:

$$y_j = \frac{\propto_{ji}\left(\frac{x_j}{1-x_j}\right)(1+ CR_{ki}+ CR_{li})}{1 + \propto_{ji}\left(\frac{x_j}{1-x_j}\right)(1+ CR_{ki}+ CR_{li}) + \propto_{ki}(CR_{ki}) + \propto_{li}(CR_{li})} \quad (6.16)$$

Where:

$$CR_{ki} = \frac{x_k}{x_i} \quad (6.16a)$$

or

$$CR_{ki} = \frac{y_k}{y_i} \quad (6.16b)$$

$$CR_{li} = \frac{x_l}{x_i} \quad (6.16c)$$

or

$$CR_{li} = \frac{y_l}{y_i} \quad (6.16d)$$

$$y_k = \frac{\propto_{ki}\left(\frac{x_k}{1-x_k}\right)(1+CR_{ji}+CR_{li})}{1+\propto_{ki}\left(\frac{x_k}{1-x_k}\right)(1+CR_{ji}+CR_{li})+\propto_{ji}(CR_{ji})+\propto_{li}(CR_{li})} \quad (6.17)$$

Where

$$CR_{ji} = \frac{x_j}{x_i} \quad (6.17a)$$

or

$$CR_{ji} = \frac{y_j}{y_i} \quad (6.17b)$$

$$CR_{li} = \frac{x_l}{x_i} \quad (6.17c)$$

or

$$CR_{li} = \frac{y_l}{y_i} \quad (6.17d)$$

$$y_l = \frac{\propto_{li}\left(\frac{x_l}{1-x_i}\right)(1+CR_{ji}+CR_{ki})}{1+\propto_{li}\left(\frac{x_l}{1-x_i}\right)(1+CR_{ji}+CR_{ki})+\propto_{ji}(CR_{ji})+\propto_{ki}(CR_{ki})} \quad (6.18)$$

Where

$$CR_{ji} = \frac{x_j}{x_i} \quad (6.18a)$$

or

$$CR_{ji} = \frac{y_j}{y_i} \quad (6.18b)$$

$$CR_{ki} = \frac{x_k}{x_i} \quad (6.18c)$$

or

$$CR_{ki} = \frac{y_k}{y_i} \quad (6.18d)$$

Unlike ternary systems, quaternary systems require two ratios of the other three components in the system. In addition, the method can be further adapted to any number of components. As the number of components increases, the number of ratios increases by one. Therefore, the general rule is that (*n*-2) ratios are required for a system of *n* components (refer to Figure 6.21). However, for higher order

systems, the contours cannot be pre-drawn and only the specific contour representing the component ratios can be plotted. From these contours, the number of theoretical stages and the feed stage location can be determined. Although equations (6.15)-(6.18) are for ideal constant relative volatility, once the ratios required are known, the method can incorporate any thermodynamic model to plot the contours of VLE for ideal and non-ideal systems. In this Chapter, a sharp split in an ideal system will be depicted, but the method can also be applied to non-ideal systems as well as indirect splits. The method for indirect splits is outlined in Figure 6.21b

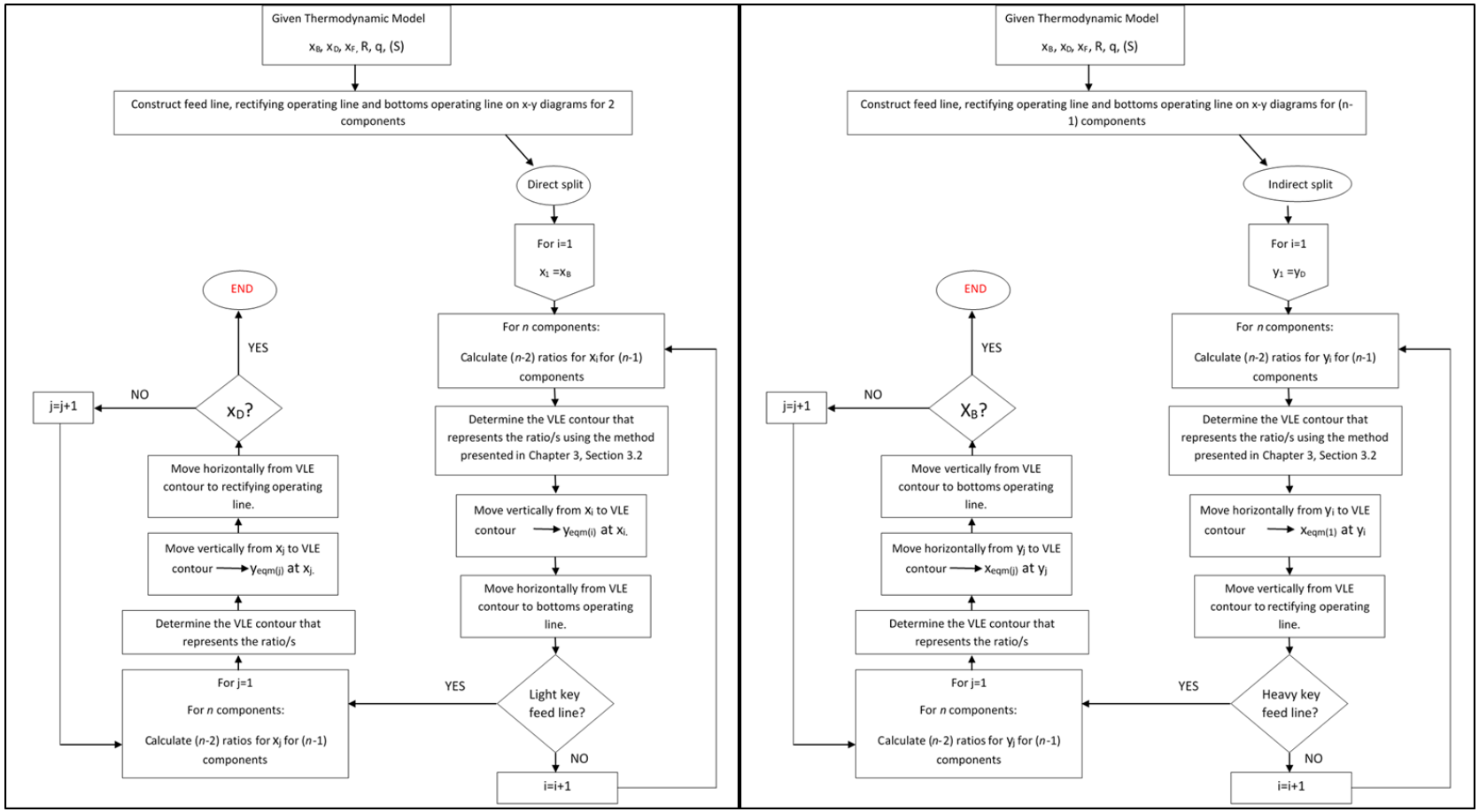

Figure 6.21: Generalised method to determine the number of theoretical stages and feed stage location at finite reflux for n number of components for (a) direct splits and (b) indirect splits

6.4.1 Example 6.3: Quaternary Ideal Simple Separation (n-hexane, n-heptane, n-nonane and n-decane)

An ideal system of n-hexane, n-heptane, n-nonane and n-decane will be considered for a simple separation. N-hexane is the light key component (normal boiling point (nbpt) – 68.9°C), n-heptane (nbpt – 98.4°C) is the intermediate component, n-nonane is the heavy key component (nbpt – 150.78°C) and n-decane is the non-heavy key component (nbpt- 174.1°C) (Wahnschafft & Westerberg, 1993; Gamba et al., 2009). The relative volatilities of the components are used to determine the equilibrium data for the contours of VLE (Equations 6.15-6.18). The relative volatilities of the components are calculated using K-values, which are dependent on temperature and pressure. The De-Priester chart is used to determine the K-values for n-hexane, n-heptane, n-nonane and n-decane at 373 K and 600 kPa. The values obtained are given in Table 6.4:

Table 6.4: K-values and relative volatilities for n-hexane, n-heptane, n-nonane and n-decane

Component	K value	Relative volatility (α)
n-hexane	0.450	7.03
n-heptane	0.220	3.44
n-nonane	0.064	1.00
n-decane	0.020	0.313

Design problem: An equimolar saturated liquid (q=1) mixture of n-hexane, n-heptane, n-nonane and n-decane feeds into a finite reflux column at constant pressure (1 bar). The aim of the separation is to achieve a mole fraction of 0.950 of n-hexane recovered in the distillate product and 0.020 mole fraction of n-hexane in the bottoms product. The feed, bottoms and distillate compositions can be found in Table 6.5. The distillate compositions for n-nonane and n-decane are chosen to be negligible in order to obtain the direct split configuration. The implications of this

choice is that more stages are required to obtain the desired product. Determine the number of theoretical stages required, and the feed stage location to achieve a feasible separation, if the reflux and reboil ratios are 3.50 and 1.48 respectively

Table 6.5: The liquid feed, distillate and bottom product compositions for n-hexane, n-heptane, n-nonane and n-decane

Component	x_F	x_D	x_B
n-hexane	0.250	0.950	0.020
n-heptane	0.250	0.050	0.316
n-nonane	0.250	1.00e-10	0.332
n-decane	0.250	1.00e-17	0.332

Before looking at the finite reflux design, the minimum number of stages at total reflux for higher order systems will be presented. The method for quaternary systems is merely an extension of that proposed in Chapter 4 for ternary systems and will be compared to the Fenske method. The general solution is applicable for any number of components, as well as for ideal and non-ideal systems, and is presented below.

A general solution for total reflux calculation involves the following algorithm:

1. Consider the first component *i* in a mixture of *n* components. Component *i* will require (*n*-2) ratios to determine the first VLE contour to step towards. For a quaternary system, n-hexane will require two ratios to be calculated. Calculate the ratios defined in Equations 6.15a and 6.15c, using the given liquid bottoms product composition. $CR_{1,(C7/C9)} = x_{C7} / x_{C9} = 0.316/0.332 = 0.952$ and $CR_{1,(C10/C9)} = x_{C10} / x_{C9} = 0.332/0.332 = 1$.
2. For *n* components, the ratios for (*n*-1) components need to be determined. For the quaternary system, in addition to n-hexane, the ratio for n-heptane (Equations 6.16a and 6.16c) and n-nonane (Equations 6.17a and 6.17c) can be determined. The fourth component (n-decane) composition can be found from a mass balance.

3. Using the ratios calculated in steps 1-2, determine the VLE contour that represents the ratios using Equations 6.15-6.17 for ideal quaternary systems or the thermodynamic model for non-ideal systems.

   For LK (n-hexane)
   x(p)=0
   y(p)=0
   x(p+1)=x(p)+0.1
   CR_{jk} = 0.952
   CR_{lk} = 1

   $$y(p+1)=\frac{\propto_{ik}\left(\frac{x_i(p+1)}{1-x_i(p+1)}\right)(1+CR_{jk}+CR_{lk})}{1+\propto_{ik}\left(\frac{x_i(p+1)}{1-x_i\,(p+1)}\right)(1+CR_{jk}+CR_{lk})+\propto_{jk}(CR_{jk})+\propto_{lk}(CR_{lk})}$$

4. Move vertically towards the VLE contour determined in step 3 to determine the liquid equilibrium composition of the vapour (y_{eqm}) at x_B.
5. Move horizontally towards the 45 degree line. Determine the new liquid composition from $x_1 = y_{eqm}$.
6. Calculate the second set of ratios (steps 1-2) using the new composition obtained in step 5 for all the components, and repeat steps 3-5 until the distillate composition is reached.

Figures 6.22 – 6.25 represent the proposed graphical method at total reflux for a quaternary system. It can be seen that the minimum number of stages required to achieve 0.95 mole fraction of n-hexane in the distillate product from the bottoms composition in Table 6.5, is 8 stages. The Fenske equation also predicts a minimum number of stages of 8, and hence correlates with that predicted by the proposed graphical method. It is important to note that the behaviour of the systems depicted by the contours of VLE are retained for quaternary systems. The LK depicts contours of VLE above the 45 degree line, the IK on both sides of the 45 degree line, the HK and non-HK below the 45 degree line.

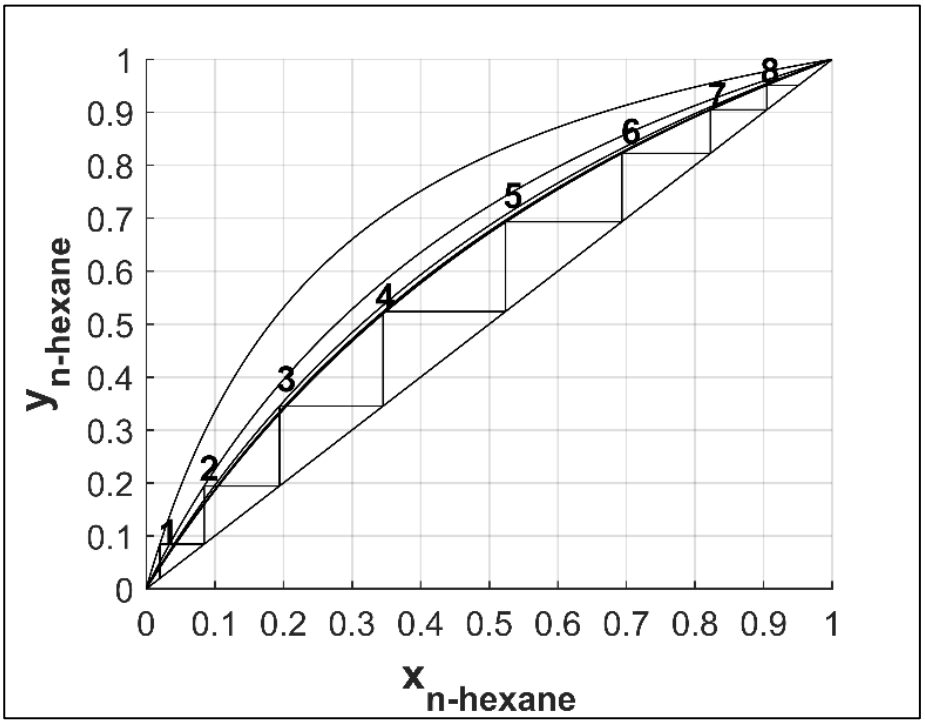

Figure 6.22: Minimum number of stages determined from the bottoms to distillate composition at total reflux using the McCabe-Thiele method for n-hexane

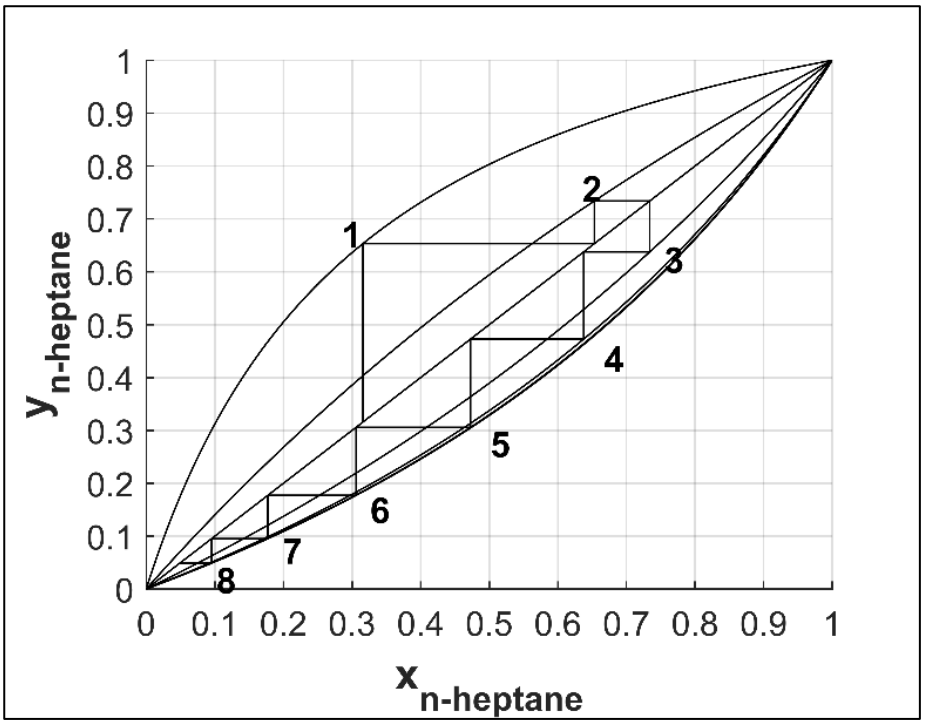

Figure 6.23: Minimum number of stages determined from the bottoms to distillate composition at total reflux using the McCabe-Thiele method for n-heptane

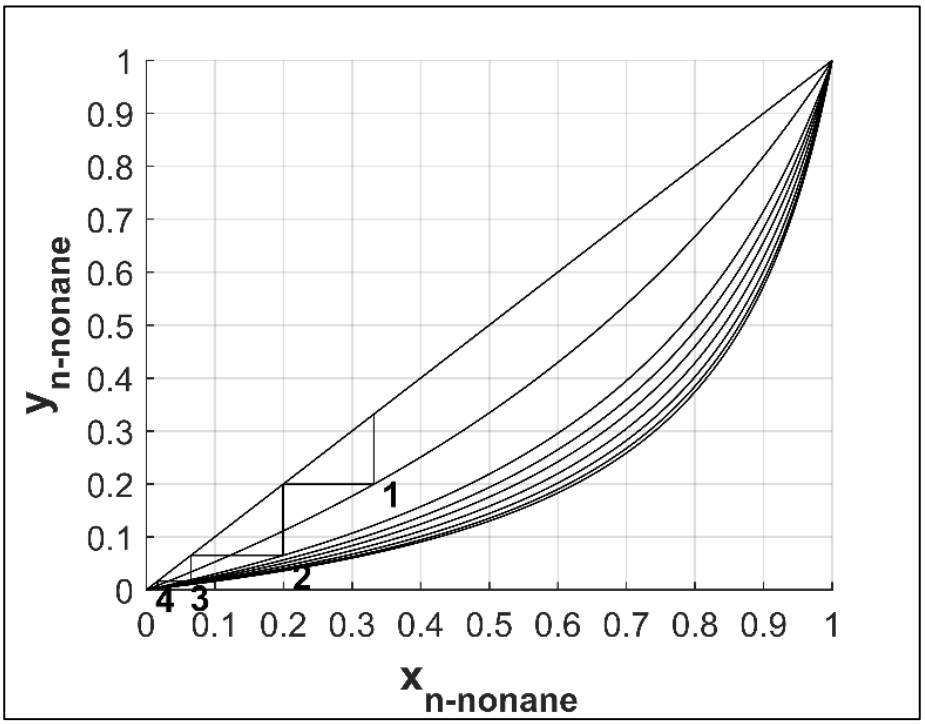

Figure 6.24: Minimum number of stages determined from the bottoms to distillate composition at total reflux using the McCabe-Thiele method for n-nonane

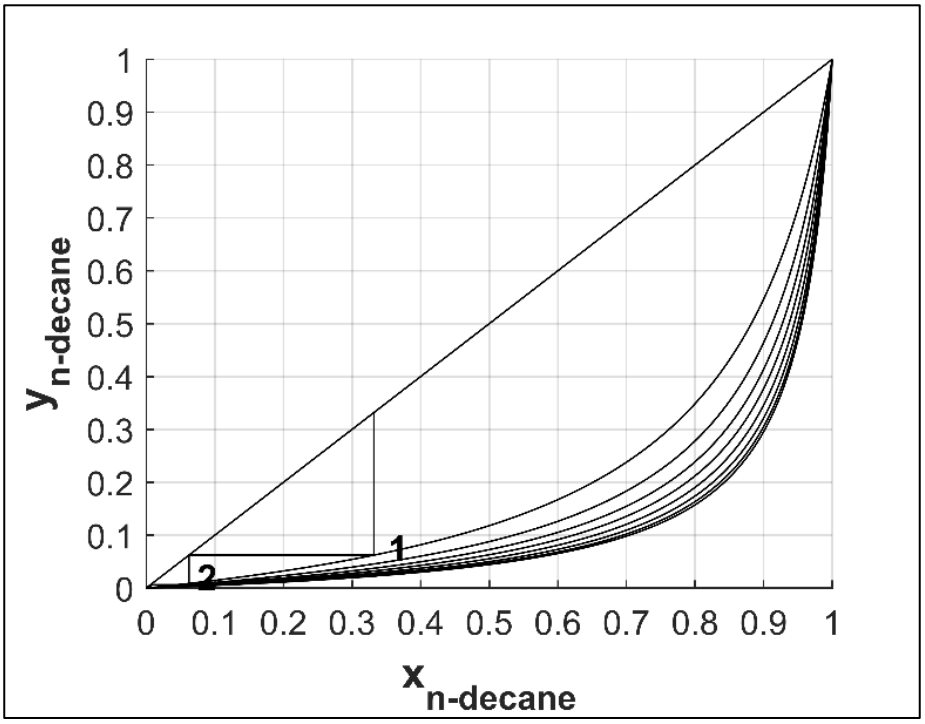

Figure 6.25: Minimum number of stages determined from the bottoms to distillate composition at total reflux using the McCabe-Thiele method for n-decane

The split is classified as direct as the process recovers a high amount of n-hexane (LK) in the distillate product. The general algorithm for direct splits in Figure 6.21a was applied to the design problem in example 6.3. The general algorithm will be applicable to any number of components, as well as ideal and non-ideal systems. The step by step method is as follows.

A general solution for finite reflux direct split calculation involves the following algorithm:

1. To construct the McCabe-Thiele diagram, the 45 degree line, feed line, rectifying operating line and bottoms operating line is plotted using Equations 6.8, 6.12 and 6.13 respectively, on x-y diagrams for (*n*-1) components. For a quaternary system, it is only necessary to plot three components as the fourth component's composition can be calculated from a material balance.
2. For a mixture of *n* components, calculate the first set of (*n*-2) ratios for (*n*-1) components. For the quaternary system, the set of ratios requires 2 ratios to be calculated for 3 components. For n-hexane (LK) calculate the two ratios required using Equations 6.15a and 6.15c and using the given liquid bottoms product composition. $CR_{1,(C7/C9)} = x_{C7} / x_{C9} = 0.316/0.332 = 0.952$ and $CR_{1,(C10/C9)} = x_{C10} / x_{C9} = 0.332/0.332 = 1$.
3. Likewise, calculate the first set of two ratios for n-heptane (Equations 6.16a and 5.16c) and n-nonane (Equations 5.17a and 5.17c).
4. Using the ratios calculated in steps 2-3, determine the VLE contour that represents the ratio using Equations 6.15-6.18 for ideal quaternary systems or the thermodynamic model for non-ideal systems.

   For LK (n-hexane)
   x(p)=0
   y(p)=0
   x(p+1)=x(p)+0.1
   CR_{jk} = 0.952
   CR_{lk} = 1

$$y(p+1)=\frac{\propto_{ik}\left(\frac{x_i(p+1)}{1-x_i(p+1)}\right)(1+CR_{jk}+CR_{lk})}{1+\propto_{ik}\left(\frac{x_i(p+1)}{1-x_i(p+1)}\right)(1+CR_{jk}+CR_{lk})+\propto_{jk}(CR_{jk})+\propto_{lk}(CR_{lk})}$$

5. Move vertically from the bottoms product composition on the 45 degree line towards the VLE contour determined in step 4, to determine the equilibrium composition of the vapour (y_{eqm}) at x_B.
6. Move horizontally from the VLE contour towards the bottoms operating line. Determine the new liquid composition for the (*n*-1) components. The composition of the last component can be calculated from a material balance.
7. Calculate the second set of (*n*-2) ratios (step 2-3) for (*n*-1) using the new composition obtained in step 6, and repeat steps 4-6 until the feed line of the light key is reached.
8. Once at the feed line for the light key, swop over towards the rectifying operating line from the contour of VLE. Determine the new liquid composition from $x_{1,R}= y_{eqm}$.
9. Repeat steps 2-5 and then step 8 until the required distillate product is obtained.

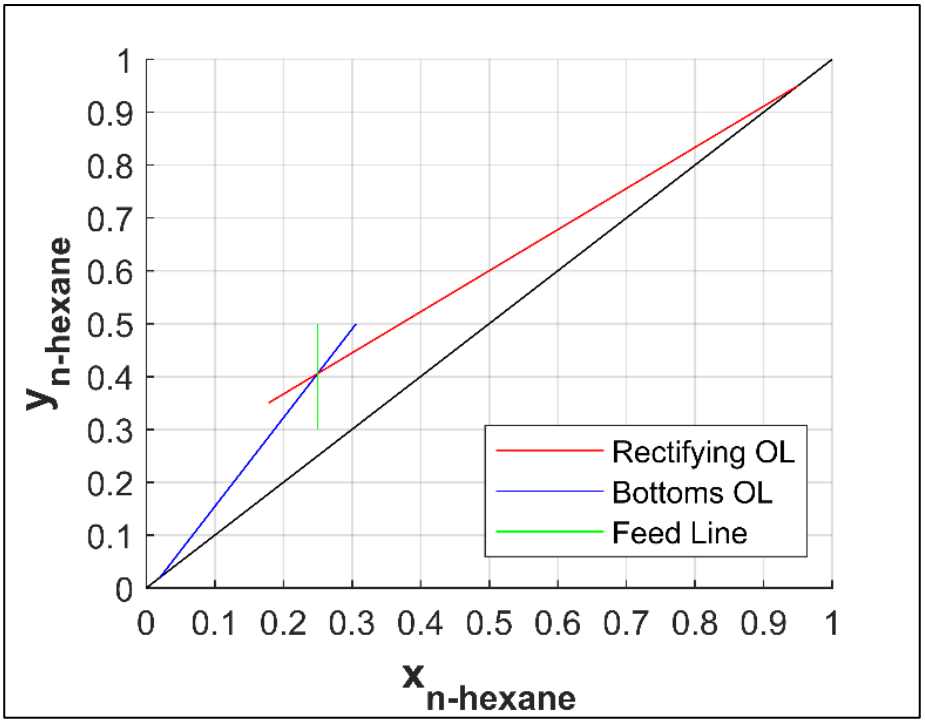

Figure 6.26: McCabe-Thiele diagram for n-hexane depicting the rectifying, bottoms and feed operating lines at finite reflux

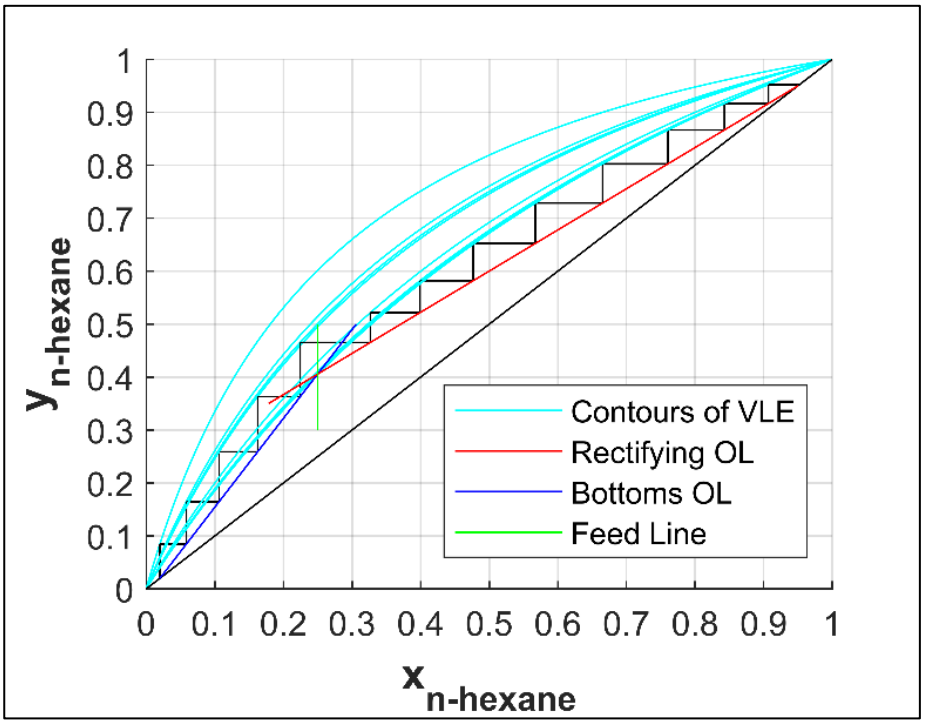

Figure 6.27: McCabe-Thiele diagram for n-hexane used to determine the number of theoretical stages at finite reflux and feed stage location for direct split

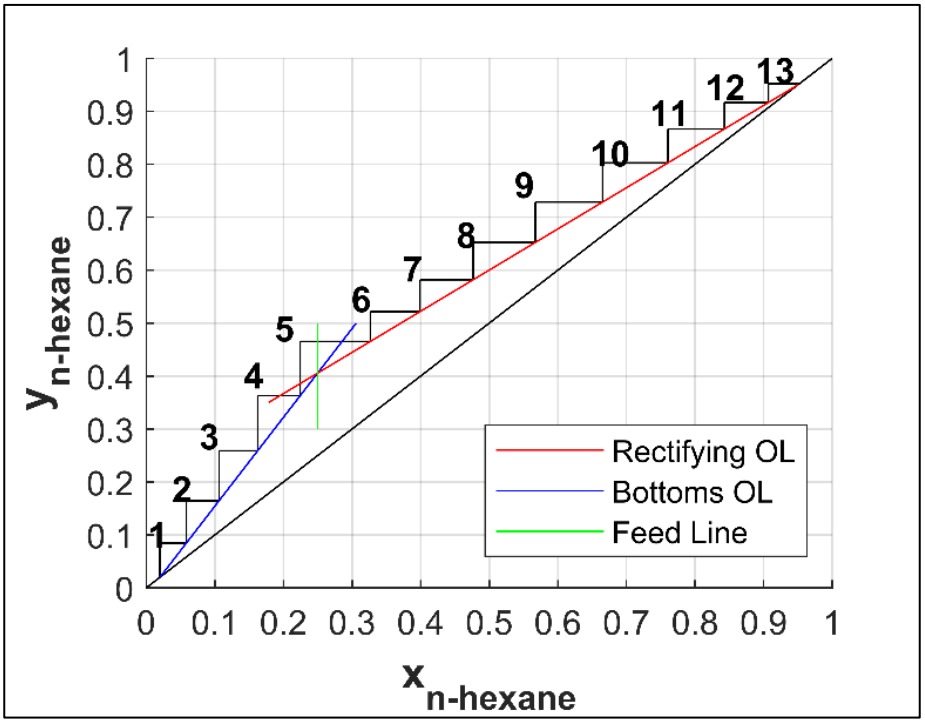

Figure 6.28: McCabe-Thiele diagram for n-hexane demonstrating the number of stages required for the direct split

Figures 6.26 – 6.28 demonstrate the proposed graphical method for a finite reflux direct separation for the LK component, n-hexane. As with ternary systems for direct splits, the LK component is analysed for feed stage location. From Figure 6.27, it can be seen that for a feed stage at stage 5, 13 stages are required to achieve a mole fraction of 0.950 for n-hexane in the distillate product. The Fenske-Underwood-Gilliland method calculates the number of theoretical stages. As presented above, the minimum number of stages at total reflux is 8 stages, using the Fenske equation. The minimum reflux ratio predicted by Underwood is 1.75 and the finite reflux will be taken to be 2 times (3.50) the minimum reflux ratio. Using the Gilliland correlation, the number of theoretical stages at finite reflux is 12.077 ~ 13 stages which correlated closely to the 13 stages calculated from the proposed graphical method. It can be concluded that the proposed graphical method correlates with the FUG method for the quaternary direct split. Although the method is shown only for ideal and direct splits, it is applicable to indirect splits as well as non-ideal systems.

6.5 Extension to Non-Constant Molar Overflow

According to McCabe & Thiele (1925), there are three cases which lead to the invalidity of CMO. The first two reasons, of varying boiling points and heat losses balance each other out and hence can be neglected (McCabe & Thiele, 1925). The third case is the considerable difference in the molar latent heat of vaporization of the components in the systems. McCabe & Thiele (1925) presented a method, developed by Peters (1922) to accommodate and correct the assumption of CMO if molar latent heat of vaporization of the components is considerably different. The correction is made by representing quantities in ‘latent heat units’ and not moles presented by Peters (1922). If quantities are changed to ‘latent heat unit’, consistency needs to be maintained hence both the equilibrium curve and well as the operating lines need to be transformed into ‘latent heat unit’. On the other hand, Fisher (1963) simplified the Peter (1922) method by using and representing the operating lines as curves and not straight lines. The Fisher (1963) method is simpler

as the equilibrium curve can be kept in mole and even mass fractions hence requiring fewer calculations.

Equations 6.19 and 6.20 give the rectifying and bottoms operating lines derived by Fisher (1963), but extended to multicomponent systems for non-CMO. Equation 6.21 provides the relationship between the reboil ratio (S) and reflux ratio (R).

Rectifying operating line:

$$y_{n,i}\left[1+\frac{(g-1)(x_{D,i}-x_{n+1,i})}{(R+1)[g-(g-1)x_{D,i}]}\right]=x_{n+1,i}+\frac{g(x_{D,i}-x_{n+1,i})}{(R+1)[g-(g-1)x_{D,i}]} \quad for\ i=1,2,\dots j \tag{6.19}$$

Bottoms operating line:

$$y_{m,i}\left[1+\frac{(g-1)(x_{m+1,I}-x_{B,i})}{S[g-(g-1)x_{B,i}]}\right]=x_{m+1,i}+\frac{g(x_{m+1,i}-x_{B,i})}{S[g-(g-1)x_{B,i}]} \qquad for\ i=1,2,\dots \tag{6.20}$$

Where $g={}^{\lambda_i}/_{\lambda_{HK}}$ $\quad for\ i=1,2\dots j\ \ and\ \lambda_{HK}$ is the molar latent heat of vaporization of the component with the lowest molar latent heat of vaporization in the mixture.

Relationship between S and R:

$$S=\frac{(R+1)[g-(g-1)x_{D,i}]\left({}^{(x_{F,i}-x_{B,i})}/_{(x_{D,i}-x_{B,i})}\right)-[g-(g-1)y_{F,i}]q}{[g-(g-1)x_{B,i}]\left({}^{(x_{D,i}-x_{F,i})}/_{(x_{D,i}-x_{B,i})}\right)} \tag{6.21}$$

The feed line is the same as the original McCabe-Thiele method (Equation 6.13) and the graphical method presented in Figure 6.6b for direct splits, and Equation 6.17a for indirect splits, and will be followed in determining the number of theoretical stages at finite reflux for ternary systems, but using Equations 6.19 and 6.20 for the operating lines. The method can also be adapted to higher order systems using Figure 6.17a for direct splits and 6.17b for indirect splits and the new operating lines.

6.6 Conclusion

With the establishment of a novel method of representing VLE, a graphical method is proposed to determine the theoretical number of stages and feed stage location for ideal and non-ideal systems. The binary McCabe-Thiele method for visualising distillation design problems is extended to ternary systems. The equations for the feed, rectifying and bottoms operating lines are presented for ternary systems along with the representation of the VLE as contours, and form the basis of representing the McCabe-Thiele diagram (x-y plot). The procedures for the original McCabe-Thiele design method are retained. A graphical method based on the McCabe-Thiele method has been proposed for ideal and non-ideal azeotropic ternary systems at finite reflux. The method calculates the number of theoretical stages and feed stage location for sharp direct and indirect splits for ideal and non-ideal systems. The proposed graphical method correlates with the FUG method for ideal ternary and quaternary systems. It has been shown that the proposed graphical method predicts the feed stage more accurately and with fewer calculations than the Kirkbride (1944) and FUG methods for ternary ideal systems. For non-ideal systems, the preliminary design parameters obtained from the proposed graphical method have been used to initialise a rigorous simulation using Aspen Plus^{TM}. The design parameters provided good initial estimates to the rigorous simulator, such that an appropriate starting point for more detailed design is achieved. The assumption of CMO provides a reasonable approximation for the highly non-ideal system of acetone-benzene-chloroform, as shown with the correlation with the rigorous simulator. Nevertheless, the method has been extended to systems in which calculations at non-CMO are necessary. In addition, the effectiveness of plotting the novel contours of VLE to analyse the behaviour of the system, as well as determine design variables, is applicable to quaternary systems. In conclusion, the proposed graphical method is an efficient and effective conceptual and preliminary design tool which retains the simplicity of the original McCabe-Thiele method.

REFERENCES

Brown, G.G., & Martin, H. Z., **1939**. An empirical relationship between reflux ratio and the number of equilibrium plates in fractionating columns. *AIChE J*. 35, pp. 679-708.

Brown, G.G., Sauders, M., Nyland, H.V., **1932**. V. Fundamental Design of Fractionating Columns for Complex Mixtures. *Ind. Eng. Chem.* 24(5), pp. 522-527.

Colburn, A.P. **1941**. The Calculation of Minimum Reflux Ratio in the Distillation of Multicomponent Mixtures. *Trans. Am. Inst. Chem. Engrs. 37*, pp. 805-825.

Cope, J.Q. & Lewis, W.K., **1932**. Studies in Distillation-Graphical Method of Computation for Rectifying Complex Hydrocarbon Mixtures. *Ind. Eng. Chem.* 24(5), pp. 498-501.

Doherty, M.F. & Malone, M.F., **2001.** Conceptual Design of Distillation Systems. *McGraw-Hill, Inc:* New York.

Erbar, J.H., & Maddox, R.N., **1961**. Latest score: reflux vs. Trays. *Petroleum Refiner*. 40 (5), pp. 183-188.

Fidkowski, Z.T., Malone, M.F., Doherty, M.F., **1991**. Nonideal Multicomponent Distillation: Use of Bifurcation Theory for Design. *AIChE J*. 37(12), pp. 1761-1779.

Fisher, G.T., **1963**. Modification of the McCabe-Thiele method for systems of unequal heats of vaporization. *Ind. Eng. Chem. ProcF. Des. Dev*. 2(4), pp. 284-288.

Gamba, S., Soave, G.D., Pellegrini, L.A., **2009**. Use of normal boiling point correlations for predicting critical parameters of paraffins for vapour-liquid equilibrium calculations with the SRK equation of state. *Fluid Phase Equilib*. 276(2), pp. 133-141.

Gani, R. & Bek-Pedersen, E., **2000**. Simple New Algorithm for Distillation Column Design. *AIChE J*. 46(6), pp. 1271-1274.

Gilliland, E.R. **1940**. Multicomponent rectification. Estimation of the Number of Theoretical Plates as a Function of the Reflux Ratio. *Ind. Eng. Chem*. 32(9), pp. 1220-1223.

Górak, A. & Sorensen, E., **2014**. Distillation: Fundamentals and Principles. *Elsevier: Academic Press*: London.

Hengstebeck, R.J., **1946**. A Simplified Method for Solving Multicomponent Distillation Problems. *Trans. AIChE*. 42, pp. 309-329.

Hengstebeck, R.J., **1961**. Distillation: Principles and Design Procedures. *Reinhold Publishing Corp:* New York.

Ho, T.J., Huang, C.T., Lee, L.S., Chen, C.T, **2010**. Extended Ponchon-Savarit Method for Graphically Analyzing and Designing Internally Heat-Integrated Distillation Columns. *Ind. Eng. Chem. Res*. 49(1), pp. 350-358.

.

Jenny, F.J., **1939**. Graphical solution of problems in multicomponent fractionation. *Trans. Am. Inst. Chem. Eng.* 35, pp. 635-677.

Julka, V, & Doherty, M.F., 1990. Geometric behavior and minimum flows for nonideal multicomponent distillation. *Chem. Eng. Sci*. 45(7), pp.1801-1822.

Kirkbride, G.G. **1944**. Process Design Procedure for Multicomponent Fractionators. *Pet. Refin*, 23(9), pp. 23-87.

Kister, H.Z., **1992**. Distillation Design. *McGraw-Hill, Inc: USA.*

Kojima, K., Katsumi, T., Kiyofumi, K., Mikiyoshi, N., **1991**. Isobaric vapor-liquid equilibria for acetone+benzene+chloroform and the three constituent binary systems. J. *Chem. Eng. Data.* 36(3), pp. 343-345.

Kong, L. & Maravelias, C.T., **2019**. From graphical to model-based distillation column design: A McCabe-Thiele-inspired mathematical programming approach. *AIChE J*. 65(11), p.e16731.

Kubicek, A.J. & Eubank, P.T., 1972. Thermodynamic Properties of n-Propanol. *J. Chem. Eng. Data*. 17(2), pp. 232-235.

Lee, J.W., Hauan, S., Lien, K.M., Westerberg, A.W., **2000a**. A graphical method for designing reactive distillation columns. I. The Ponchon-Savarit method. P*roceedings of the Royal Society of London*. 456(2000), pp. 1953-1964.

Lee, J.W., Hauan, S., Lien, K.M., Westerberg, A.W., **2000b**. A graphical method for designing reactive distillation columns. II. The McCabe-Thiele method. P*roceedings of the Royal Society of London*. 456(2000), pp. 1965-1978.

Lewis, W. **1922**. The Efficiency and Design of Rectifying Columns for Binary Mixtures. *Ind. End. Chem.* 14(6), pp. 492-496.

Mathias, P.M., **2009**. Visualizing the McCabe-Thiele Diagram. *Chem. Eng. Prog*. 105(12), pp. 36-44.

McCabe, W.L. & Thiele, E.W., **1925**. Graphical Design of Fractionating Columns. *Ind. Eng. Chem.* 17(6), pp. 605-611.

Neri, B., Mazzotti, M., Storti, G., Morbidelli, M., **1998**. Multicomponent Distillation Design through Equilibrium Theory. *Ind. Eng. Chem. Res*. 37(6), pp. 2250-2270.

Peters, JR, W.A., **1922**. The Efficiency and Capacity of Fractionating Columns. *Ind. Eng. Chem.* 14(6), pp. 476-479.

Reyes, J.A., Gomez, A., Marcilla, A., **2000**. Graphical Concepts to Orient the Minimum Reflux Ratio Calculation on Ternary Mixtures in Distillation. *Ind. Eng. Chem. Res*. 39(10), pp. 3912-3919.

Smoker, E., **1938**. Analytical Determination of Plates in Fractionating columns. *Trans. Am. Inst. Chem. Eng*. 34, pp.165.

Sorel, E. **1889**. Sur la rectification de l'alcool. *Comptes Rendus*. 58, pp. 1128.

Thong, D.Y.C., Castillo, F.J.L., Towler, G.P., **2000**. Distillation design and retrofit using stage-composition lines. *Chem. Eng. Sci*. 55(3), pp. 625–640.

Underwood, A.J.V. **1948**. Fractional Distillation of Multicomponent Mixtures. *Chem. Eng. Prog*. 44(8), pp. 603-614.

Van Winkle, M., **1967**. Distillation. *McGraw-Hill, Inc: USA*.

Vogelpohl, A., **2015**. Distillation. *Walter De Gruyter*: Berlin/Munich/Boston.

Wahnschafft, O.M. & Westerberg, A.W., **1993**. The Product Composition Regions of Azeotropic Distillation Columns. 2. Separation in Two-Feed Columns and Entrainer Selection. *Ind. Eng. Chem. Res*. 32(6), pp. 1108-1120.

Wankat, P. C. **2012**. Separation Process Engineering, Third edition. *Pearson: Upper Saddle River*, NJ.

Wasylkiewicz, S.K., Kobylka, L.C., Castillo, F.J.L., **2000**. Optimal design of complex azeotropic distillation columns. *Chem. Eng. J*. 79(3), pp. 219-227.

Widago, S. & Seider, W.D., **1996**. Azeotropic Distillation. *AIChE J*. 42(1), pp. 96-130.

Chapter 7

Reactive Distillation Design

The work in this chapter will be submitted for publication as: Seedat, N., Kauchali, S., Patel, B. A graphical method for the preliminary design of ternary reactive-hybrid distillation processes.

Abstract

This work presents a graphical method using the contours of VLE (as covered in Chapter 3) to design reactive-hybrid columns without the traditional approach of transformation of composition variables as done by Barbosa & Doherty (1987). The graphical method used to determine the minimum reflux ratio, the number of theoretical stages and the feed stage location is applied to an ideal system for reaction on the feed stage without any change in the number of moles due to the reaction ($v_T = 0$). The graphical method is extended to determine the number of theoretical stages and the reactive feed stage location for non-ideal systems with a change in the number of moles due to the reaction ($v_T \neq 0$).

Additionally, the graphical method for reaction in the rectifying section only, stripping section only and rectifying and feed stage for ideal systems was presented. The analysis of minimum reflux, feed stage location, reactive stage location and multiple reactive stages in the rectifying section is shown which in a similar manner, can be applied to the other hybrid reactive configurations. Finally, it was shown the parameters obtained from the reaction on feed stage for non-ideal systems can be used to initialise a rigorous simulation for preliminary design calculations. This chapter presents a graphical tool for the initial design of reactive-hybrid systems without the transformation of composition variables such that rigorous simulations can be initialised.

7.1 Introduction

Reactive distillation is an established process intensification technology, which combines both reaction and distillation separation in a single unit resulting in significant capital and energy savings (Kiss et al., 2019; Orjuela et al., 2016; Taylor & Krishna, 2000). According to Kiss et al., (2019), reactive distillation is one of the best applications of process intensification technologies since 1920. Reactive distillation in general has shown capital and energy savings of between 15% and 80% over conventional set-ups (Harmsen, 2007). In addition, environmental advantages, improved selectivity, avoidance of azeotropes, heat integration and increased conversions for equilibrium reactions are amongst other advantages for the combined process (Harmsen, 2007; Thotla & Mahajani, 2009).

There has been extensive research on reactive distillation in recent years. However, by 2011, the industrial implementation of reactive distillation had not matched this increased interest in the topic due to the difficulty in designing and operating reactive distillation processes (Chen et al., 2011). After further advancements post-2011, Orjuela et al., (2016) observed that reactive distillation has gained some maturity in process development, with several processes implemented in industry. Etherification, esterification, hydrogenation, hydrodesulphurisation, hydrolysis, alkylation and polymerisation are among the reactions that have been successfully implemented and investigated using reactive distillation (Hiwale et al., 2004; Muthia et al., 2018). Over the last 10 years, focus has shifted to combining intensified distillation technologies with reactive distillation processes such as divided-wall columns (DWC) (Zheng et al., 2017; Gor et al., 2020; Harding & Fieg, 2020; Weinfeld et al., 2018), heat-integrated distillation columns (Lee et al., 2021; Anbreen et al., 2022; León-Pulido et al., 2017; Jiao et al., 2012) and thermally coupled columns (Zhao et al., 2018; Santaella et al., 2017; Zhang et al., 2017) among other technologies (Kiss et al., 2019).

The successful implementation of reactive distillation processes requires the products to be either the light or heavy key such that the product can be recovered

in the either the distillate or bottoms product respectively. Additionally, in terms of reaction feasibility, the kinetics are required to be fast at the operating conditions of the reactive stages, such that reaction equilibrium is reached during the residence time of the liquid in contact with a stage (Orjuela et al., 2016). In designing reactive distillation processes, the combined separation and reaction feasibility factors need to be considered unlike conventional distillation and reactor design which accounts individually for the respective design and feasibility factors. In conventional single feed distillation processes, the main design variables are the number of stages, feed stage location and operating reflux. Reactive distillation has additional design variables such as the location of the number of reactive stages and liquid hold-up (Almeida-Rivera et al., 2004). Additionally, CMO only holds if the column is operated as thermally neutral and stoichiometrically balanced (Almeida-Rivera et al., 2004). Hence, there are several further design considerations than conventional distillation design that even differ from one reactive distillation design to another (Almeida-Rivera et al., 2004). Whilst there are economic benefits to reactive distillation processes, the complexity of designing such processes remains an integral area of research and hence limited application in chemical industries. It can also be concluded that there cannot be a single unique design solution for reactive distillation processes.

In a similar design approach, as used for non-reactive distillation processes, reactive distillation processes require three essential steps, namely: conceptual design, preliminary design and detailed design. Design methods for reactive distillation are more complex in comparison to the methods discussed in Chapters 3-6, for non-reactive distillation processes, which are to design a separation-only process (Thery et al., 2005). Reactive distillation design requires the equilibrium constants for reaction, thermodynamic models for phase equilibrium, reaction yield and purity of products in order to begin the design of a reactive distillation process (Thery et al., 2005).

Numerous methods have been developed on new concepts as well as existing non-reactive distillation concepts for reactive distillation design (Thery et al., 2005).

Short-cut methods are preliminary design tools based on using approximate equations derived from making simplifying assumptions to calculate preliminary design variables (Taylor & Krishna, 2000). Chemical reactions influence the process in reactive distillation, and these simplifying assumptions do not hold for reactive distillation processes. Hence, short-cut methods are not appropriate for reactive distillation design (Taylor & Krishna, 2000).

Almeida-Rivera et al., (2004) designated conceptual/preliminary design methods into three categories namely: graphical, optimization and heuristic methods. Each category has its place in the overall reactive distillation design procedure stated above. Graphical methods are applicable to the conceptual and preliminary design stages, to analyse feasibility and determine preliminary design variables required to initialize rigorous simulators (Gani & Bek-Pedersen, 2000). Optimization methods are developed on mathematical based models, taking into consideration material, energy balances, kinetics, and thermodynamic models as well as economic factors (operating and capital costs) (Domingues et al., 2014). Since each application of reactive distillation is unique due to the chemical systems present in the column, heuristic models calculations will differ for unique designs (Domingues et al., 2014). Since this thesis is centred on graphical methods, further elaboration on graphical methods will be presented.

According to Dragomir (2004), graphical methods can be classified as a conventional graphical method or in the group of methods based on the Boundary Value Methods (BVM) using residue curve maps (RCM). Barbosa & Doherty (1987) laid the foundation of many conceptual/preliminary graphical design methods for reactive distillation. Barbosa & Doherty (1987) presented a set of transformed composition variables, such that the mass balance equations can be represented without the reaction term analogous to non-reactive distillation systems (Barbosa & Doherty, 1988b). In reactive distillation the use of mole fractions (used in conventional distillation design) is not appropriate as the non-reactive limits are not accurately determined (Barbosa & Doherty, 1987). Barbosa & Doherty (1988a) used the transformed variables to depict phase diagrams for a single equilibrium

reaction to locate reactive azeotropes. Barbosa & Doherty (1988b) presented the mass balance equations, and hence differential equations used to plot RCMs for reactive systems, in order to identify feasible designs by identifying distillation boundaries for ideal and non-ideal ternary and quaternary systems. Barbosa & Doherty (1988c) and Barbosa & Doherty (1988d) used the foundations of transformed variables and derived a new set of differential equations to extend the BVM of Levy et al., (1985a) to reactive distillation processes for single-feed and double-feed columns respectively. Additionally, Barbosa & Doherty (1988c) and Barbosa & Doherty (1988d) presented a method of calculating minimum reflux for reactive distillation based on the Levy et al., (1985b) method for conventional distillation.

All the above-mentioned methods use the transformed compositions and assume reaction on every stage in the column, and hence are not applicable to columns with non-reacting stages (Taylor & Krishna, 2000). Hybrid columns incorporate both reactive and non-reactive stages in a column in order to obtain the desired product, which otherwise cannot be obtained from a fully reactive column (Dragomir & Jobson 2005). Espinosa et al., (1996) looked at reaction only at the core of the column (middle section) using transformed variables. Dragomir & Jobson (2005) stated that the method presented by Espinosa et al., (1996) provides an approximation and hence Dragomir & Jobson (2005) presented a method with reactive zones in different column sections (either stripping, core or rectifying) using stage composition lines and the BVM.

The Hengstebeck, Ponchon-Savarit and McCabe-Thiele methods are classified as conventional graphical methods. Jantharasuk et al., (2011) presented a graphical method for multicomponent systems by representing the components in the system as elements. A key element of the method is based on the assumption made by Hengstebeck (1946) of reducing multicomponent systems to a pseudo-binary system, in order to represent the system on a two dimensional (2D) plane. Additionally, a reactive driving force diagram (Gani & Bek-Pederson, 2000) can be incorporated, using the largest driving force, into the graphical representation of the

pseudo-binary elemental system (Jantharasuk et al., 2011). The resulting graph can be used to determine the conventional design parameters in a similar manner to the McCabe-Thiele method (Jantharasuk et al., 2011). This method can only be applied if the intermediate components can be neglected and for ideal systems. In addition, it has been shown in Chapter 3 that VLE for multicomponent systems cannot be approximated by a single VLE curve for one component.

Espinosa et al., (1993) extended the Ponchon-Savarit method to reactive distillation processes. Lee et al., (2000a, b) and Sánchez-Daza et al., (2003) provided methods applicable to both the McCabe-Thiele and Ponchon-Savarit methods. Espinosa et al., (1993) used the transformed variables of Barbosa & Doherty (1987) to reduce ternary systems to binary system. The model incorporates the energy and mass balance under reaction equilibrium, hence the Ponchon-Savarit method is used to determine key design variables (Espinosa et al., 1993). Sánchez-Daza et al., (2003) did not use the transformed variables of Barbosa & Doherty (1987) but rather the elements mass balance concept first presented by Pérez-Cisneros et al., (1997). The mixture could contain three components but contains binary elements. If the equilibrium curve can be represented as an 'element' VLE curve, and not component VLE curve and assuming constant total elemental mass overflow (CTEMO) the equilibrium curves can be plotted on an x-y diagram (without non-key consideration) to perform the McCabe-Thiele method (Sánchez-Daza et al., 2003). The VLE is calculated from sequential computation of reactive bubble points (Sánchez-Daza et al., 2003). Factoring in heat effects, allows the plot of an equivalent diagram to be used to perform the Ponchon-Savrit method to determine key design parameters (Sánchez-Daza et al., 2003). The methods by Sánchez-Daza et al., (2003) are limited if the system contains more than two elements and non-key components cannot be neglected.

Lee et al., (2000b) identified that the majority of the design methods for reactive distillation were based on transformed coordinates. In particular, the simple graphical method of Ponchon-Savarit and the McCabe-Thiele method, with untransformed mole fraction coordinates were not available for reactive distillation

processes. Transformed coordinates reduce the composition space using the stoichiometric lines, such that visual insights are lost in the graphical representation (Lee et al., (2000d). Hence, Lee et al., (2000b; 2000c) extended the original Ponchon-Savarit and McCabe-Thiele methods to binary reactive distillation systems without transforming the composition variables. The aim was to retain the powerful visual insights of conventional distillation and extend the visual impacts to reactive distillation.

The Ponchon-Savarit method is applied to isomerization reactions (with no net change in the number of moles) and decomposition reaction (with a net change in the number of moles) (Lee et al., 2000a). Reactive fixed points are defined by Hauan et al., (1999) as the phenomenon when the sum of the individual mixing, separation and reaction vectors is zero. Furthermore, Hauan et al., (1999) developed the concept of reaction difference points. All reactions follow a straight line and pass through a locus known as the reaction difference point, and hence can also be defined as the flows generated by the reactions taking place (Dragomir, 2004; Huerta- Garrido et al., 2004). The Ponchon-Savarit method is based on the lever rule developed extensively by Hauan et al., (2000) and reactive difference points (Hauan et al., (1999, 2000); Lee et al., 2000a). From these two concepts a set of new operating lines is derived from the energy and mass balances. The number of stages can be determined by stepping off stages on the Ponchon- Savarit diagram using the difference points for a reactive cascade (Lee et al., 2000b). The adapted Ponchon-Savarit method is applied to hybrid columns, determines the optimal feed stage location and determines the reaction distribution in the column (Lee et al., 2000b). The Ponchon-Savarit method is only extended to binary reactive systems, and the accuracy of the method relies on the correct enthalpy and heat of reaction data while the design variables have a large dependence on the extent of the reaction (Lee et al., 2000b).

Lee et al., (2000c) developed methods applicable to reactive-hybrid columns and of particular interest, the reaction on the feed stage using the McCabe Thiele method. Espinosa et al., (1996) and Dragomir & Jobson (2005) looked at reactive

cores and other hybrid configurations but not the reaction on the feed stage. Lee et al., (2000c) looks at isomerization reactions (no net changes in moles- assume CMO) and decomposition (net changes in moles) which the construction of the McCabe-Thiele diagram based on constant mass overflow if the mass heat of vaporization is constant (Lee et al., 2000c).

As with the Ponchon-Savarit method, a set of new reactive operating lines is derived by adding the normalized reactant/product coefficient to the non-reactive McCabe-Thiele operating lines (Lee et al., 2000c). This allows the diagram to be constructed in a finite composition space (Lee et al., 2000d). Columns with a reaction in the stripping / rectifying section will have a unique operating line, such that the intersection of the operating line for each reactive stage, with the 45 degree line, will shift by an amount equal to the ratio of the reaction extent to the product flowrate $\left(\frac{\xi_n}{D}\right)$ (Lee et al., 2000c). The moving intersection points are termed the reactive difference points, and the series of difference points is known as the reactive cascade difference points (Lee et al., 2000c). In addition, Lee et al., (2000c; 2000d) derived a modified q-line (feed line) for a decomposition reaction on the feed stage which requires accounting for the thermal conditions of the feed, heat of reactions and heat of vaporization. For a feed stage reactions, the concept of a pseudo-feed was introduced (Lee et al., 2000c). Huerta-Garrido et al., (2004) extended the concepts of pseudo-feeds and reactive difference points to binary batch distillation processes. The method presented by Lee et al., (2000c) is limited to binary reactive systems but the concept of reactive cascade difference points can be extended to multicomponent systems. The graphical method for designing ternary reactive distillation processes, proposed in this chapter, will use the concepts developed by Lee at al., (2000c, 2000d).

Sundmacher & Qi (2003) presented the McCabe-Thiele method for ideal binary systems undergoing isomerization reactions. The method incorporates the Damköhler number to analyse the conceptual design of different configurations namely: fully reactive columns, hybrid columns and a non-reactive column on top of a reactive reboiler. The method is confined to isomerization reactions in which

there is no net change in the number of moles, as well as not being extended to non-ideal and multicomponent mixtures. Flores-Estrella et al., (2016) proposed an extension of the McCabe-Thiele method to reactive distillation using the transformed reaction-invariant compositions (Ung & Doherty, 1995). The VLE is represented by the transformed variables and hence, the operating lines required for the reactive McCabe-Thiele method, is plotted for one component (Flores-Estrella et al., 2016). The work also extends the graphical method to incorporating Murphee tray efficiencies (Flores-Estrella et al., 2016). The method is applied to both ideal and non-ideal systems and the authors state that it can be applied to any thermodynamic model but since the VLE is approximated by a linear correlation it cannot correctly predict pinch points and reactive azeotropes (Flores-Estrella et al., 2016). The method can determine all the conventional preliminary design parameters as the non-reactive McCabe-Thiele method. The method is only applied to fully reactive columns and cannot be directly applied to hybrid columns as rigorous calculation will be required for non-reactive stages and the method can be applied to reactive stages (Flores-Estrella et al., 2016).

The earliest work of using McCabe-Thiele diagrams for the preliminary design of reactive distillation systems was presented by Marek (1954). Unlike all the methods mentioned above, of reducing a multicomponent mixtures to pseudo-binary pairs, Marek (1954) depicted both the light and heavy key components. This aspect correlates with the graphical method presented in this thesis (Chapter 3-6). Marek (1954) plotted the light key liquid (x_1) and vapour (y_1) at constant heavy key liquid values of heavy key component 3 (x_3) to depict the VLE of component 1. In addition, the method is not based on a transformed or equivalent composition variable. Marek (1954) developed a set of reactive operating lines, including reactions to accommodate a change in the number of moles due to reaction. The method requires VLE data, kinetics of reaction, molal volumes and enthalpy of phases and reaction in order to calculate the number of stages (Marek, 1954). The application of the method is a combined numerical-graphical method and is limited to ideal systems and fully reactive columns (Marek, 1954).

Although several graphical methods based on the McCabe-Thiele method have been developed for reactive distillation systems, these methods are limited in at least one aspect. The methods of Lee et al., (2000c) and Sundmacher & Qi (2003) are limited to binary systems and isomerization/decomposition reactions, The Jantharasuk et al., (2011) and Sánchez-Daza et al., (2003) methods rely on transformed variables, fully reactive columns and reducing the system to pseudo-binary pairs. The Marek (1954) method is restricted to ideal systems, fully reactive columns and requires numerical calculation to aid the graphical method. Hence, a comprehensive, purely graphical tool that is intuitive to the McCabe-Thiele method is lacking. A method that does not require transformed composition variables, reduction to a pseudo-binary system or which is limited to ideal systems is required. In addition, the method should be able to design hybrid combined reactive and non-reactive zones in one column.

The proposed graphical method in this chapter will be applicable to ideal and non-ideal systems, hybrid columns, and will not require transformed composition variables or reduction to a pseudo-binary system. The method is applicable to any type of reaction and not restricted to isomerization or decomposition reactions. Section 7.2 presents an extension of the method by Lee et al., (2000c) for feed stage reaction using the contours of VLE for ideal and non-ideal ternary systems. The method by Lee et al., (2000c) is particularly attractive as it retains the powerful visual insights of non-reactive distillation McCabe-Thiele diagrams. In addition, the reaction extent on each stage can be visualized graphically. It will also be shown that the method for minimum reflux, presented in Chapter 5 can be applied to feed stage reaction design cases. Once again, the proposed graphical method is to be used in conceptual and preliminary design of reactive distillation processes. From the insights gained in the conceptual and preliminary design stages, design engineers can perform detailed design calculations. Hence the design variables obtained from the design of reaction on the feed stage for a non-ideal system of isobutene, methanol and methyl tert-butyl ether (MTBE) will be used to initialise a rigorous simulation in Apsen Plus^{TM}. The method is applicable to single reaction, simple (one feed and 2 product) columns where VLE is reached on each stage.

Section 7.3 explains the method of reaction in the rectifying section, the configuration feed of rectifying sections and stripping section only for the same reaction based on reactive cascade difference points (Lee et al., 2000c; 2000d).

7.2 The Feed Stage Reaction

Of the several design methods mentioned in Section 7.1, the design method for reaction on the feed stage was presented by Lee et al., (2000c) only for binary reactive systems. Although the method was applied to decomposition reactions, it can be applied to any type of reaction. Since reaction only takes place on the feed stage, the composition on only the feed is altered. Hence, the following observations are made (Lee et al., 2000c; 2000d):

1. The configuration is equivalent to a reactor followed by a conventional distillation column.
2. The rectifying and bottoms operating lines are the same as in the non-reactive McCabe-Thiele method (Chapter 6).
3. The intersection of the operating lines is shifted linearly and does not intersect at the original feed composition fed to the column but rather at the pseudo-feed resulting from reaction on the feed stage.
4. Hence, the pseudo-feed, distillate and bottoms products are collinear on a mass balance triangle.

The proposed graphical method for the different reaction zones will apply the following assumptions (Lee et al., 2000c):

- Constant molar overflow (CMO)
- Heat losses to surroundings are negligible (adiabatic) in comparison to heat carried by vapour in the column

- Boiling points of all the components must not be significantly different and do not change at any point in the column (the temperature range of the column must not be substantial)
- Molar latent heat of vaporization of all the components must not be considerably different and constant at all conditions of the column
- Sensible heat and heat of mixing effects are negligible in comparison to latent heat changes
- On a stage, the vapour and liquid are in equilibrium
- 100% tray efficiency
- Constant pressure
- Reaction takes place in the liquid phase only

All the assumptions, besides the last, form the basis of all non-reactive distillation column designs. The last assumption is related to reactive columns. For the method to hold the extent of the reaction on the feed stage has to be determined, and for which equilibrium must be obtained.

If CMO does not hold, such that the net number of moles changes or the heat of reaction cannot be neglected, the method for reaction on the feed stage can still be applied. The method below explains both cases of no net change in moles ($v_T = 0$) and net change in moles $v_T \neq 0$ for a single reaction.

7.2.1 The McCabe-Thiele Method for Multicomponent Systems for Reaction on the Feed Stage

The general method and equations that govern a multicomponent reactive distillation column with reaction on the feed stage will be presented. The method and equations are independent of the type of reaction, but will differ if the total net number of moles changes or not. The method proposed is an extension of the method presented by Lee et al., (2000c), by adapting the idea of reactive difference points to multicomponent systems.

Consider Figure 7.1 for a reactive zone on the feed stage. The overall and component material balances, including reaction terms, can be derived for multicomponent systems.

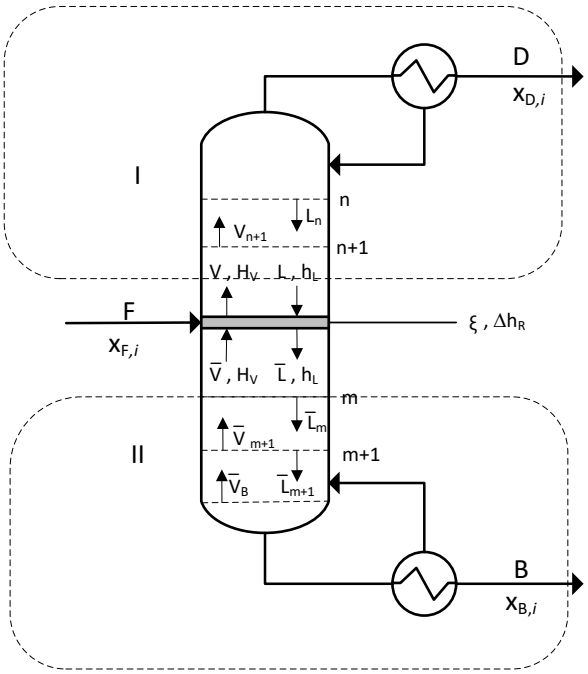

Figure 7.1: A schematic of internal and external flows for a reactive distillation column with a reaction zone on the feed stage

The overall and component material balances over the column are defined in Equations 7.1 and 7.2 and adapted for multicomponent systems.

$$F = D + B - v_T \xi \tag{7.1}$$

Where F, D and B are the molar flowrates of the feed, distillate and bottoms streams; v_T is the sum of the stoichiometric coefficients; and ξ is the total of the reaction molar turnover flowrate for a single reaction on the feed stage (extent of reaction- kmol/h).

$$Fx_{F,i} = Dx_{D,i} + Bx_{B,i} - v_i \xi \qquad for\ i = 1,2 \ldots j \tag{7.2}$$

Where $x_{F,i}$, $x_{D,i}$, $x_{B,i}$ are the molar compositions of component *i* in the feed, distillate and bottoms streams respectively; v_i is the stoichiometric coefficient of component *I;* and ξ is the extent of the reaction.

As stated in section 7.2, the operating lines of the rectifying and bottoms sections remain the same as for the non-reactive columns but due to reaction on the feed stage the intersection of the operating line shifts proportionally to the feed. The new intersection is termed as the pseudo-feed composition and can be defined as the ratio of the stoichiometric amount of the molar extent to the product flowrate$\left({}^{v_i\xi}/_{(D+B)}\right)$. The pseudo-feed is defined from the observation that the distillate and bottoms compositions are collinear with the pseudo-feed composition. Lee et al., (2000c; 2000d) defined the pseudo-feed in Equation 7.3, which has been extended to multicomponent systems.

$$x_{\hat{F},i} = \frac{Dx_{D,i}+Bx_{B,i}}{D+B} \qquad for\ i = 1,2 \dots j \tag{7.3}$$

Where $x_{\hat{F},i}$ is the molar composition of component *i* in the pseudo-feed.

Substitution of Equation 7.1 into 7.2, and defining the reaction difference point of component *i* as $\delta_{R,i} = {}^{v_i}/_{v_T}$ and using the pseudo-feed in Equation 7.3, results in Equation 6.4 (refer to Appendix D).

$$(D+B)\left(x_{F,i} - x_{\hat{F},i}\right) = v_T\xi\left(x_{F,i} - \delta_{R,i}\right) \qquad for\ i = 1,2 \tag{7.4}$$

The overall and component material balances over the feed stage (reaction zone) in Figure 7.1 are defined in Equation 7.5 and 7.6 respectively and adapted for multicomponent systems.

$$(V_i - \bar{V}_i) = F - (\bar{L}_i - L_i) + v_T\xi \quad for\ i = 1,2 \dots j \tag{7.5}$$

$$y_i(V_i - \bar{V}_i) = Fx_{F,i} + x_i(L_i - \bar{L}_i) + v_i\xi \quad for\ i = 1,2 \dots j \tag{7.6}$$

Where V_i and $\bar{L}_i$ are the vapour and liquid flowrates leaving the feed stage, and $\bar{V}_i$ and L_i are the vapour and liquid flowrates entering the feed stage.

Rearranging Equation 7.4 to make $x_{F,i}$ the subject of the formula (Equation 7.7), and substituting Equations 7.7 and 7.1 into Equation 7.6, yields the component balance in terms of the pseudo-feed composition (Equation 7.8).

$$x_{F,i} = \frac{(D+B)x_{\hat{F},i} - v_i\xi}{F} \qquad for\ i = 1,2 \dots j \tag{7.7}$$

$$y_i(V_i - \bar{V}_i) = (L_i - \bar{L}_i) + (F + v_T\xi)x_{\hat{F},i} \quad for\ i = 1,2 \dots j \tag{7.8}$$

To obtain the modified feed equation for the reaction on the feed stage, Equation 7.5 is substituted into Equation 7.8 and incorporating Equation 7.9.

$$q \equiv \frac{\bar{L}_i - L_i}{F} \tag{7.9}$$

Equation 7.10 represents the modified feed (q) line for reactive distillation columns with a reaction zone on the feed stage. The feed line intersects the 45 degree line at the pseudo-feed composition.

$$y_i = \left(\frac{q}{(q-1)-({}^{v_T\xi}/_{F})}\right)x - \left(\frac{1+({}^{v_T\xi}/_{F})}{(q-1)-({}^{v_T\xi}/_{F})}\right)x_{\hat{F},i} \quad for\ i = 1,2 \dots j \tag{7.10}$$

From the energy balance over the feed stage represented by Equation 7.11 and substituting Equation 7.5 into 7.11, the correlation to calculate q is provided in Equation 7.12.

$$h_v F + H_V\bar{V} + h_L L - \Delta h_R\xi = H_V V + h_L\bar{L} \tag{7.11}$$

$$q = \frac{H_V - h_F}{H_V - h_L} + \frac{({}^{v_T\xi}/_{F})\left(H_V + \left({}^{\Delta h_R}/_{v_T}\right)\right)}{H_V - h_L} \tag{7.12}$$

Where Δh_R is the heat of reaction

H_V is the enthalpy of the feed at the dew point

h_F is the enthalpy of the feed

h_L is the enthalpy of the feed at the bubble point

For reactions in which there is no net change in the number of moles, such as isomerization reactions and the dehydration of methanol to form dimethyl ether (DME), Equation 7.10 can be reduced to Equation to 7.13 as v_T is taken as 0.

$$y_i = \left(\frac{q}{(q-1)}\right)x - \left(\frac{x_{\tilde{F},i}}{(q-1)}\right) \quad for\ i = 1,2 \ldots j \tag{7.13}$$

The feed operating line is determined using Equation 7.10 for a net change in the number of moles and 7.13 for no net change in the number of moles. Once the feed line is determined, the rectifying and bottoms operating lines are determined using Equations 6.8 and 6.12 respectively in Chapter 6, Section 6.2.2.The operating lines are plotted on an x-y diagram and stepping off stages takes place in accordance with the rules for non-reactive systems, as set out in Chapter 6 (Figures 7.9-7.11).

7.2.2 Ideal System: No Net Change in the Number of Moles

An ideal ternary system will be used to demonstrate the basis of the method for determining the minimum reflux, the number of stages as well as the feed stage location for the reaction on the feed stage, for no net change in the number of moles ($v_T = 0$). The reaction of the form of: $2A \rightarrow B + C$, where A, B and C are fictitious components. The reactant, component A, is the intermediate key component, product B is the light key and product C is the heavy key. Hence, Component B will be recovered in the distillate and Component C in the bottoms product.

Design problem: A mixture of components A, B and C is fed to a reactive distillation column at constant pressure (1 bar). The relative volatilities are presented in Table 7.1. The reaction zone is confined to the feed stage. The bottoms and distillate flowrates are 30 kmol/h and 20kmol/h respectively. The compositions of the pseudo-feed, saturated liquid feed, distillate and bottoms composition is provided in Table 7.1. The target distillate composition for the light key component

(B) should be a minimum of 0.980. The extent of reaction on the feed stage is 5 kmol/h.

Table 7.1: Relative volatilities, pseudo-feed, feed, distillate and bottoms compositions for components A, B and C

Component	Relative volatility (α)	$x_{\widehat{F}}$	x_F	x_B	x_D
A	1.90	0.2780	0.4780	0.4500	0.020
B	3.25	0.3950	0.2950	0.0050	0.980
C	1.00	0.3270	0.2270	0.5495	5×10^{-11}

For the reaction under investigation, there is no net change in the number of moles, hence v_T = 0. Equation 7.1 is reduced to the overall mass balance of a non-reactive distillation column such that F=D+B. The feed required is presented in Table 7.1.

7.2.2.1 Minimum Reflux

The method for minimum reflux presented in Chapter 5 can be applied to reactive distillation columns with a reaction on the feed stage. Since a high purity of the LK, component B, is to be recovered in the distillate product, the operation of the column is classified as a sharp direct split. Hence, the first step is to determine the minimum reflux of the transition split, followed by the procedure for minimum reflux calculations for a sharp direct split. The steps remain the same as in Sections 4.3.1 and 4.3.2, nevertheless a brief explanation will be provided in this section.

Transition split

Step 1 in the graphical method is to determine the minimum reflux for a transition split, given a specified feed. Since the reaction zone is on the feed stage, the feed composition entering the column is altered hence the pseudo-feed in Table 7.1 will be used instead of the actual feed composition. Direct splits produce a distillate product rich in the light key, Component B, and contain very little of the heavy

component, Component C. Hence, once the transition point in the rectifying section is reached, the system can be approximated as a binary mixture of Components A and B. In order to determine the transition point in the rectifying section, the transition split, in which very little of Component C is present in the distillate product. To determine the minimum reflux of the transition split for a direct split the distillate composition of Component C is set to 1.00×10^{-10} in the distillate product (Figure 7.2). It should be highlighted that to enhance the clarity of figures in this chapter, a few contours of VLE will be shown and not all the contours required in the simulation.

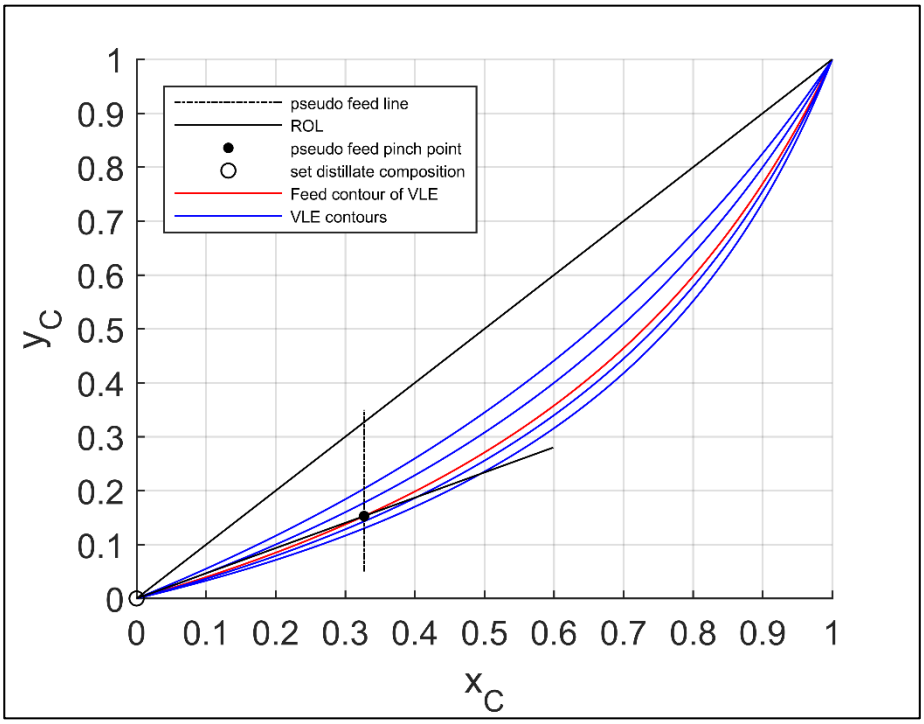

Figure 7.2: McCabe-Thiele diagram for Component C (HK), used to determine the minimum reflux for the transition split in a direct split in a feed stage reactive column

The minimum reflux ratio is calculated using the gradient of the rectifying operating line that passes through the distillate composition and the point of intersection of the feed VLE contours and feed line for Component C. The minimum reflux ratio is found to be 0.878 and the resulting adjusted distillate composition of Component B is 0.780 (Figure 7.3). The distillate and bottoms products to obtain the pinch at the feed can be found in Table 7.2.

Table 7.2: Feed, distillate and bottoms compositions for Components A, B and C in a transition split for reaction on the feed stage.

Component	$x_{\widehat{F}}$	y_F^*	x_B	x_D
A	0.2780	0.513	0.3378	0.2197
B	0.3950	0.250	1.00×10^{-10}	0.7800
C	0.3270	0.237	0.6622	1.00×10^{-10}

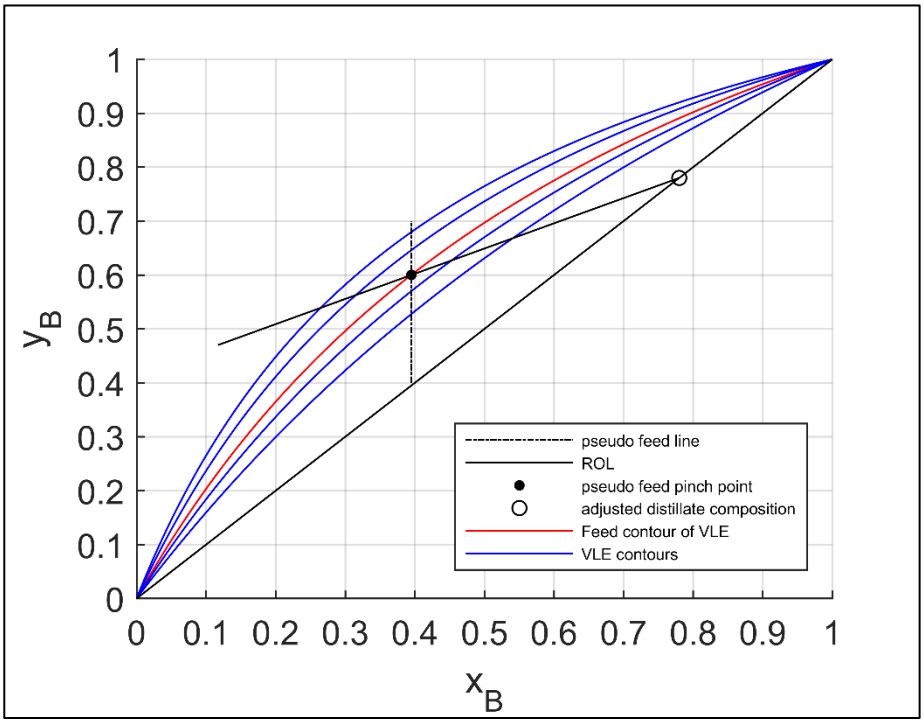

Figure 7.3: McCabe-Thiele diagram showing the adjusted distillate composition for Component B (LK), at the transition split in a direct split in a feed stage reactive column

Sharp Direct split

For direct splits, the binary equilibrium curve for Component C (HK) and B (LK), as well as the rectifying operating line at the transition split for Component B (LK), is plotted on the x-y diagram for Component B. Figure 7.4 depicts the rectifying operating line and binary equilibrium curve on the x-y plot for Component B (LK).

The intersection of the rectifying operating line and the binary equilibrium curve (Components A and B) represents the transition point in the rectifying section for a direct split. Using the estimated minimum reflux ratio of 0.878 (Step 1), the rectifying operating line for Component B (LK) for the transition split can be plotted from the calculated adjusted distillate composition (0.780) calculated from the transition split depicted in Figure 7.3. The transition point ($x_{TR,i}^{*}$, $y_{TR,i}^{*}$) is read off Figure 7.4 at the intersection of the binary equilibrium curve and the rectifying operating line for the transition split. The transition point for the specified pseudo-feed is (0.541, 0.668).

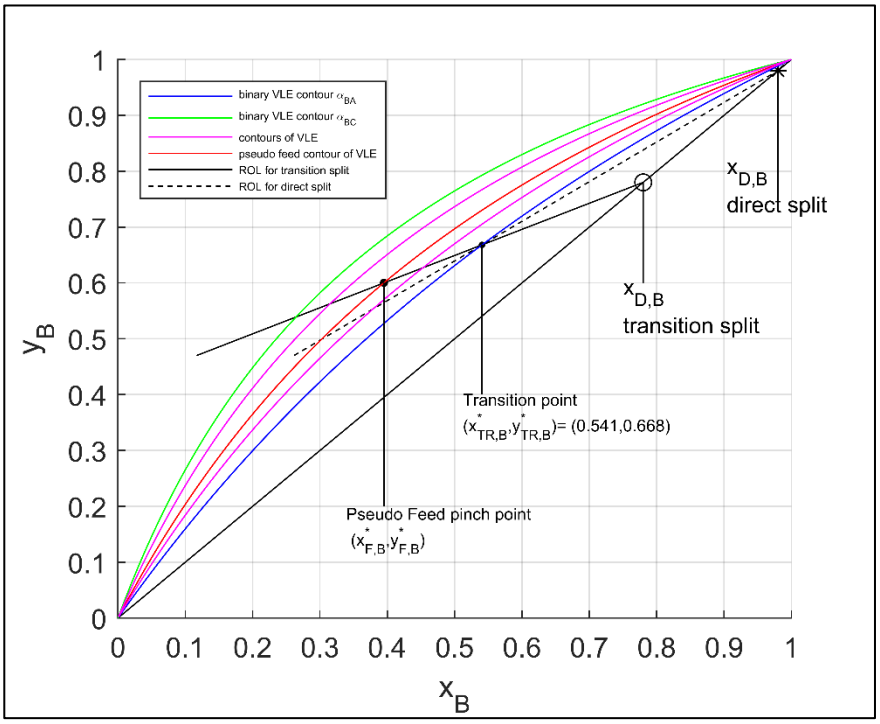

Figure 7.4: McCabe-Thiele plot for component B to determine the transition point and hence the minimum reflux ratio for a direct split in a feed stage reactive column

The gradient of the new rectifying operating line at the desired split (Component B = 0.98) can be calculated using Equation 5.6 and using the transition point calculated in Step 2. The gradient is found to be 0.710 and hence the minimum reflux for the direct split is found to be 2.45 (Figure 7.4). The compositions on each stage can be plotted on a mass balance triangle (MBT). Figure 7.5 depicts the rectifying and bottoms composition profiles for the direct split analysed above, using the distillate product compositions in Table 7.1. It can be seen that both

profiles just intersect indicating that the estimate for minimum reflux is sufficiently accurate (Levy et al., 1985a). Hence, the proposed method provides a simple graphical technique for calculating the minimum reflux in reactive distillation columns with a reaction zone on the feed stage, and provides good estimates.

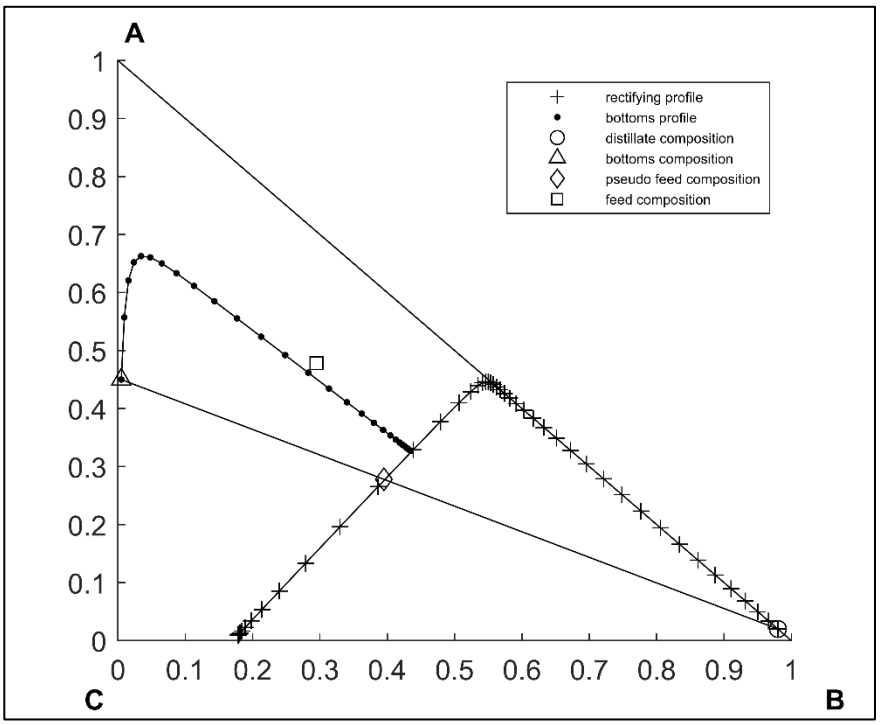

Figure 7.5: Distillation curve map (DCM) depicting the rectifying and bottoms operating profiles at the minimum reflux predicted by the proposed graphical method for a direct split in a feed stage reactive column

Analysis 7.1: Minimum Reflux with no reaction

The minimum reflux for a column with no reaction, such that the actual feed in Table 7.1 is fed to the column and 0.98 mole fraction of Component B is achieved in the distillate was determined. The minimum reflux and reboil ratio for the double feed pinch were determined to be 0.9141 and 1.8113 respectively. A summary of the double feed pinch distillate and bottoms compositions can be found in Table 7.3.

Table 7.3: Feed, distillate and bottoms compositions for Components A, B and C in transition split for a non-reactive column

Component	x_F	y_F^*	x_B	x_D
A	0.478	0.434	0.5582	0.3933
B	0.295	0.458	1.00×10^{-10}	0.6067
C	0.227	0.108	0.4418	1.00×10^{-10}

Figure 7.6 was used to determine the minimum reflux of 3.78 for the direct split using the method illustrated in Chapter 5 for non-reactive columns. Figure 7.7 plots the rectifying and bottoms profiles of the distillate composition (as in Table 7.1) and the bottoms composition for this split. A comparison of the minimum reflux ratio for a non-reactive (3.78) column and reactive column (2.45) for the given case shows that a larger reflux is required for non-reactive columns.

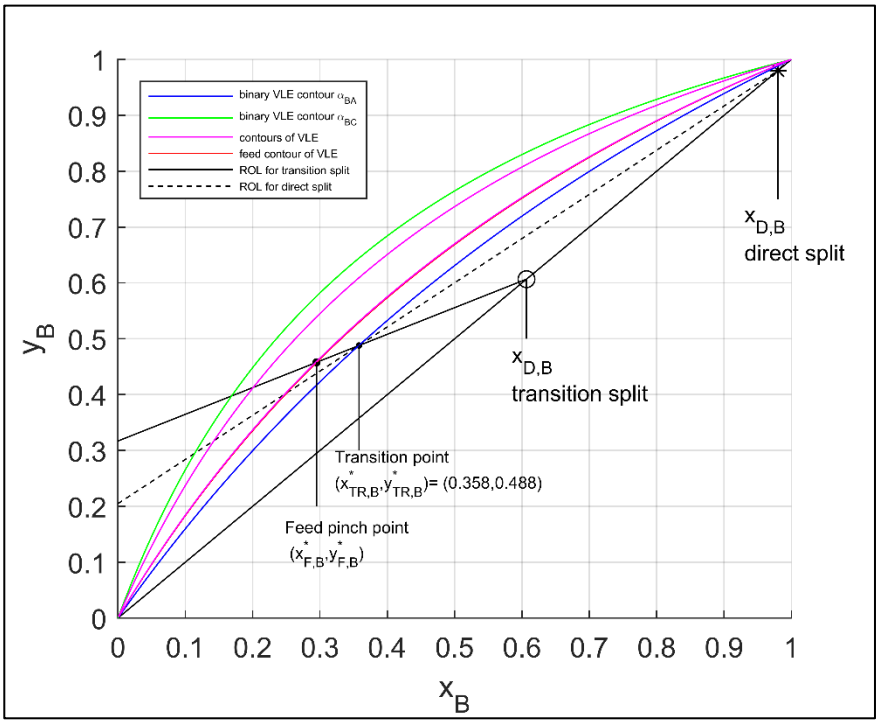

Figure 7.6: McCabe-Thiele plot for component B to determine the transition point and hence the minimum reflux ratio for a direct split in a non-reactive column

In addition, a comparison of Figures 7.5 and 7.7 illustrating the distillation curve map (DCM) at minimum reflux for reaction and no reaction respectively, shows that the reactive column recovers a higher amount of Component C in the bottoms product due to continuous and simultaneous reaction and separation of products, hence the amount of Component A decreases in the column (Malone & Doherty, 2001). Hence, feed stage reactive columns are advantageous in terms of lowering the operating reflux and the separation of components. Nevertheless, designers would have to do a cost analysis of the benefits of a lower reflux and higher recovery of components (reboiler and condenser duty) over the higher costs of the implementation of a reaction and catalyst addition on the feed stage.

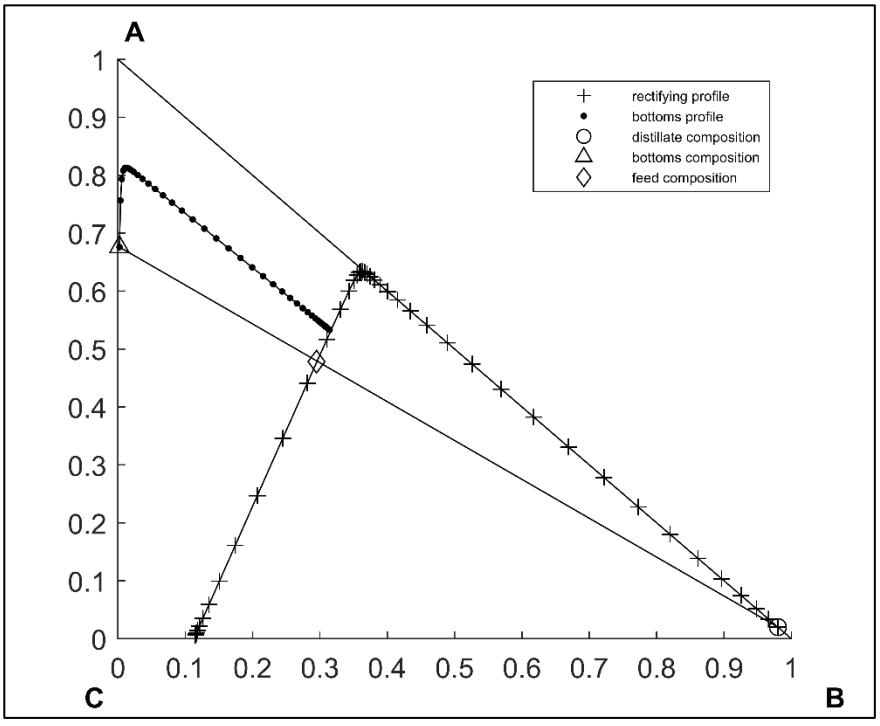

Figure 7.7: Distillation curve map (DCM) depicting the rectifying and bottoms operating profiles at the minimum reflux predicted by the proposed graphical method for a direct split in a non-reactive column

The method for minimum reflux was depicted for a sharp direct split for reaction on the feed stage but can be applied for sharp indirect splits (not shown in this chapter) by following the method presented in Chapter 4, Section 4.2.2 and using the pseudo-feed compositions and not the actual feed compositions.

7.2.2.2 Finite Reflux: Theoretical number of stages and feed stage location

The method of determining the number of theoretical stages and the reactive feed stage location for direct and indirect splits is analogous to the method for the non-reactive column design method as presented in Chapter 6. The method for both direct and indirect splits is presented in Figure 7.8. The only point of difference is that instead of the actual feed, the pseudo-feed is plotted and the changeover from one operating lines to the next is at the pseudo-feed line. It should be noted that the design specifications (x_D, x_B, x_F, $x_{\hat{f}}$, q, R and S) have to be defined beforehand, without which the method cannot be applied as depicted in Figure 7.8. This work does not present a method to determine the process specifications, (x_D, x_B, x_F, $x_{\hat{f}}$) but any appropriate method or simulation software can be used to determine these specifications.

Consider the feed, pseudo-feed, bottoms and distillate product compositions can be found in Table 7.1. The operating reflux ratio will be taken as double the minimum reflux ratio (calculated in section 7.2.2.1 as 2.45) which is 4.89 and the corresponding reboil ratio is 3.93 (calculated using Equation 6.14). The pseudo-feed location is dependent on the extent of the reaction, and the bottoms and distillate flowrates. Hence, the greater the reaction extent, the further the pseudo-feed moves from the original feed to the column. This will be analysed further when considering a pure feed of component A. As shown in Figures 7.9 and 7.10, the pseudo-feed lies to the right of the original feed by a ratio of $\left({}^{v_i\xi}/_{(D+B)}\right)$, which is 0.1 for Components B and C. Since both Component B and C are products, the shift is to the right but for the reactant (Component A) the shift would be to the left (Figure 7.11). This is due to the negative stoichiometric coefficient associated with reactants. Hence, it is possible for a column with feed stage reaction to operate with a pure reactant feed.

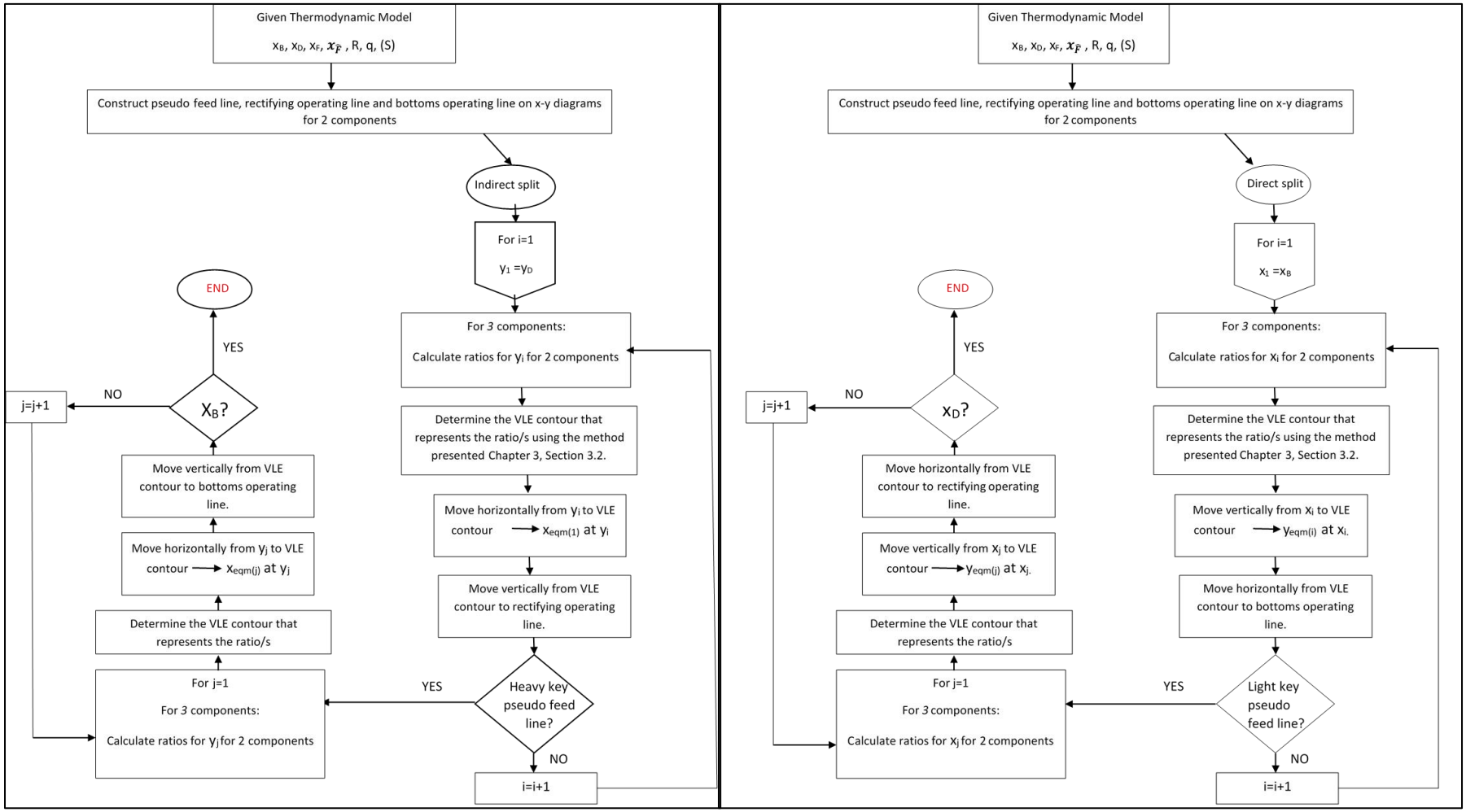

(a) (b)

Figure 7.8: Method to determine the number of theoretical stages and feed stage location for a reactive distillation column with reaction on feed stage location at finite reflux for 3 component systems for (a) indirect splits and (b) direct splits

Figures 7.9, 7.10 and 7.11 depict the McCabe-Thiele diagrams for the light key (Component B), heavy key (Component C) and intermediate key (Component A) which depict the stepping off stages to determine the number of stages required. The number of theoretical stages required is 23, and the feed stage location is stage 12 from the top of the column. It is important to emphasise that the rectifying and bottoms operating lines remain the same as non-reactive distillation for reaction on the feed stage. Hence, stepping off stages begins at the bottoms composition for direct splits using the bottoms operating line (Equation 6.12) for non-reactive columns. Change over (feed stage location) takes place at the pseudo-feed line of the light key component in Figure 7.9 (direct split).

The algorithm below, for reaction on the feed stage below is followed to determine the number of theoretical stages for a direct split.

1. To construct the McCabe-Thiele diagram, the 45 degree line, pseudo-feed line, rectifying operating line and bottoms operating line are plotted using Equation 7.10, 6.8 and 6.12 respectively on x-y diagrams for the light key (Component B) and heavy key (Component C). It is only necessary to plot two components as the third component's composition can be calculated from a material balance.
2. Calculate the first ratio for Component B (LK) (Equation 6.1a) using the given liquid bottoms product composition. $CR_{1,(Component\ A/Component\ C)} = x_{comp(A)} / x_{comp(C)} = 0.450/0.545 = 0.825$.
3. Calculate the first ratio for Component C (HK) using the given liquid bottoms product composition. $CR_{1,(Component\ B/Component\ A)} = x_{comp(B)} / x_{comp(A)} = 0.005/0.450 = 0.011$.
4. Using the ratios calculated in steps 2-3, determine the VLE contour that represents the ratio using the method presented in Section 6.2.1 or Chapter 3.
5. Move vertically from the bottoms product composition on the 45 degree line towards the VLE contour determined in step 4, to determine the equilibrium composition of the vapour (y_{eqm}) at x_B.

6. Move horizontally from the VLE contour towards the bottoms operating line. Determine the new liquid composition for the light and heavy key. The composition of the intermediate key can be calculated from a material balance.
7. Calculate the second ratio (steps 2-3) for the light and heavy key using the new composition obtained in step 6. Repeat steps 4-6 until the feed line of the light key is reached.
8. Once at the **pseudo-feed** line for Component B (light key) (Figure 7.9), swop over towards the rectifying operating line from the contour of VLE. Determine the new liquid composition from $x_1 = y_{eqm}$.
9. Repeat steps 7- 8 until the required distillate product is obtained.

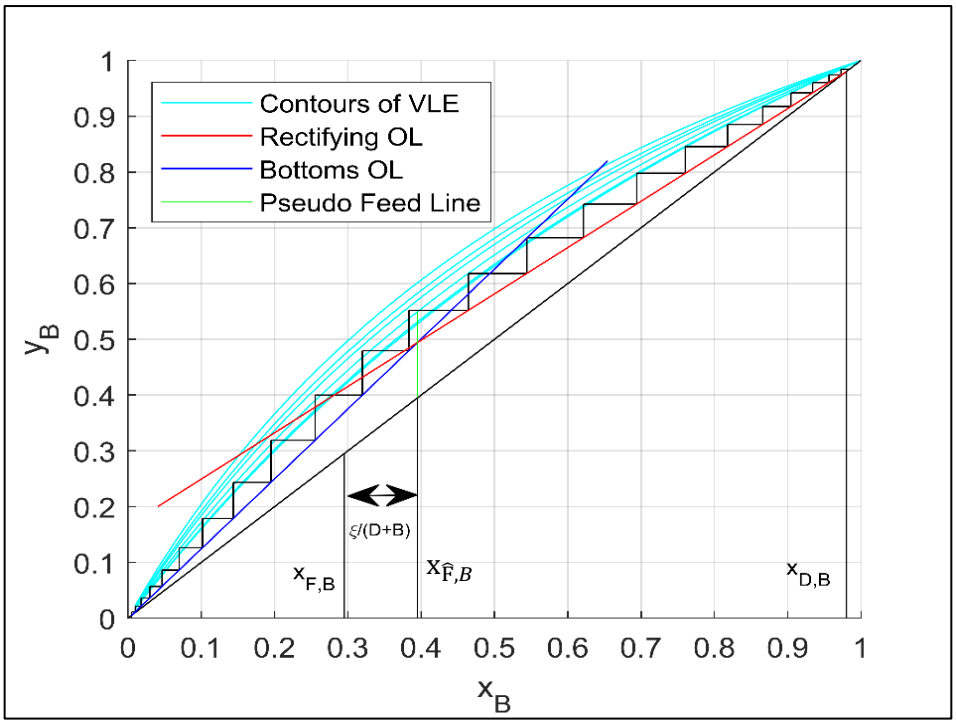

Figure 7.9: McCabe-Thiele diagram for Component B (LK) showing the pseudo-feed and actual feed used to determine the number of theoretical stages at finite reflux and the feed stage location for a direct split

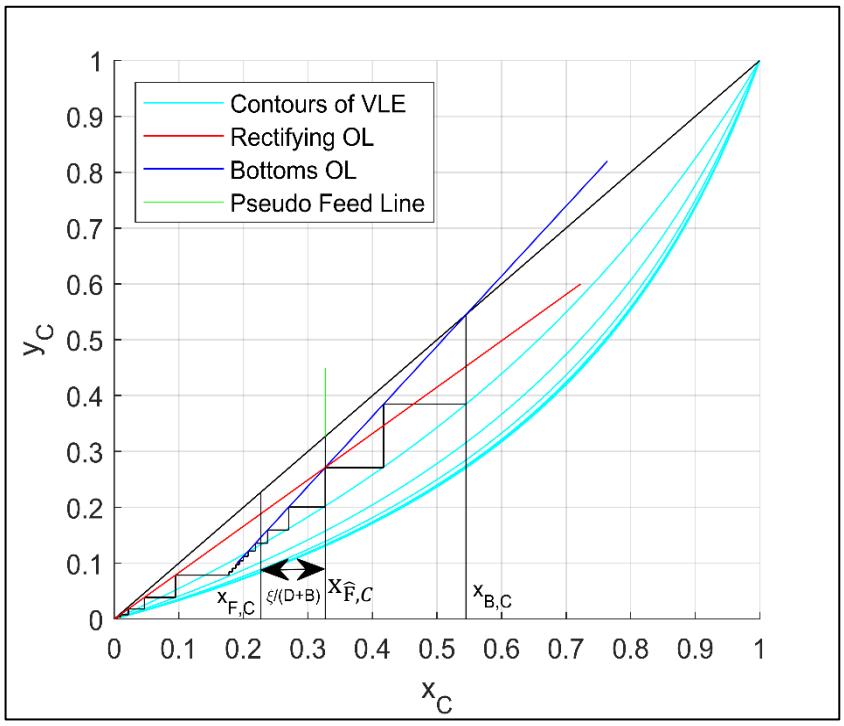

Figure 7.10: McCabe-Thiele diagram for Component C (HK) showing the pseudo-feed and actual feed used to determine the number of theoretical stages at finite reflux and the feed stage location for a direct split

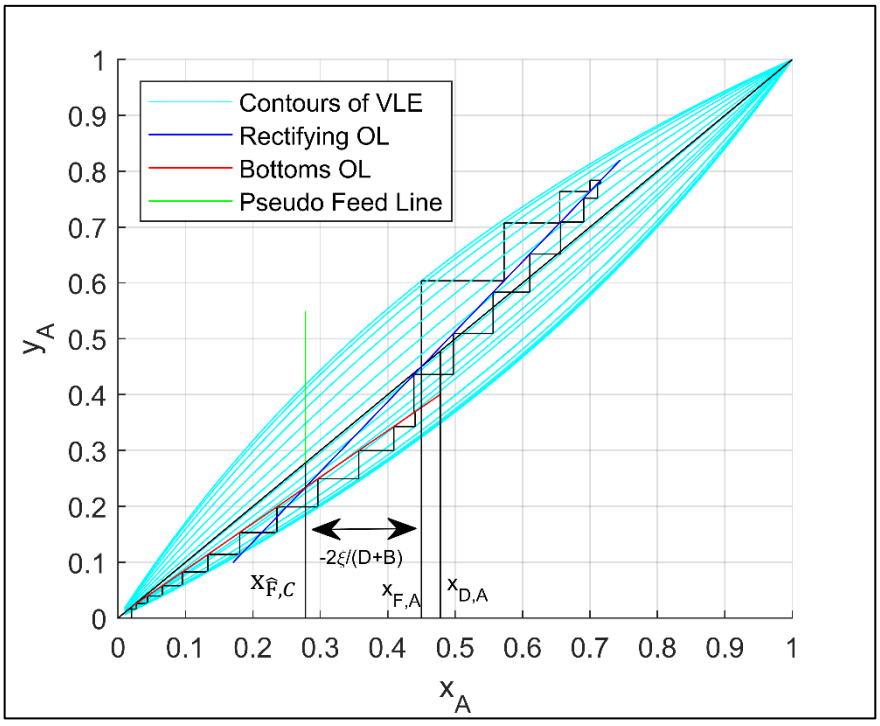

Figure 7.11: McCabe-Thiele diagram for Component A (IK) showing the pseudo-feed and actual feed used to determine the number of theoretical stages at finite reflux and the feed stage location for a direct split

Figure 7.12 plots the rectifying and bottoms profiles for reaction on feed stage on a MBT. Hence using the graphical method, the compositions on each stage can be plotted on a MBT in untransformed variables such that the visual insights are easier to interpret.

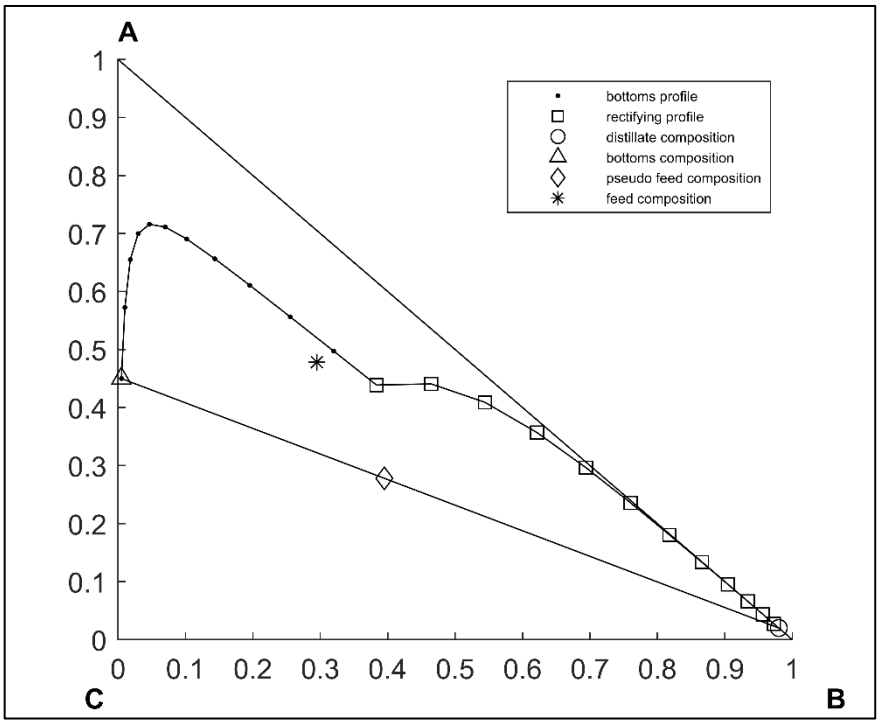

Figure 7.12: Distillation curve map (DCM) depicting the rectifying and bottoms operating profiles at the finite reflux as predicted by the proposed graphical method for a direct split in a reactive column

Analysis 7.2: Pure reactant feed

Since the proposed graphical method does not require transformation of coordinates, it is possible to depict a pure reactant feed and the corresponding product compositions in finite composition space. The addition of the reaction on the feed stage results in a pseudo-feed composition which is dependent on the reaction extent, since the stoichiometric coefficient is constant and constant product flowrates are assumed. Figure 7.13 depicts the resulting pseudo-feeds at reaction extents of 5, 10, 15, 20 kmol/h for pure feed of Component A. The reaction extent is dependent on the operating conditions of the column such as temperature, catalyst loading and hold-up rate on each stage (Marek, 1954). By changing these variables, the extent can be increased or decreased to obtain the suitable reaction extent

required. Keeping the distillate product composition constant as per the specification of the requirement of a high recovery of Component B (LK), at different extent and hence pseudo-feed compositions, different bottoms products can be obtained. By increasing the reaction extent, more reactant is consumed and hence a higher recovery of the heavy key (Component C) is achieved in the bottoms product. At high extents of 20 and greater separation and reaction become impossible. From Figure 7.13 it can be deduced that extents of less than 10 will not be feasible in terms of reaction as greater quantities of the reactant will not have reacted (higher molar fraction of Component A in the bottoms product). It is also noted that due to pseudo-feed shift being defined by a proportional ratio of $\left({}^{v_i\xi}/_{(D+B)}\right)$ for each component, the pseudo-feeds lie collinear with the original feed.

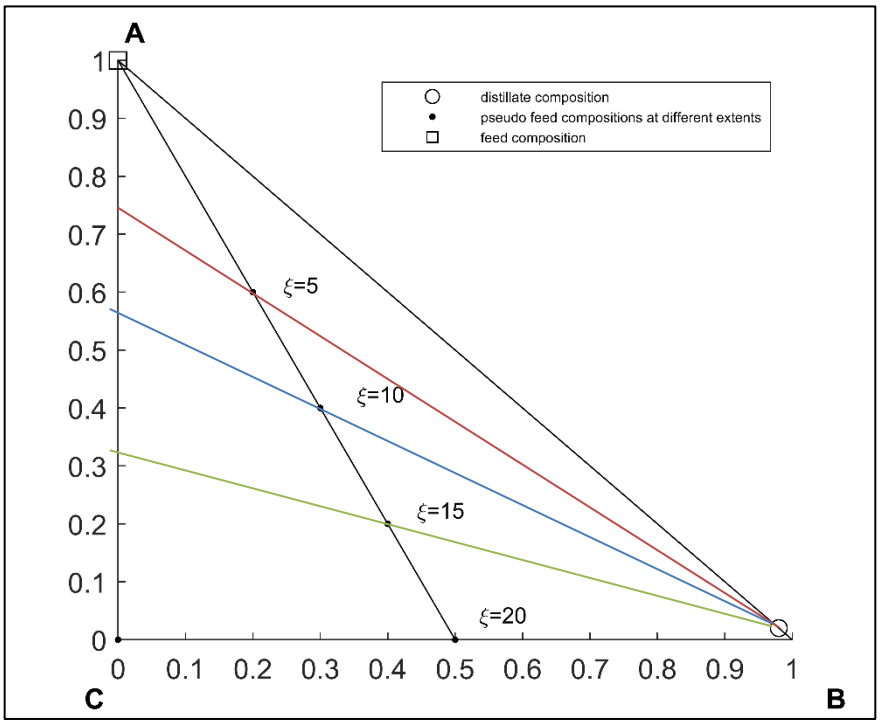

Figure 7.13: Analysis of the pseudo-feed composition at different extents for a pure Component A (reactant) feed.

7.2.3 Non-Ideal System: Net Change in Number of Moles

The method presented in Section 7.2.2 can be applied to non-ideal systems in which there may or may not be a net change in the number of moles. A non-ideal ternary system will be used to demonstrate the basis of the method for determining the number of stages required with a net change in the number of moles. The primary synthesis of methyl tert-butyl ether (MTBE) is from the etherification of isobutene (C_4H_8) with methanol (CH_3OH) in the presence of an acidic, homogeneous catalyst (Singh et al., 2005). The reaction is in the form of: $isobutene + methanol \rightarrow MTBE$, hence the total net change in moles is $v_T = -1$.

Methanol (nbpt 64.7°C) is a reactant and the heavy key component (Doherty & Malone, 2001). Isobutene (nbpt – -6.9C) is the light key component and a reactant (Doherty & Malone, 2001). MTBE (nbpt 55.1°C) is the intermediate key and the only product (Doherty & Malone, 2001). The extended Antoine equation and the Wilson activity coefficient model were used to model the equilibrium data. The Wilson model was used to model the VLE for the system as it correlated accurately with experimental data (Lísal et al., 1999). In addition, several publications have reported designs reactive distillation columns producing MTBE, using the Wilson activity coefficient model (Ung & Doherty, 1995; Singh et al., 2005). To provide a consistent basis, for comparison of results of the rigorous Aspen Plus™ simulation and the proposed graphical method, the thermodynamic parameters were taken from the rigorous simulator (Aspen Plus™). (Refer to Appendix B for the parameters).

Figure 7.14 depicts the residue curve map (RCM) for the isobutene, methanol, MTBE system. It can be seen that the system exhibits two binary azeotropes; a minimum boiling azeotrope between methanol and MTBE (51.2°C) and a minimum boiling azeotrope between Isobutene and methanol (-7.1°C) (Stichlmair & Frey, 1999). Two distillation regions exist as a result of the distillation boundary that connects the two minimum boiling azeotropes. Doherty and Malone (2001) state that, due to the two distillation regions, the difficulty in designing a feasible column

arises. In order to obtain pure MTBE (recovery of the product is the goal of the separation), the separation has to be designed in the lower distillation region B, where MTBE is the stable node (Doherty & Malone, 2001).

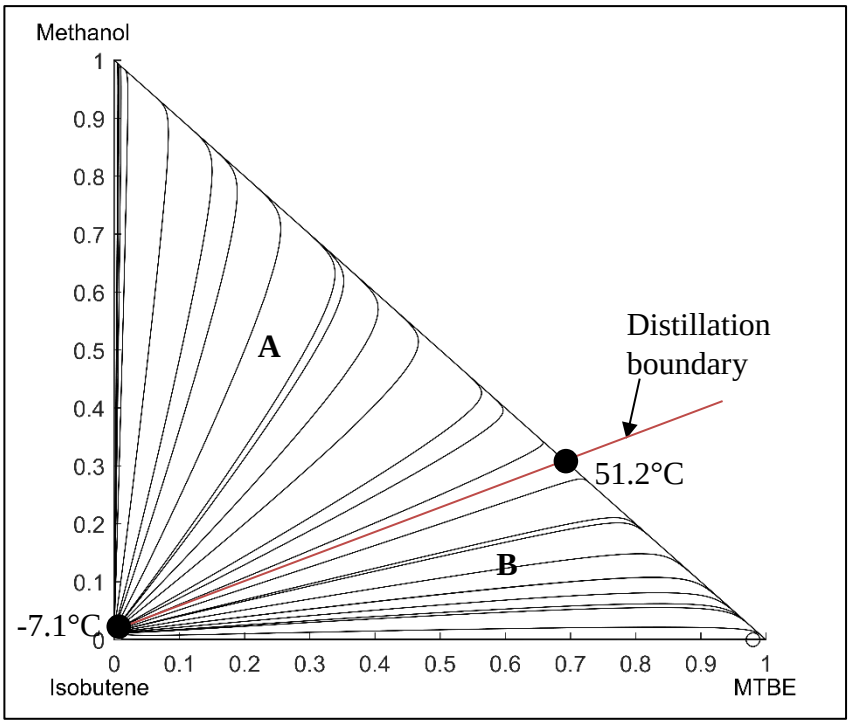

Figure 7.14: Residue curve map (RCM) for isobutene-methanol-MTBE system.

It should be noted that in distillation region B, MTBE is the intermediate key, hence the recovery of the intermediate key in the bottoms product cannot be classified as a sharp direct or a sharp indirect split. The method of determining minimum reflux in Chapter 5 is limited to sharp direct and indirect splits, and hence will not be suitable for this design problem. In addition, due to the geometry of the two azeotropes in such a system, it is not possible to obtain a sharp direct or indirect split, as isobutene is an unstable node. Nevertheless, the graphical method of determining the number of theoretical stages and the feed stage location can be applied to the desired separation. The design of the recovery of MTBE in the bottoms product in distillation region B will be produced using the graphical method. The design parameters obtained from the proposed graphical method will be used to initialise a rigorous simulation using Aspen Plus™.

Design problem: A saturated liquid feed of isobutene, methanol and MTBE enters a reactive distillation column at constant pressure (1 bar). The feed flowrate is 165 kmol/hr and the extent of reaction on the feed stage is 65 kmol/h such that an almost pure feed of the reactants is fed to the column (Figure 7.15). The pseudo-feed and feed composition are calculated using Equations 7.6 and 7.7 respectively where $v_T = -1$. The pseudo-feed and feed compositions can be found in Table 7.4. The aim of the separation is to achieve a mole fraction of 0.9999 of MTBE recovered in the bottoms product and 0.5500 mole fraction of MTBE in the distillate product. Determine the number of theoretical stages required and the reactive feed stage location to achieve a feasible separation, if the reflux and reboil ratio are 1.5 and 8.03 respectively.

Table 7.4: Pseudo-feed, feed, distillate and bottoms compositions for isobutene, methanol and MTBE

Component	$x_{\widehat{F}}$	x_F	x_B	x_D
isobutene	0.1800	0.5015	5×10^{-11}	0.2300
methanol	0.1720	0.4969	0.0001	0.2200
MTBE	0.6480	0.0016	0.9999	0.5500

The method of calculating the number of theoretical stages will follow Figure 7.8a for an indirect splits and hence step off stages from the distillate composition. The column will be designed such that the feed stage location and the reaction will be on stage 5 from the top of the column (Figures 7.15-7.16). The reflux ratio is 1.5, the q value is 0.411 and the corresponding reboil ratio is 8.03.

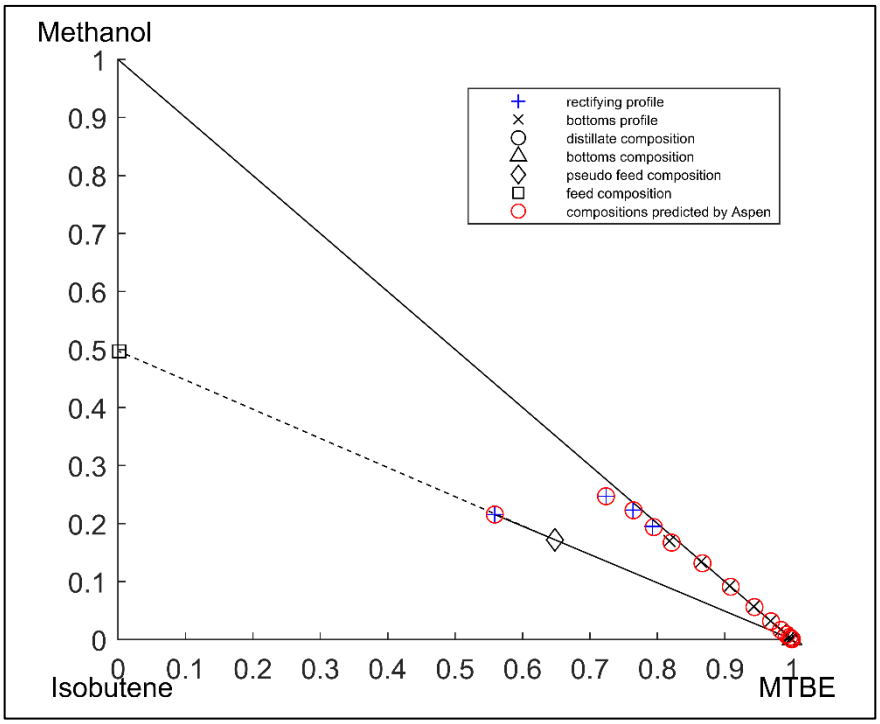

Figure 7.15: Distillation curve map (DCM) depicting the rectifying and bottoms operating profiles at the finite reflux predicted by the proposed graphical method and Aspen Plus™ for the reaction on the feed stage to produce MTBE using a reactive distillation column

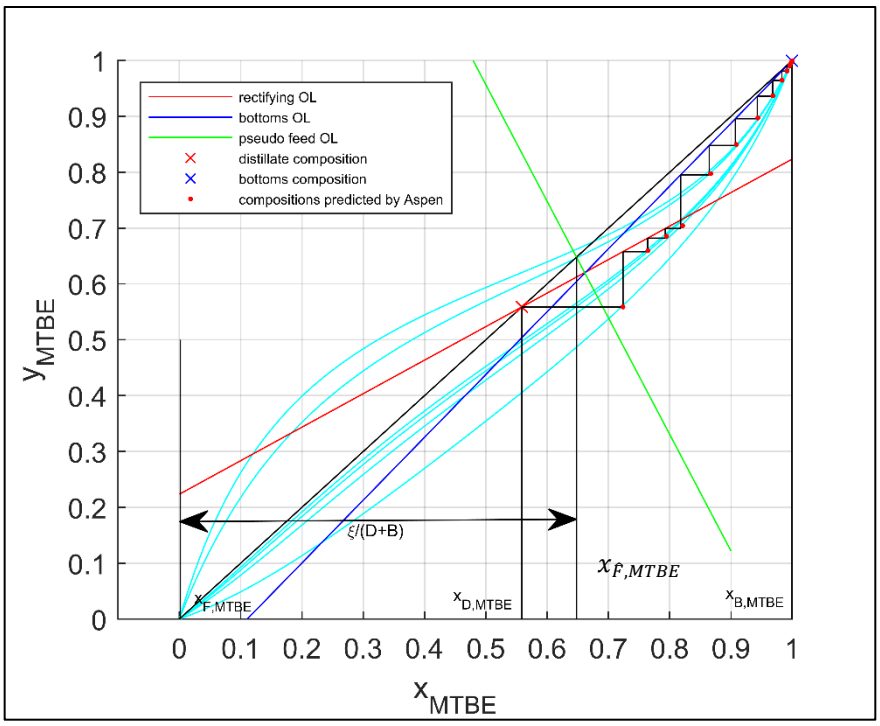

Figure 7.16: McCabe-Thiele diagram for MTBE and the Aspen Plus™ compositions on each stage at finite reflux for reaction on the feed stage

Figures 7.15 and 7.16 depict the DCM and McCabe-Thiele plot for MTBE for the desired separation, respectively, using the proposed graphical method. The McCabe-Thiele plot for isobutene and methanol can be found in Appendix F. The number of stages required is 15, with the feed stage location on stage 5.

Analysis 7.3: Initializing a rigorous simulation in Aspen Plus™

A Radfrac column is used with a single feed and two products. For pure components, vapour pressures were determined using the extended Antoine equation and the Wilson activity coefficient model. The feed is defined as a saturated liquid at 1 bar, with a feed flowrate of 165 kmol/h and feed the compositions (not pseudo-feed) in Table 7.4 are used as inputs. The column is set to have a total condenser, reflux ratio of 1.5, reboil ratio of 8.03 and 16 stages (including condensor). The feed stage is set on stage 5 with reaction only on stage 5, and a corresponding conversion 0.476 (key component is methanol). The reaction is defined as: $isobutene + methanol \rightarrow MTBE$, hence both reactants have a coefficient of -1 and the product, 1. An Aspen Plus™ simulation was initialised with the parameters from the graphical method.

The Aspen Plus™ simulation converged with the design parameters obtained from the graphical method. Hence, the graphical method will save the designer time in trying to produce a converged design from which detailed calculations can be done. The liquid compositions on each stage obtained from the Aspen Plus™ simulation and the proposed graphical method are depicted on the DCM for the system in Figure 7.15. Figure 7.16 shows the compositions on each stage obtained from Aspen Plus™ and the graphical method for MTBE on the McCabe-Thiele diagram. Figures 7.15 and 7.16 show that the graphical method correlates sufficiently with the Aspen Plus™ simulation.

Hence, it can be concluded that the proposed graphical method proves to be a beneficial preliminary design tool that can be used in the conceptual and preliminary design phases of reactive distillation processes for non-ideal systems

with reaction on the feed stage. It can also be concluded, through the correlation with Aspen Plus^{TM}, that the effect of the assumption of CMO in the method is not significant.

7.3 Reaction in the Stripping/Rectifying Section

Lee et al., (2000c; 2000d) extended the McCabe-Thiele method to accommodate reaction in the rectifying or stripping sections of a distillation column. Lee et al., (2000c; 2000d) have limited their analysis to isomerization reactions, but this can be applied to any reaction type. The graphical method in this section will extend the method by Lee et al., (2000c; 2000d) to ternary systems using the contours of VLE. The graphical method for reactive distillation systems will be based on the observations presented by Lee et al., (2000c; 2000d) namely:

1. Flow generated by the reaction is represented by the reaction difference point.
2. Infinite composition spaces are avoided by decomposing the total stoichiometric coefficient vector into coefficient vectors for reactants and products.
3. From the collinearity of the reaction difference point, the feed and product compositions result in a generalized cascade difference point, which moves as stepping off reactive stages. Hence, reactive stages will have unique operating lines depending on the section in which the reaction takes place. Non-reactive stages will have the same operating line as in non-reactive distillation.
4. The linear composition changes caused by the reaction are depicted in the original composition space (Huanan et al., 1999).

The assumptions for the graphical method for a reaction in different reaction zones are stated in Section 7.2 for the feed stage reaction. If CMO does not hold, design problems can be analysed by assuming constant mass overflow (Lee et al., 2000c; 2000d). The latter method can be applied to cases in which the net number of moles

changes with the reaction, or where the heat of reaction cannot be assumed to be negligible. Future work will look at developing the method for non-CMO design problems.

7.3.1 McCabe-Thiele Method for a Multicomponent System for a Reaction in the Rectifying or Stripping Section Only

The general method and equations that govern a multicomponent reactive distillation column, with a reaction on stages in either the rectifying or stripping sections, will be presented. The method and equations are independent of the type of reaction. The method proposed is an extension of the method presented by Lee et al., (2000c) by adapting the idea of reactive cascade difference points to multicomponent systems.

Reaction zone in the rectifying section

Consider Figure 7.17 for reactive zone in the rectifying section stage (Zone I). The overall and component material balances, including reaction terms, can be derived for multicomponent systems.

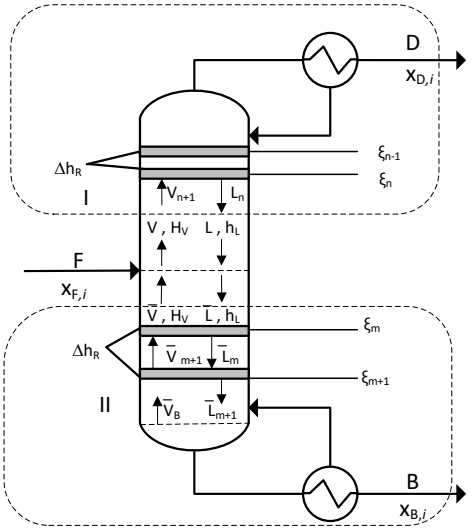

Figure 7.17: A schematic of the internal and external flows for a reactive distillation column with a reaction zone in the rectifying and bottoms sections

The overall and component material balances over the rectifying section are defined in Equations (7.14) and (7.15) and adapted for multicomponent systems.

$$V_{n+1} = L_n + D - v_T \sum_{n=1}^{n} \xi_n \tag{7.14}$$

Where V_{n+1}, D and L_n are the molar flowrates of the vapour entering stage n / leaving stage n+1, distillate and liquid leaving stage n / entering stage n+1. v_T is the sum of the stoichiometric coefficients, and $\sum_{n=1}^{n} \xi_n$ is the sum of the reaction molar turnover flowrate occurring on all stages from the top stage to stage n, the final reactive stage (extent of reaction- kmol/h).

$$V_{n+1,i}\ y_{n+1,i} = L_{n,i}\ x_{n,i} + D x_{D,i} - \boldsymbol{v} \sum_{n=1}^{n} \xi_n \qquad for\ i = 1,2 \ldots j \tag{7.15}$$

Where $\boldsymbol{v}$, the stoichiometric coefficient vector.

For reactions in which $v_T = 0$, the difference point is infinite $\left(\delta_{R,i} = {}^{v_i}/_{v_T} = \infty\right)$. The stoichiometric coefficient vector, $\boldsymbol{v}$, can be separated into the product coefficient vector c_P and the reactant coefficient vector c_R overflow (Lee et al., 2000c; 2000d). The infinite difference point can therefore be overcome by analysing each component material balance over the rectifying section by using v_i the stoichiometric coefficient for component *i* (Equation 7.16). Hence, the operating lines for each component can be plotted on the McCabe-Thiele diagram in finite space.

$$V_{n+1,i}\ y_{n+1,i} = L_{n,i}\ x_{n,i} + D x_{D,i} - v_i \sum_{n=1}^{n} \xi_n \qquad for\ i = 1,2 \ldots j \tag{7.16}$$

Equation 7.16 can be rearranged to derive the rectifying operating line for reactive stages (Equation 7.17). If a stage is non-reactive, Equation 5.8 will be used to plot the rectifying operating line.

$$y_{n+1,i} = \frac{L_{n,i}}{V_{n+1,i}} x_{n,i} + \frac{D}{V_{n+1,i}} x_{D,i} - \frac{v_i \sum_{n=1}^{n} \xi_n}{V_{n+1,i}} \qquad for\ i = 1,2 \ldots j \tag{7.17}$$

For a reaction with no net change in the number of moles, assuming constant liquid and vapour flowrates in the rectifying section and defining the reflux ratio (R) as $R = L_n/D$, the reactive rectifying operating line in terms of reflux ratio is defined in Equation 7.18.

$$y_{n+1,i} = \frac{R}{R+1}x_{n,i} + \frac{1}{R+1}x_{D,i} - \frac{v_i \sum_{n=1}^{n} \xi_n}{D(R+1)} \quad for\ i = 1,2 \ldots j \tag{7.18}$$

The slope of the reactive rectifying operating line (L/V or R/R+1) is independent of the extent of reaction overflow (Lee et al., 2000c; 2000d). For several reactive stages, the rectifying operating lines are parallel lines with the same gradient (Lee et al., 2000c; 2000d). The shift in the parallel operating lines is due to the moving y-intercept which is dependent on the stoichiometric coefficient and reaction extent, which for reaction in the forward direction will increase as one moves down the column (Lee et al., 2000c; 2000d). Hence, for products (positive coefficient), the intercept will move down, and for the reactants (negative coefficient), the intercept will move up with each operating line. The new moving intercepts of the operating line and the 45 degree line are defined as the difference point overflow (Lee et al., 2000c; 2000d) (Figure 7.18-7.19). The difference points can be determined by setting $y_{n+1,i} = x_{n,i}$ in Equation 7.17. Equation 7.19 shows that the intersection with the 45 degree line moves from $x_{D,i}$ by a ratio of the stoichiometric extent to the distillate flowrate, for the specific reactive stage (Lee et al., 2000c; 2000d). For products, the reactive difference points move to the left, and for reactants to the right of the distillate composition.

$$x_{n,i} = \delta^{r}{}_{R,i,n} = x_{D,i} - {}^{v_i \xi_n}/_{D} \qquad for\ i = 1,2 \ldots j \tag{7.19}$$

For cases in which the reactive zone is solely in the rectifying section, the feed line and the bottoms operating line will be the same as the non-reactive Equations 6.13 and 6.12 respectively. It is also possible to consider reaction in the rectifying section as well as the feed stage and this will be illustrated in Section 7.3.3.

Reaction zone in the stripping section

Consider Figure 7.17 for reactive zone in the stripping section stage (Zone II). The overall and component material balances, including reaction terms, can be derived for multicomponent systems.

The overall and component material balances over the bottoms section are defined in Equations (7.20) and (7.21) and adapted for multicomponent systems.

$$\bar{V}_{m+1} = \bar{L}_m - B + v_T \sum_{m=0}^{m+1} \xi_{m+1} \tag{7.20}$$

Where $\bar{V}_{m+1}$, B and $\bar{L}_m$ are the molar flowrates of the vapour entering stage m / leaving stage m+1, bottoms and liquid leaving stage m / entering stage m+1. v_T is the sum of the stoichiometric coefficients and $\sum_{m=1}^{m+1} \xi_{m+1}$ is the sum of the reaction molar turnover flowrate occurring on all stages, from the top stage in the bottoms section to stage m+1, the final reactive stage in the section (extent of reaction-kmol/h).

$$\bar{V}_{m+1,i}\ y_{m+1,i} = \bar{L}_{m,i}\ x_{m,i} - B x_{B,i} + \boldsymbol{v} \sum_{m=0}^{m+1} \xi_{m+1} \qquad for\ i = 1,2 \ldots j \tag{7.21}$$

As with reaction in the rectifying section, the stoichiometric coefficient vector, $\boldsymbol{v}$, can be separated into the product coefficient vector c_P and the reactant coefficient vector c_R overflow (Lee et al., 2000c; 2000d). Hence, the infinite difference point can therefore be overcome by analysing each component material balance over the stripping section, using v_i the stoichiometric coefficient for component *i.* The reactive operating line for the stripping section for each component is derived in Equation 7.22.

$$y_{m+1,i} = \frac{\bar{L}_m}{\bar{V}_{m+1,i}}\ x_{m,i} - \frac{B}{\bar{V}_{m+1,i}} x_{B,i} + \frac{v_i \sum_{m=0}^{m+1} \xi_{m+1}}{\bar{V}_{m+1,i}} \qquad for\ i = 1,2 \ldots j \tag{7.22}$$

Defining the reboil ratio (S) as $S = \frac{V_{m+1}}{B}$, assuming constant liquid and vapour flowrates in the stripping section, and specific vapour reaction extent $\hat{\xi}_{m+1} = \frac{\xi_{m+1}}{\bar{V}_{m+1}}$

then the reactive stripping operating line in terms of reboil ratio is defined in Equation 7.23.

$$y_{m+1,i} = \frac{S+1}{S}\ x_{m,i} - \frac{1}{S}x_{B,i} + \frac{v_i \sum_{m=0}^{m+1} \xi_{m+1}}{BS} \qquad for\ i = 1,2 \ldots j \tag{7.23}$$

The slope of the stripping operating line ($\bar{L}/\bar{V}$ or S+1/S) is independent of the extent of reaction overflow (Lee et al., 2000c; 2000d). For several reactive stages, the stripping operating lines are parallel lines with the same gradient, but move up as reaction proceeds up the column (Lee et al., 2000c; 2000d). Similar to reaction in the rectifying section only, for products (positive coefficient) the intercept will move down and for reactant (negative coefficient) the intercept will move up with each operating line. The new moving intercepts of the operating line and the 45 degree line is defined as the difference points overflow (Lee et al., 2000c; 2000d) (Figure 7.55-7.57). The difference points can be determined by setting $y_{m+1,i} = x_{m,i}$ in Equation 7.22. Equation 7.24 shows that the intersection with the 45 degree line moves from $x_{B,i}$ by a ratio of the stoichiometric extent to the bottoms flowrate for the specific reactive stage (Lee et al., 2000c; 2000d).

$$x_{m,i} = \delta^{s}{}_{R,i,n} = x_{B,i} - {}^{v_i \xi_{m+1}}/_{B} \qquad for\ i = 1,2 \ldots j \tag{7.24}$$

For cases in which the reactive zone is solely in the stripping section, the feed line and rectifying operating line will be the same as the non-reactive Equations 6.13 and 6.8 respectively.

The ideal reaction $2A \rightarrow B + C$ presented in Section 7.2.2 for an ideal system undergoing reaction on the feed stage will be applied to three cases namely: reaction in rectifying section only, reaction in the rectifying and feed stage and reaction in the stripping section only. The analysis will be limited to ideal systems and where $v_T = 0$. Further work would look at extending the method to non-ideal systems and systems in which $v_T \neq 0$.

7.3.2 Case A: Reaction in the Rectifying Section Only

An ideal mixture of Components A, B and C following the reaction $2A \rightarrow B + C$ presented in Section 7.2.2 will be fed to a simple reactive distillation column such that the relative volatilities, saturated feed (q=1) bottoms and distillate product are presented in Table 7.5. In this example no reaction will take place on the feed stage and in the stripping section. Reaction will occur on a single rectifying stage. Hence one extent of reaction (ξ_n) will be defined to be 5 kmol/h. An analysis of the minimum reflux followed by the finite reflux design method will be explained for the ideal system.

Table 7.5: Relative volatility, feed, bottoms, distillate and adjusted distillate compositions for reaction in the rectifying section only.

Component	**Relative volatility (α)**	x_F	x_B	x_D	x_{D1}
A	1.900	0.4640	0.4500	0.0200	0.5200
B	3.250	0.1500	0.0050	0.9800	0.7300
C	1.000	0.3860	0.5495	5×10^{-11}	-0.2500

For reaction in the rectifying section only, the stripping operating line (Equation 6.12) and feed line (Equation 6.13) remain the same as for non-reactive distillation design. In addition to the non-reactive rectifying operating line (Equation 6.8), the reactive rectifying operating line defined in Equation 7.18 is plotted. In this example, a single reactive stage with an associated reaction extent is defined. Hence there in one reactive rectifying operating line. In conclusion, *n* reaction stages in the rectifying column section will result in *n* reactive rectifying operating lines.
Figures 7.18-7.20 for component B (LK), component A (IK) and component C (HK) respectively, plot the stripping, feed, non-reactive rectifying and reactive rectifying operating lines on x-y diagrams. The adjusted distillate composition (also known as the difference point overflow) of the reactive rectifying operating line is

found using the reaction difference point (Equation 7.19). The adjusted distillate composition is visually depicted at the point which the new reactive rectifying operating line passes through the 45 degree line. The adjusted distillate composition can be identified on Figures 7.18-7.20 and the adjusted distillate composition can be found in Table 7.5.

The reactive rectifying operating lines lie below the non-reactive rectifying operating lines for products. Hence, the adjusted distillate composition shifts down, below the distillate composition (Figure 7.18 and 7.20). For reactants, the reactive rectifying operating lines, lie above the non-reactive rectifying operating lines hence the adjusted distillate composition shifts up, above the distillate composition (Figure 7.19).

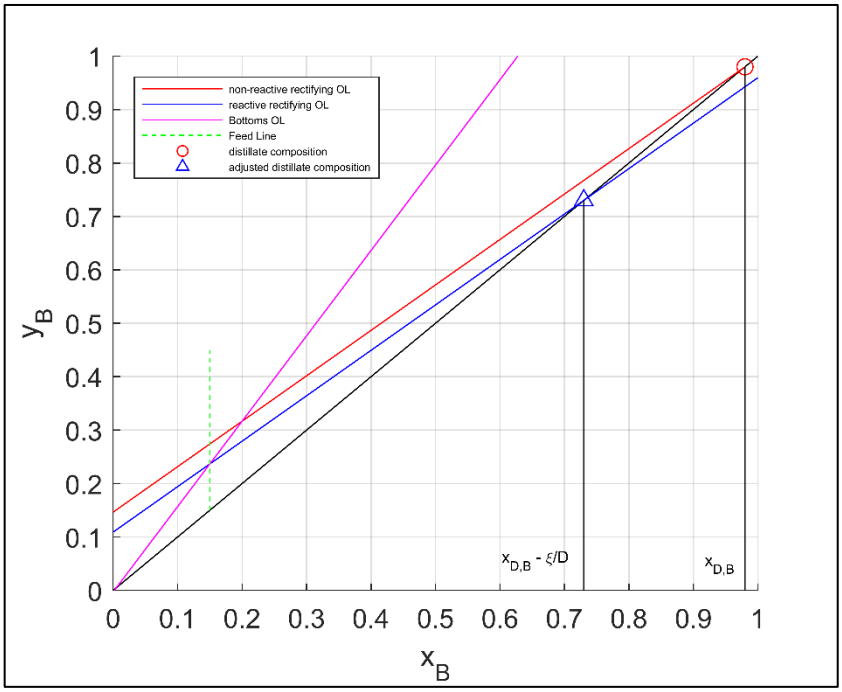

Figure 7.18: McCabe-Thiele diagram for Component B (LK) depicting the reactive rectifying, non-reactive rectifying, bottoms and feed operating lines at finite reflux.

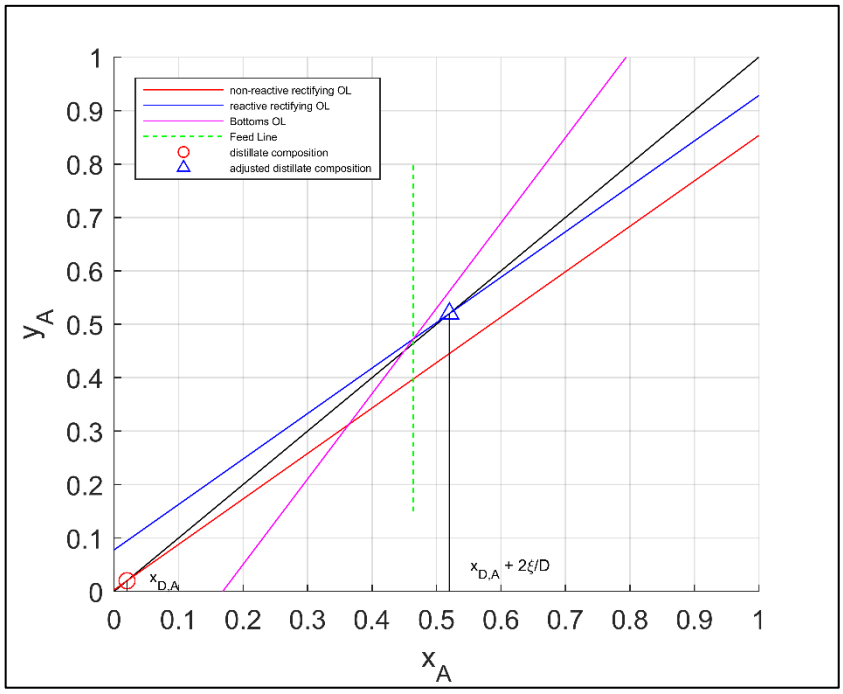

Figure 7.19: McCabe-Thiele diagram for Component A (IK) depicting the reactive rectifying, non-reactive rectifying, bottoms and feed operating lines at finite reflux.

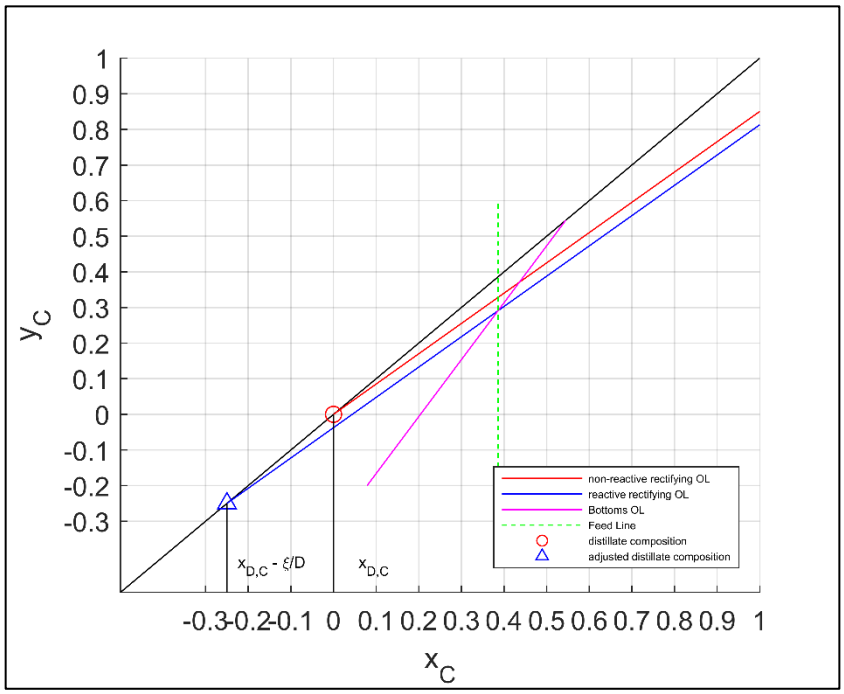

Figure 7.20: McCabe-Thiele diagram for Component C (HK) depicting the reactive rectifying, non-reactive rectifying, bottoms and feed operating lines at finite reflux.

Due to reaction, the bottoms composition, feed composition and the adjusted distillate composition (not the distillate composition) must satisfy a mass balance. Hence, in Figures 7.18-7.20 the bottoms operating line and the reactive rectifying operating line intersect at the feed line.

7.3.2.1 Minimum Reflux

The method for determining minimum reflux for the reaction in a section of a column is not as simple as for the reaction on feed stage. The method is trial-and-error in nature, and requires the assistance of DCMs to determine minimum reflux. The trial-and-error method requires the designer to select a reflux and reboil ratio, using the ternary McCabe-Thiele method the rectifying and stripping profiles are plotted on a DCM. If the profiles do not intersect then the reflux is adjusted until the profiles just meet at the minimum reflux. Since the separation is a sharp direct split, the saddle in the rectifying profile controls the separation. Hence, stepping off stages begins at the distillation composition using the non-reactive rectifying operating line indicated on Figures 7.21-7.23, which are the McCabe-Thiele plots at minimum reflux for the separation.

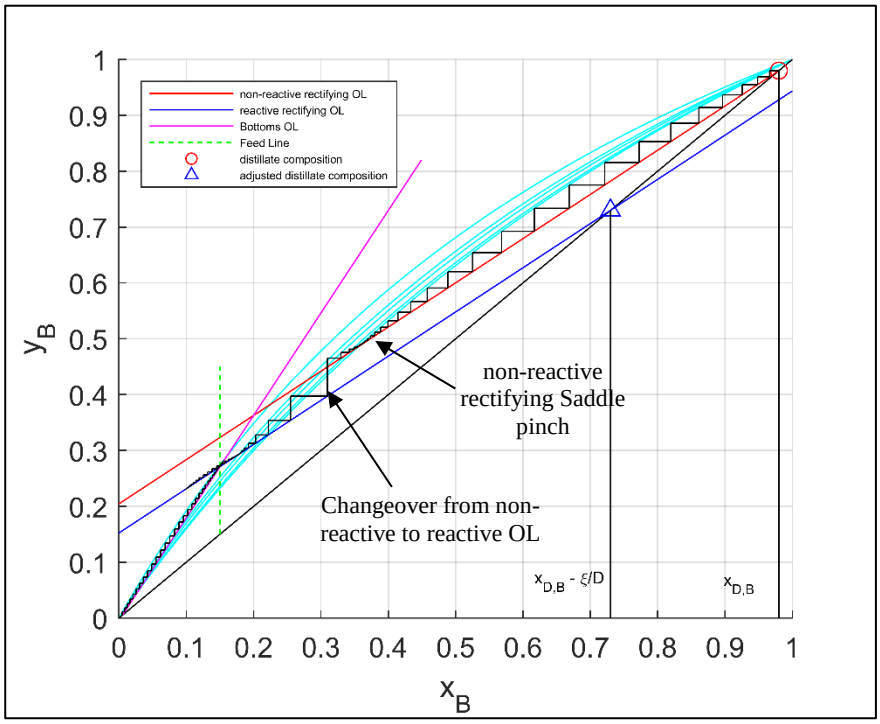

Figure 7.21: McCabe-Thiele diagram for Component B at minimum reflux for reaction in the rectifying section only.

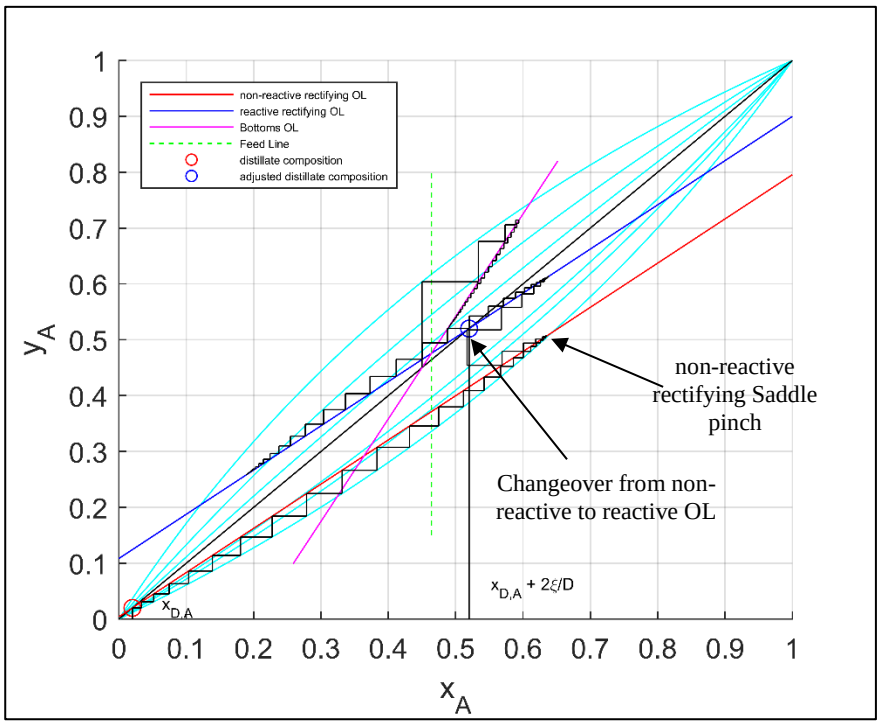

Figure 7.22: McCabe-Thiele diagram for Component A at minimum reflux for reaction in the rectifying section only.

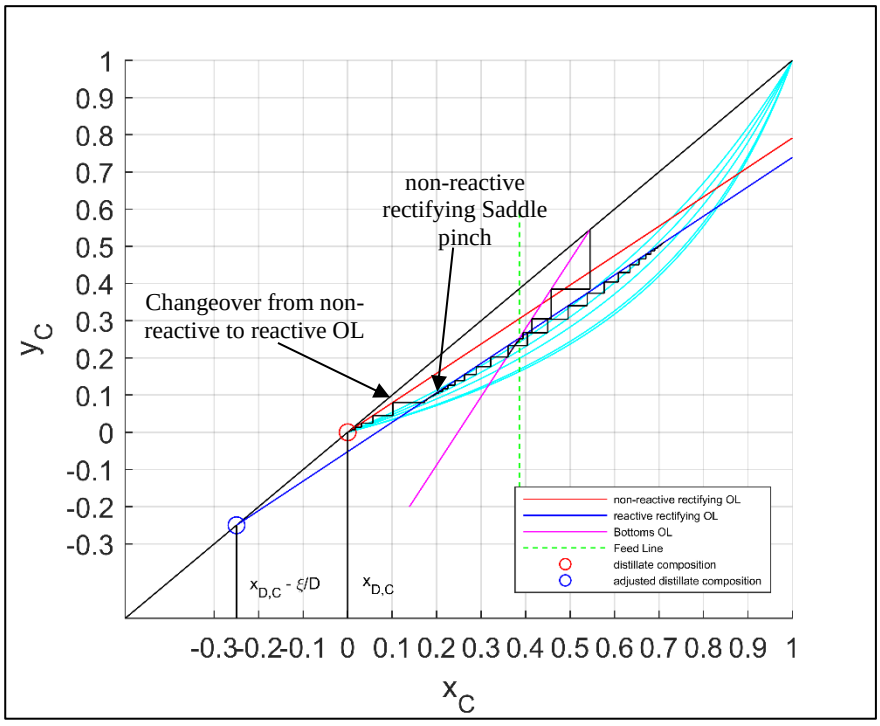

Figure 7.23: McCabe-Thiele diagram for Component C at minimum reflux for reaction in the rectifying section only.

The stepping off stages proceeds using the non-reactive rectifying operating line until the profile exits the saddle pinch (Figure 7.24 for changeover on stage 30). The changeover from the non-reactive to the reactive operating lines occurs after exiting the saddle (Figures 7.21-7.23). The reactive rectifying operating lines are used to step off stages in order to generate the reactive rectifying profile (Figures 7.21-7.24).

The method for determining the number of stages from the distillate composition presented in Chapter 6 was used to find the non-reactive and reactive rectifying profiles. The bottoms profile was determined using the method for stepping off stages from the bottoms composition in Chapter 6. The reflux ratio is increased (by trial-and-error) whilst also ensuring the changeover from reactive to non-reactive is after the non-reactive profile exits the saddle pinch. For reaction in the rectifying section, minimum reflux is indicated when the stripping profile pinches on the profile of the last reactive rectifying profile and not the non-reactive rectifying profile. The minimum reflux ratio is found to be 3.79 and changeover from rectifying to non-rectifying operating line at stage 30. Figure 7.24 shows that the stripping and reactive rectifying profiles just intersect at a reflux of 3.79 and changeover on stage 30. Figure 7.24 shows the bottoms, reactive and non-reactive profiles at the minimum reflux of 3.79 and changeover at stages 29, 30 and 31 on a DCM. It can be seen that changeover on stage 29, or below, results in the rectifying profiles turning away and hence are not feasible designs. Hence, changeover from the non-reactive to the reactive operating line before exiting the saddle pinch will yield designs that’s are not feasible. Changeover at stage 31 and above does not result in the stripping profile terminating on either the non-reactive or reactive rectifying profile. It can be concluded that, in addition to determining the minimum reflux, the stage at which the changeover from the non-reactive to reactive operating line affects the minimum reflux calculations.

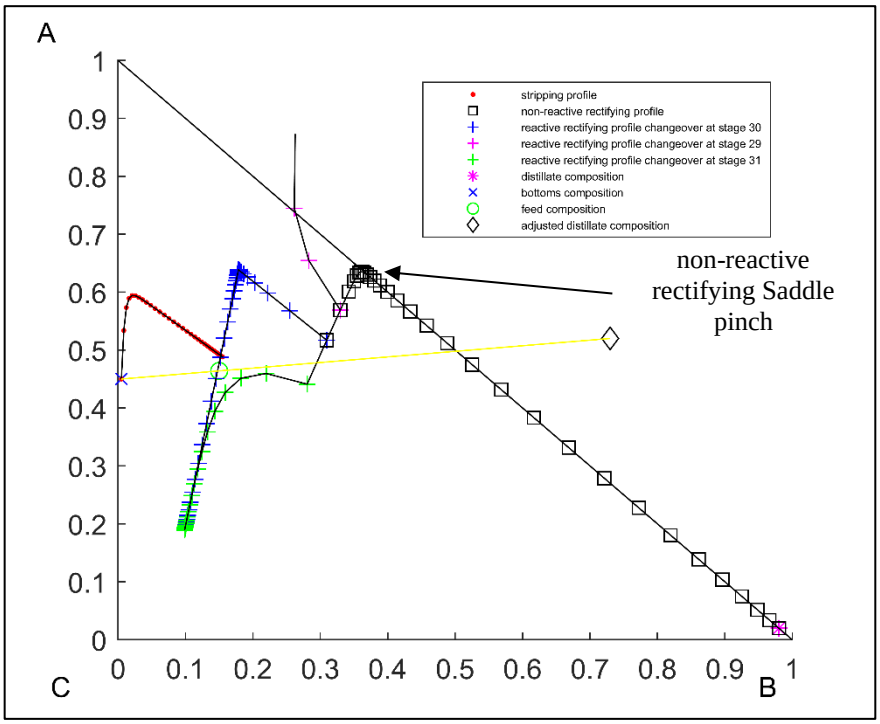

Figure 7.24: Distillation curve map (DCM) plotting the stripping, non-reactive and reactive rectifying profiles at minimum reflux for changeover from non-reactive to reactive operating lines at stage 29, 30 and 31

The desired product specification and feed composition results in a unique separation at the minimum reflux ratio of 3.79 and changeover stage of 30. The reactive profile exhibits a saddle pinch that aligns with the feed transition point (0.209, 0.7908) for the feed, depicted by the red triangle on Figure 7.25. The feed transition point for a sharp split was determined using the method in Chapter 5, Section 5.2.1. The occurrence of a saddle pinch in the reactive profile requires the minimum reflux to correlate with the changeover of stages on a whole stage hence the occurrence of the saddle pinch in the reactive profile. Two analyses will be demonstrated by changing the distillate composition and extent to show that the saddle in the reactive profile is a unique case study.

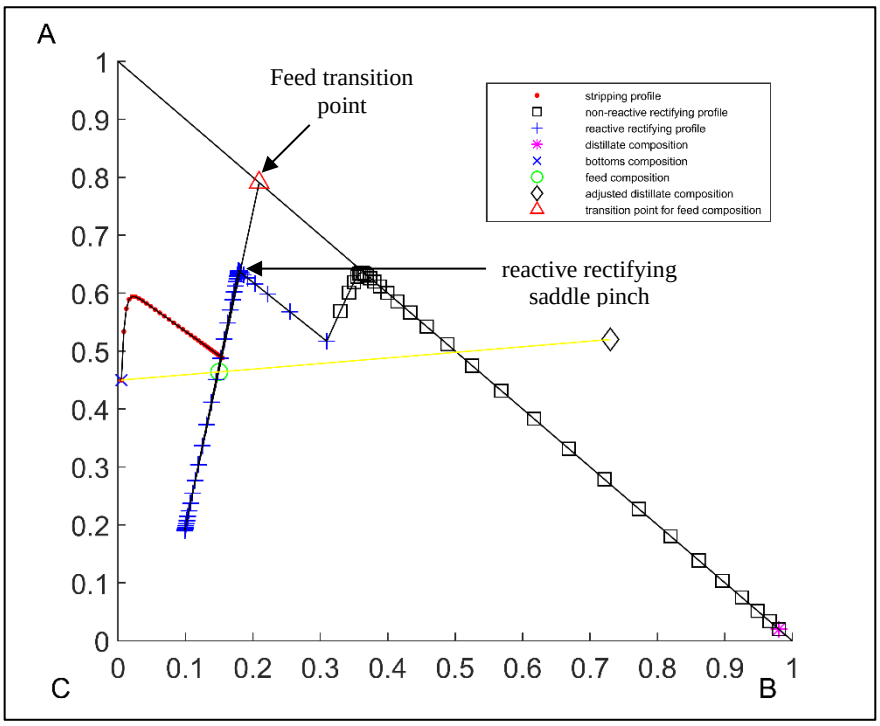

Figure 7.25: Distillation curve map (DCM) plotting the stripping, non-reactive and reactive rectifying profiles at minimum reflux

It should be noted that, for the system, the minimum reflux ratio required to obtain the same product specifications is lower for reaction on feed stage (2.45) than reaction in the rectifying section (3.79). Hence, it can be concluded that to obtain the same extent and product specification, reaction on the feed stage would be a more favourable design.

Analysis 7.3: Change in extent

An analysis of the minimum reflux ratio and changeover stage for three extents of 4, 5 and 6 kmol/h were analysed for the stipulated product specifications in Table 7.5. With a change in extent, the adjusted distillate composition (Equation 7.19) and, hence the feed composition (by material balance) changes as depicted in Figure 7.26 in order to obtain the required product compositions. The minimum reflux ratio

required decreases with increasing reaction extent, whilst the stage for changeover increases.

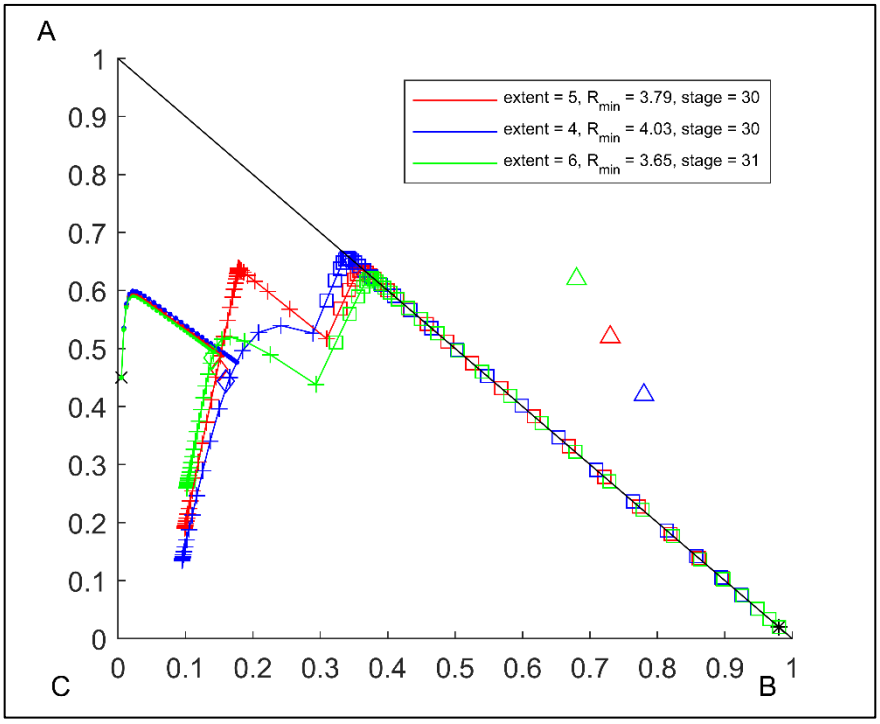

Figure 7.26: Distillation curve map (DCM) plotting the stripping, non-reactive and reactive rectifying profiles at minimum reflux at extents of 4, 5 and 6 kmol/h

Analysis 7.4: Change in distillate composition

The effect of different distillate compositions for a sharp direct split is analysed whilst fixing the feed composition specified in Table 7.5. Since the distillate composition is changing, the adjusted distillate composition shifts. The feed is fixed, hence by a mass balance, the bottoms compositions are recalculated to satisfy the mass balance with the feed and adjusted distillate compositions. Figure 7.27 shows that, for a fixed feed composition, regardless of changing the distillate products, the stripping profiles terminate on the linear plane of the feed transition point and the feed. By reducing the proportion of the light key in the distillate, lower minimum reflux ratios are required. Thus, the number of stages required to exit the saddle increases and the stage at changeover of the operating lines will be higher.

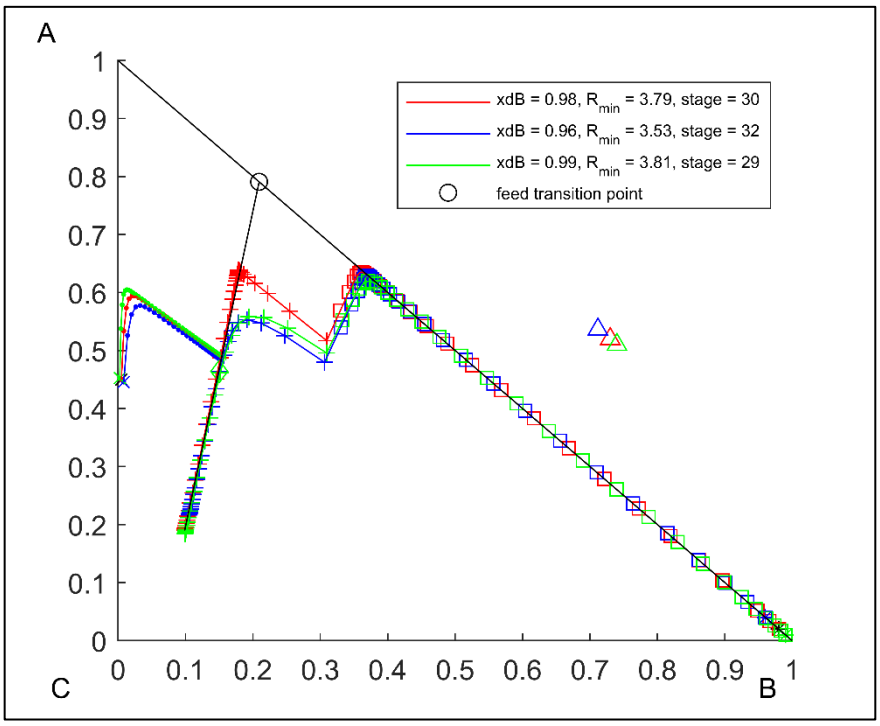

Figure 7.27: Distillation curve map (DCM) plotting the stripping, non-reactive and reactive rectifying profiles at minimum reflux for different distillate compositions

From analysis 7.3 and 7.4 it can be seen that none of the design simulations resulted in a saddle pinch in the rectifying profile, hence the original design specification results in a unique case. The method explained in this section can be applied to indirect splits with reaction in the stripping section. Although only depicted for ideal systems, the method can be applied to non-ideal systems incorporating different thermodynamic models. This Chapter lays the foundations of the graphical method. Future work will extend the method to non-ideal systems.

7.3.2.2 Finite Reflux Design

The desired product specifications, feed composition and adjusted distillate compositions remain the same as in Table 7.5. The minimum reflux ratio obtained in Section 7.3.2.1 of 3.79 was multiplied by 1.5 to calculate the operating finite reflux of 5.69. Hence using Equation 6.14, the corresponding reboil ratio is 1.67 – using the adjusted distillate composition, and not the distillate composition. The

extent of reaction is 5 kmol/h. The method presented in Figure 7.28 is used to determine the number of theoretical stages, the feed stage location and the reactive stage location at finite reflux, for reaction in the rectifying section only.

Chapter 4 and Chapter 6 showed the manual calculations for total and finite reflux non-reactive column design. Using a similar approach, this can be done for finite reflux reactive column design following the algorithm presented below.

The algorithm below is followed to determine the number of theoretical stages for a direct split.

1. To construct the McCabe-Thiele diagram, the 45 degree line, feed line, non-reactive rectifying operating line, reactive rectifying operating line/s and stripping operating line is plotted using Equation 6.13, 6.8, 7.18 and 6.12 respectively, on x-y diagrams for the light key (Component B) and heavy key (Component C). It is only necessary to plot two components as the third component's composition can be calculated from a material balance.
2. Calculate the first ratio for Component B (LK) (Equation 6.1a) using the given liquid bottoms product composition. $CR_{1,(comp\ A/comp\ C)} = x_{comp\ A} / x_{comp\ C} = 0.450/0.545 = 0.826$.
3. Calculate the first ratio for Component C (HK) using the given liquid bottoms product composition. $CR_{1,(comp\ B/comp\ A)} = x_{comp\ B} / x_{comp\ A} = 0.005/0.450 = 0.011$
4. Using the ratios calculated in steps 2-3, determine the VLE contour that represents the ratio using the method presented in Section 6.2.1 or Chapter 3.
5. Move vertically from the bottoms product composition on the 45 degree line towards the VLE contour determined in step 4, to determine the equilibrium composition of the vapour (y_{eqm}) at x_B.
6. Move horizontally from the VLE contour towards the bottoms operating line. Determine the new liquid composition for the light and heavy key. The

compositions of the intermediate key can be calculated from material balance.

7. Calculate the second ratio (steps 2-3) for the light and heavy key using the new compositions obtained in step 6. Repeat steps 4-6 until the feed line of the light key is reached.
8. Once at the feed line for component B (light key), swop over towards the reactive rectifying operating line from the contour of VLE is reached. Determine the new liquid composition from $x_i = y_{eqm}$.
10. Repeat steps 7- 8 until the changeover to the non-reactive rectifying operating line at the reactive stage from the contour of VLE. Determine the new liquid composition from $x_i = y_{eqm}$.
11. Repeat steps 7 and 10 until the required distillate product is obtained.

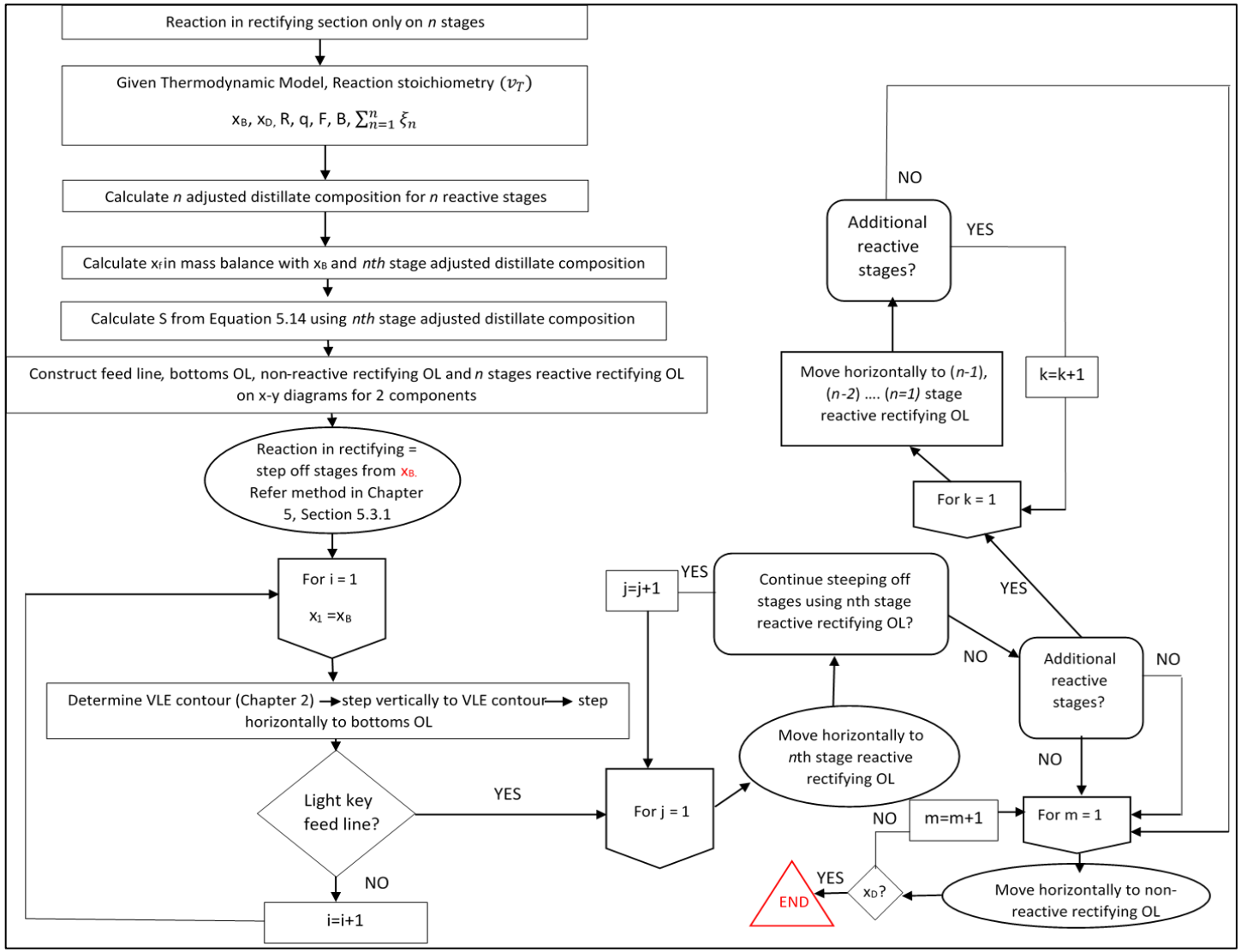

Figure 7.28: Method to determine the number of theoretical stages and feed stage location at finite reflux for 3 component systems for reaction in the rectifying section only.

Following the algorithm and method in Figure 7.28, Figures 7.29-7.31 plot the McCabe-Thiele diagrams of the LK, IK and HK respectively while Figure 7.32 plots the DCM for the separation at finite reflux. From Figures 7.29-7.32, the number of theoretical stages required is 24. The feed stage is stage 12 and the reactive stage is 5 (from the top of the column) when changeover from the bottoms operating line to reactive rectifying operating line is at the feed of the light key as shown in Figure 7.29. The effect of feed and reactive stage location on the number of theoretical stages should be analysed to understand the behaviour of systems with reaction in a specific column section.

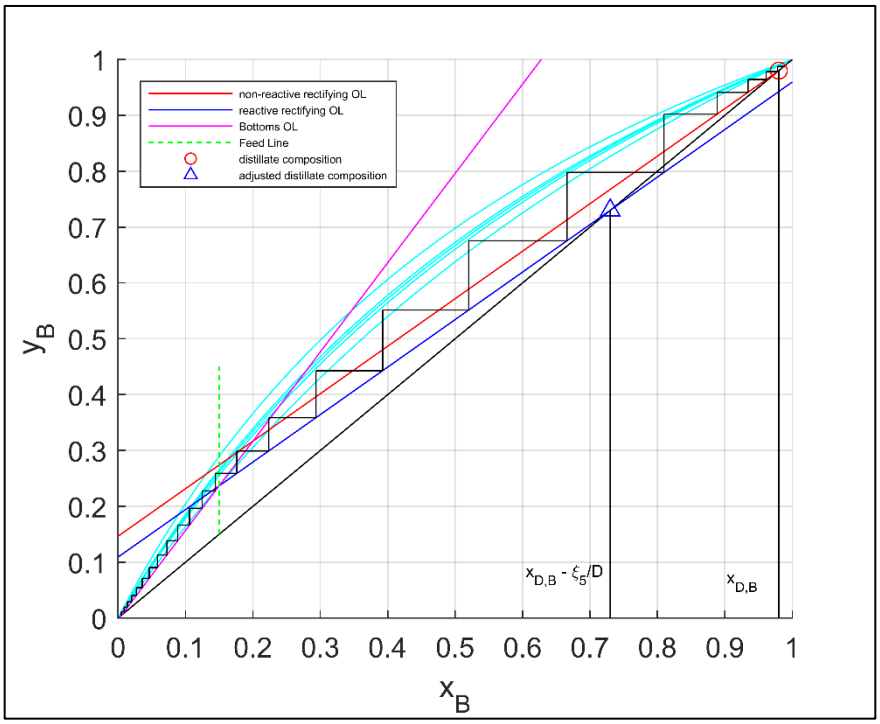

Figure 7.29: McCabe-Thiele diagram for Component B at finite reflux for reaction on stage 5 in the rectifying section and feed stage = 12

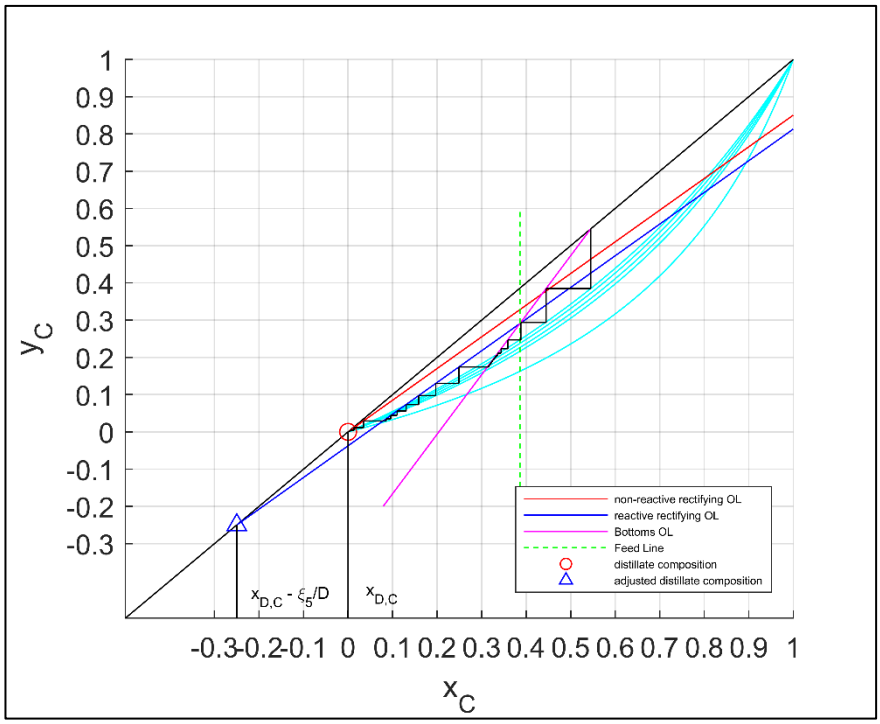

Figure 7.30: McCabe-Thiele diagram for Component A at finite reflux for reaction on stage 5 in the rectifying section and feed stage = 12

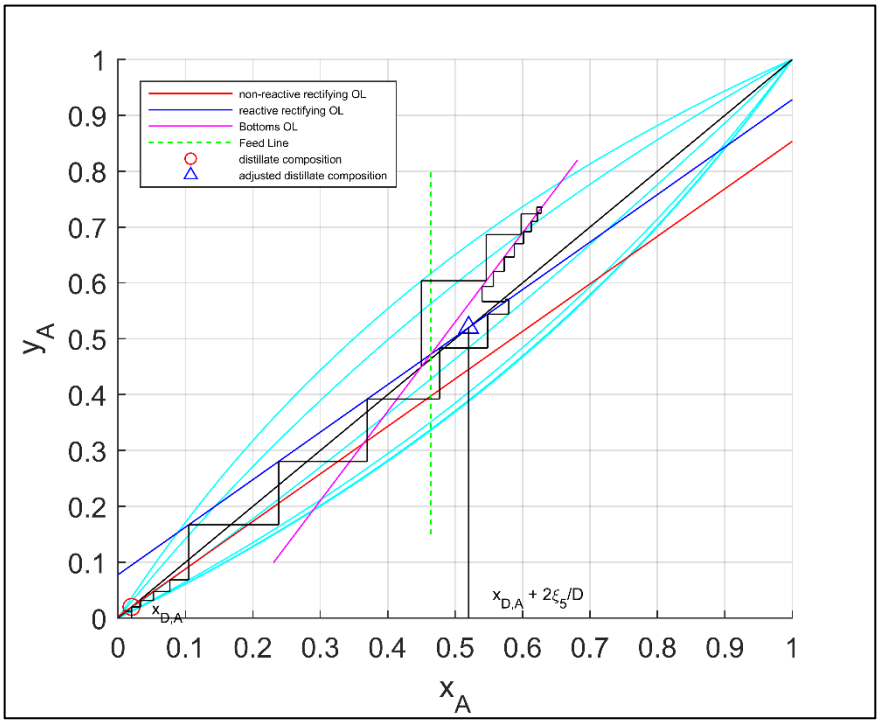

Figure 7.31: McCabe-Thiele diagram for Component C at finite reflux for reaction on stage 5 in the rectifying section and feed stage = 12

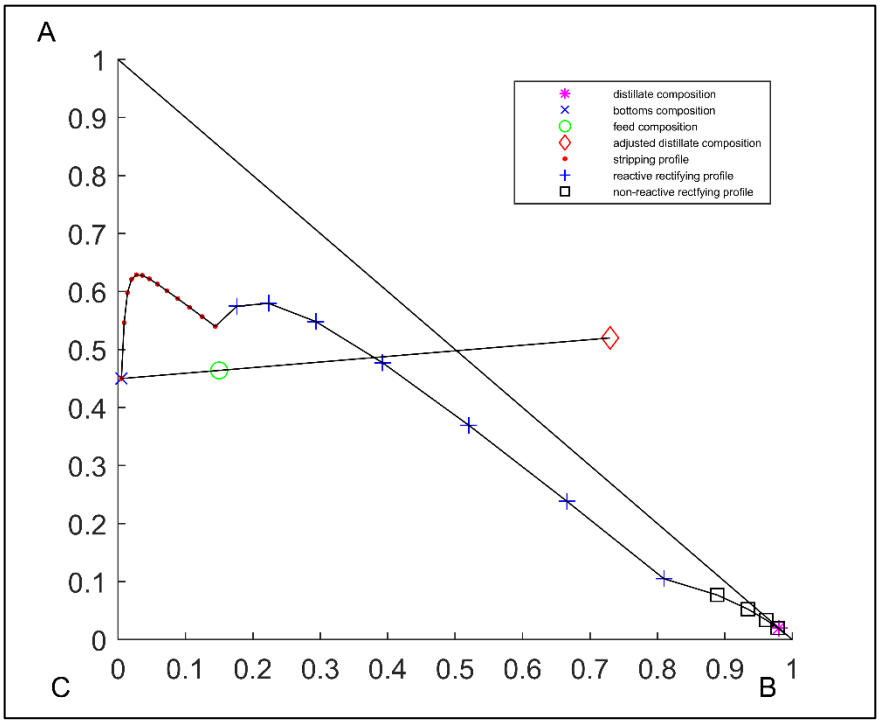

Figure 7.32: Distillation curve map (DCM) plotting the stripping, non-reactive and reactive rectifying profiles at finite reflux for reaction on stage 5 in the rectifying section and feed stage = 12

Analysis 7.4: Effect of feed position

The effect of choosing a feed position of 10, 13 and 14 (from the bottom of the column) was analysed to determine the effect of changing the feed stage position. The operating reflux ratio is 5.69 for all simulations. Figure 7.33 and 7.38 depict the McCabe-Thiele diagram for the light key and DCM for feed stage location on stage 13. Figures 7.33 and 7.38 show that by changing the feed position to stage 13, the number of theoretical stages required is 24 – the same for feed stage location on stage 12. The changeover from the reactive operating line to the non-reactive operating line is at the same position as in the original problem, on the eighth stage after the feed stage. It can be seen that changeover, one stage above the feed, does not have an immediate effect on the number of stages required and the reactive stage location.

Consider moving the feed stage two stages above the previous feed location, stage 14, and the reactive stage kept as in the original problem. It can be seen from Figures 7.34 and 7.36, the McCabe-Thiele diagram for the LK and DCM respectively for feed stage 14, the product specification cannot be met. In order for the product specification to be met, the changeover from the reactive rectifying to the non-reactive rectifying operating line has to be positioned correctly. The changeover has to be positioned such that the separation sufficiently follow the non-reactive rectifying profile in order to achieve the product specifications. By changing the reactive feed stage location to one stage lower (stage 7 after the feed location), the product specification can be met (Figure 7.35-7.36). The number of stages required is also 24. (The McCabe-Thiele plots for Components A and C can be found in Appendix F.) The theoretical number of stages required is not impacted by the location of the feed stage, above the feed line of the light key. However, the feed stage location higher up the column will require the adjustment of the reactive stage location lower down the column.

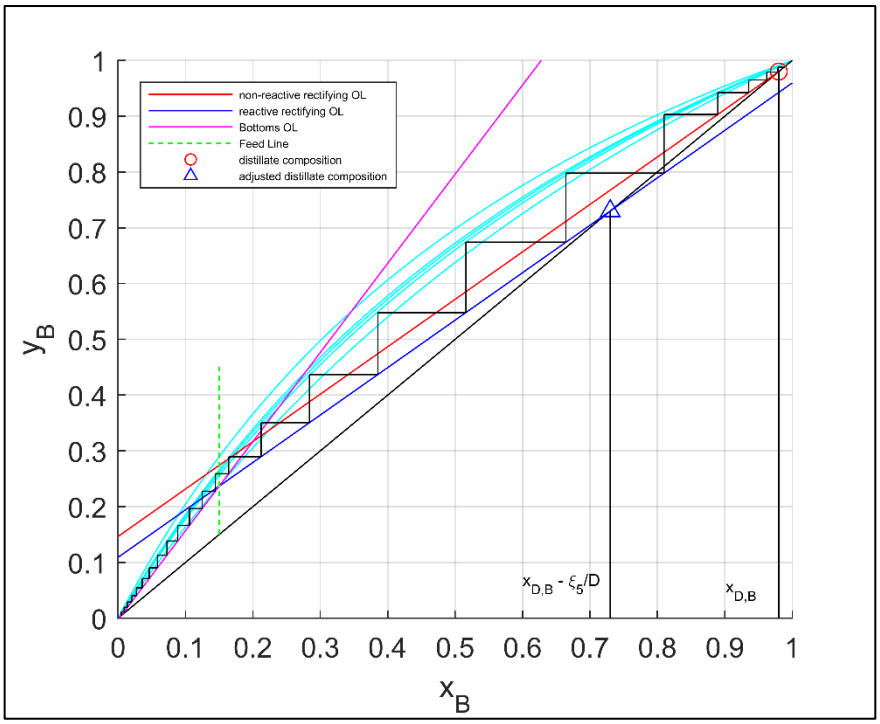

Figure 7.33: McCabe-Thiele diagram for Component B at finite reflux for reaction on stage 5 in the rectifying section and feed stage = 13

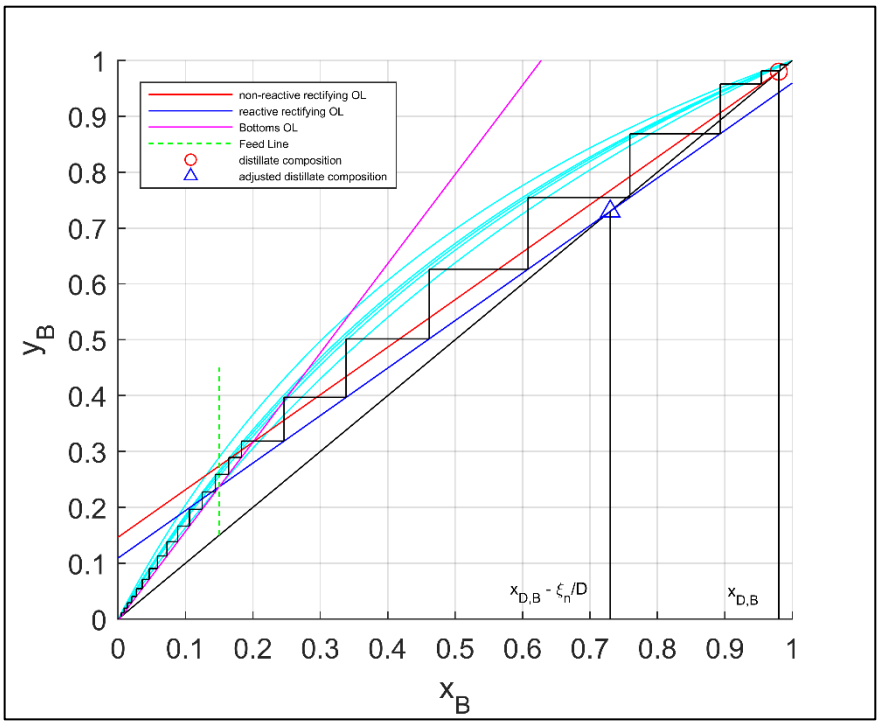

Figure 7.34: McCabe-Thiele diagram for Component B at finite reflux for reaction on stage 8 after the feed location at stage 14 in the rectifying section

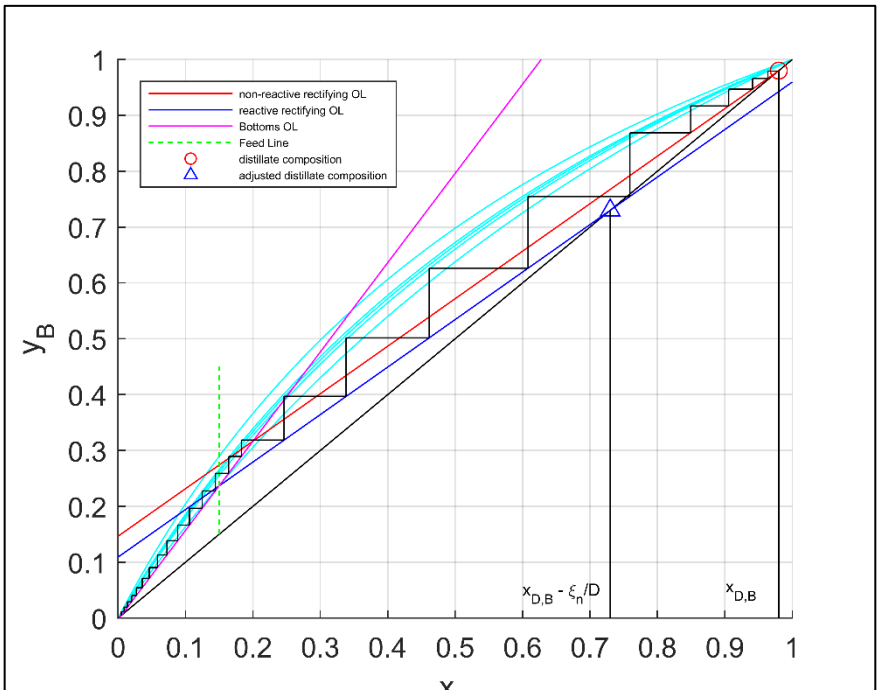

Figure 7.35: McCabe-Thiele diagram for Component B at finite reflux for reaction on stage 7 after the feed location at stage 14 in the rectifying section.

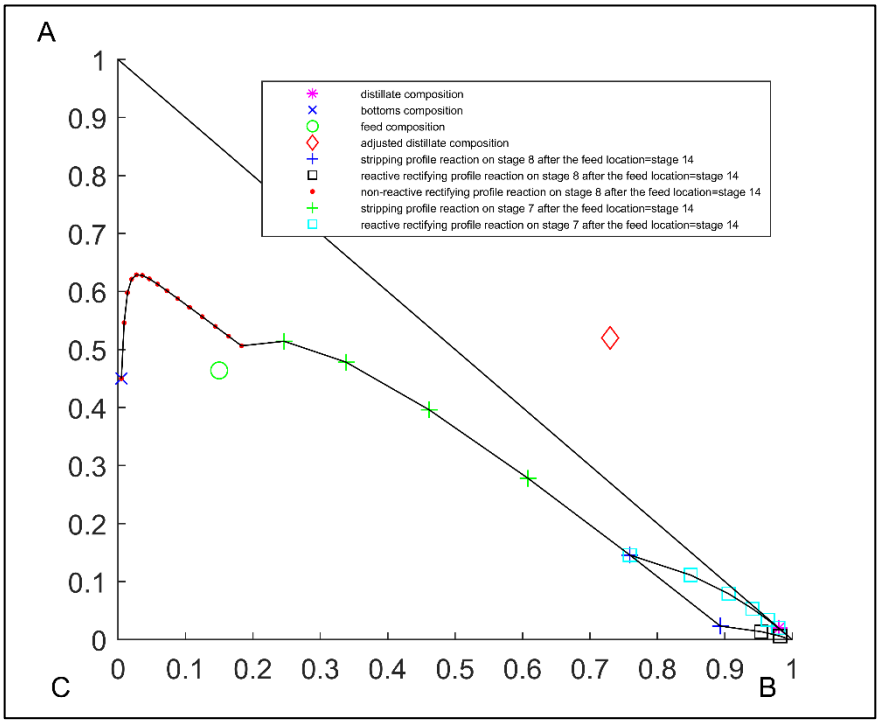

Figure 7.36: Distillation curve map (DCM) plotting the stripping, non-reactive and reactive rectifying profiles at finite reflux for reaction on stage 7 and 8 after the feed location (stage

Figures 7.37-7.38 depict the feed stage location at stage 10 below the feed line of the light key on the McCabe-Thiele diagram and DCM respectively. It can be noticed that the profile turns away from the distillate composition on the McCabe-Thiele plot and DCM hence rendering the design as not feasible. The McCabe-Thiele plots for Components A and C can be found in Appendix F. As a rule of thumb, for reaction in the rectifying section only (same applies for non-reactive direct splits), the feed stage location should be at the feed line of the light key component.

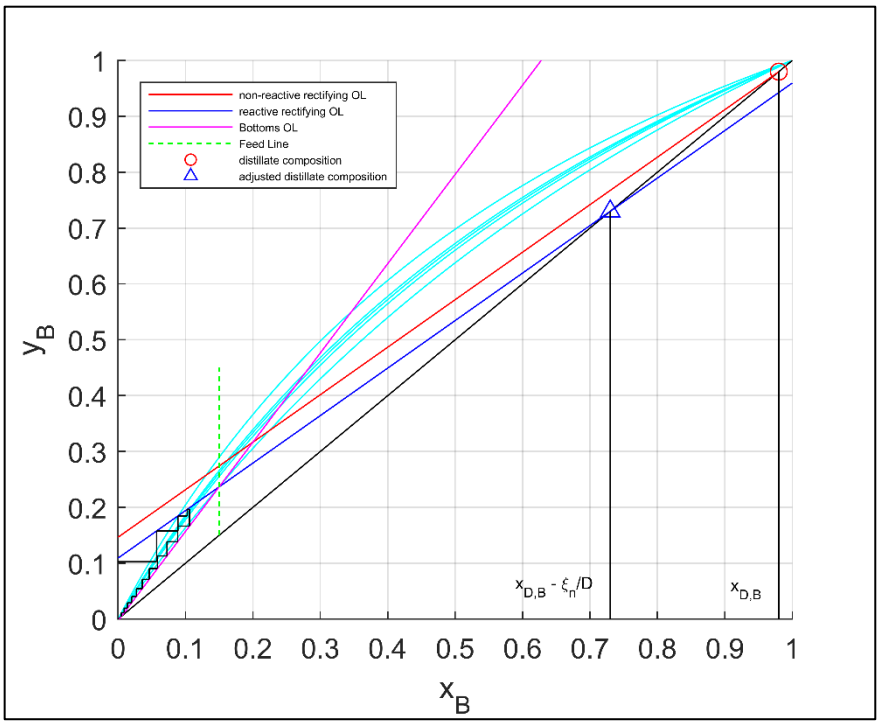

Figure 7.37: McCabe-Thiele diagram for Component B at finite reflux for reaction in the rectifying section and feed stage = 10

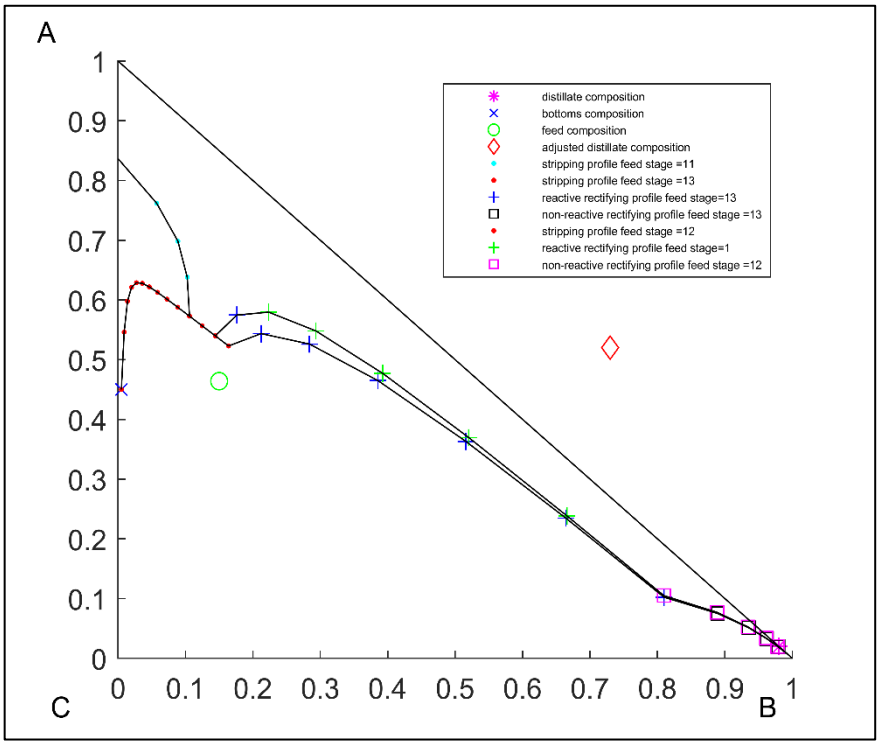

Figure 7.38: Distillation curve map (DCM) plotting the stripping, non-reactive and reactive rectifying profiles at finite reflux for reaction on stage 5 in the rectifying section and feed stage below (stage 10) at (stage 12) and above (stage 13) the feed line of Component B

Analysis 7.5: Effect of reactive stage position

To maintain a consistent comparison, the reflux ratio will be set at 5.69 and the feed stage location will be fixed at the feed line of the light key (stage 12 – from the top of the column) whilst studying the effect of changing the reactive stage. Figures 7.39 - 7.41 depict the McCabe-Thiele diagram for the light key, intermediate key and DCM respectively, for reaction on the first stage (The heavy key can be found in Appendix F). An interesting finding shown in Figures 7.39 and 7.41 is that the design is not feasible with reaction on stage 1, due to the distillate product specification not being met. This is attributed to the rectifying profile following the reactive rectifying line only, and changeover to the non-reactive rectifying line is at the last point. Hence, the rectifying profile moves towards the adjusted distillate composition and does not achieve the required distillate product composition. Figure 7.40 shows that the intermediate key component composition becomes negative in order to obtain the desired light key composition of 0.98. Depending on the system to be designed, reaction on certain stages will not produce feasible design parameters. The positioning of the reactive stage has to be such that the non-reactive rectifying profile is followed sufficiently to obtain the product specifications. McCabe-Thiele diagrams will visually depict designs that are not feasible.

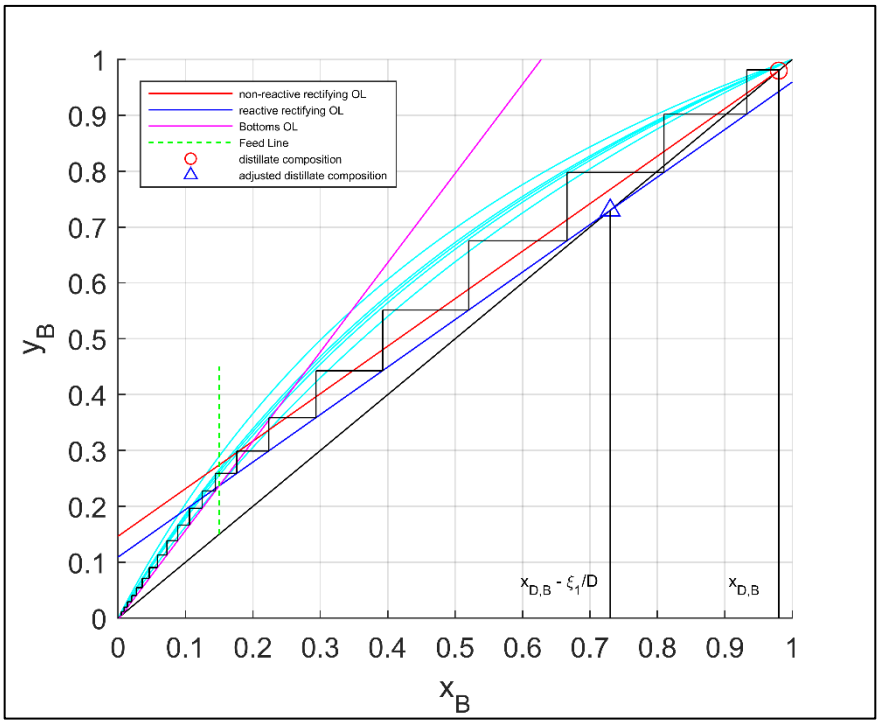

Figure 7.39: McCabe-Thiele diagram for Component B at finite reflux for reaction on stage 1 in the rectifying section and feed stage = 12

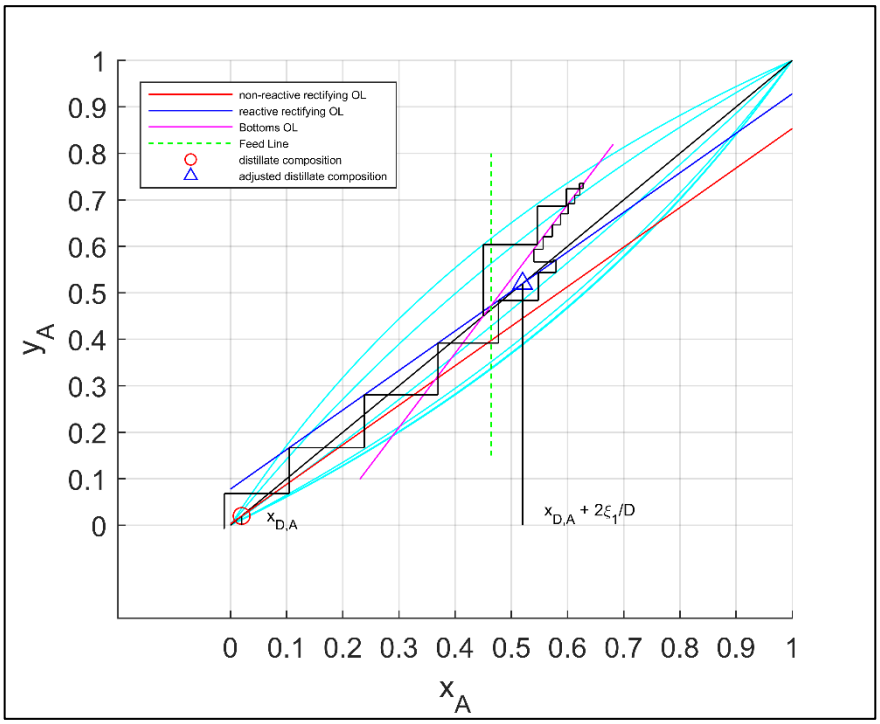

Figure 7.40: McCabe-Thiele diagram for Component A at finite reflux for reaction on stage 1 in the rectifying section and feed stage = 12

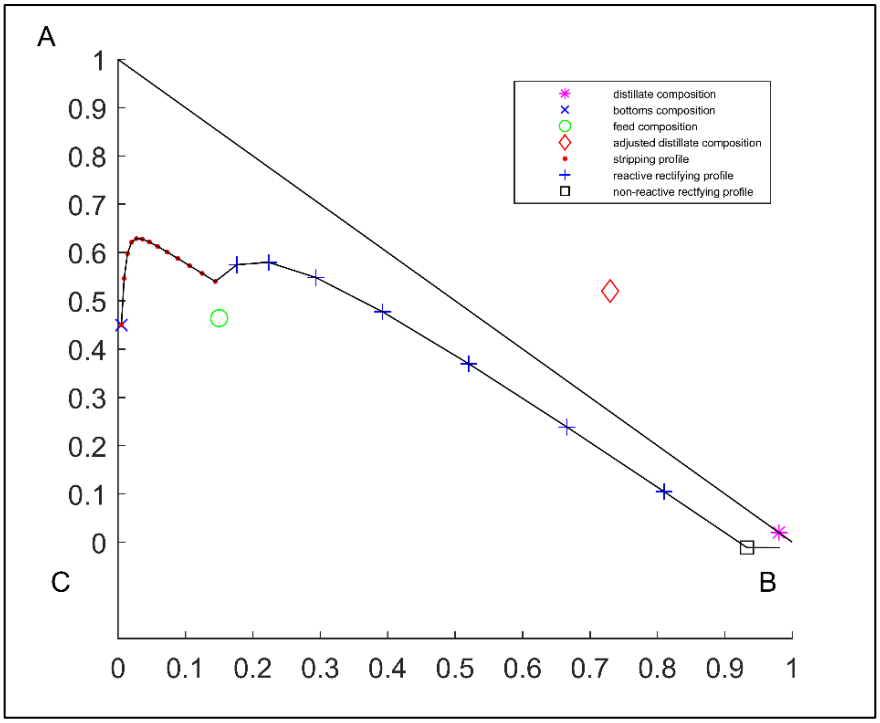

Figure 7.41: Distillation curve map (DCM) at finite reflux for reaction on stage 1 in the rectifying section and feed stage = 12

The effect of reaction stage closer to the feed rather than higher in the rectifying column is also a point of analysis. Figure 7.42 and Figure 7.43 depict the McCabe-Thiele diagram for the light key and DCM for the reactive stage on stage 14, closer to the feed for the light key component. It can be noticed that 29 theoretical stages are required to achieve the desired product specifications. Hence, 5 additional stages are required, in comparison with reaction on stage 5, with the same reflux and feed stage (Figure 7.29). Reaction stage number directly affects the number of stages required for a desired separation. Reaction stages closer to the feed will require more stages than reaction stages closer to the distillate product, at the top of the rectifying section.

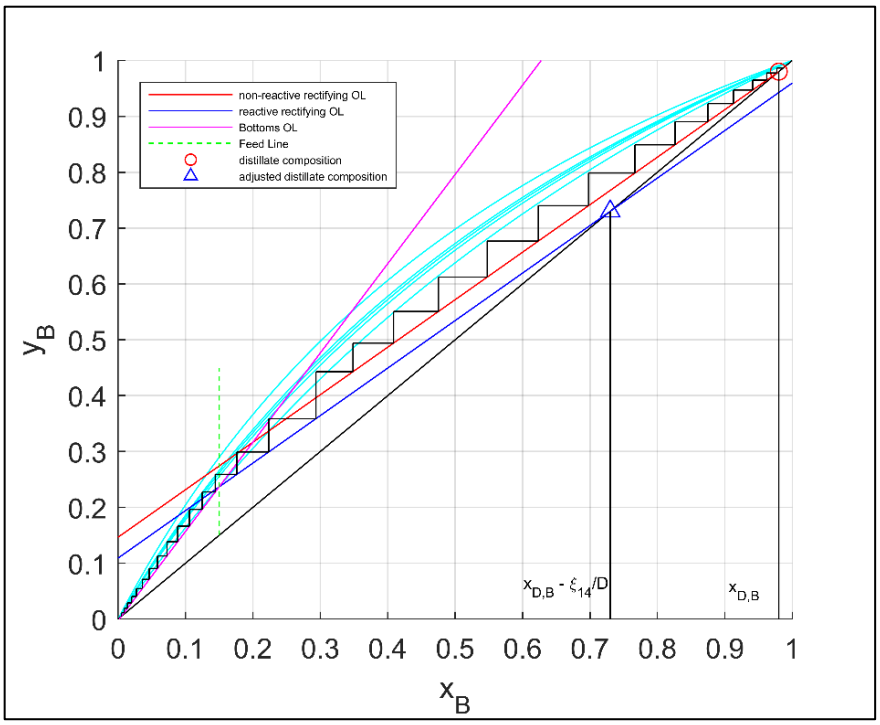

Figure 7.42: McCabe-Thiele diagram for Component B at finite reflux for reaction on stage 14 in the rectifying section and feed stage = 12

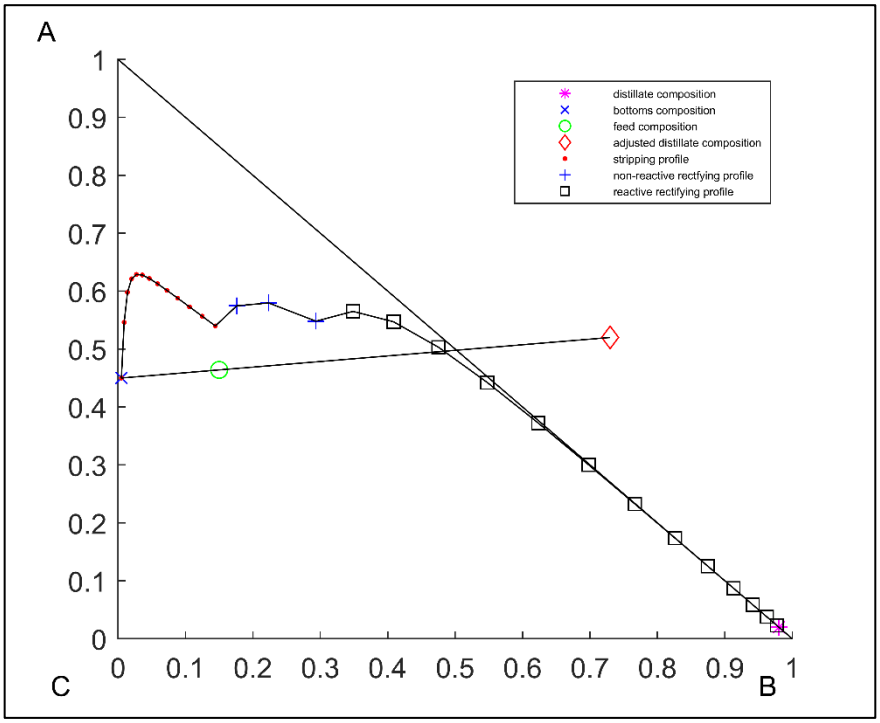

Figure 7.43: Distillation curve map (DCM) at finite reflux for reaction on stage 14 in the rectifying section and feed stage = 12

Analysis 7.6: Reaction on two stages

The desired product specification can also be obtained by multiple reactive stages in the rectifying section. In this example, two reactive stages in the rectifying section will be designed with the same product specification, as in Table 7.5. The extent (ξ_n), on the first stage from the top of the column, has a reaction extent of 5 kmol/h whilst the reactive stage below will have a reaction extent of 9 kmol/h. The reflux ratio is set to 5.69, and hence the reboil ratio is 4.46. There will be two reactive rectifying operating lines and hence two adjusted distillate compositions for each reactive stage and corresponding reaction extent. Equation 7.18 and 7.19 will be used to calculate the reactive rectifying operating line and adjusted distillate compositions respectively. Since the bottoms and distillate product compositions are fixed, the feed composition is calculated to satisfy a material balance with the bottoms compositions and second adjusted distillate composition in accordance with Figure 7.28. The feed and both adjusted distillate compositions are given in Table 7.6. The feed, bottoms, and two reactive rectifying and non-reactive operating lines are plotted on the x-y diagrams for the three components shown in Figures 7.44-7.46 and the DCM for the separation in Figure 7.47. I

It should be noted that, the reactive rectifying operating lines lie below the non-reactive rectifying operating lines for products and for reactants. It should be noted further that the reactive rectifying operating lines lie above the non-reactive rectifying operating lines for multiple reactive stages as well. The method in Figure 7.28 is followed to determine the number of theoretical stages, reactive stages and the feed stage location.

Table 7.6: Feed, bottoms, distillate and adjusted distillate compositions for reaction in the rectifying section only.

Component	x_F	x_B	x_D	x_{D1}	x_{D2}
A	0.638	0.450	0.020	0.520	0.920
B	0.215	0.005	0.980	0.730	0.530
C	0.147	0.545	5×10^{-11}	-0.250	-0.450

For multiple reactions, the location of the reactive stages affects the number of stages required. The reactive stages may or may not be consecutive. For this example, the location of the second reactive rectifying operating line (second reactive stage from the top of the column and $((\xi_n) = 9$ kmol/h) will be after the feed line of the light key component B (Figure 7.41). The location of the first reactive rectifying operating line $((\xi_n) = 5$ kmol/h) is set on the second stage, after the second reactive operating line, hence the stages will not be consecutive. The changeover to the non-reactive rectifying operating line is on the second stage after the first reactive operating line. Hence, the total number of stages required is 17 stages, with feed stage location on stage 10, first reactive stage on stage 6 and second reactive stage on stage 8 from the top of the column (Figures 7.41-7.44).

For the desired separation, and designing a column with one reactive stage, requires more stages than designs with two reactive stages. The simulations of feed stage location at the light key feed line, and reactive stage on stage 5, for one reactive stage (Figure 7.29), requires 24 stages. For two reactive stages, with feed stage location at the light key feed line and first reactive stage on stage 6, and second on stage 8, 17 stages are required. Hence, the reduction of 7 stages is achieved by an additional reactive stage. The addition of reactive stages for a specified separation at the same reflux ratio reduces the number of theoretical stages required.

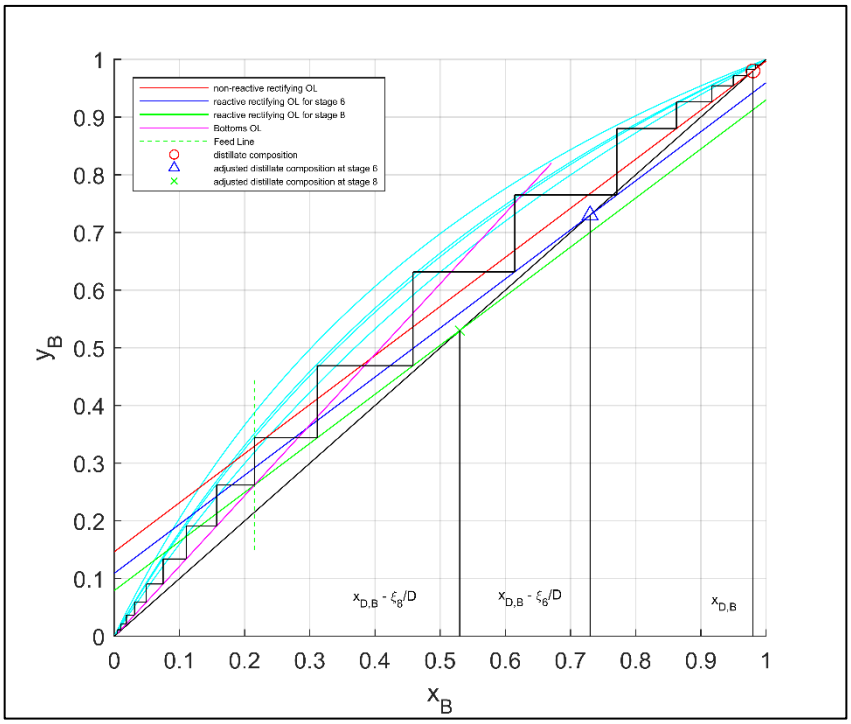

Figure 7.44: McCabe-Thiele diagram for Component B at finite reflux for reactive stage 1 on stage 6 and reactive stage 2 on stage 8 in the rectifying section and feed stage = 10

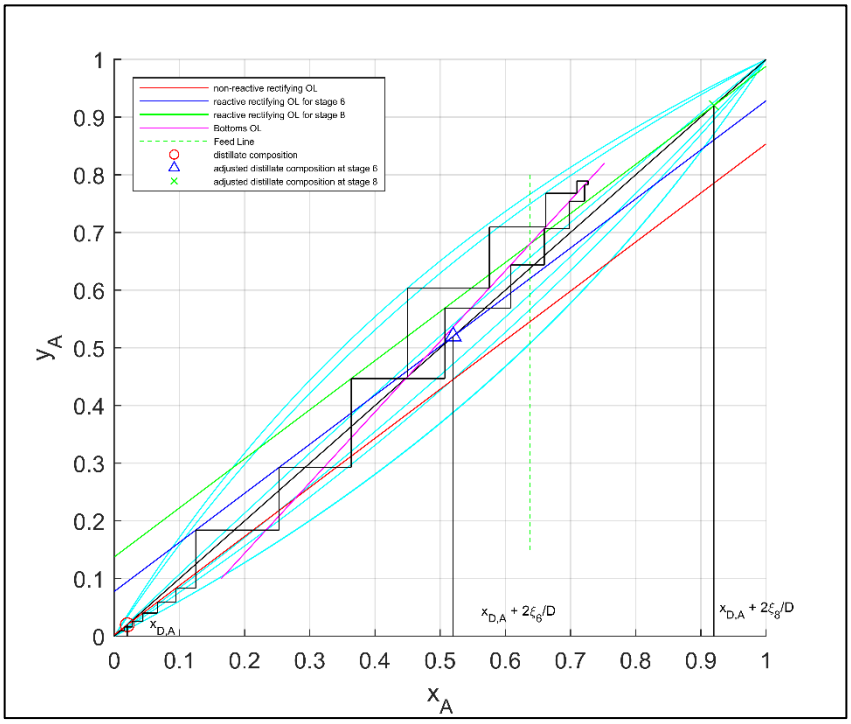

Figure 7.45: McCabe-Thiele diagram for Component A at finite reflux for reactive stage 1 on stage 6 and reactive stage 2 on stage 8 in the rectifying section and feed stage = 10

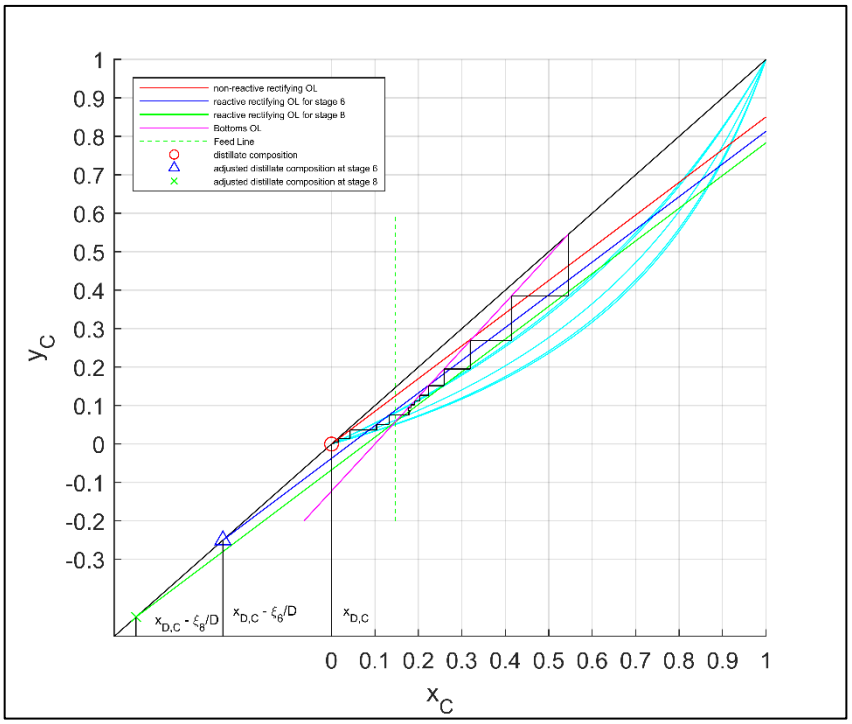

Figure 7.46: McCabe-Thiele diagram for Component C at finite reflux for reactive stage 1 on stage 6 and reactive stage 2 on stage 8 in the rectifying section and feed stage = 10

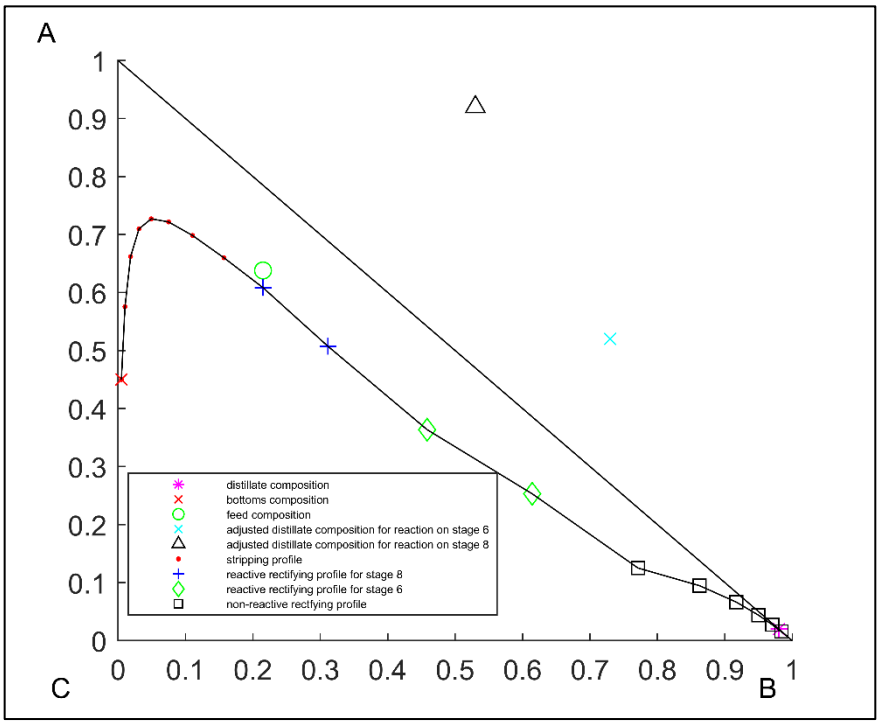

Figure 7.47: Distillation curve map (DCM) at finite reflux for reactive stage 1 on stage 6 and reactive stage 2 on stage 8 in the rectifying section and feed stage = 10

Analysis 7.7: Effect of consecutive reaction stages for reaction on two stages

A second simulation of the design presented for a separation with two reactive stages will be presented to determine the effect of consecutive reactive stages. All operating parameters will be the same, as well as the specifications in Table 7.6. The difference in this example is that the second reactive stage will be placed after the feed line (one stage after the feed stage) and the first reactive stage on the next stage, lower down in the column. Figures 7.48 and 7.49 present the McCabe-Thiele diagram for the light key and the DCM for the simulation (Refer to Appendix F for the McCabe-Thiele plots for the IK and LK). From Figures 7.48-7.49, the total number of stages required is 21 stages, with feed stage location on stage 13, first reactive stage on stage 11 and second reactive stage on stage 12, from the top of the column. The number of stages required for consecutive stages, closer to the feed, is higher than spacing the stages such that one stage is higher in the column and one lower in the column closer to the feed.

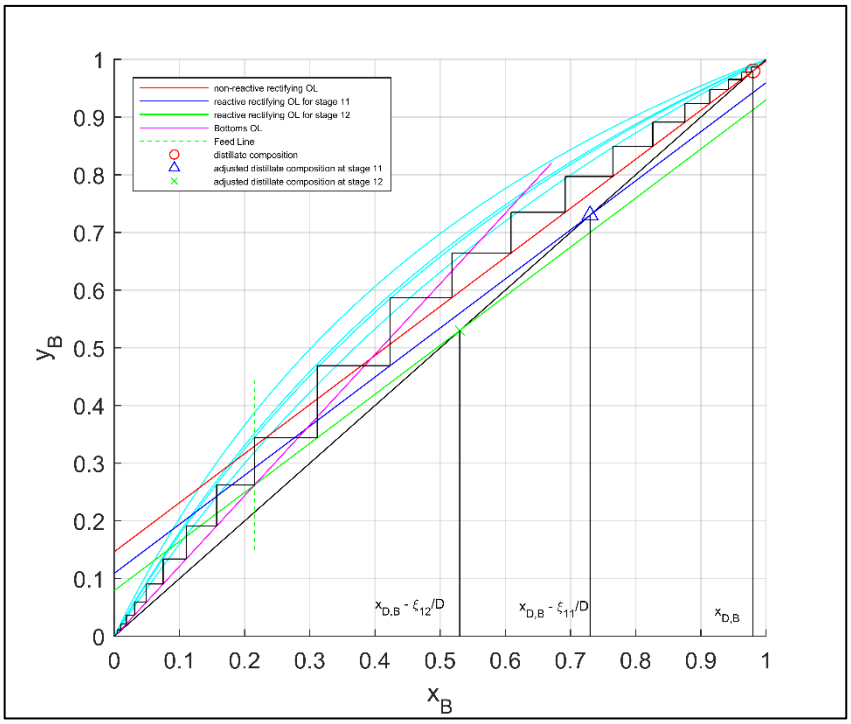

Figure 7.48: McCabe-Thiele diagram for Component B at finite reflux for reactive stage 1 on stage 11 and reactive stage 2 on stage 12 in the rectifying section and feed stage = 13

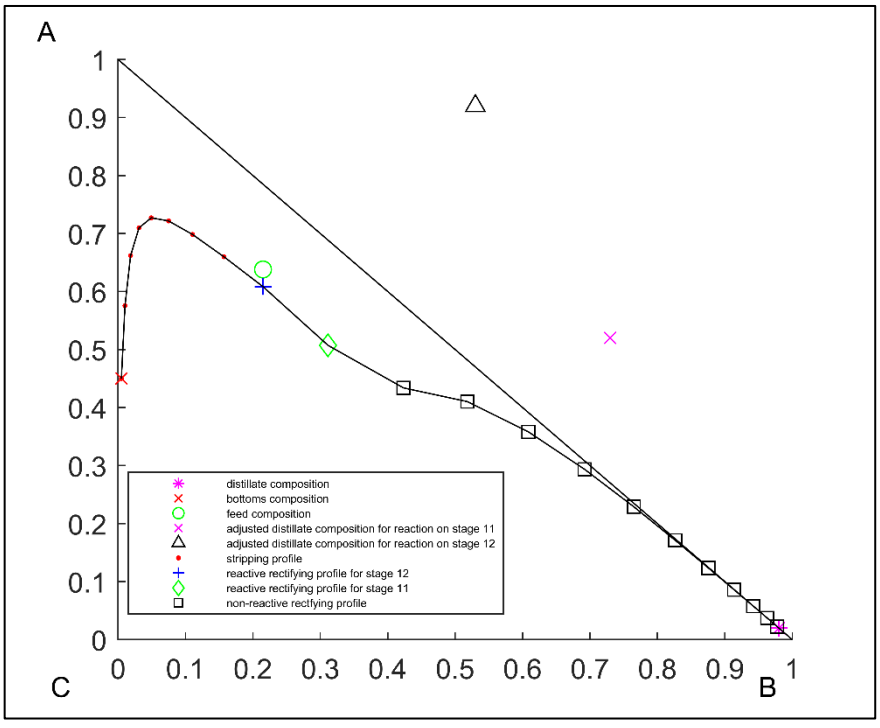

Figure 7.49: Distillation curve map (DCM) at finite reflux for reactive stage 1 on stage 11 and reactive stage 2 on stage 12 in the rectifying section and feed stage = 13

The effect of reactive feed location, feed location or a combination of both factors, as well as multiple reactive stages, can be visually investigated using the graphical method. Once the contours of VLE are plotted for the components, various design scenarios can be investigated to determine the best suited design with minimal additional calculations. A detailed analysis has been performed for Case A, with the reactive stage in the rectifying section. An explanation of the design method and parameter analysis for minimum reflux, feed stage location, reactive stage location and multiple reactive stages in the rectifying section has been presented.

Case B and Case C, for reaction in the rectifying section and feed stage and reaction in the stripping section only, respectively will focus only on determining the number of theoretical stages required. By extending the methods and principles, a similar analysis can be performed for Case B and Case C.

7.3.3 Case B: Reaction in the Rectifying Section and Feed Stage

The desired separation for the reaction in section 7.3.2 for reaction in rectifying the section only, can be achieved using a combination of reaction on feed stage and rectifying section. The feed, pseudo-feed, distillate and bottoms compositions are provided in Table 7.7. The desired product specifications are provided, and the extent of reaction on the feed stage is set to 3 kmol/h ($\xi_{n(feed)}$) and on the reactive stage to 5 kmol/h ($\xi_{n(rect)}$). The reflux and reboil are 5.69 and 1.67 respectively.

Table 7.7: Relative volatility, feed, pseudo-feed, bottoms, distillate and adjusted distillate compositions for reaction in the rectifying section and on the feed stage.

Component	**Relative volatility (α)**	x_F	$x_{\hat{F}}$	x_B	x_D	x_{D1}
A	1.90	0.524	0.464	0.450	0.020	0.520
B	3.25	0.120	0.150	0.005	0.980	0.730
C	1.00	0.356	0.386	0.545	5×10^{-11}	-0.250

The method of determining the feed, pseudo-feed, adjusted distillate compositions and hence, the number of theoretical stages in provided in Figure 7.50. The algorithm for determining the number of stages is provided below:

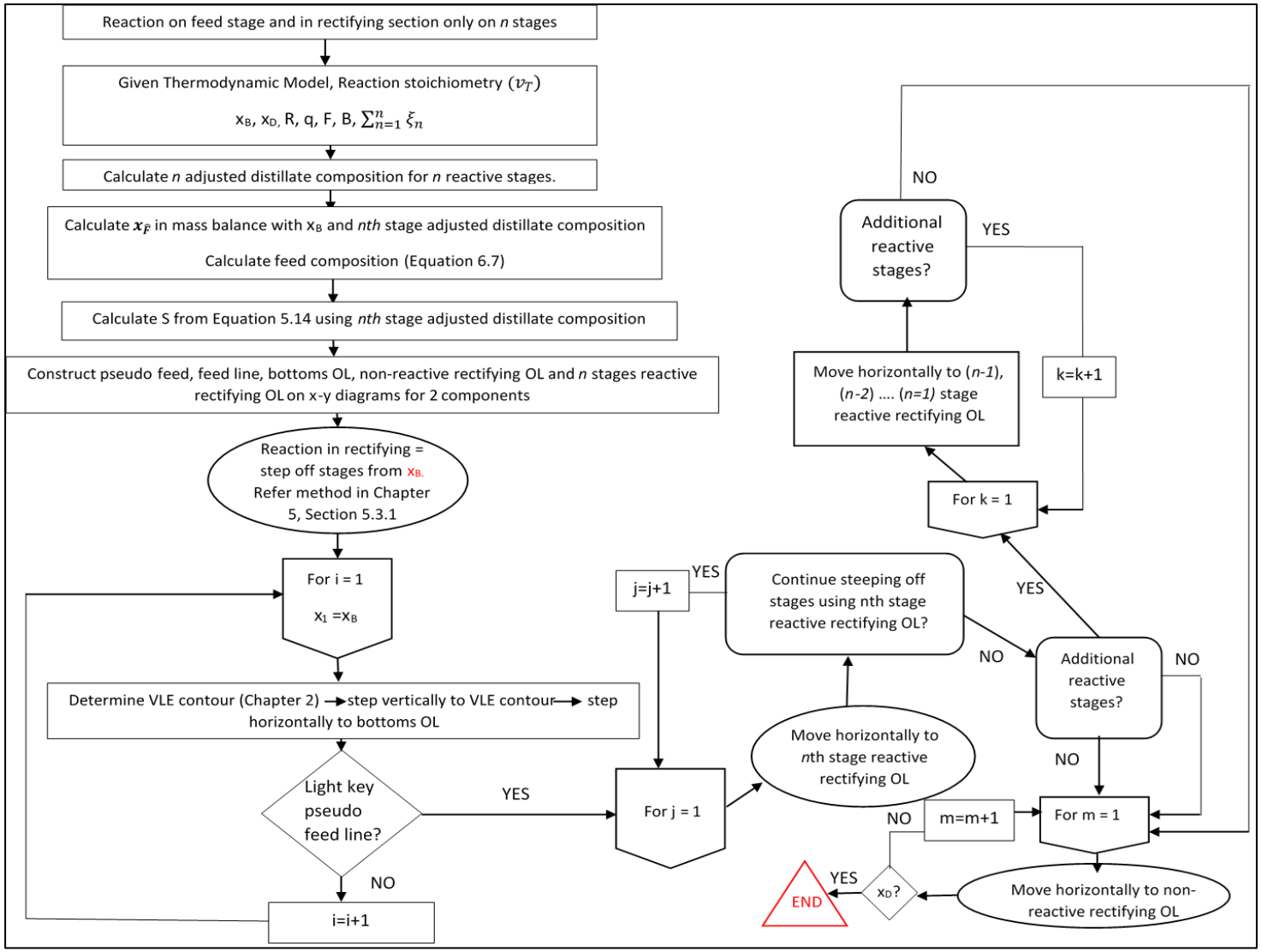

Figure 7.50: Method to determine the number of theoretical stages and feed stage location at finite reflux for 3 component systems for reaction on the feed stage and in the rectifying section only

Figures 7.51-7.52 plot the McCabe-Thiele diagrams for the light key and heavy key respectively (The IK can be found in Appendix F). Figure 7.53 depicts the DCM for the separation of reaction on the feed stage and one stage in the rectifying section. The number of theoretical stages required is 24, the feed stage is located on stage 12, and the reactive stage on stage 5 (Figures 7.51-7.53). It can be seen from Figures 7.51 and 7.52, the McCabe-Thiele diagrams for the light key and heavy key, that the simulation is identical to the design of reaction in the rectification column only (Figures 7.29-7.31). This is due to the fact that the reaction on the feed stage shifts the actual feed, such that the pseudo-feed is equivalent to the actual feed in Figures 7.29-7.31. Hence, the reaction on the feed stage would be useful in cases where the feed is required to be 'adjusted' in order to achieve the desired product specifications with reaction in the rectifying section.

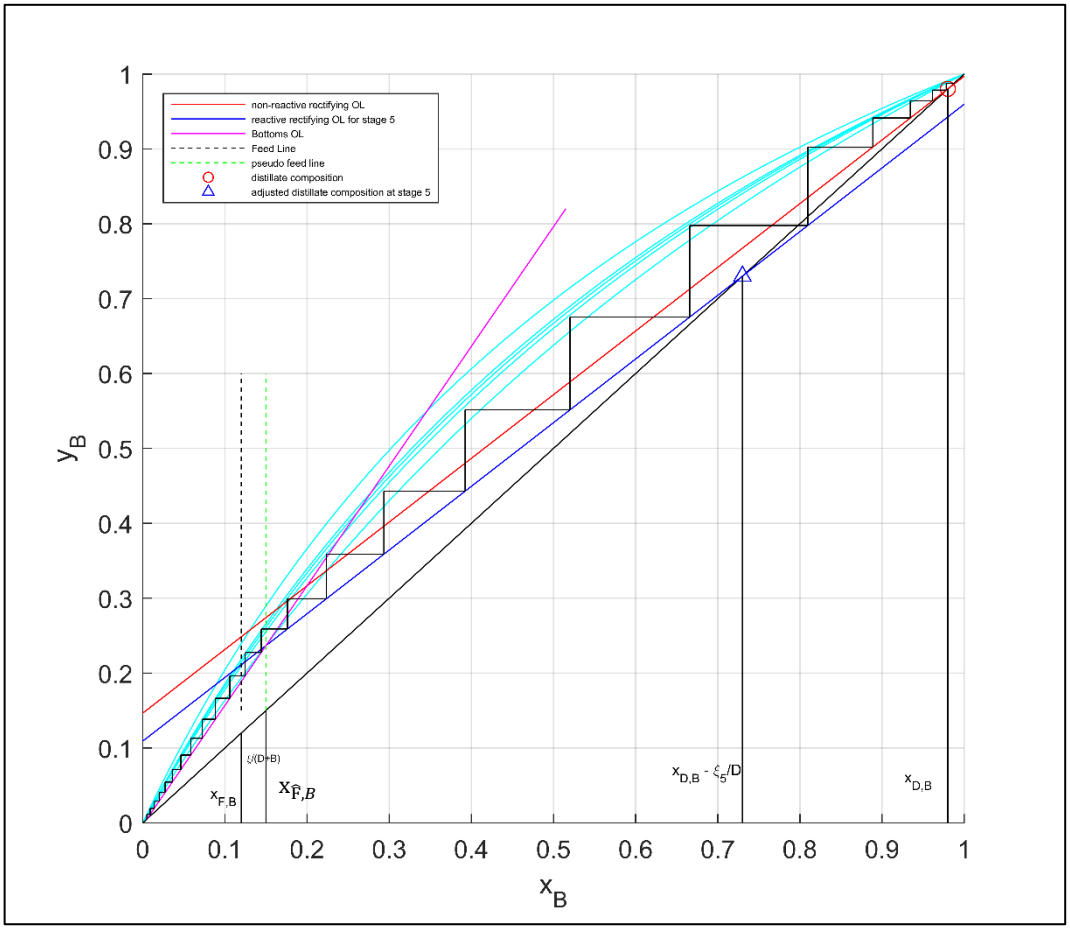

Figure 7.51: McCabe-Thiele diagram for Component B at finite reflux for reactive stage on stage 5 and feed stage reaction on stage 12

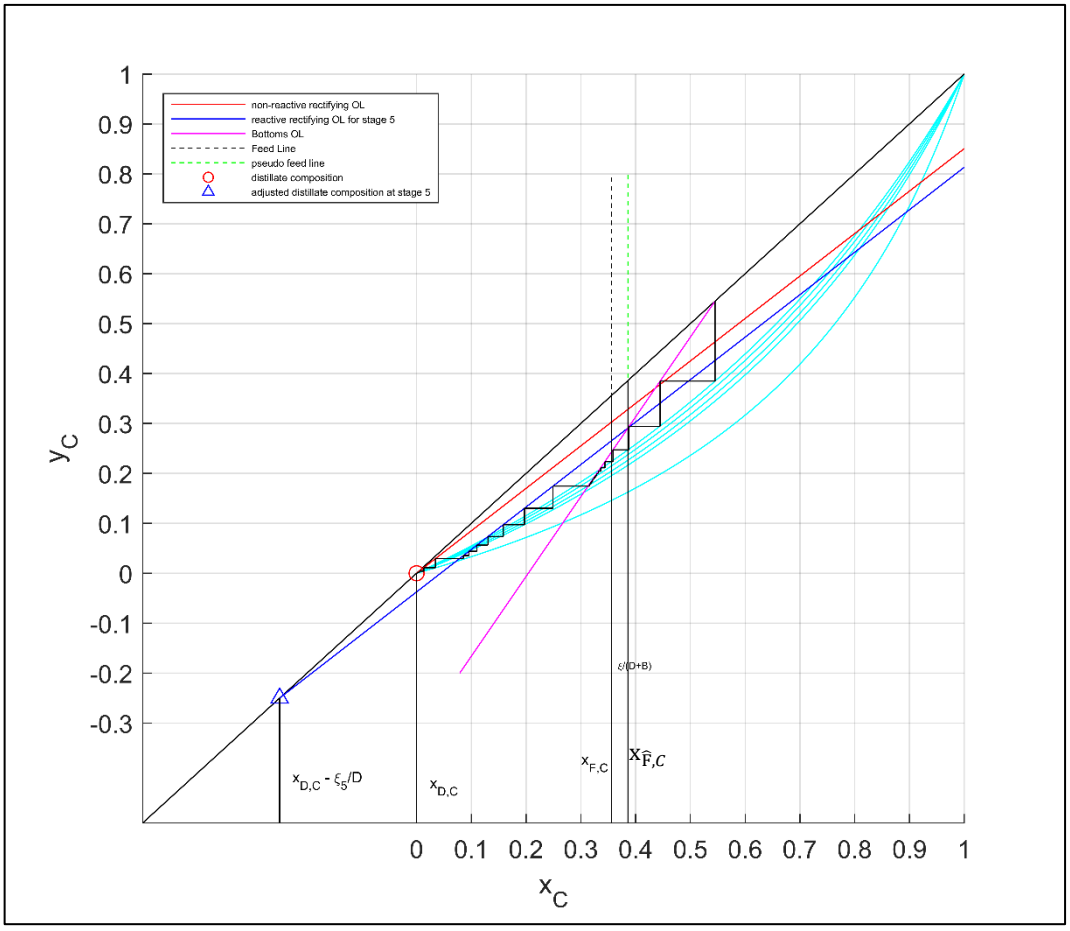

Figure 7.52: McCabe-Thiele diagram for Component C at finite reflux for reactive stage on stage 5 and feed stage reaction on stage 12

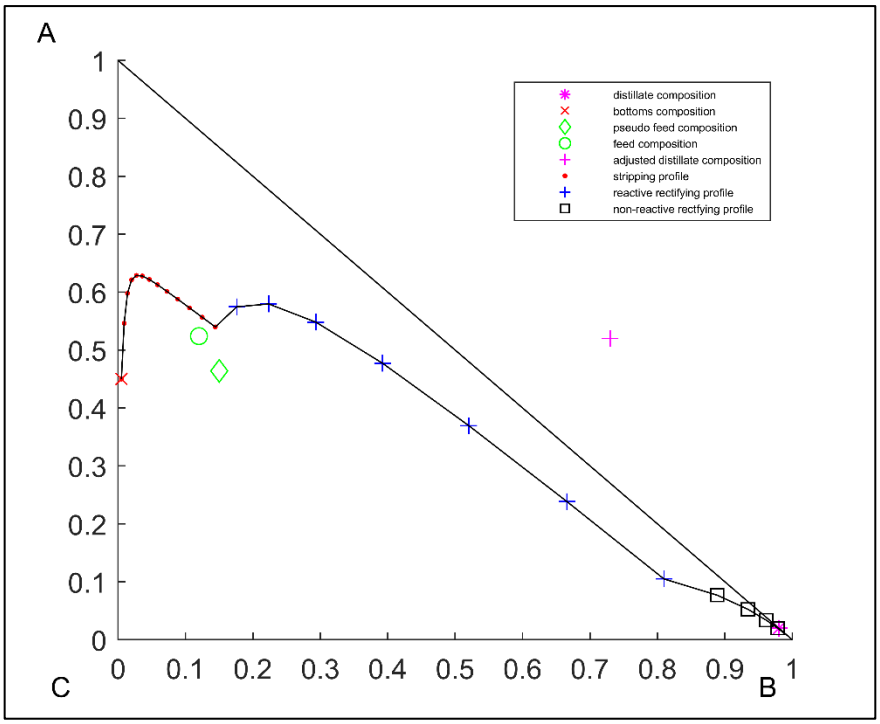

Figure 7.53: Distillation curve map (DCM) at finite reflux for reactive stage on stage 5 and feed stage reaction on stage 12

7.3.4 Case C: Reaction in the Stripping Section Only

The final Case, C, will investigate the design of columns with reaction in the stripping/bottoms section only. The method is very similar to that of reaction in the rectifying section, but instead of stepping off stages from the bottoms composition, stepping off stages will begin at the distillate product. Due to reaction now shifting to the bottoms section, stripping profile, and hence the saddle in the stripping profile, controls the separation (explained in sections 7.3.2.1 and 7.3.2.2). Reaction in the stripping section only will be more suited to indirect splits, whilst reaction in the rectifying section is suited to direct splits.

The product specifications, relative volatility, and feed composition can be found in Table 7.8 for a direct split. There will be a single reaction in the stripping section with an associated extent of 5 kmol/h (ξ_n). The reflux and corresponding reboil

ratio are 4.33 and 8 respectively. The method for determining the number of theoretical stages is presented in Figure 7.54.

Table 7.8: Relative volatility, feed, distillate, bottoms and adjusted bottoms compositions for reaction in the stripping section only

Component	**Relative volatility (α)**	x_F	x_B	x_D	x_{B1}
A	1.90	0.280	0.020	0.445	0.270
B	3.25	0.375	5×10^{-11}	0.550	-0.125
C	1.00	0.345	0.980	0.005	0.855

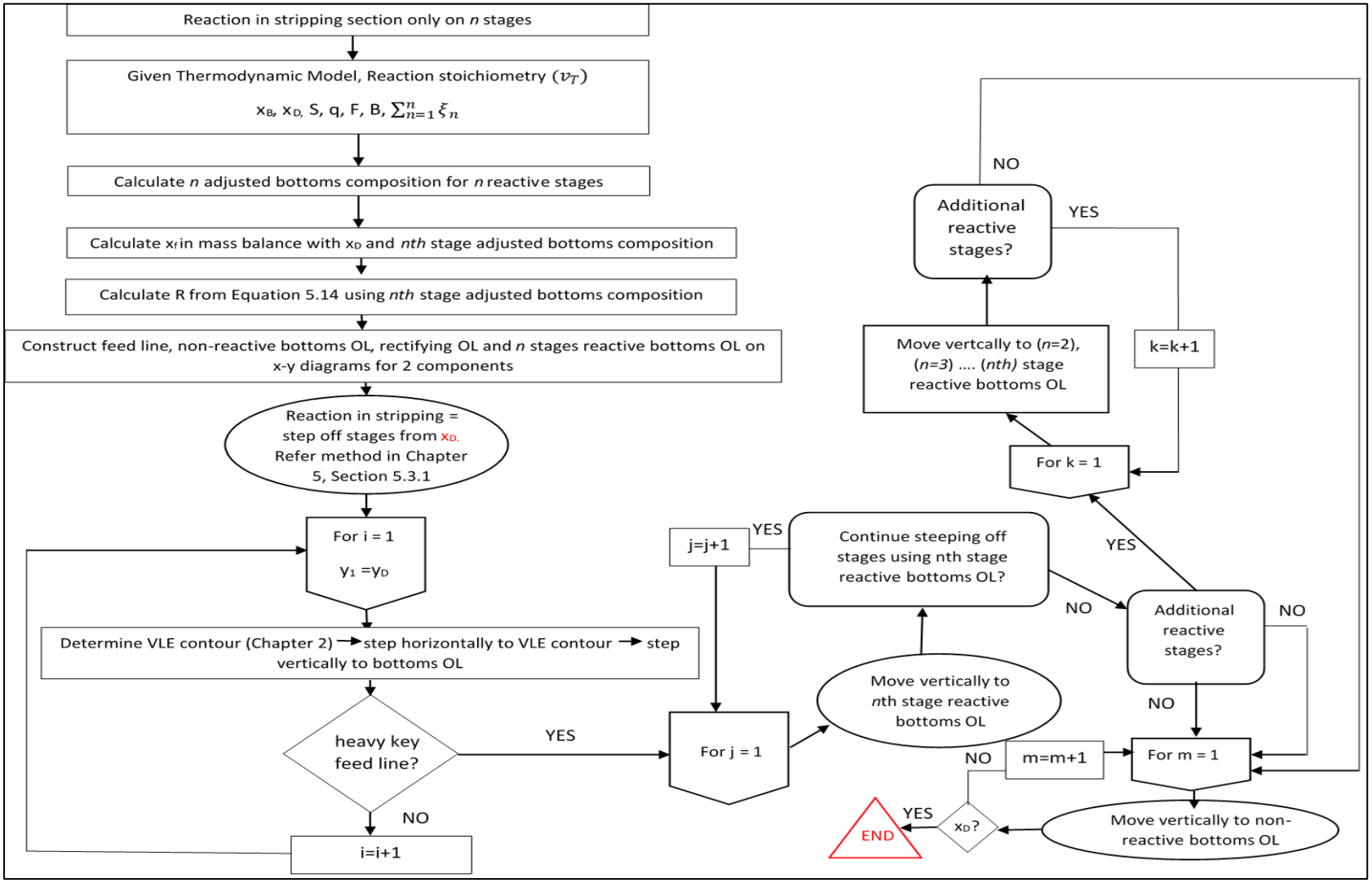

Figure 7.54: Method to determine the number of theoretical stages and feed stage location at finite reflux for 3 component systems for reaction on the bottoms section only.

Figures 7.55-7.57 depict the McCabe-Thiele diagram for reaction in the stripping section using the design problem provided for the LK, IK and HK respectively. Figure 7.58 presents the DCM for the design, with reaction in the stripping section. Reaction in the stripping section shifts the adjusted bottoms composition below the bottoms composition for products, and above the bottoms composition for reactants.

From Figures 7.55-7.58, the number of theoretical stages required are calculated to be 17. If the stages are numbered from the top of the column, the feed location is on stage 9 (10 from bottoms of the column) and reactive stage on 13 (stage 4 from the bottoms of the column).

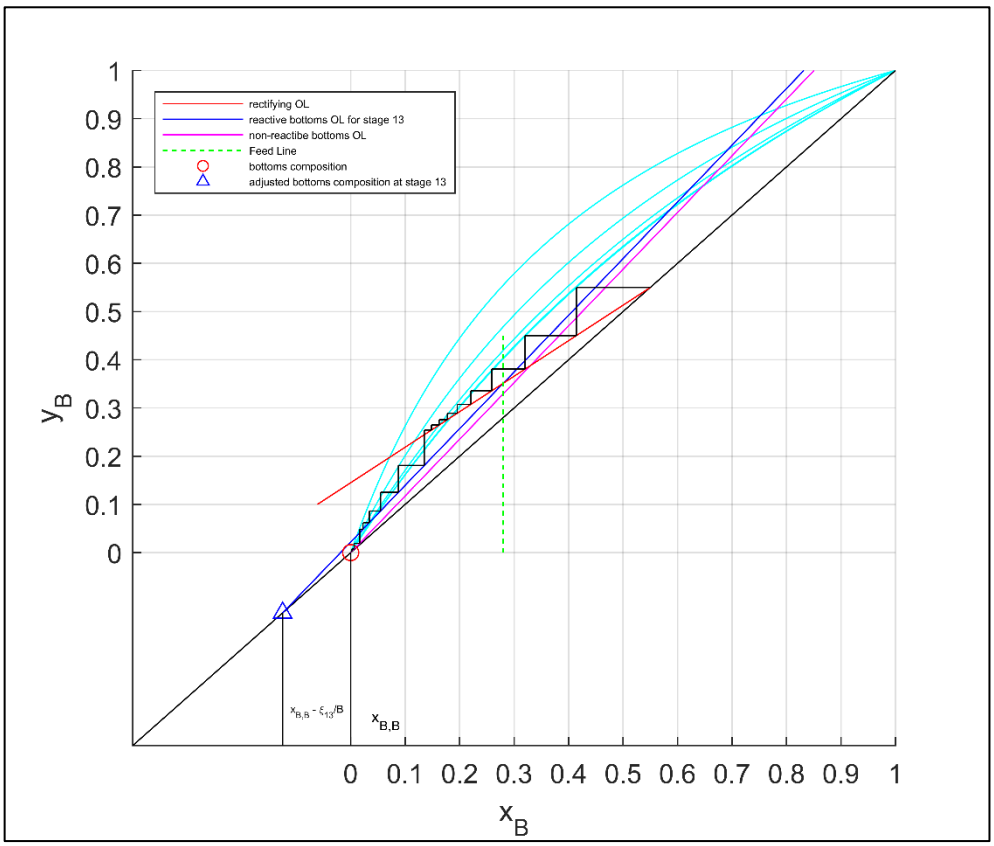

Figure 7.55: McCabe-Thiele diagram for Component B at finite reflux for reaction on stage 13 in the stripping section and feed stage = 9

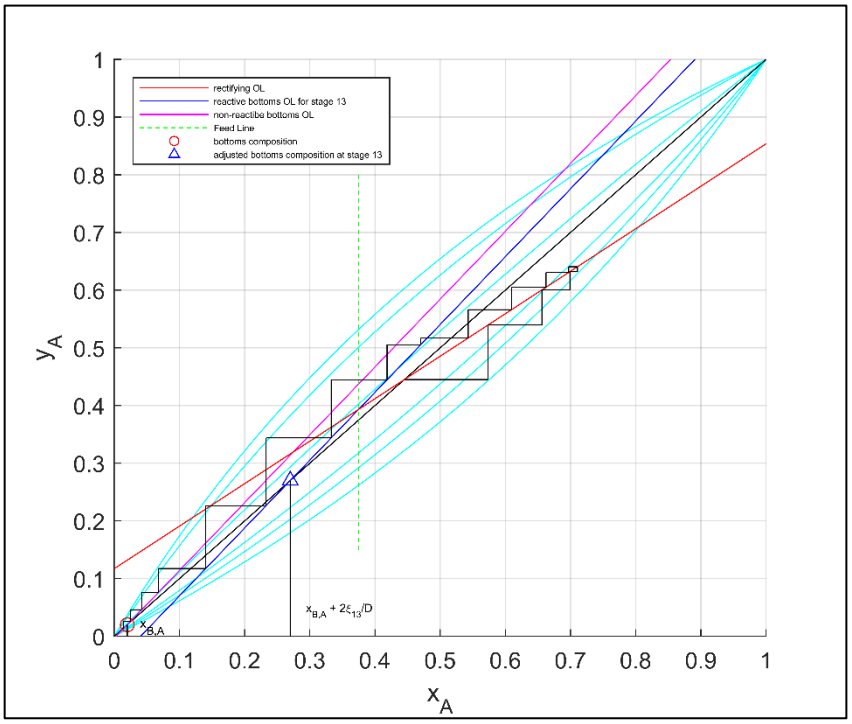

Figure 7.56: McCabe-Thiele diagram for Component A at finite reflux for reaction on stage 13 in the stripping section and feed stage = 9

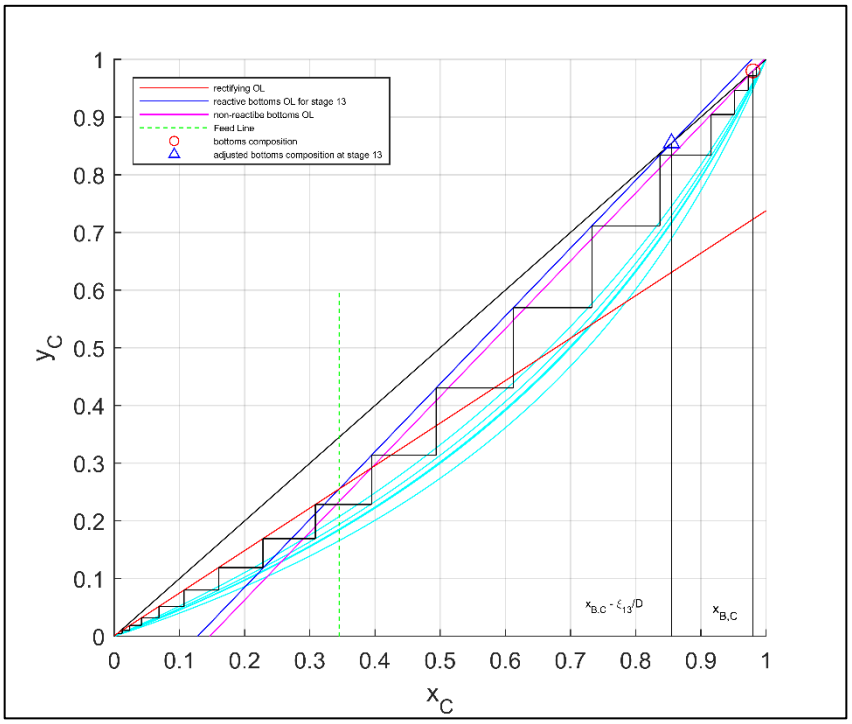

Figure 7.57: McCabe-Thiele diagram for Component B at finite reflux for reaction on stage 13 in the stripping section and feed stage = 9

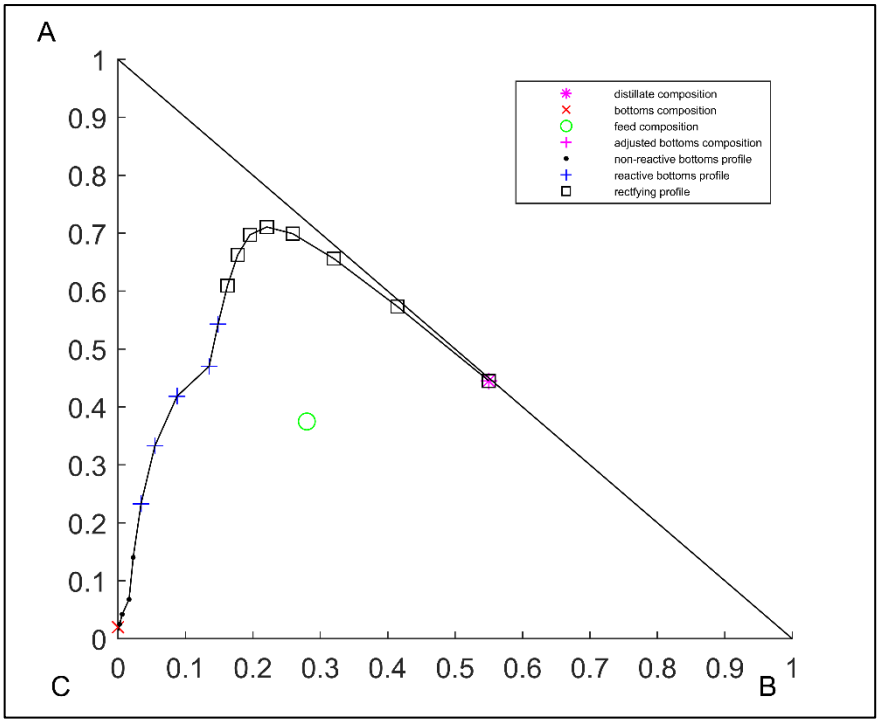

Figure 7.58: Distillation curve map (DCM) at finite reflux for reaction on stage 13 in the stripping section and feed stage = 9.

Further analysis and optimization of the feed and reactive stage location, as well as the inclusion of multiple reactive stages in the stripping section can be investigated, as shown in Section 7.3.2.2. In addition, analysis of feed stage reaction and reaction on the stripping section can be performed by combining the methods in Section 7.3.3 and 7.3.4.

Future work

The methods presented above – for reaction in the rectifying section only, and the feed and rectifying section and stripping section only – can be extended to non-ideal systems, as presented in Section 7.2.3, for reaction on the feed stage only. Future work will present the methods of reaction in a column section for non-ideals systems in which $v_T = 0$ and $v_T \neq 0$ by extending the methods presented in this chapter. In addition, the method can be extended to quaternary systems with particular attention to the esterification reaction of lactic acid with methanol producing methyl lactate and water.

7.4 Conclusion

The graphical technique for determining design parameters at finite reflux (Chapter 6) using the novel representation of VLE (Chapter 3) for ternary ideal and non-ideal systems is adapted for reactive-hybrid distillation columns in this work. The theoretical basis of reactive cascade difference points presented by Lee et al., (2000c; 2000d) for binary reactive-hybrid columns is extended to ternary reactive-hybrid systems. Through the graphical depiction of the reactive cascade difference points, a modified McCabe-Thiele method can be derived for the preliminary design of ternary reactive-hybrid distillation columns, without the transformation of composition variables. Hence, the powerful visual insights of non-reactive columns are retained on the x-y plot. In this chapter, the method derived by Lee et al., (2000c; 2000d) for binary feed stage reaction, reaction in the rectifying section only and stripping section only, is applied to ternary reactive design simulations. In addition, this work also presents the method for reaction on the feed stage and in the rectifying section. In a similar manner, it is possible to use the graphical technique to design a column with reaction in the stripping section and on the feed stage.

It was shown that, for reaction on the feed stage for an ideal system and $v_T = 0$, the minimum reflux can be determined using the method presented in Chapter 5. Using the concept of pseudo-feed due to reaction on the feed stage, the feed stage location is shifted to the pseudo-feed line for LK for direct splits and pseudo-feed line for HK for indirect splits. The method of determining the number of theoretical stages remains the same as in Chapter 6. In addition, it was concluded that a reduction in the reflux ratio and enhanced separation is achieved in a feed stage reactive distillation column, in comparison with separate units. A rigorous Aspen Plus™ simulation was initialised with the design parameters obtained from a non-ideal system of isobutene-methanol-MTBE. The reaction of isobutene and methanol to form MTBE is a widely researched application of reactive distillation. In this reaction, there is a net change in the number of moles due to reaction. It was shown

that the rigorous simulation successfully converged, using the design parameters obtained from the graphical technique. Hence, it can be concluded that the graphical technique is a useful preliminary design tool that can aid the successful use of rigorous simulators.

A detailed analysis of the design for reaction in the rectifying section for an ideal system and $v_T = 0$ was presented. The method of determining minimum reflux is complex and requires the additional help of DCMs, and is iterative in nature. The number of stages required is determined from the bottoms composition for reaction in the rectifying section, incorporating a reactive rectifying operating line. Hence it is concluded that reaction in the rectifying section is better suited for sharp direct splits. Additionally, it was demonstrated that the reaction stage and number of reactive stages directly impact the theoretical number of stages required. Reaction stages closer to the feed will require more stages than reaction stages closer to the distillate product at the top of the rectifying section. The addition of reactive stages for specified separation, at the same reflux ratio, reduces the number of theoretical stages required. The graphical technique is beneficial in that once the VLE for the components are plotted, various scenarios can be analysed in order to choose the optimal design variables with minimal additional calculations.

Reaction on the feed stage and reaction in the rectifying section is not articulated by Lee et al., (2000c; 2000d). The method of determining the number of stages is a combination of incorporating the pseudo-feed and reactive rectifying operating line. The number of stages is determined from the bottoms composition following the method of sharp direct splits, and the feed stage location is at the pseudo-feed line of the LK. Finally, the method of determining the number of stages and feed stage location for reaction in the stripping section is demonstrated. The number of stages is determined from the distillate composition and the feed stage is located at the feed line of the HK. The method requires the inclusion of a reactive bottoms operating line. Hence, reaction in the stripping section is more suited for sharp indirect splits. Both configurations are designed for ideal systems and $v_T = 0$.

The work in this chapter forms the foundation upon which further research can be performed in the future. The methods presented above, for reaction in the rectifying section only, feed and rectifying section and stripping section only, can be extended to non-ideal systems as presented in Section 7.2.3 for reaction on the feed stage only. Future work will present the methods of reaction in a column section for non-ideal systems in which $v_T = 0$ and $v_T \neq 0$ by extending the methods presented in this chapter.

REFERENCES

Almeida-Rivera, C.P., Swinkels, P.L.J., Grievink, J., **2004**. Designing reactive distillation processes: present and future. *Comp. Chem. Eng.* 28(10), pp. 1997-2020.

Anbreen, A., Ramzan, N., Faheem, M., **2022**. A Heat-Integrated Reactive Distillation Process for Methyl Lactate Hydrolysis. *Chem. Eng. Process. Process Intensif.* 170, pp. 108695.

Barbosa, D. & Doherty, M.F., **1987**. A new set of transformed variables for the representation of reactive-phase diagrams. *Proc. R. Soc. Lond.* 413(1845), pp. 459-464.

Barbosa, D. & Doherty, M.F., **1988a**. The influence of chemical reactions on vapour-liquid phase diagrams. *Chem. Eng. Sci*. 43(3), pp. 529-540.

Barbosa, D. & Doherty, M.F., **1988b**. The simple distillation of homogeneous reactive mixtures. *Chem. Eng. Sci*. 43(3), pp. 541-550.

Barbosa, D. & Doherty, M.F., **1988c**. Design and minimum-reflux calculations for single-feed multicomponent reactive distillation columns. *Chem. Eng. Sci*. 43(7), pp. 1523-1537.

Barbosa, D. & Doherty, M.F. **1988d**. Design and minimum-reflux calculations for double-feed multicomponent reactive distillation columns. *Chem. Eng. Sci*. 43(9), pp. 2377-2389.

Carrera-Rodriguez, M., Segovia-Hernandez, J.G., Bonilla-Petriciolet, A., **2011**. Short-Cut Method for the Design of Reactive Distillation Columns. *Ind. Eng. Chem. Res.* 50(8), pp. 10730-10743.

Chen, A.R., Ward, J.D., & Yu, C.C., **2011**. Feasibility of Reactive Distillation for Ternary Systems with Azeotropic Mixtures: Decomposition reaction. *Ind, Eng, Chem. Res.* 50(3), pp. 1305-1320.

Doherty, M.F. & Malone, M.F., **2001.** Conceptual Design of Distillation Systems. *McGraw-Hill, Inc:* New York.

Domingues, L., Pinheiro, C.I.C., Oliveira, N.M.C., **2014**. Optimal design of reactive distillation systems: Application to the production of ethyl tert- butyl ether (ETBE). *Comp. Chem. Eng.* 64, pp. 81-94.

Dragomir, R.M., **2004**. Synthesis and Design of Reactive Distillation Columns. PHD Thesis, UMIST, UK.

Dragomir, R.M & Jobson, M., **2005**. Conceptual design of single-feed hybrid reactive distillation columns. *Chem. Eng. Sci.* 60(16), pp. 4377-4395.

Espinosa, J., Scenna, N., Pérez, G., **1993**. Graphical procedure for reactive distillation systems. *Chem. Eng. Com.* 119(1), pp. 109-124.

Espinosa, J., Aguirre, P.A., Pérez, G., **1996**. Some Aspects in the Design of Multicomponent Reactive Distillation Columns with a Reacting Core: Mixtures Containing Inerts. *Ind. Eng. Chem. Res.* 35(12), pp. 4537-4549.

Flores-Estrella, R.A. & Iglesias-Silva, G.A., **2016**. Reactive McCabe-Thiele: Short-cut method including reactive vapor-liquid efficiency. *Rev. Mex. Ing. Quim.* 15(1), pp. 193-207.

Gani, R. & Bek-Pedersen, E., **2000**. Simple New Algorithm for Distillation Column Design. *AIChE J*. 46(6), pp. 1271-1274.

Gor, N.K., Mali, N.A., Joshi., S.S., **2020**. Intensified reactive distillation configurations for production of dimethyl ether. *Chem. Eng. Process. Process Intensif*. 148, pp. 107824.

Harding, L.S & Fieg, G., **2020**. Energy saving potential of reactive dividing wall columns with azeotropic reaction systems. *Chem. Eng. Sci*. 227(9), pp. 115888.

Harmsen, G.J., **2007**. Reactive distillation: The front-runner of industrial process intensification: A full review of commercial applications, research, scale-up, design and operation. *Chem. Eng. Proc.* 46(9), pp. 774-780.

Hauan, S., Westerberg, A.W., Lien, K.M., **1999**. Phenomena-based analysis of fixed point in reactive separation systems. *Chem. Eng. Sci*. 55(6), pp. 1053-1075.

Hauan, S., Ciric, A.R., Westerberg, A.W., Lien, K.M., **2000**. Difference points in extractive and reactive cascades. I - Basic properties and analysis. *Chem. Eng. Sci*. 55(16), pp. 3145-3159.

Hengstebeck, R.J., **1946**. A Simplified Method for Solving Multicomponent Distillation Problems. *Trans. AIChE*. 42, pp. 309-329.

Hiwale, R.S., Bhate, N.V., Mahajan, Y.S., Mahajan, S.M., **2004**. Industrial Application of Reactive Distillation: Recent Trends. *Int. Jour. Chem. Reac. Eng*. 2(1).

Huerta-Garrido, M.E., Rico-Ramirez, V., Hernandez-Castro, S., **2004**. Simplified Design of Batch Reactive Distillation Columns. *Chem. Eng. Res. Des*. 43(14), pp. 4000-4011.

Jantharasuk, A., Gani, R., Górak, A., & Assabumrungrat, S. **2011**. Methodology for design and analysis of reactive distillation involving multielement systems. Chem. Eng. Res. Des. 89(8), pp. 1295-1307.

Jiao ,Y., Wang, S.J., Huang. K., Chen, H., Liu, H., **2012**. Design and Analysis of Internally Heat-Integrated Reactive Distillation Processes. *Ind. Eng. Chem. Res.* 51(10), pp. 4002−4016.

Kiss, A.A., Jobson, M., Goa, X., **2019**. Reactive Distillation: Stepping Up to the Next Level of Process Intensification. *Ind. Eng. Chem. Res.* 58(15), pp. 5909−5918.

Lee, J.W., Hauan, S., Lien, K.M., Westerberg, A.W., **2000a**. Difference points in extractive and reactive cascades. II—Generating design alternatives by the lever rule for reactive systems. *Chem. Eng. Sci*. 55(16), pp. 3161-3174.

Lee, J.W., Hauan, S., Lien, K.M., Westerberg, A.W., **2000b**. A graphical method for designing reactive distillation columns. I. The Ponchon-Savarit method. P*roceedings of the Royal Society of London*. 456(2000), pp. 1953-1964.

Lee, J.W., Hauan, S., Lien, K.M., Westerberg, A.W., **2000b**. A graphical method for designing reactive distillation columns. I. The Ponchon-Savarit method. P*roceedings of the Royal Society of London*. 456(2000), pp. 1953-1964.

Lee, J.W., Hauan, S., Lien, K.M., Westerberg, A.W., **2000c**. A graphical method for designing reactive distillation columns. II. The McCabe-Thiele method. P*roceedings of the Royal Society of London*. 456(2000), pp. 1965-1978.

Lee, J.W., Hauan, S., Westerberg, A.W., **2000d**. Graphical Methods for Reaction Distribution in a Reactive Distillation Column. *AIChE J*. 46(6), pp. 1218-1233.

Lee, H.Y., Novita, F.J., Weng, K.C., **2021**. Hybrid heat-integrated design and control for a diphenyl carbonate reactive distillation process. *Chem. Eng. Process*. *Process Intensif*. 162, pp. 108344.

León-Pulido, J., Sarmiento, M.P., Garzon, D.M., Hernandez, M.A., Gonzalez, A.D., Peralta-Ruiz, Y.Y., Duran, M.A., **2017**. Energy Study of Reactive-HIDiC Simulation for Ethyl Acetate Synthesis from Acetic Acid. *Chem. Eng. Trans*. 58, pp. 547−552.

Levy, S.G., Van Dongen, D.B., Doherty, M.F., **1985a**. Design and Synthesis of Homogeneous Azeotropic Distillations. 1. Problem Formulation for a Single Column. *Ind. Eng. Chem. Fundam*. 24(4), pp. 454–463.

Levy, S.G., Van Dongen, D.B., Doherty, M.F., **1985b**. Design and Synthesis of Homogeneous Azeotropic Distillations. 2. Minimum Reflux calculations for Nonideal and Azeotropic Columns. *Ind. Eng. Chem. Fundam*. 24(4), pp. 463–474.

Lísal, M., Smith, W.R., Nezbeda, I., **1999**. Accurate Computer Simulation of Phase Equilibrium for Complex Fluid Mixtures. Application to Binaries Involving Isobutene, Methanol, Methyl *tert*-Butyl Ether, and *n*-Butane. *J. Phys. Chem. B.* 103(47), pp. 10496–10505.

Lísal, M., Smith, W.R., Nezbeda, I., **2000**. Molecular Simulation of Multicomponent Reaction and Phase Equilibria in MTBE Ternary System. *AIChE J.* 46(4), pp. 866–875.

Malone, M.F & Doherty, M.F., **2000**. Reactive Distillation. *Ind. Eng. Chem. Res*. 39(11), pp. 3953–3957.

Marek, J., **1954**. Rectification with a chemical reaction. I. Calculation of the number of theoretical plates for continuous plate columns. *Collection of Czechoslovak Chemical Communications*. 19(6), pp. 1055-1073.

Muthia, R., Reijneveld, A.G.T., van der Ham, A.G.J., ten Kate., A.J.B., Bargeman, G., Kerstena, S.R.A., Kiss, A.A., **2018**. Novel method for mapping the applicability of reactive distillation. *Chem. Eng. Process. Process Intensif*. 128, pp. 263–275.

Orjuela A., Santaella M.A., Molano P.A., **2016**. Process Intensification by Reactive Distillation. In: Segovia-Hernández J., Bonilla-Petriciolet A. (eds) Process Intensification in Chemical Engineering. *Springer International Publishing*, Cham. pp. 131-181.

Pérez-Cisneros, E.S., Gani, R., Michelsen, M.L., **1997**. Reactive separation systems – I. Computation of physical and chemical equilibrium. *Chem. Eng. Sci*. 52(4), pp. 527-543.

Pérez-Cisneros, E.S. **1997**. Modelling, Design and Analysis of Reactive Separation Process. Technical Univ. of Denmark.

Santaella, M.A., Jiménez, L.E., Orjuela, A., Segovia-Hernández, J.G., **2017.** Design of thermally coupled reactive distillation schemes for triethyl citrate production using economic and controllability criteria. *Chem. Eng. J*. 328, pp. 368−381.

Sánchez-Daza, O., Pérez-Cisneros, E.S., Bek-Pedersen, E., Gani, R., **2003**. Graphical and stage-to-stage methods for reactive distillation column design. *AIChE J*. 49(11), pp. 2822-2841.

Singh, B.P., Singh, R., Kumar, M.V.P., Kaistha, N., **2005**. Steady-state analyses for reactive distillation control: An MTBE case study. *J Loss Prev Process Ind.* 18(4-6), pp. 283–292.

Spes, H., **1966**. Katalytische Reaktionen in Ionenaustauscherkolonnen unter Verschiebung des chemischen Geleichgewichts. *Chemiker Atg/Chemische Aparatur*. 90(13), pp. 443-446.

Stichlmair, J. & Frey, T., **1999**. Review: Reactive Distillation Processes. *Chem. Eng. Technol. 22*(2), pp. 95-103.

Sundmacher, K. & Qi, Z., **2003**. Conceptual design aspects of reactive distillation processes for ideal binary mixtures. *Chem. Eng. Proc*. 42(3), pp. 191-200

Taylor, R. & Krishna, R., **2000**. Modelling reactive distillation. *Chem. Eng. Sci*. 55(22), pp. 5183-5229.

Thery, R., Meyer, X.M., Joulia, X., Meyer, M., **2005**. Preliminary design of reactive distillation columns. *Chem. Eng. Res. Des*. 83(4), pp. 379-400.

Thotla, S. & Mahajani, S.M., **2009**. Conceptual design of reactive distillation for selectivity improvement in multiple reactant systems. *Chem. Eng. Res. Des*. 87(1), pp. 61-81.

Ung, D. & Doherty, M.F., **1995**. Synthesis of reactive distillation systems with multiple equilibrium chemical reactions. *Ind. Eng. Chem. Res*. 34(8), pp. 2555-2565.

Weinfeld, J.A., Owens, S.A., Eldridge, R.B., **2018**. Reactive dividing wall columns: A comprehensive review. *Chem. Eng. Process. Process Intensif*. 123, pp. 20-33.

Zhang, Q., Guo, T., Yu, C., Li., Y., **2017**. Design and control of different pressure thermally coupled reactive distillation for amyl acetate synthesis. *Chem. Eng. Process. Process Intensif*. 121, pp. 170–179.

Zhao, T., Li, J., Zhou, H., Ma, Z., Sun, L., **2018**. A thermally coupled reactive distillation process to intensify the synthesis of isopropyl acetate. *Chem. Eng. Process. Process Intensif*. 124, pp. 97–108.

Zheng, L., Cai, W., Zhang, X., Wang, Y., **2017**. Design and control of reactive dividing-wall column for the synthesis of diethyl carbonate. *Chem. Eng. Process. Process Intensif*. 111, pp. 127−140.

Chapter 8

Conclusions and Summaries

8.1 Overview

The aim of this thesis is to present a simple, quick, effective and comprehensive graphical tool/technique that can be used for preliminary design as well as to analyse system behaviour. The graphical method retains the simplicity and effectiveness of the original binary McCabe-Thiele method. The purpose of the graphical tool is to aid in an efficient design process by complementing the proper and effective usage of rigorous design simulation packages.

Chapter 3 postulates the novel method of depicting the contours of VLE for ideal and non-ideal systems. The method is general in nature, but application is restricted to ternary mixtures only, in this chapter. The mathematical foundation of the method is presented followed by a general method of plotting the vapour-liquid equilibrium (VLE) on an x-y two dimension (2D) plot for each component under investigation. The method is applicable to all types of components, thermodynamic models or equilibrium data. In this chapter the visual insights of an easy and difficult separation were portrayed such that a designer can quickly 'see' if a separation is viable before beginning to design a column. In addition, non-ideal azeotropic systems that exhibit both binary and ternary azeotropes were visually identified as intersections of one or more contours of VLE with the 45 degree line. The designer can also identify the composition of each component of the azeotrope. The intersection of the specific VLE contour with the 45 degree line is the fraction of the component in the azeotrope. The ratio that represents the specific VLE contour at the azeotrope is either 0 or infinity for binary azeotropes, or a specific value for ternary azeotropes. Lastly, it was shown that tangent pinch point for

multicomponent systems are visually identified on a 2D plot as multiple intersections of the equilibrium curve and operating line. Since binary systems are represented by a single unique equilibrium curve, and a single unique tangent pinch exists. Ternary mixtures on the other hand will have multiple unique tangent pinch points, as the contours of VLE are represented as many equilibrium curves as a function of the other components in the system.

Chapter 4 uses the method of plotting the novel contours of VLE to present a method to calculate the minimum number of stages at total reflux. The method is simple and analogous to the binary McCabe-Thiele method to determine the preliminary design parameters, including the minimum number of stages. The method for determining the number of stages from the distillate to the bottoms products, and from the bottoms to distillate product is presented. The importance of stepping in either direction is depicted in Chapter 6 for determining the number of theoretical stages at finite reflux, for sharp direct and indirect splits. The method is demonstrated for both ideal and non-ideal systems. In addition, it is shown that the results for ideal systems correlate with the short-cut empirical correlation method by Fenske (1932) for ideal systems and for non-ideal systems with a rigorous simulator, Aspen Plus^{TM}. It was further shown that designers and students can do a quick manual calculation once the contours of VLE are plotted, and that the results obtained correlate closely with those performed using computation. Finally, it was shown the proposed graphical method correlated more closely with rigorous simulations than the method proposed by Hengstebeck (1946), of reducing multicomponent systems to a pseudo-binary system. Hence, it can be concluded that the VLE of non-ideal, multicomponent systems cannot be represented as a single curve on an x-y plot.

Chapter 5 incorporates the contours of VLE presented in Chapter 3, and the observations made by Stichlmair (1993), that for sharp splits with nearly pure products the internal liquid concentration profiles are characterized by ‘transition points’. Using the notion of transition points, a graphical method for determining the transition point for a specified feed, and hence the minimum reflux, is proposed.

The method requires the calculation of minimum reflux for the transition splits first, in order to locate the transition point. Once the transition point is located, the minimum reflux for sharp direct and indirect splits can be determined. Once the minimum reflux is obtained, the operating reflux can be calculated by multiplying the minimum reflux by a certain design factor. The operating reflux is required in Chapter 6 for finite reflux calculations. The method is applied to both ideal and non-ideal systems, and the minimum reflux calculated corresponds to both Underwood (1948) and the Boundary Value Method (Doherty & Malone, 2001).

Chapter 6 extends the method presented for total reflux in Chapter 4 to preliminary design calculations, at finite reflux. The novel representation of contours of VLE, presented in Chapter 3, are used once again as the foundation of the method. Once the minimum reflux is calculated using the method explained in Chapter 5, the operating reflux can be set. Once the product specification are obtained along with the operating reflux, the designer can then determine two important preliminary design parameters. These are the feed stage location and the number of theoretical stages. Once the design parameters are obtained, the values are used to initialise a rigorous design simulator. The simulation for a non-ideal system of acetone-benzene-chloroform was initialised on Aspen Plus™, and converged on the first simulation using the preliminary design parameters obtained from the proposed graphical technique. This reiterating the importance of the graphical technique as a preliminary design tool in the overall distillation design process, and hence greatly supports and complements rigorous design simulation packages for detailed column design. It should also be mentioned that, for ideal systems, the method correlated closely with the Fenske-Underwood-Gilliland (FUG) method. It must be stressed that the graphical method allows the location of the feed stage to be determined while determining the number of theoretical stages simultaneously. No additional calculations are required as with other methods. Finally, the method at finite reflux for ternary systems is extended to quaternary systems and non-CMO systems.

Chapter 7 presents a graphical technique for the design of reactive-hybrid columns without the transformation of composition variables. Hence, the powerful visual

insights gained from the McCabe-Thiele method, for non-reactive distillation columns, is retained. The technique incorporates the novel representation of VLE (Chapter 3), the method for determining design parameters at finite reflux (Chapter 6), and reactive cascade difference points presented by Lee et al., (2000a; 2000b) to develop a method for determining design variables for reactive-hybrid distillation columns. The design method for several reactive-hybrid configurations were developed, namely: reaction on the feed stage, reaction in the rectifying section or stripping section only and a combination of reaction on the feed stage and rectifying section. The graphical technique will enhance, support and complement the efficient use of rigorous design simulation packages for detailed column design. The method for determining design parameters for reaction on the feed stage and rectifying section, rectifying section only and stripping section was developed for ideal systems with no net change in the number of moles. It was shown the reactive stage location, and multiple reactive stages in a column section, directly influence the number of stages required. The graphical technique is beneficial in that, once the VLE for the components are plotted, various scenarios can be analysed in order to choose the optimal design variables, with minimal additional calculations. The minimum reflux for reaction on the feed stage can be determined using the method in Chapter 5 for sharp direct and indirect splits. The graphical technique to determine feed stage location and number of theoretical stages for reaction on the feed stage is applicable to ideal and non-ideal systems, with or without a change in net number of moles. The design parameters obtained from the simulation of a non-ideal system of isobutene-methanol-MTBE, were successfully initialised and produced a converged design using a rigorous simulator, Aspen Plus^{TM}. Once again, the importance of the graphical technique as a preliminary design tool in the overall distillation design process is highlighted.

8.2 Summary of Method Rules and Graphical Representations

8.2.1 Comparison of Characteristics for Binary and Multicomponent McCabe-Thiele Diagrams

Figure 8.1 presents a summary and comparison of the characteristics of binary VLE and multicomponent contours of VLE for the examples presented in this thesis. Figure 8.1a shows the representation of ideal VLE for binary systems as a single equilibrium curve, and multicomponent systems as contours of VLE on an x-y diagram. Azeotropes in binary mixtures exhibit a single equilibrium curve with one intersection with the 45 degree line, representing a single binary azeotrope in the mixture (Figure 8.1b). Multicomponent systems can display multiple contours intersecting the 45 degree line, as depicted in Figure 8.1b. The intersection of the contours and the 45 degree line can represent binary azeotropes, ternary azeotropes and turning points. The visual depiction of VLE tangent to the 45° line represents tangent pinches in both ideal and multicomponent systems (Figure 8.1c). The difference is that a single curve becomes tangent to the 45 degree line for binary systems, and all the contours of VLE for multicomponent mixtures become tangent to the 45 degree line. For binary systems, the stepping off stages are between the 45 degree line and a single equilibrium curve. Figure 8.1d illustrates that the stepping off stages for multicomponent systems is from the 45 degree line to a different contour at each step, depending on the ratio of the compositions of the other components in the system. At finite reflux for binary systems, the light key is plotted and stepping takes place from the distillate to the bottoms composition. Stepping takes place between a single equilibrium curve and the relevant operating line. The changeover from the rectifying to the bottoms operating line takes place at the feed line for the light key. For multicomponent systems, either the light key (LK) or heavy key (HK) is plotted, depending on whether the separation is sharp direct or indirect respectively. Stepping takes place between the relevant operating line and a unique VLE contour, depending on the ratio of the compositions of the other components in the system. Changeover from one operating to the next is at the LK feed line for direct splits and HK for indirect splits.

Property	Binary system	Multicomponent system
(a) Ideal VLE	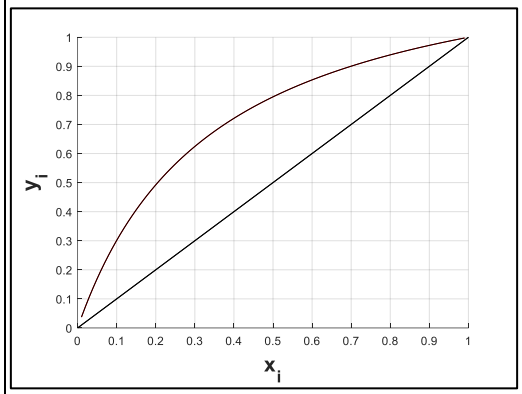	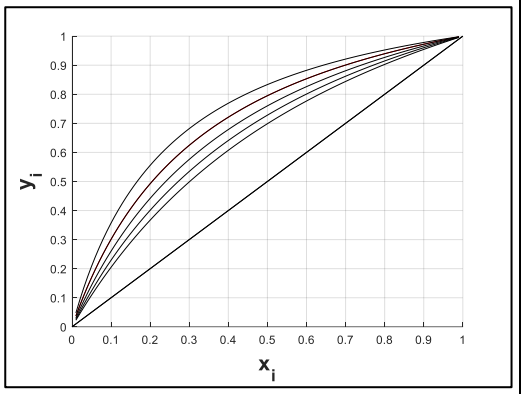
(b) Azeotropic VLE	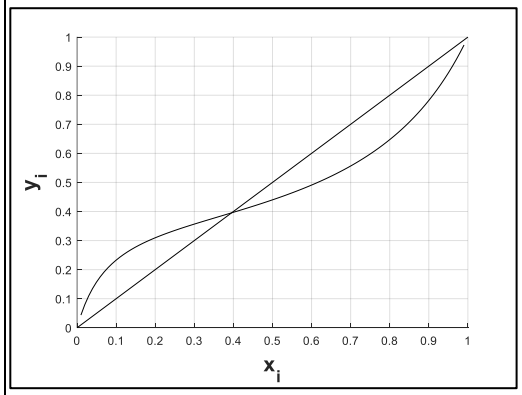	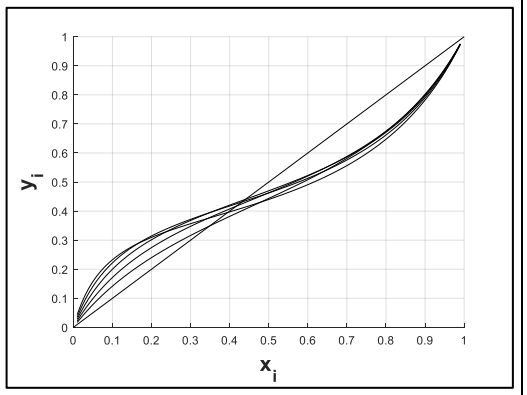

(c) Tangent pinch	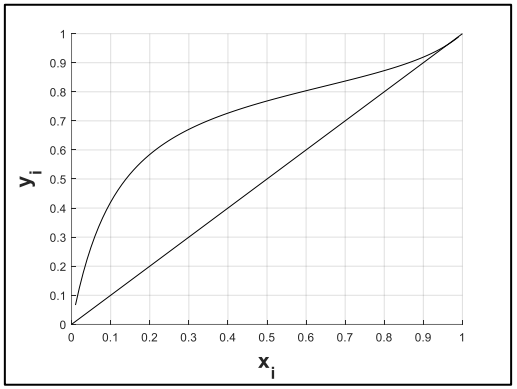	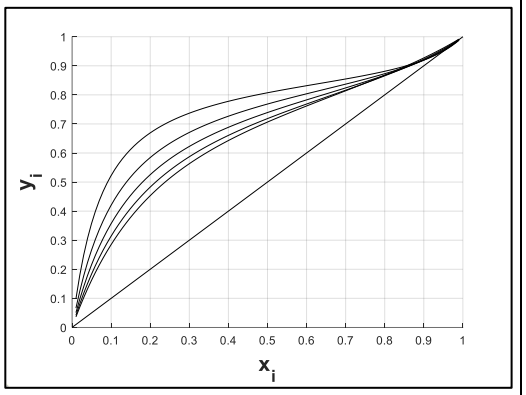
(d) Total reflux (minimum stages)	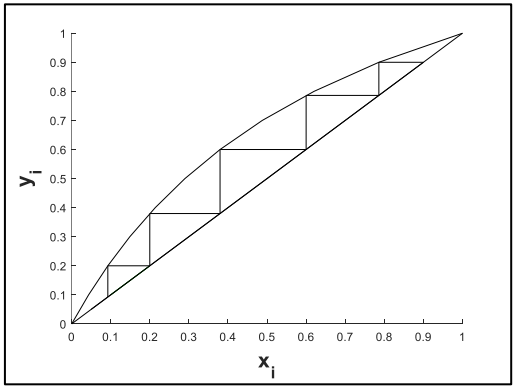	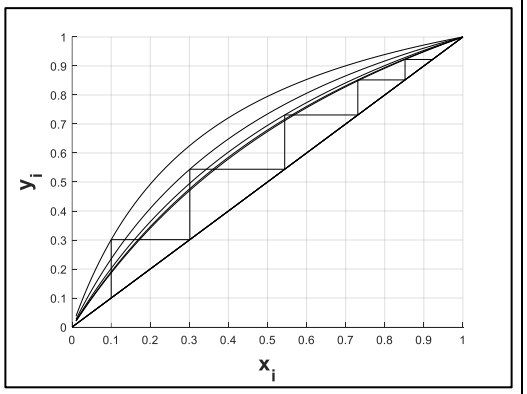

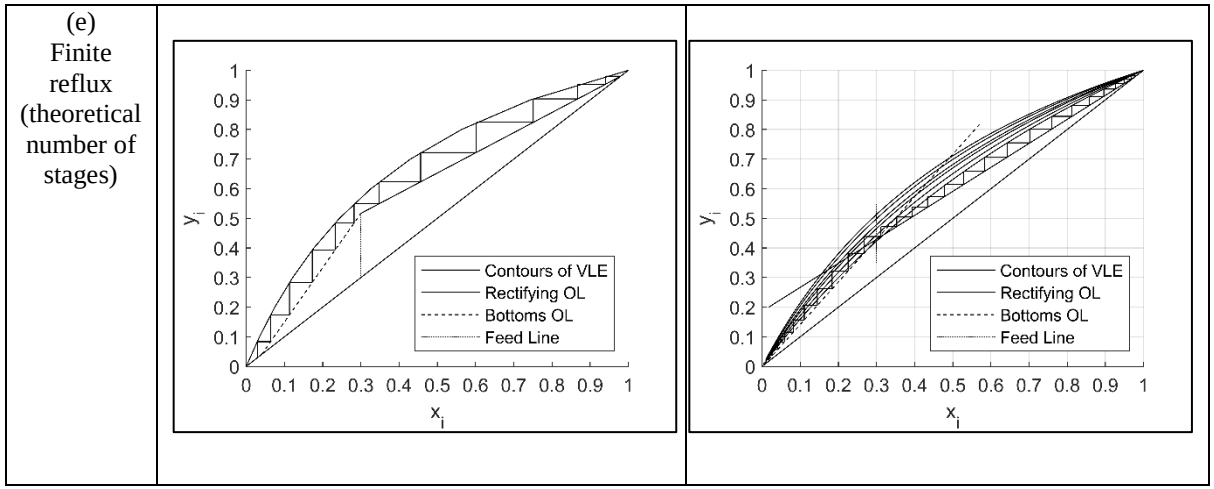

Figure 8.1: Comparison of the visual representation of binary VLE and multicomponent contours of VLE for (a) ideal systems (b) azeotropic systems (c) tangent pinches (d) total reflux (e) finite reflux

8.2.2 Summary of the Procedures for Direct and Indirect Splits for Minimum Reflux and Finite Reflux.

Table 8.1 provides the designer with a summary and guidelines for the rules of thumb to be followed when designing direct and indirect splits. Table 8.1 stipulates the guidelines for the number of theoretical stages at finite, feed stage location and minimum reflux.

Table 8.1: The procedures to be followed for direct and indirect splits to determine minimum reflux, number of theoretical stages and feed stage location

Procedure	Type of split	
Finite Reflux	**Direct split**	**Indirect split**
Target composition:	LK	HK
Number of stages is determined from:	bottoms to distillate composition	distillate to bottoms composition
Feed stage location	At feed line of LK-changeover from bottoms to rectifying operating line	At feed line of HK-changeover from rectifying to bottoms operating line
Minimum reflux	**Direct split**	**Indirect split**
Binary VLE required to determine transition point to be plotted for :	LK and IK	HK and IK
McCabe-Thiele diagram required to be plotted for:	LK	HK
Transition point found in:	Rectifying section	Bottoms section

8.2.3 Summary of the Procedures for Reactive-Hybrid Distillation Design

Table 8.2 provides the designer with a summary and guidelines for the rules of thumb to be followed when designing finite reflux, reactive-hybrid distillation columns. The general procedures are summarized for reaction on the feed stage, rectifying section only, stripping section only, and feed and rectifying section respectively.

Table 8.2: The procedures to be followed for reaction in the feed stage, rectifying section only, stripping section only and feed and rectifying section

	Reactive Column Configuration			
Procedure	**Feed stage**	**Rectifying section only**	**Stripping section only**	**Feed stage and rectifying section**
Suited type of separation	All types of separation	Direct split	Indirect split	Direct split
Number of stages is determined from:	Direct split- bottoms to distillate composition Indirect split- distillate to bottoms composition	bottoms to distillate composition	distillate to bottoms composition	bottoms to distillate composition
Calculation of pseudo-feed	Yes Reactant- pseudo-feed shift to the left of actual feed Products- shift to the right of the actual feed	No	No	Yes Reactant- pseudo-feed shift to the left of actual feed Products- shift to the right of the actual feed
Feed stage location	At pseudo-feed line of LK- changeover from bottoms to rectifying operating line	At feed line of LK- changeover from bottoms to reactive rectifying operating line	At feed line of HK- changeover from rectifying to reactive bottoms operating line	At pseudo-feed line of LK- changeover from bottoms to reactive rectifying operating line

Calculation of adjusted x_D	No	Yes Reactant-adjusted distillate composition shifts above the distillate composition Products-adjusted distillate composition shifts below the distillate composition	No	Yes Reactant-adjusted distillate composition shifts above the distillate composition Products-adjusted distillate composition shifts below the distillate composition
Calculation of adjusted x_B	No	No	Yes Reactants-adjusted bottoms composition shifts above the bottoms composition Products-adjusted bottoms composition shifts below the bottoms composition	No

8.3 Recommendations for Future Research

This work lays the foundation for the development of a comprehensive, preliminary design graphical tool that can be used widely by designers and students alike to design ternary distillation processes. The establishment of the fundamentals and basis of the graphical method in this work paves a way for future work to establish the graphical method presented in this thesis, as a leading graphical design tool. The idea is to provide a simple graphical method that complements the use of residue curve maps.

The general method for determining preliminary design parameters such as minimum number of stages, number of theoretical stages and feed stage location can be extended to system for 4 components and higher for ideal and non-ideal systems applicable to both reactive and non-reactive distillation processes.

While the work in this thesis looked at simple columns with a single feed and two products, further work is recommended on complex columns such as multiple feed, single/multiple side streams, Petlyuk and Keibel configurations. Several emerging intensified distillation technologies such as divided wall columns (DWC), heat-integrated distillation columns (HIDiC), thermally-coupled columns can also be designed using the proposed graphical method in this thesis. This thesis presented the basis of reactive-hybrid distillation column design using the proposed graphical technique. Future work will build on the principles provided, to extend the graphical technique of reaction on feed stage and rectifying section, rectifying section only and stripping section only to non-ideal systems and systems with a net change in the number of moles. Once the graphical method for non-ideal simple reactive processes is established, the design of reactive columns combined with DWC, HIDiC and thermally-coupled columns can be developed.

The graphical method presented in this thesis covers continuous distillation columns and not batch operated distillation columns. The binary McCabe Thiele method has been applied to binary batch systems with reflux. Hence, it can be hypothesized that the method presented in this thesis for continuous multicomponent systems can be applied to multicomponent batch systems in future work.

It would be very useful to solve the problem of determining minimum reflux for non-sharp splits in a simple graphical manner as presented in Chapter 5 for sharp splits. There are very few solutions to the problem currently implemented in the field of distillation design.

REFERENCES

Doherty, M.F. & Malone, M.F., **2001.** Conceptual Design of Distillation Systems. *McGraw-Hill, Inc:* New York.

Fenske, M.R., **1932**. Fractionation of Straight-Run Pennsylvania Gasoline. *Ind. Eng. Chem.* 24(5), pp. 482–485.

Hengstebeck, R.J., **1946**. A Simplified Method for Solving Multicomponent Distillation Problems. *Trans. AIChE*. 42, pp. 309-329.

Lee, J.W., Hauan, S., Lien, K.M., Westerberg, A.W., **2000a**. A graphical method for designing reactive distillation columns. II. The McCabe-Thiele method. P*roceedings of the Royal Society of London*. 456(2000), pp. 1965-1978.

Lee, J.W., Hauan, S., Westerberg, A.W., **2000b**. Graphical Methods for Reaction Distribution in a Reactive Distillation Column. *AIChE J*. 46(6), pp. 1218-1233.

Levy, S.G. & Doherty, M.F., **1986**. A simple exact method for calculating tangent pinch points in multicomponent nonideal mixtures by bifurcation theory. *Chem. Eng. Sci.* 41(12), pp. 3155-3160.

Stichlmair, J., Offers, H., Potthoff, R.W., **1993**. Minimum Reflux and Minimum Reboil in Ternary Distillation. *Ind. Eng. Chem. Res*. 32(1), pp. 2438-2445.

Underwood, A.J.V. **1948**. Fractional Distillation of Multicomponent Mixtures. *Chem. Eng. Prog*. 44(8), pp. 603-614.

Appendix A

Derivation of the correlation to generate the contours of VLE for ideal systems

Define an ideal ternary systems containing Components *i, j, k.*

Where the distribution coefficients and relative volatilities are defined in Equations (A.1) and (A.2). Assume constant relative volatility.

Distribution coefficient, K_i:

$$K_i = \frac{y_i}{x_i} \tag{A.1}$$

Relative Volatilities, α:

$$\alpha_{ik} = {}^{y_i/x_i}\Big/_{y_k/x_k} \tag{A.2}$$

Solve for y_i in Equation (A.2) as generally equilibrium curves are expressed in terms of the vapour composition (y).

$$y_i = \alpha_{ik} y_k \left({}^{x_i}/_{x_k}\right) \tag{A.3}$$

From the summation of vapour compositions of components *i, j, k*:

$$y_k = 1 - y_i - y_j \tag{A.4}$$

Substitute Equation (A.4) into (A.3)

$$y_i = \alpha_{ik}\left(1 - y_i - y_j\right)\left({}^{x_i}/_{x_k}\right) \tag{A.5}$$

Furthermore:

$$\alpha_{ij} = {}^{y_i/x_i}\Big/_{y_j/x_j} \tag{A.6}$$

$$\alpha_{ij} = \frac{y_i x_j}{x_i y_j} \tag{A.7}$$

$$y_j = {}^{y_i}/_{\alpha_{ij}}\left({}^{x_j}/_{x_i}\right) \tag{A.8}$$

Substitute Equation (A.8) into (A.5)

$$y_i = \alpha_{ik}\left(1 - y_i - \left({}^{y_i}/_{\alpha_{ij}}\left({}^{x_j}/_{x_i}\right)\right)\right)\left[{}^{x_i}/_{x_k}\right] \tag{A.9}$$

$$y_i = \alpha_{ik}\left(1 - y_i\left[1 + \frac{x_j}{\alpha_{ij}x_i}\right]\right)\left[{}^{x_i}/_{x_k}\right] \tag{A.10}$$

$$y_i = \alpha_{ik}\left({}^{x_i}/_{x_k} - \left(y_i\left[{}^{x_i}/_{x_k}\right]\left[1 + \frac{1}{\alpha_{ij}}\left[{}^{x_j}/_{x_i}\right]\right]\right)\right) \tag{A.11}$$

$$y_i = \alpha_{ik}\left[\left({}^{x_i}/_{x_k}\right) - y_i\left({}^{x_i}/_{x_k}\right) - y_i\frac{1}{\alpha_{ij}}\left({}^{x_j}/_{x_k}\right)\right] \tag{A.12}$$

$$y_i = {}^{\alpha_{ik}\left({}^{x_i}/_{x_k}\right)}\Big/_{1 + \alpha_{ik}\left({}^{x_i}/_{x_k}\right) + \frac{\alpha_{ik}}{\alpha_{ij}}\left({}^{x_j}/_{x_k}\right)} \tag{A.13}$$

Let the component ratio of component *i* be defined as CR_{jk}:

$$CR_{jk} = {}^{x_j}/_{x_k} \tag{A.14}$$

$$x_j = x_k CR_{jk} \tag{A.15}$$

From the summation of liquid compositions of components *i, j, k:*

$$x_i + x_j + x_k = 1 \tag{A.16}$$

$$x_i + x_k CR_{jk} + x_k = 1 \tag{A.17}$$

$$x_k = {}^{1 - x_i}\Big/_{\left(CR_{jk} + 1\right)} \tag{A.18}$$

Substitute Equation (A.18) into (A.13)

$$y_i = \frac{\alpha_{ik}\left(\frac{x_i}{1-x_i}\right)\left(CR_{jk}+1\right)}{1+\alpha_{ik}\left(\frac{x_i}{1-x_i}\right)\left(CR_{jk}+1\right)+\frac{\alpha_{ik}}{\alpha_{ij}}CR_{jk}} \tag{A.19}$$

Equation (A.19) is the final equation used to determine the vapour and liquid compositions at equilibrium for component *i* at ratios of component *j* and *k* such that the contours of VLE can be generated for ideal systems. Equation (A.20) is presented as Equation (3.1) in Chapter 3. The same method can be followed to derive Equations (3.2) and (3.3).

Appendix B

Thermodynamic Properties

In this Appendix, the relevant physical property data for the examples (non-ideal mixtures only) studied in this thesis are presented. The vapour pressures are calculated using the extended Antoine equation presented in Equation B.1 and the parameters are provided in Table B.1 obtained from Aspen Plus™.

$$\ln p_i = C_{1i} + \frac{C_{2i}}{T+C_{3i}} + C_{4i}T + C_{5i}\ln T + C_{6i}T^{C_{7i}} \quad for\ C_{8i} \le T \le C_{9i} \tag{B.1}$$

Table B.1: Pure component constants for extended Antoine equation

	Component								
	C_1	C_2	C_3	C_4	C_5	C_6	C_7	C_8	C_9
Acetone	57.4931	-5599.6	0	0	-7.098	6.2237×10^{-6}	2	-94.7	235.05
Benzene	71.5941	-6486.2	0	0	-9.2194	6.9844×10^{-6}	2	5.53	288.9
Chloroform	134.917	-7792.3	0	0	-26.614	0.024578	1	-66	263.25
Ethanol	61.7911	-7122.3	0	0	-7.1424	2.8853×10^{-6}	2	-114.1	240.85
Water	62.1361	-7258.2	0	0	-7.3037	4.1653×10^{-6}	2	0.01	373.95
Methanol	71.2051	-6904.5	0	0	-8.8622	7.4710^{-6}	2	-97.68	239.35
Isobutene	66.4971	-4634.1	0	0	-8.9572	1.3413e-05	2	-140.34	144.75
MTBE	45.6171	-5200.7	0	0	-5.1398	1.6513e-17	6	-108.6	233.95

The Wilson activity coefficient model (Equation B.2) has been used to predict the activity coefficients of the species in the non-ideal mixtures and the binary parameters are provided in Table B.2 obtained from Aspen Plus™.

$$\ln \gamma_i = 1 - ln\left(\sum_j A_{ij}x_j\right) - \sum_j \frac{A_{ji}x_j}{\sum_k A_{jk}x_k} \tag{B.2}$$

Table B.2: Binary interaction parameters for the Wilson equation

Component *i*	Component *j*	A_{ij}	A_{ji}	B_{ij}	B_{ji}	C_{ij}	C_{ji}	D_{ij}	D_{ji}
Acetone	Benzene	-0.4336	0.0849	184.624	-237.196	0	0	0	0
Acetone	Chloroform	-0.7683	-0.7191	262.179	435.144	0	0	0	0
Benzene	Chloroform	-2.4936	1.2772	598.487	-188.941	0	0	0	0
Acetone	Ethanol	0.8452	0.7465	-405.215	-346.039	0	0	0	0
Acetone	Water	-0.4374	-9.7051	-291.079	2719.21	0	0	0	0
Ethanol	Water	-2.5035	-0.0503	346.151	-69.6372	0	0	0	0
Acetone	Methanol	0	0	-115.663	-108.526	0	0	0	0
Chloroform	Methanol	0	0	-32.5972	-652.896	0	0	0	0
Isobutene	Methanol	0	0	-328.818	-1100.59	0	0	0	0
Isobutene	MTBE	0	0	-342.508	208.572	0	0	0	0
Methanol	MTBE	0	0	-237.859	-218.606	0	0	0	0

The NRTL liquid activity coefficient model (Equation B.3) has been used to predict the activity coefficients of a non-ideal mixture of acetone-benzene-chloroform and the binary parameters are provided in Table B.3 obtained from Aspen Plus™.

$$\ln \gamma_i = \frac{\sum_j x_j \tau_{ji} G_{ji}}{\sum_k x_k G_{ki}} + \sum_j \frac{x_j G_{ij}}{\sum_k x_k G_{kj}} \left(\tau_{ij} - \frac{\sum_m x_m \tau_{mj} G_{mj}}{\sum_k x_k G_{kj}} \right) \quad \text{(B.3)}$$

Table B.3: Binary interaction parameters for the NRTL liquid coefficient model

Component *i*	Component *j*	A_{ij}	A_{ji}	B_{ij}	B_{ji}	C_{ij}	D_{ij}	E_{ij}	E_{ji}	F_{ij}	F_{ji}
Acetone	Benzene	-0.1015	0.4224	306.066	-239.901	0.3	0	0	0	0	0
Acetone	Chloroform	0.9646	0.5382	-590.026	-106.422	0.3	0	0	0	0	0
Benzene	Chloroform	0.6209	-1.0488	-480.842	607.006	0.3	0	0	0	0	0

Appendix C

Calculation of Minimum Number of Stages using the Fenske Equation

The calculation of the minimum number of stages using the Fenske equation (1932) is presented in this Appendix.

For multicomponent systems the separation will be specified in terms of the light key and heavy key components and provided in Equation C.1 below (Górak & Sorensen, 2014):

$$N_{min} = \frac{log\left[\left(\frac{x_{LK}}{x_{HK}}\right)_D\left(\frac{x_{HK}}{x_{LK}}\right)_B\right]}{log(\propto_{LK,HK})} \quad \text{(C.1)}$$

Where:

N_{min} = Minimum number of stages

$\left(\frac{x_{LK}}{x_{HK}}\right)_D$ = the ratio of the mole fractions of the light and heavy key components in the distillate product

$\left(\frac{x_{HK}}{x_{LK}}\right)_B$ = the ratio of the mole fractions of the light and heavy key components in the bottoms product

$\propto_{LK,HK}$ = is the average volatility

$(x_{HK})_B = 0.6000$
$(x_{LK})_B = 0.1000$
$(x_{HK})_D = 0.0003220$
$(x_{LK})_D = 0.9224$
$K_{hexane} = 0.45$
$K_{heptane} = 0.22$

Since the relative volatilities are assumed constant through the column:

$$\alpha_{LK,HK} = \frac{K_{hexane}}{K_{heptane}} = \frac{0.45}{0.22} = 7.031$$

$$N_{min} = \frac{log\left[\left(\frac{0.9224}{0.0003220}\right)_D\left(\frac{0.6000}{0.1000}\right)_B\right]}{log(7.031)}$$

$$N_{min} = 5.00$$

Appendix D

Calculation of Minimum Reflux Ratio Using the Underwood Method

The calculation of the minimum reflux and reboil ratios for n-pentane, n-hexane and n-heptane system using the Underwood method (1948) is presented in this Appendix.

For multicomponent systems the separation will be specified in terms of the light key and heavy key components and provided in Equation D.1 below (Underwood, 1948):

$$\sum_{i=1}^{c} \frac{\alpha_{i/ref} z_{i,F}}{\alpha_{i/ref} - \theta} = 1 - q \quad \text{(D.1)}$$

$$\sum_{i=1}^{c} \frac{\alpha_{i/ref} x_{i,D}}{\alpha_{i/ref} - \theta} = R_{min} + 1 \quad \text{(D.2)}$$

$$\sum_{i=1}^{c} \frac{\alpha_{i/ref} x_{i,B}}{\theta - \alpha_{i/ref}} = S_{min} \quad \text{(D.3)}$$

Where:

$$\theta = \frac{V_{min}}{L_{min} K_{ref}}$$

Where:

R_{min} = Minimum reflux ratio

S_{min} = Minimum reboil ratio

V_{min}= minimum vapour flow in the column

L_{min}= minimum liquid flow in the column

$z_{i,F}$= feed composition of component *i*

$x_{i,D}$= distillate composition of component *i*

$x_{i,B}$= bottoms composition of component *i*

$$\alpha_{i/ref} = {K_i}/{K_{ref}}$$

Since the relative volatilities are assumed constant through the column and generally K_{ref} is the heavy key component:

$\alpha_{M,P} = 3.25$
$\alpha_{E,P} = 1.90$

$\alpha_{P,P} = 1$

Since the feed is a saturated liquid hence:
$q = 1$
Feed compositions:
$z_{F,M} = 0.30$
$z_{F,E} = 0.25$
$z_{F,P} = 0.45$

Distillate compositions:
$x_{D,M} = 0.730$
$x_{D,E} = 0.250$
$x_{D,P} = 0.020$

Bottoms compositions:
$x_{B,M} = 0.010$
$x_{B,E} = 0.250$
$x_{B,P} = 0.740$

Step 1: use equation D.1 to determine θ:

$$\frac{3.25\times0.30}{3.25-\theta} + \frac{1.90\times0.25}{1.90-\theta} + \frac{1\times0.45}{1-\theta} = 1 - 1 = 0$$

$$\theta = 1.33 \; or \; \theta = 2.44$$

Step 2: use Equations D.2 and D.3 to determine R_{min} and S_{min} respectively:

$$\frac{3.25\times0.73}{3.25-\theta} + \frac{1.90\times0.25}{1.90-\theta} + \frac{1\times0.02}{1-\theta} = R_{min} + 1$$

$$R_{min} = 1.02$$

$$\frac{3.25\times0.01}{3.25-\theta} + \frac{1.90\times0.25}{1.90-\theta} + \frac{1\times0.74}{1-\theta} = S_{min}$$

$$S_{min} = 1.36$$

Appendix E

Derivation of equation for reaction on the feed stage for reactive distillation columns

$$F = D + B - v_T\xi \tag{E.1}$$

$$Fx_{F,i} = Dx_{D,i} + Bx_{B,i} - v_i\xi \qquad for\ i = 1,2 \dots j \tag{E.2}$$

Substitute Equation E.1 into Equation E.2

$$(D + B - v_T\xi\ )x_{F,i} = Dx_{D,i} + Bx_{B,i} - v_i\xi \qquad for\ i = 1,2 \dots j \tag{E.3}$$

Simplify Equation E.3:

$$Dx_{F,i} + Bx_{F,i} - v_T\xi x_{F,i} = Dx_{D,i} + Bx_{B,i} - v_i\xi \tag{E.4}$$

$$x_{F,i} = \frac{Dx_{D,i}+Bx_{B,i}}{(D+B)} + \frac{v_T\xi x_{F,i}-v_i\xi}{(D+B)} \tag{E.5}$$

$$x_{F,i} = \frac{Dx_{D,i}+Bx_{B,i}}{(D+B)} + \frac{v_T\xi x_{F,i}-v_i\xi}{(D+B)} \tag{E.6}$$

$$x_{F,i} = \frac{Dx_{D,i}+Bx_{B,i}}{(D+B)} + \frac{v_T\xi\left(x_{F,i}-v_i/v_T\right)}{(D+B)} \tag{E.7}$$

Where:

$$x_{\hat{F},i} = \frac{Dx_{D,i}+Bx_{B,i}}{D+B} \qquad for\ i = 1,2 \dots j \tag{E.8}$$

$$\delta_{R,i} = {}^{v_i}/_{v_T} \tag{E.9}$$

Substitute E.8 and E.9 into E.7 to obtain an expression (Equation E.10) that relates the feed, pseudo-feed and reactive difference point.

$$(D + B)x_{F,i} = x_{\hat{F},i} + v_T\xi\left(x_{F,i} - \delta_{R,i}\right)$$

$$(D + B)\left(x_{F,i} - x_{\hat{F},i}\right) = v_T\xi\left(x_{F,i} - \delta_{R,i}\right) \tag{E.10}$$

Appendix F

Reactive Distillation: Additional Figures

Feed stage reaction: Non-ideal system: net change in number of moles

Figures F.1 and F.2 present the McCabe-Thiele diagrams at finite reflux for reaction on the feed stage only for isobutene and methanol. The number of stages required is 15 with feed stage location on stage 5

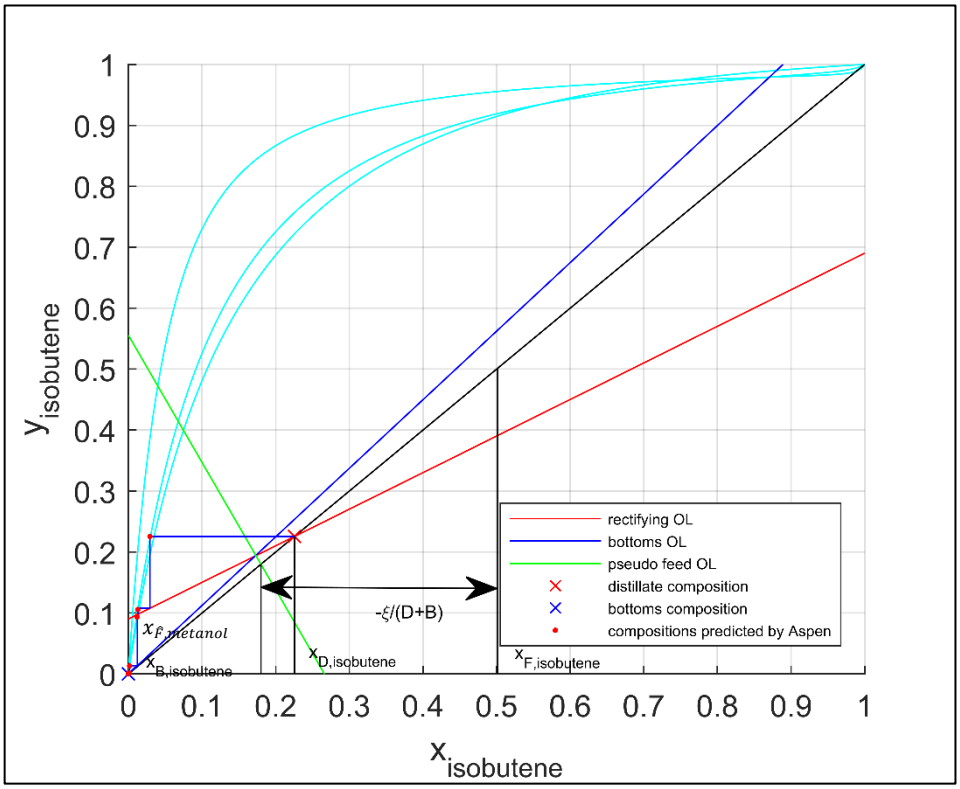

Figure F.1: McCabe-Thiele diagram for isobutene and Aspen Plus™ compositions on each stage at finite reflux for reaction on the feed stage

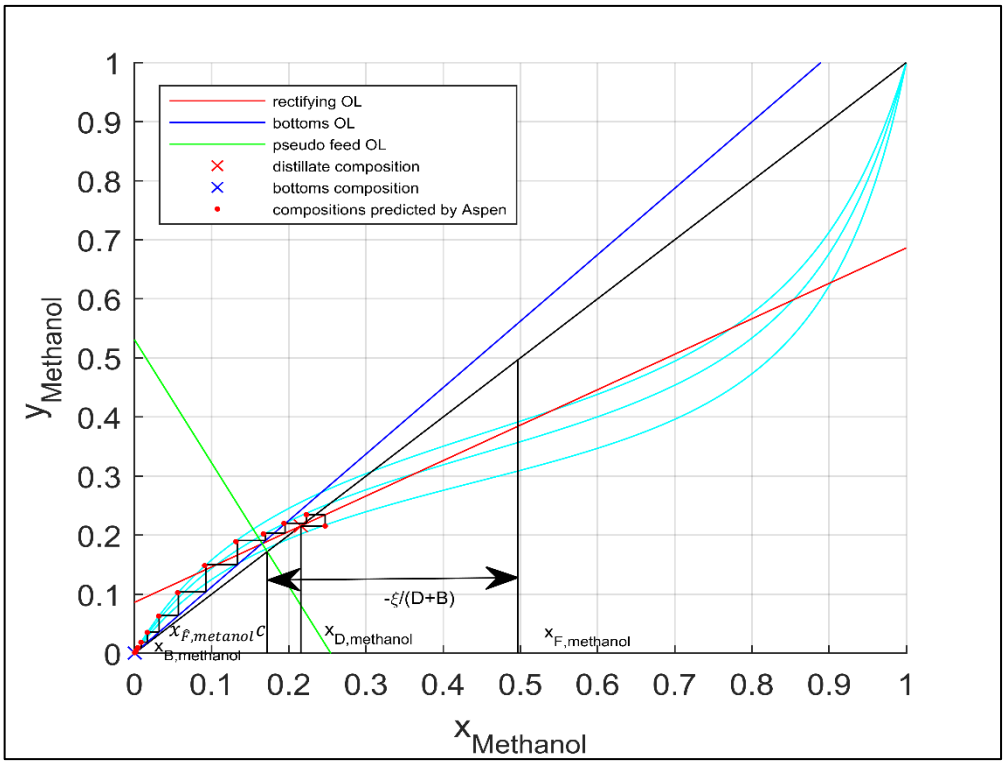

Figure F.2: McCabe-Thiele diagram for methanol and Aspen Plus™ compositions on each stage at finite reflux for reaction on the feed stage

Effect of feed position

Figures F.3 and F.4 present the McCabe-Thiele diagrams at finite reflux for reaction in the rectifying section only for Component A (IK) and C (HK). The feed stage and reactive stage location are stage 13 and 5 respectively

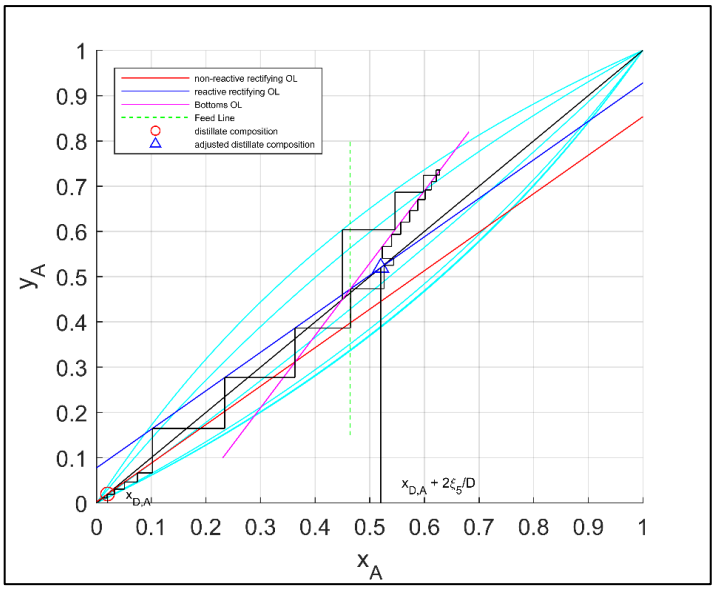

Figure F.3: McCabe-Thiele diagram for Component A at finite reflux for reaction on stage 5 in the rectifying section and feed stage = 13

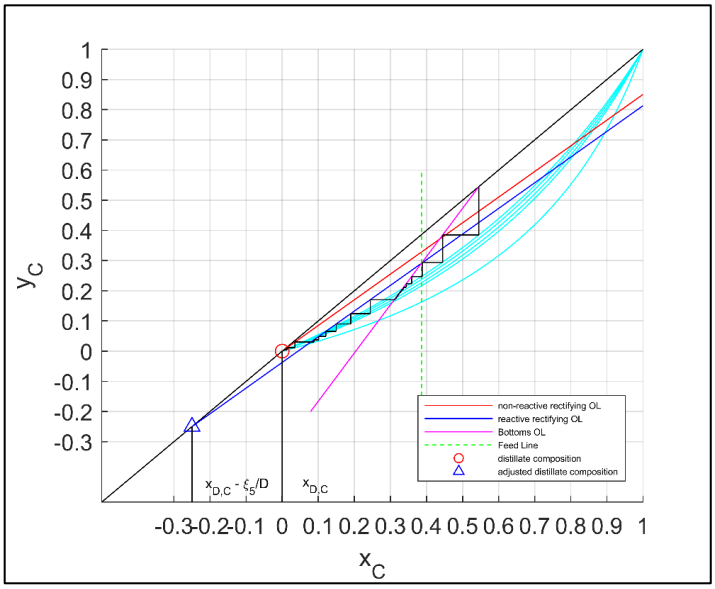

Figure F.4: McCabe-Thiele diagram for Component A at finite reflux for reaction on stage 5 in the rectifying section and feed stage = 13

Figures F.5 and F.6 present the McCabe-Thiele diagrams at finite reflux for reaction in the rectifying section only for Component A (IK) and C (HK). Feed stage location on stage 14 and reactive stages, 8 stages above the feed location.

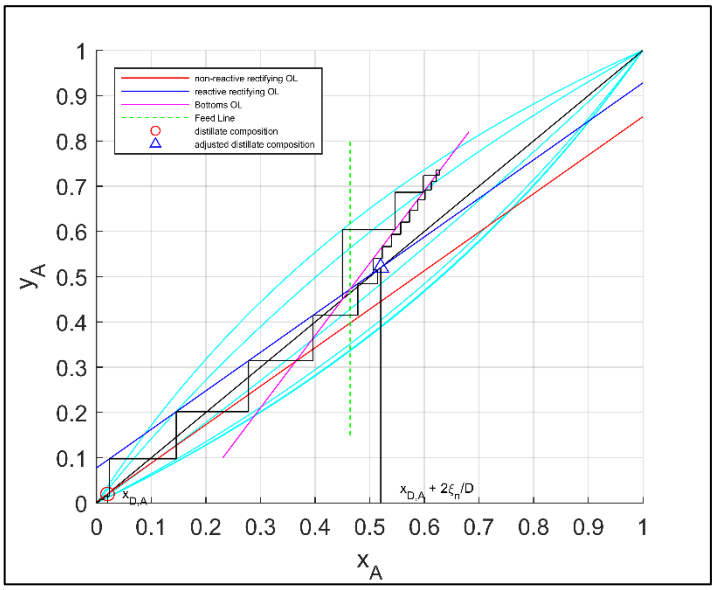

Figure F.5: McCabe-Thiele diagram for Component A at finite reflux for reaction on stage 8 after the feed location at stage 14 in the rectifying section.

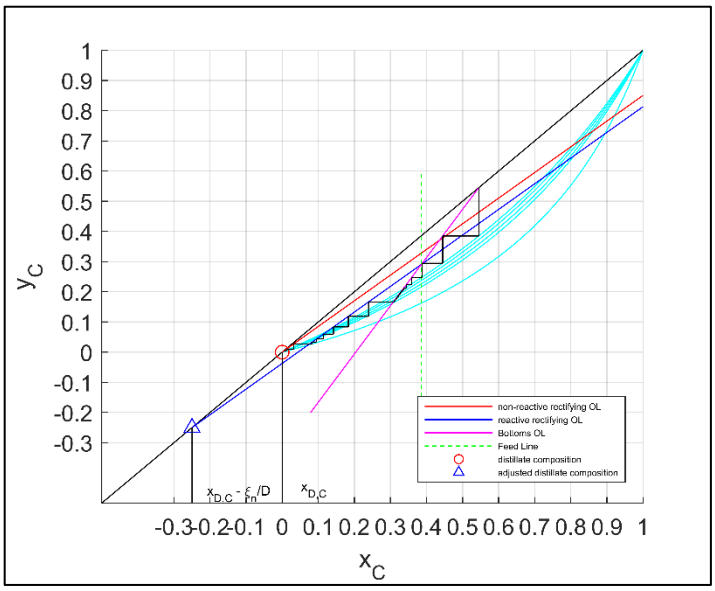

Figure F.6: McCabe-Thiele diagram for Component C at finite reflux for reaction on stage 8 after the feed location at stage 14 in the rectifying section.

Figures F.7 and F.8 present the McCabe-Thiele diagrams at finite reflux for reaction in the rectifying section only for Component A (IK) and C (HK). Feed stage location on stage 14 and reactive stages, 7 stages above the feed location.

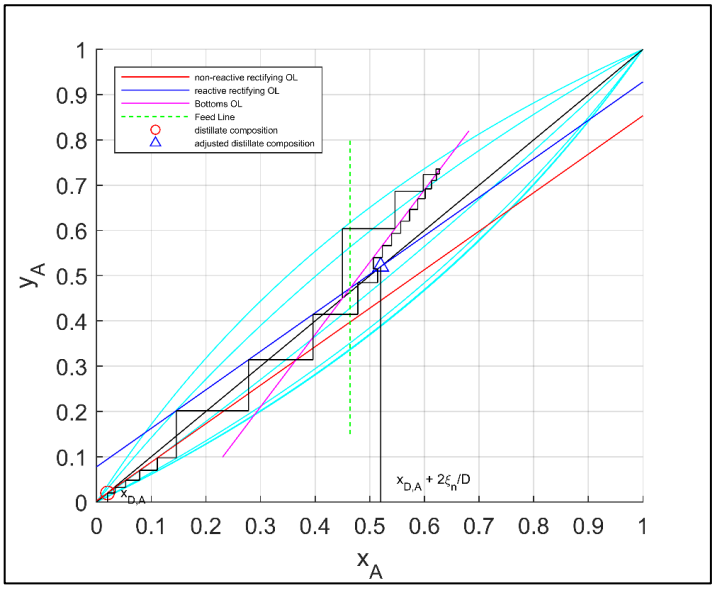

Figure F.7 McCabe-Thiele diagram for Component A at finite reflux for reaction on stage 7 after the feed location at stage 14 in the rectifying section

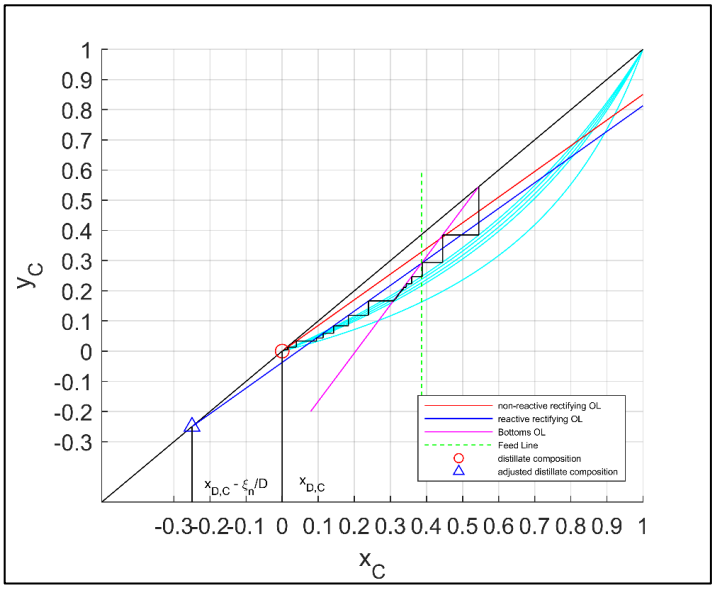

Figure F.8: McCabe-Thiele diagram for Component A at finite reflux for reaction on stage 7 after the feed location at stage 14 in the rectifying section

Figures F.9 and F.10 present the McCabe-Thiele diagram at finite reflux for reaction in the rectifying section only on stage 5 and feed stage location onstage 10 for Component A (IK) and C (HK).

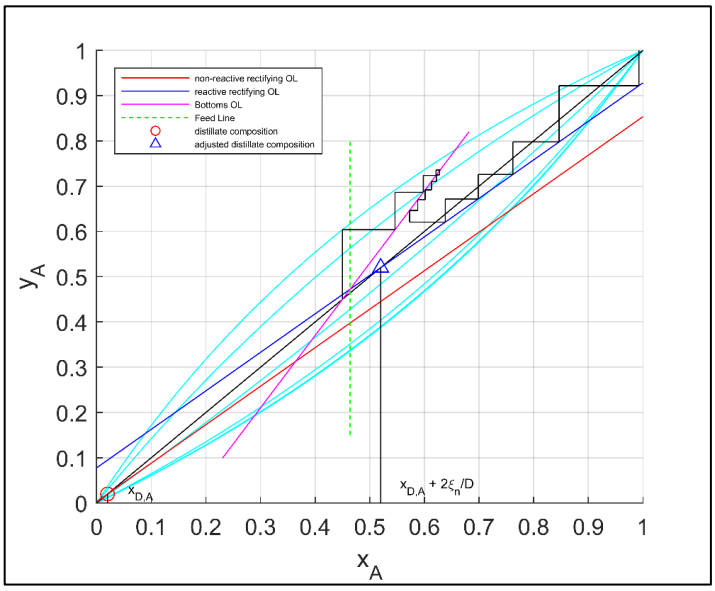

Figure F.9: McCabe-Thiele diagram for Component A at finite reflux for reaction on stage 5 in the rectifying section and feed stage = 10

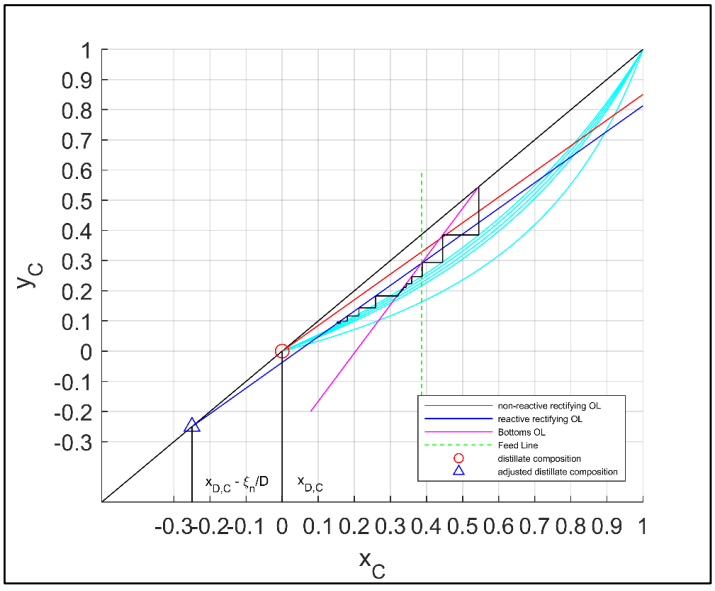

Figure F.10: McCabe-Thiele diagram for Component A at finite reflux for reaction on stage 5 in the rectifying section and feed stage = 13

Effect of reactive stage position

Figures F.11 present the McCabe-Thiele diagrams at finite reflux for reaction in the rectifying section only (stage 1) for Component C (HK).

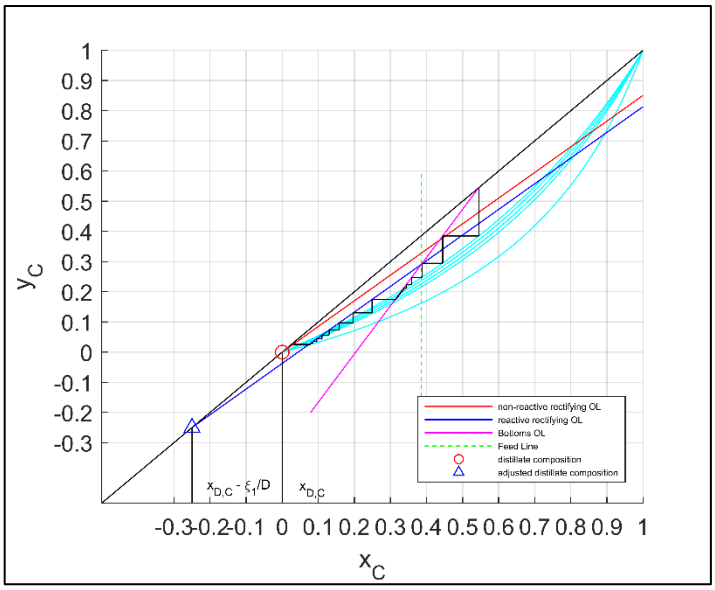

Figure F.11: McCabe-Thiele diagram for Component A at finite reflux for reaction on stage 5 in the rectifying section and feed stage = 13

Figures F.12 and F.13 present the McCabe-Thiele diagram at finite reflux for reaction in the rectifying section only (stage 12) for Component A (IK) and C (HK).

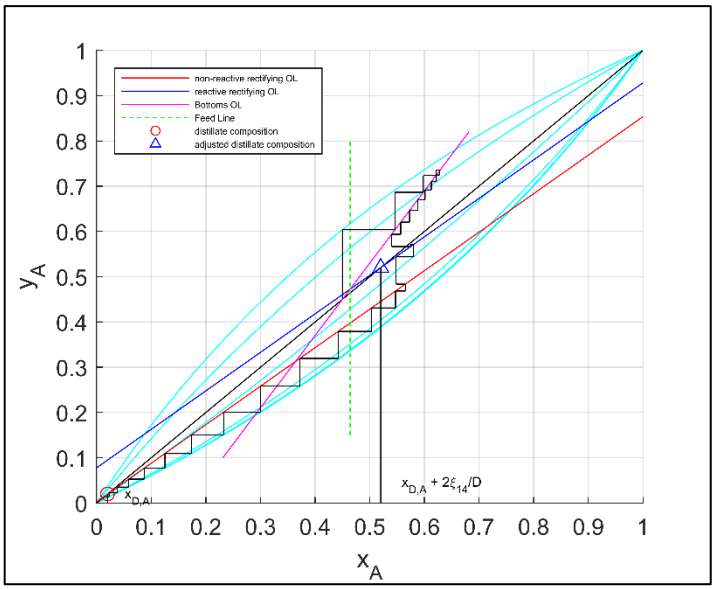

Figure F.12: McCabe-Thiele diagram for Component A at finite reflux for reaction on stage 14 in the rectifying section and feed stage = 12

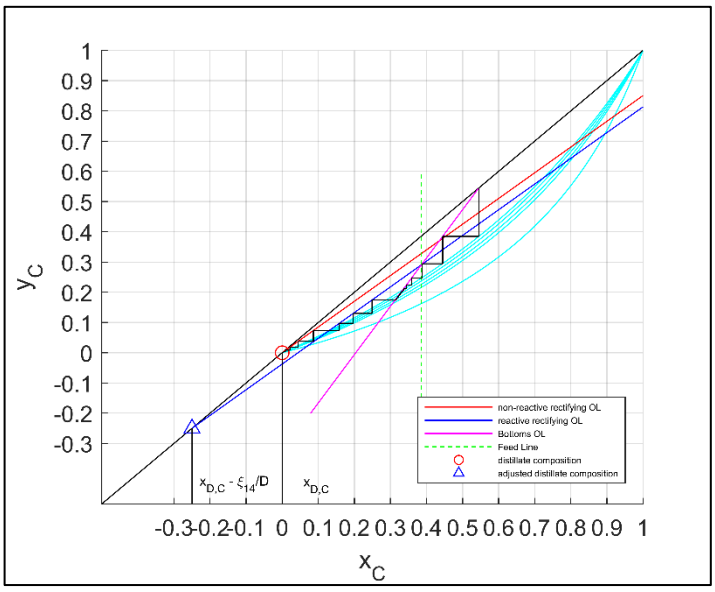

Figure F.13: McCabe-Thiele diagram for Component C at finite reflux for reaction on stage 14 in the rectifying section and feed stage = 12

Effect of consecutive reaction stages for reaction on two stages

Figures F.14 and F.15 present the McCabe-Thiele diagram at finite reflux for two consecutive reaction stages in the rectifying section only. Feed stage 12, Reactive stage number 11 and 12 for Component A (IK) and C (HK).

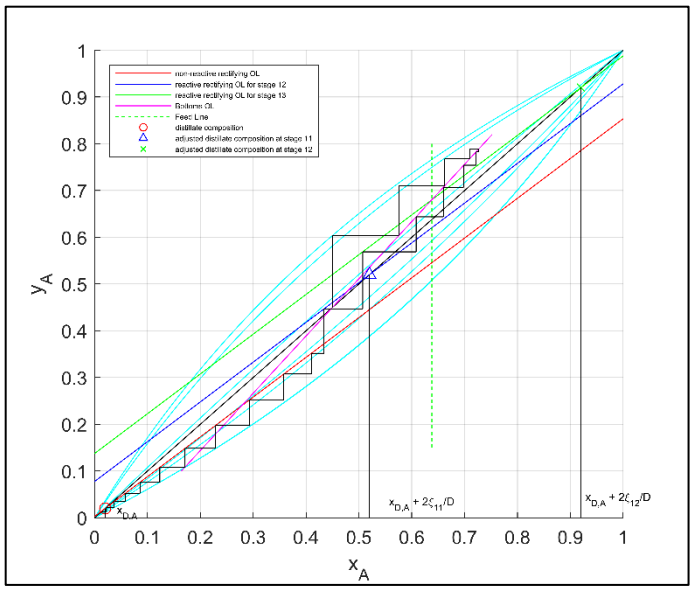

Figure F.14: McCabe-Thiele diagram for Component A at finite reflux for reactive stage 1 on stage 11 and reactive stage 2 on stage 12 in the rectifying section and feed stage = 13

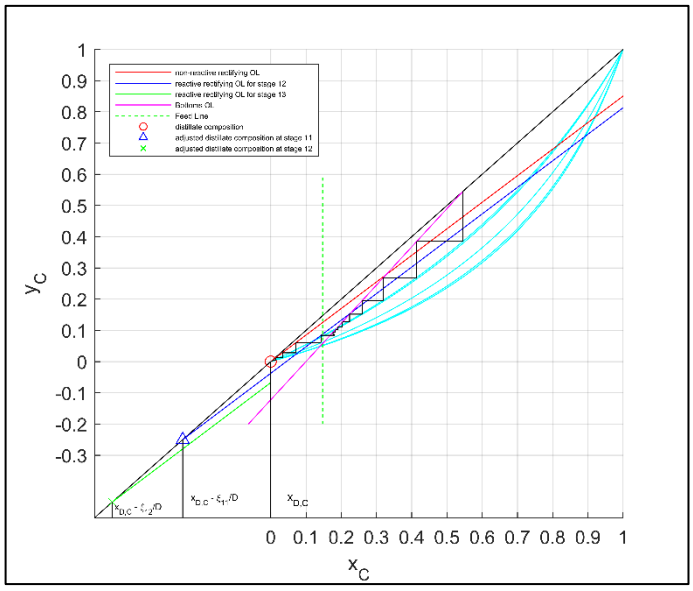

Figure F.15: McCabe-Thiele diagram for Component B at finite reflux for reactive stage 1 on stage 11 and reactive stage 2 on stage 12 in the rectifying section and feed stage = 13

Reaction in rectifying section and feed stage

Figure F.16 presents the McCabe-Thiele diagram at finite reflux for reaction in rectifying section (stage 5) and feed stage (stage 12) for Component A (IK).

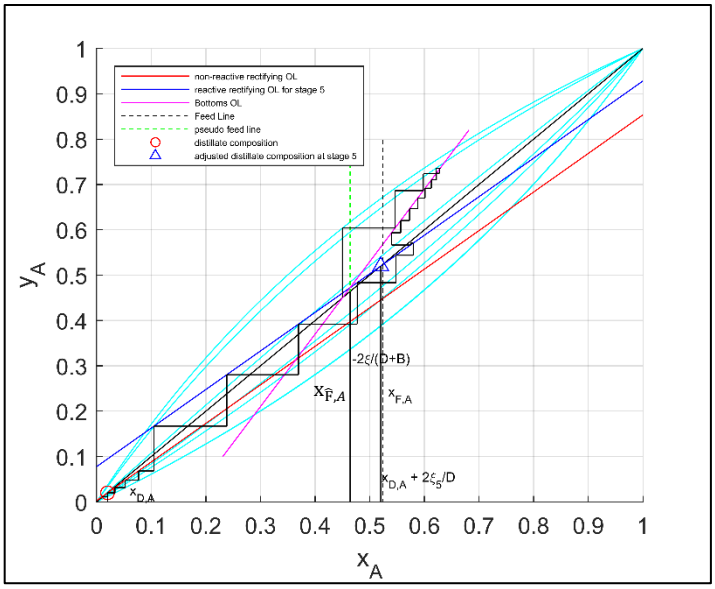

Figure F.16: McCabe-Thiele diagram for Component A at finite reflux for reactive stage on stage 5 and feed stage reaction on stage 12